Gas-phase Ion-electron and Ion-photon Reactions for Structural Characterization of Protein Glycosylation

by

Wen Zhou

A dissertation submitted in partial fulfillment
of the requirements for the degree of
Doctor of Philosophy
(Chemistry)
in The University of Michigan
2011

Doctoral Committee:

      Associate Professor Kristina I. Håkansson, Chair
      Professor David M. Lubman
      Professor Michael D. Morris
      Professor Nils G. Walter

To My Parents and My Husband

Acknowledgements

First, I would like to express my deepest gratitude to my supervisor, Dr. Kristina Håkansson. I sincerely thank Kristina for all the encouragement, guidance, support, and persistent help through my Ph.D. research. Her enthusiasm, dedication, and wide knowledge of science have inspired all her students. I could not have imagined having a better advisor and mentor for my Ph.D. study.

Second, I would like to thank my Ph.D. committee, including Professor David M. Lubman, Professor Michael D. Morris, and Professor Nils G. Walter, for all the valuable suggestions and comments during my candidacy, data meeting, and dissertation. This dissertation could not have been completely without their critique, guidance, and feedback. Special thanks go to Professor David M. Lubman for leading me into the fantastic world of mass spectrometry during my rotation.

Third, I would like to express my warm and sincere thanks to the former and present colleagues in the Håkansson lab: Jiong, Hye Kyong, Haichuan, Jingjie, Julie, Natasa, Jason, Bo, Hyun Ju, Hangtian, Yibing, Chris, Katie, Ashley, Noah, Di, and Ning. I am fortunate to have awesome colleagues like you, and thank you all for your help, support, and friendship.

Financial support from Eli Lilly & Company (to Kristina), National Science Foundation (NSF), National Institutes of Health (NIH), George Ashworth Analytical

Table of Contents

List of Figures

Figures

List of Tables

Tables

List of Abbreviations

2-AA	2-aminobenzoic acid
2-AB	2-aminobenzamide
AGC	Automatic gain control
AI-ECD	Activated-ion ECD
BIRD	Blackbody infrared radiative dissociation
CAD	Collision activated dissociation
CI	Chemical ionization
DMSO	Dimethyl sulfoxide
ECD	Electron capture dissociation
EDD	Electron detachment dissociation
EID	Electron induced dissociation
Endo-H	Endoglycosidase-H
ESI	Electrospray ionization
ETD	Electron transfer dissociation
FTICR-MS	Fourier transform ion cyclotron resonance mass spectrometry
GAG	Glycosaminoglycan
GC	Gas chromatography
GlcNAc	N-acetyl glucosamine
HeCAD	High-energy CAD
HCD	High-energy C-trap dissociation
HILIC	Hydrophilic interaction chromatography
IRMPD	Infrared multiphoton dissociation
LC	Liquid chromatography
LID	Laser induced dissociation
MALDI	Matrix-assisted laser desorption/ionization
MCDT	Multicollision dissociation threshold
MS	Mass spectrometry
MS/MS or MS^n	Tandem mass spectrometry
m/z	Mass-to-charge ratio
Nano ESI	Nano electrospray ionization
NETD	Negative electron transfer dissociation

NeuAc	*N*-acetyl neuraminic acid
NMR	Nuclear magnetic resonance
PGC	Porous graphitized carbon
PNGase F	Peptide-*N*-glycosidase F
PTM	Posttranslational modification
Q	Quadrupole
S/N	Signal to noise
SID	Surface induced dissociation
SORI-CAD	Sustained off-resonance irradiation collision activated dissociation
SPE	Solid phase extraction
T	Tesla, a unit of magnetic field
TOF	Time of flight
UVPD	Ultraviolet photodissociation

Abstract

Gas-phase Ion-electron and Ion-photon Reactions for Structural Characterization of Protein Glycosylation

by

Wen Zhou

Chair: Kristina I. Håkansson

Glycosylation is one of the most prevalent post-translational modifications (PTMs), playing key roles in various biological activities. Characterization of protein glycosylation faces unique challenges due to the highly diverse structures of glycans and the heterogeneity of glycoforms at a specific glycosylation site. Fourier transform ion cyclotron resonance mass spectrometry (FT-ICR MS) is an extremely valuable tool for glycosylation analysis, benefiting from high resolution, ultrahigh mass accuracy, and a multitude of tandem mass spectrometric capabilities.

In this thesis, ion-electron and ion-ion based fragmentation techniques such as electron capture dissociation (ECD), electron transfer dissociation (ETD), and electron

detachment dissociation (EDD) are explored for structural characterization of glycosylation. Acidic glycans such as sulfated and sialylated glycans have been linked to cancer metastasis. EDD and metal-assisted ECD/ETD are utilized for structural elucidation of acidic and neutral oligosaccharides, and complementary structural information is obtained compared to collision activated dissociation and infrared multiphoton dissociation (IRMPD). Compared to ECD, ETD is less efficient for fragmenting low charge state precursor ions. For sialylated glycans, negative-ion mode analysis is more advantageous due to the abundant signal and the ability of EDD to generate extensive glycosidic and cross-ring cleavages.

We explore EDD and IRMPD of fluorescently labeled oligosaccharides, and compare the influence of different labels. Complementary structural information can be obtained from EDD and IRMPD. Acidic labels promote glycan signal in negative-ion mode, but also introduce competition of deprotonation sites which impedes the formation of cross-ring cleavages. IRMPD and EDD are also utilized for structural characterization of N- and O-linked glycopeptides. For N-linked glycopeptides, EDD fragmentation efficiency decreases with increased peptide length. For O-linked glycopeptides, EDD is able to yield peptide backbone, glycosidic, and cross-ring cleavages in the same spectrum, suggesting EDD as a powerful tool for structural analysis of *O*-glycopeptides.

Finally, development of LC-FT-ICR MS methods to separate and identify neutral and acidic *N*-glycans using hydrophilic interaction chromatography and graphitized carbon columns is also described. The methods explored in this thesis can contribute to the process of decoding the glycome, and yield new insights into the highly diverse functions of protein glycosylation.

Chapter 1

Introduction

1.1 Glycosylation and Mass Spectrometry

Glycosylation is one of the most prevalent posttranslational modifications (PTMs) and a variety of different types of glycans are also frequently attached to lipids. Glycans participate in many important biological processes, including protein folding and assembly, cell adhesion, cell signaling, immune response, molecular trafficking, and cancer metastasis.[1-5] Altered glycosylation patterns have been associated with cancer malignancy, such as modification of core structures, increased branching, and increased sialylation.[6-9] Therefore, therapeutics or vaccines that target cancer-associated glycans or, in the former case, their down-stream interactions will potentially impede tumor progression. Several glycan-based therapeutics and vaccines are already available clinically or in various clinical stages, such as Fragmin® from Pfizer, and Aranesp® from Amgen.[10,11]

Although the biological significance of glycosylation is well established, the structural diversity arising from complex nontemplate-based biosynthesis, makes glycan structural characterization a highly challenging task. Glycosylation encompasses, e.g.,

N-linked glycans, O-linked glycans, and the glycosaminoglycan (GAG) family of polysaccharides. As shown in Figure 1.1,[10] *N*-glycans are branched carbohydrates containing a pentasaccharide core, normally attached to asparagine residues of proteins in an Asn-Xxx-Ser (or Thr) amino acid consensus sequence with Xxx $\neq$ proline. *N*-glycans are classified into three sub-categories based on the structures at each branch.[12] "High-mannose" type only contains mannose residues that are attached to the core structure. "Complex" type contains only *N*-acetyllactosamine in the antenna region. "Hybrid" type contains both mannose and *N*-acetyllactosamine residues in the antenna. *O*-glycans are branched and linked with either serine or threonine but without a consensus amino acid sequence. In addition, there are several core structures for *O*-glycans. GAGs are also attached to serine or threonine, but they are linear carbohydrates and often highly sulfated.[12,13]
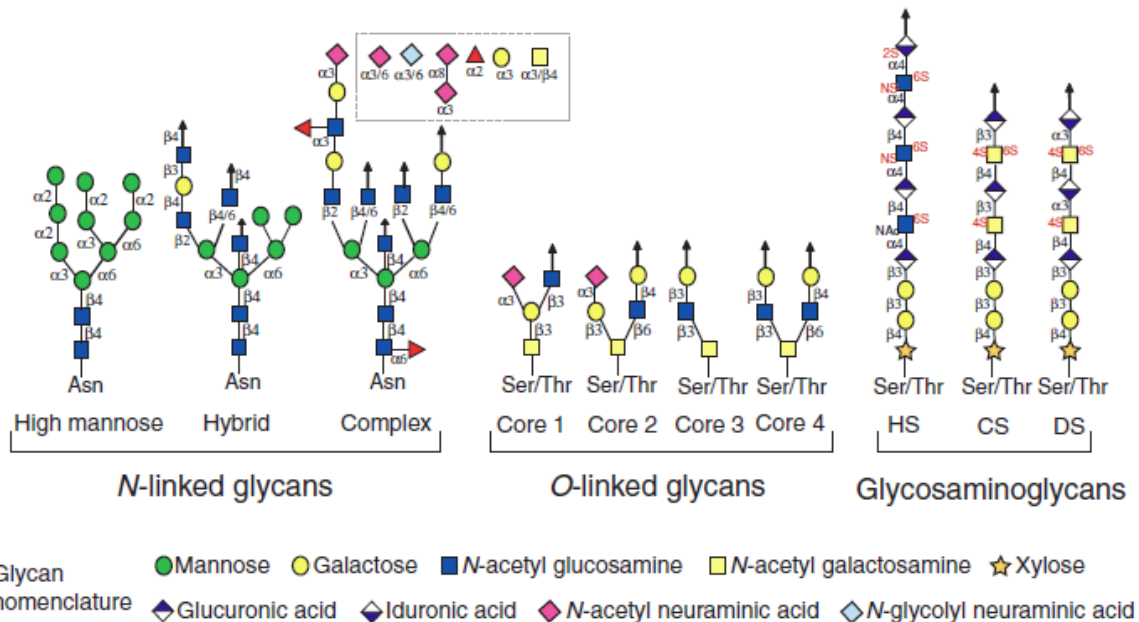
Figure 1.1. Representative structures of N-linked glycans, O-linked glycans, and glycosaminoglycans.[10]

In order to fully understand the key roles glycosylation plays in various cellular processes, knowledge of only the sequence of these compounds is far from sufficient. The linkage, degree of branching, and stereochemistry should also be determined. Traditionally, exoglycosidase digestion, nuclear magnetic resonance (NMR) spectroscopy, X-ray crystallography, and gas chromatography/mass spectrometry (GC/MS) have all been used for structural characterization of carbohydrates.[14] However, such methods do not provide the required sensitivity for glycoproteomics. Modern mass spectrometry is an important tool for structural analysis of carbohydrates, offering high sensitivity, high precision, and analytical versatility.[15-17] Accurate masses obtained from high-resolution tandem mass spectrometry (MS/MS or MS^n) provide reproducible and reliable information for glycan and glycopeptide structural characterization, and glycosylation site determination.[18,19] Fourier transform ion cyclotron resonance mass spectrometry (FT-ICR MS) provides the highest resolution and resolving power of current mass spectrometers.[15] FT-ICR MS is discussed in Section 1.3.

1.2 Strategies for Glycosylation Characterization by Mass Spectrometry

1.2.1 Overview

Glycoproteomics and glycomics constitute emerging fields with the goal of establishing a better understanding of the various essential roles protein glycosylation play in cellular processes.[4,13,20-23] However, the study of glycosylation is still far from routine, due to the enormous structural diversity of glycans and glycopeptides. Mass spectrometry-based glycosylation studies can generally be assigned to one of three categories: glycosylation site determination, glycan analysis (glycomics), and glycopeptide analysis.[24]

In studies where the focus is on glycosylation site determination, glycoproteins are often enriched by affinity chromatography or covalent coupling chemistry and then either investigated as glycoproteins directly, or as deglycosylated proteins. Deglycosylation is often performed by applying peptide-*N*-glycosidase F (PNGase F) digestion to *N*-glycosylated proteins, which cleaves the amide bond between asparagine residues and the glycan, converting the asparagine into aspartic acid.[25] The mass shift of 1 Da after deglycosylation could be used to identify the former glycosylation site.[26] Reverse phase liquid chromatography (LC) separation is commonly used to separate the resulting non-glycosylated peptides after proteolytic digestion, and large-scale analysis can be achieved.[27] One drawback of this approach is that the glycan moiety is discarded and, thus, no glycan structural information can be obtained.

Glycomics studies aim to obtain information regarding monosaccharide composition, i.e., "sequence" of glycans, as well as glycan linkage type. This approach is complementary to glycosylation site determination. PNGase F cleavage, β-elimination, and hydrozinolysis are some of the commonly employed sample preparation methods for glycan release in glycomics. Following glycan release, solid phase extraction (SPE) or LC are applied for purification and enrichment of native or derivatized glycans, followed by mass spectrometric strategies for glycan identification and characterization.[28-32] Glycan release and derivatization methods are discussed in Section 1.2.3. In glycomics approaches, glycosylation site information is not obtained.

Glycopeptide analysis involves proteolytic digestion of glycoproteins and analysis of the resulting glycopeptides with their glycans still attached. Traditionally, amino acid specific enzymes such as trypsin and Glu-C are primarily used. However, in the resulting

peptide mixture, glycopeptides can suffer from significant ion suppression from non-glycosylated peptides, which increases the difficulty in analyzing glycopeptides. Non-specific enzymes, such as pronase and proteinase K, have received increasing attention recently, due to their ability to completely digest non-glycosylated peptides into single amino acids, and generate short glycopeptides at the same time.[24,28,33-35] MS/MS of glycopeptides, particularly the combination of different fragmentation techniques, generates not only peptide backbone cleavages, but also glycosidic and cross-ring cleavages on the glycan moiety, providing rich structural information.[36-44]

1.2.2 Ionization Methods

Matrix-assisted laser desorption/ionization (MALDI) and electrospray ionization (ESI) are the two major modern ionization methods for glycans and glycoconjugates. MALDI involves co-crystallization of analytes and an organic matrix, which acts as a chromophore for ultraviolet laser irradiation. The MALDI mechanism is still under debate, but it has been demonstrated that the choice of matrix plays a crucial role in obtaining strong signals from carbohydrates.[16] MALDI demonstrates high sensitivity, relatively high tolerance to contamination, and predominantly produces singly charged ions, such as $(M + H)^+$ and $(M + Na)^+$ ions in positive-ion mode. However, acidic (sialylated, sulfated, or phosphorylated) carbohydrates may undergo fragmentation in positive-ion mode during ionization, both in-source and post-source.[45,46] In negative-ion mode, MALDI mostly produces $(M - H)^-$ ions.

ESI is a soft ionization method and particularly suitable to use with LC. Depending on sample composition, ESI produces both singly and multiply charged ions, which makes ESI more compatible with various MS/MS strategies than MALDI. It is

believed that the sensitivity of ESI for carbohydrates is limited by their hydrophilicity:[47] There are three major steps in the formation of gas-phase ions during the ESI process: (a) formation of charged analyte-containing droplets; (b) disruption of charged droplets due to solvent evaporation and Coulomb repulsion; (c) formation of gas-phase ions from secondary droplets.[48] When the initial droplets are formed, hydrophobic analytes (such as most proteins and peptides) are distributed preferentially on the droplet surfaces, whereas hydrophilic analytes (such as glycans or heavily glycosylated proteins and peptides) are located inside the droplets. Consequently, ion signal from hydrophilic compounds is suppressed in the ESI process, resulting in low sensitivity.[47] Permethylated oligosaccharides and oligosaccharides derivatized with hydrophobic tags thus demonstrate enhanced sensitivity, up to 1,000 fold.[17,49,50] Nano electrospray ionization (nano-ESI) shows significantly improved sensitivity and higher tolerance to salts and other contaminants compared to conventional ESI due to decreased initial droplet sizes.[47,51] Nano-ESI also facilitates glycan structural analysis with extremely low sample consumption and has been widely utilized with nano-scale LC.[32,52-54]

1.2.3 Sample Preparation Methods of Glycans

Enzymatic and Chemical Release Methods. For enzymatic release of N-linked glycans, PNGase F is most commonly used. This enzyme cleaves the amide bond between asparagine residues and the glycan, releasing most N-linked glycans, except for those containing an α1→3 fucose linkage at the reducing end *N*-acetyl glucosamine (GlcNAc).[25] In such cases, peptide-N-glycosidase A (PNGase A) can be used as an alternative. Endoglycosidase-H (Endo-H) is another popular enzyme for *N*-glycan release. This enzyme cleaves the glycan between the two GlcNAcs at the chitobiose core

of high-mannose and hybrid glycans.[55] However, Endo-H derived *N*-glycans do not provide information regarding core fucosylation, because the reducing end GlcNAc remains bound to the protein. There is currently no universal enzyme for releasing *O*-glycans. Endo-α-N-acetylgalactosaminidase (*O*-glycanase) cleaves exclusively at serine/threonine-glycan bonds, but it is only active for core-1 type *O*-glycans.[56] Therefore, chemical release methods are more commonly used for releasing *O*-glycans.

Hydrazinolysis is a widely used chemical method,[57-59] which has the advantage of releasing both N- and O-linked oligosaccharides, but also frequently introduces side reactions, such as loss of *N*- and *O*-acetyl and glycolyl groups under harsh reaction conditions.[60] Reductive β-elimination with sodium hydroxide and borohydride is also a popular method to chemically release *O*-glycans. When using strong base such as sodium hydroxide, non-selective release of other Ser/Thr PTMs and glycan degradation (peeling) are often observed.[61,62] Therefore, usage of mild bases such as ammonia or dimethylamine[61] has been explored. Recently, a novel *O*-glycan release method combining complete enzyme degradation with chemical release during the process of solid-phase permethylation was introduced.[63] Glycans attached to serine and threonine are effectively cleaved, but those attached to arginine are not, rendering this strategy highly specific.

Derivatization Methods. Permethylation of glycans prior to mass spectrometric analysis is a widely used method. When glycans are permethylated, they become significantly more hydrophobic, which has been reported to increase glycan sensitivity in MS with both ESI and MALDI.[16,64] Moreover, permethylation enables structural analysis of sialylated glycans in positive-ion mode by stabilizing the labile sialic acid in MALDI.[65,66]

Traditionally, permethylation is based on the reaction of glycans with iodomethane and sodium hydroxide prepared in dimethyl sulfoxide (DMSO).[67] More recently, Novotny, Mechref and co-workers have developed high-throughput solid-phase permethylation of glycans prior to MS[68,69] by utilizing fused-silica capillaries or spin columns packed with sodium hydroxide powders or beads, and also demonstrated that sequential double-permethylation can be used for improved structural characterization of sulfated glycans, including localization of sulfate groups.[70]

Reductive amination is another widely used derivatization method. 2-aminobenzoic acid (2-AA), 2-aminobenzamide (2-AB) and 2-aminopyridine (2-AP) are some of the commonly used reagents.[16,71-74] Reductive amination serves multiple purposes: first, by introducing a chromophore to the reducing end of glycans, UV or fluorescence detection becomes possible in LC. Second, because the introduced chromophore is hydrophobic, the retention in reverse phase LC improves at the same time as MS sensitivity increases. However, in order to ensure high yield of labeled oligosaccharides, excess of labeling reagent is used, which requires a clean-up step.

In addition to protonated/deprotonated oligosaccharides, alkali, alkaline earth, and transition metals are widely used for ionization of glycans prior to MS/MS analysis.[75-81] Metal cations can stabilize labile acidic groups, e.g. sulfate groups.[82,83] It has also been demonstrated that metal-adducted glycans result in more cross-ring cleavages than their protonated counterparts in collision activated dissociation (CAD).[75,78,81] Another advantage of metal adduction is elimination of rearrangement reactions during fragmentation. Tandem mass spectrometry of reductively aminated glycans and glycopeptides in their protonated form is known to result in fucose and hexose

rearrangements, but this phenomenon is not observed for their sodium-adducted counterparts.[74,84-87] Therefore, one should be aware of the possibility of rearrangements when assigning MS/MS spectra of protonated glycans and glycoconjugates.

Compared to metal adducts, anionic adducts are not as frequently used in mass spectrometry. Harvey explored a variety of anions in negative-ion mode ESI and reported that nitrate adducts yielded the most satisfactory spectra of N-linked glycans with little in-source fragmentation and high signal abundance.[88] CAD of nitrate- and chloride-adducted *N*-glycans resulted in abundant A- and C-type product ions, whereas bromide and iodide adducts generated few fragments. Cole and co-workers examined chloride adducts in both negative-ion MALDI and ESI, and found unique structurally-informative product ions.[89-91] For example, the abundance ratio of Cl⁻-adducted/non-Cl⁻-adducted product ions in CAD spectra was utilized to differentiate anomeric configurations of disaccharides.[90]

1.3 Fourier Transform Ion Cyclotron Resonance Mass Spectrometry

1.3.1 Overview and Operating Principles

The tremendous complexity of biological samples continues to push the technical limitations of analytical instrumentation. FT-ICR[92] and orbitrap mass analyzers[93-95] provide the highest resolving power of current mass spectrometers and such high-end instruments are utilized in a number of areas, including biomolecular identification, characterization of PTMs, quantification in proteomics, glycomics, and metabolomics, as well as petroleum characterization. In addition to the superior resolution, FT-ICR and orbitrap also provide ultrahigh mass accuracy.[15,96] Both mass analyzers are able to

achieve <5 ppm mass error for externally calibrated spectra and <2 ppm for internally calibrated spectra.[15]

Unlike mass analyzers that measure ion deflection (electric/magnetic sectors), stability of ion trajectories (quadrupole mass analyzer, quadrupole ion trap), or time of ion transit (TOF), FT-ICR is based on detection of induced image current in the time domain followed by Fourier transformation to yield a frequency domain spectrum, which is then converted to an *m/z* spectrum through the ion cyclotron equation (equation (1)) for FT-ICR mass analyzers (shown in Figure 1.2):[15,92,97]

$$\omega_c = \frac{zeB}{m} \qquad (1)$$

in which ω_c is the ion cyclotron frequency, z is an integer, e is the elementary charge, B is the magnetic field strength, and m is the ion mass.
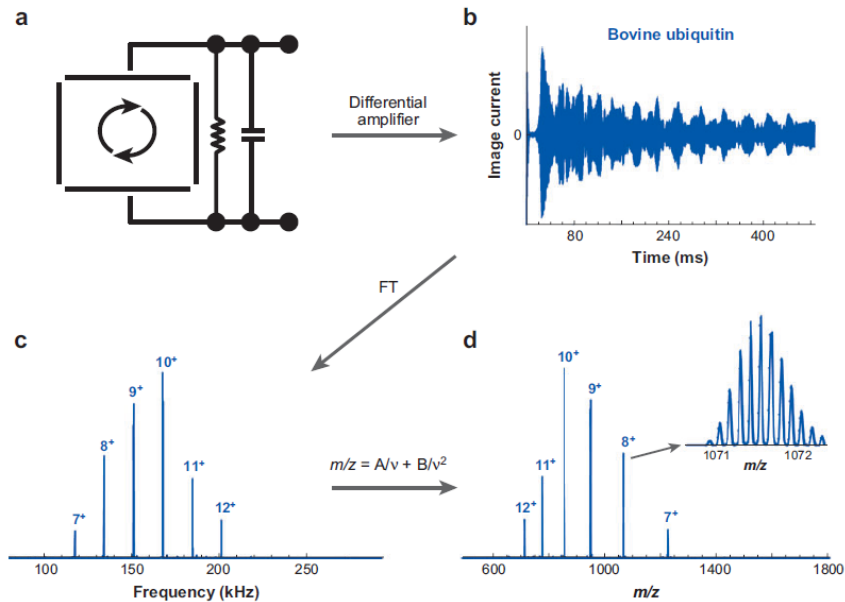
Figure 1.2. (a) Schematic representation of excited ion cyclotron rotation, (b) time-domain image-current signal from opposed detection electrodes, (c) frequency-domain spectrum obtained by fast Fourier transformation of the digitized time-domain signal, and (d) Fourier transform–ion cyclotron resonance m/z spectrum obtained by calibrated frequency-to-m/z conversion.[15]

In the ICR cell, ions are first trapped radially and axially, coherently excited to larger cyclotron radii by applying an rf voltage containing the resonance frequency of the ions between one pair of plates, and then the image current of the orbiting cloud is measured by another pair of plates (shown in Figure 1.3). This principle inherently allows high resolution because resolution is proportional to the ion observation time and this time can be rather long (several seconds) because FT-ICR mass analyzers operate at ultrahigh vacuum, typically in the region of 10^{-9} to 10^{-10} torr.[15]
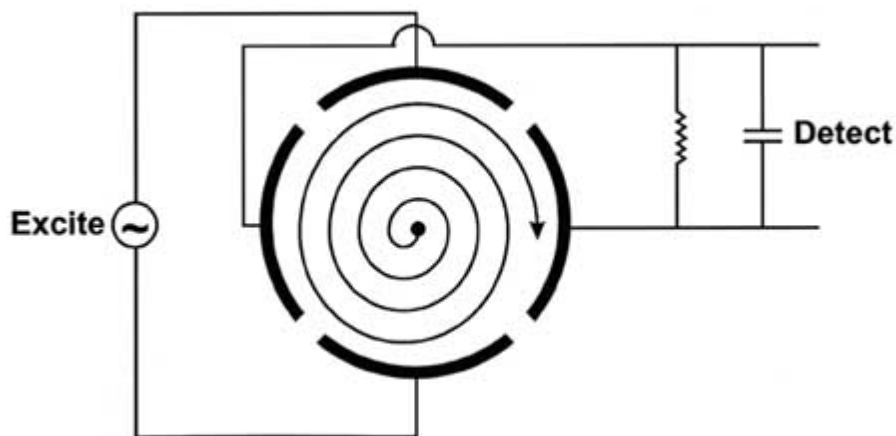
Figure 1.3. Excitation of an ion trapped inside the ICR cell. An rf voltage waveform containing the resonance frequency of the ion is applied between one pair of opposite cell plates. An image current of the orbiting ion cloud is detected on the other pair of plates.

Typically, the superconducting magnetic field utilized in FT-ICR mass spectrometer is 7 - 18 Tesla, while a new 21 Tesla FT-ICR mass spectrometer is currently under development.[98] With increased magnetic field, several FT-ICR MS parameters are improved, including mass resolving power, mass accuracy, signal-to-noise ratio, and dynamic range.[99] Sufficiently accurate mass measurements allow unique identification of biomolecular elemental composition. For example, the mass difference between potassium and sodium is 16 Da, which is also the mass difference between hexose (Hex,

e.g., mannose or glucose) and deoxyhexose (dHex, e.g., fucose or rhamnose), and between N-glycolyl neuraminic acid (NeuGc) and N-acetyl neuraminic acid (NeuAc). With a conventional ion trap mass analyzer, it is impossible to distinguish, e.g., (Hex + Na − H) (mass 184.03029) and (dHex + K − H) (mass 184.00931),[100] whereas high resolution mass analyzers demonstrate outstanding capability for such applications.[101] In addition, high resolution mass spectrometers combined with isotopic labeling of glycans is a powerful tool for glycan quantification. For example, Orlando and co-workers reported a novel permethylation method using $^{13}CH_3I$ and $^{12}CH_2DI$ for comparative glycomics, introducing a mass difference of 0.002922 Da at each permethylation site.[102,103]

Another advantage of FT-ICR is its ability to couple with various tandem mass spectrometric techniques.[97,104] Gas-phase ion-electron reactions, such as electron capture dissociation (ECD),[105] electron detachment dissociation (EDD),[106] and electron transfer dissociation (ETD)[107] have received increasing attention as alternative MS/MS strategies to CAD and infrared multiphoton dissociation (IRMPD), particularly for structural characterization of PTMs (see discussion in Section 1.4). ECD and EDD are best implemented in FT-ICR mass spectrometers, although ECD is also available in three-dimensional quadrupole ion traps[108-110] and digital ion traps[111,112]. The superiority of the FT-ICR for ECD and EDD is due to the required trapping of both electrons and polycations or anions, respectively, which is challenging in ion traps due to their low m/z cut-off.[93] In addition, ECD and EDD often generate complex MS/MS spectra, including mixtures of radical and even-electron species. Therefore, high resolution mass analysis is essential for unambiguously assigning product ions. ETD was first introduced in a radio-

frequency linear quadrupole ion trap instrument,[107] however, analogous to ECD and similar to EDD, ETD generates complex product ion spectra that are challenging to interpret without high resolving power and high mass accuracy.[113-115]

1.3.2 Experimental Setup

The instruments used throughout the dissertation are both 7 Tesla Fourier transform ion cyclotron resonance mass spectrometers (Bruker Daltonics, MA). Schematic diagrams of the instruments are shown in Figure 1.4. The Bruker Apex FT-ICR MS is equipped with an ESI source, which can produce multiply charged ions and therefore is highly compatible with various fragmentation techniques such as ECD, ETD, and EDD. Dual ion funnels provide improved ion transmission efficiency and ion sensitivity.[116,117] The quadrupole before the collision cell allows external mass selection of ions. The hexapole collision cell can store ions for a selected time, or be used to induce fragmentation (CAD, see discussion in Section 1.4.1) of selected precursor ions. Ion transfer optics are required to accelerate and focus the ions coming out of the collision cell in order to overcome the magnetic mirror effect.[118] The mass analyzer in this instrument is an infinity cell, which has a cylindrical geometry design. Located at the back of the instruments is a hollow cathode that can generate electrons for ion-electron reactions such as ECD and EDD, and a 10.6 μm CO_2 laser for IRMPD.

The Solarix mass spectrometer shares a similar design with the Apex, but there are some differences. A transfer hexapole is used instead of high voltage ion transfer optics to achieve improved ion transfer efficiency and higher sensitivity. A chemical ionization (CI) source is coupled to the instrument after the dual ion funnels, to allow

generation of radical anions for ETD events (see Section 1.4.2). In addition, a CO_2 IR

laser is currently not available for Solarix.
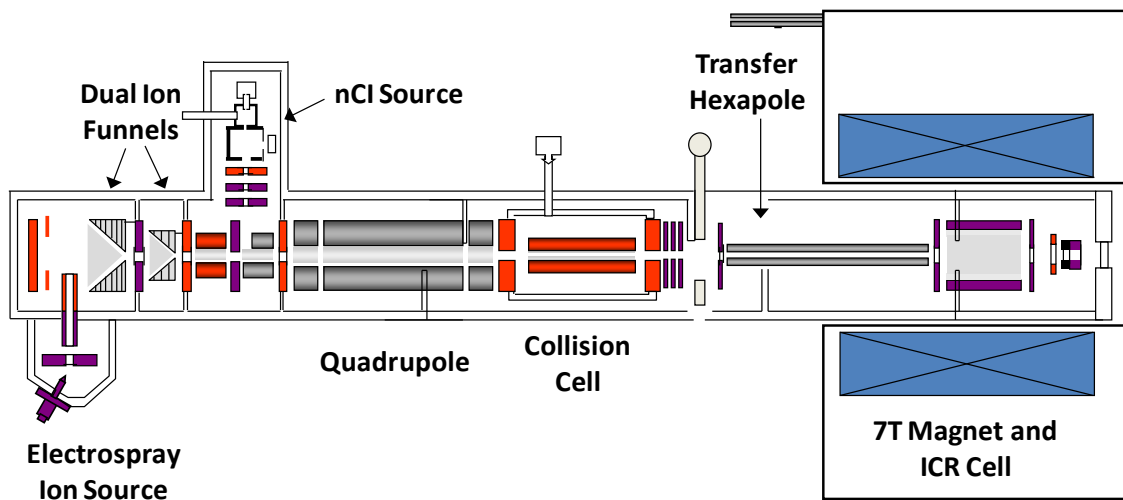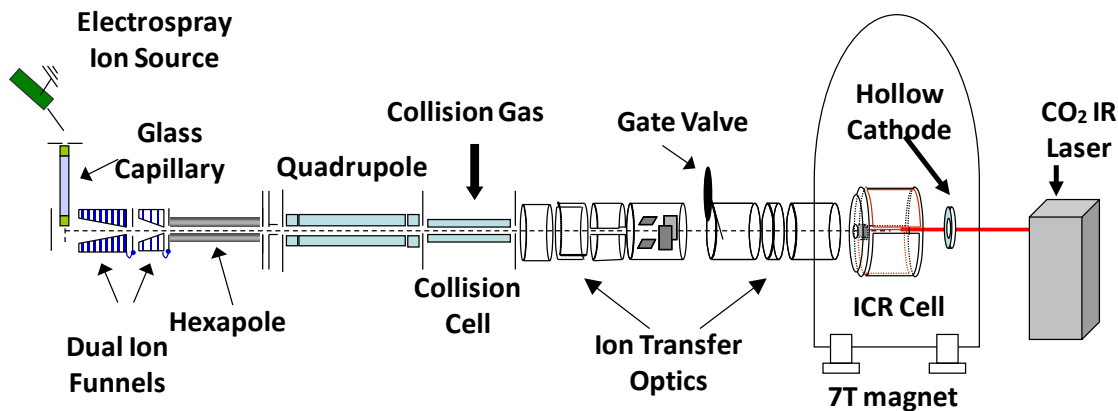
Figure 1.4. Schematic diagrams (top, Bruker Apex; bottom, Bruker Solarix) of 7 Tesla Fourier transform ion cyclotron resonance mass spectrometers used in the dissertation. The instruments are equipped with an ESI source, dual ion funnels, a quadrupole for mass selection, a hexapole as collision cell for CAD, and ICR cells as mass analyzers.

1.4 Tandem Mass Spectrometry

In tandem mass spectrometry (MS/MS),[119] precursor ions are isolated in the gas-

phase and subjected to fragmentation. One major advantage of MS/MS is its ability to

provide extensive sequence information of the precursor ions in a single experiment.[120] A variety of MS/MS techniques are compatible with FT-ICR mass spectrometers, including sustained off-resonance irradiation (SORI)-CAD,[121-127] IRMPD,[30,37,124,128-130] blackbody infrared radiative dissociation (BIRD),[131-133] surface induced dissociation (SID),[134-136] ECD,[105,137-139] EDD,[106,140,141] ETD, [107,142,143] and electron induced dissociation (EID).[144,145] The fragmentation techniques utilized in this dissertation include CAD, IRMPD, ECD, ETD, and EDD (see Figure 1.5).

<div style="border:1px solid black; padding:1em;">

Vibrational Activation Methods

- **Collision Activated Dissociation (CAD)**

  $[M +/- nH]^{n+/-} + \text{collision} \rightarrow [M +/- nH]^{n+/-*} \rightarrow \text{fragments}$

- **Infrared Multiphoton Dissociation (IRMPD)**

  $[M +/- nH]^{n+/-} + mh\nu \rightarrow [M +/- nH]^{n+/-*} \rightarrow \text{fragments}$

Ion-electron Reactions

- **Electron Capture Dissociation (ECD)**

  $[M + nH]^{n+} + e^-_{<1 \text{ eV}} \rightarrow [M + nH]^{(n-1)+\bullet} \rightarrow \text{fragments}$

- **Electron Transfer Dissociation (ETD)**

  $[M + nH]^{n+} + A^- \rightarrow [M + nH]^{(n-1)+\bullet} + A \rightarrow \text{fragments}$

- **Electron Detachment Dissociation (EDD)**

  $[M - nH]^{n-} + e^-_{>10 \text{ eV}} \rightarrow [M - nH]^{(n-1)-\bullet} \rightarrow \text{fragments}$

</div>

Figure 1.5. Summary of tandem mass spectrometric techniques used in this dissertation.

1.4.1 Vibration Excitation Methods

CAD. CAD is the most widely utilized fragmentation technique for structural analysis of glycans and glycoconjugates. There are two types of cleavages in MS/MS, including glycosidic cleavages (B-, C-, Y-, Z-type) and cross-ring cleavages (A- and X-type) as shown in Figure 1.6.[146] Glycosidic cleavages involve bond rupture between monosaccharides and provide information regarding monosaccharide composition. Cross-ring cleavages, which occur across carbohydrate rings, are particularly helpful in

determining linkage type. Low-energy CAD, which involves multiple inelastic collisions with neutral molecules or atoms, typically produces glycosidic cleavages.[17] Cross-ring cleavages are less likely to be formed because higher energy is required to break two covalent bonds.
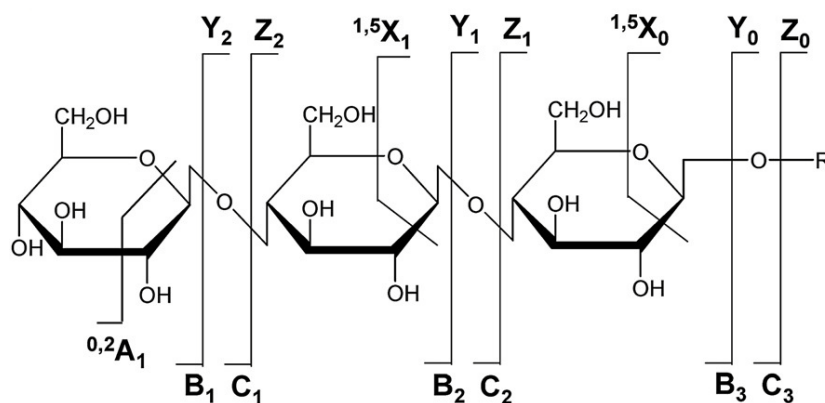
Figure 1.6. Nomenclature for tandem mass spectrometric product ions of glycans.[146]

In positive-ion mode of neutral oligosaccharides, B- and Y-type ions are commonly observed, whereas in negative ion mode, cross-ring and abundant C-type fragments are often generated.[88,147-149] For sialylated oligosaccharides, negative-ion CAD is dramatically different compared to non-sialylated glycans and higher energy is required for dissociation.[150] High-energy CAD provides more cross-ring cleavages, such as ^{1,5}X- and ^{3,5}A-type ions in both positive- and negative-ion mode[72,151-153] compared to low-energy CAD. In addition to providing extensive structural information regarding glycan sequence and branching, high-energy CAD is capable of differentiating structural isomers.[152,154] However, high-energy CAD is currently mainly available in MALDI tandem time-of-flight (TOF)/TOF instruments, which limits its applicability. Further, high-energy CAD involves significant ion scattering which reduces sensitivity.

In Fourier transform mass spectrometry, low-energy CAD can be performed external to the mass analyzer, either in a linear quadrupole ion trap (for orbitrap and FT-ICR instruments), or in a hexapole collision cell (for FT-ICR). The FT-ICR mass analyzer also allows CAD inside the ICR cell by adding collision gas. In the latter case, two main variants of CAD can be performed: in on-resonance CAD, an excitation frequency equal to the ICR frequency of a precursor ion is applied while collision gas is pulsed into the ICR cell.[18] In this approach, product ions are formed off-axis, which limits the practicality of further fragmentation stages and also limits resolving power.[97] In SORI-CAD, the excitation frequency is slightly offset from the precursor ions' cyclotron frequency. Consequently, ions are repeatedly excited to a relatively small cyclotron radius and then come back to the center of the ICR cell, thereby removing the shortcomings of on-resonance CAD. "In cell" CAD and CAD in an external linear ion trap both have the advantage of allowing multiple stages of tandem mass spectrometry, MS^n where n>2.

In SORI-CAD, precursor ions undergo multiple low-energy collisions with added background gas and are continuously vibrationally excited in a manner analogous to IRMPD.[121] Solouki *et al*. reported that SORI-CAD MS^n (n>2) of permethylated oligosaccharides provided more extensive fragmentation compared to conventional CAD in a triple quadrupole mass spectrometer.[155] SORI-CAD has also been applied to protonated carrageenan sulfated oligosaccharides for determining the positions of sulfated residues,[125] to deprotonated monosaccharides for determining phosphate locations,[124] and to alkali metal-adducted di-saccharides for studying the influence of metal ions on fragmentation behavior.[156] The latter work showed that, in SORI-CAD, the

dissociation thresholds of oligosaccharide glycosidic cleavages depend on the size of alkali metals, while activation barriers for cross-ring cleavages are independent of alkali metal identity, but dependent on linkage type.[156]

IRMPD. IRMPD is a valuable tool in FT-ICR and other ion trap instruments because of its ability to readily yield secondary fragmentation and thereby provide higher fragmentation efficiency compared to CAD.[18] IRMPD has been applied to various kinds of biomolecules, such as proteins, peptides, carbohydrates, and oligonucleotides.[130] Typically, a 10.6 µm CO_2 laser is used for infrared irradiation, but tunable CO_2 laser IRMPD has recently been implemented.[157-159] The latter approach was able to differentiate anomers of lithium-adducted methyl-glucopyranoside by comparing relative product ion abundances as function of laser wavelength.[158] Differentiation of lithium-tagged glucose-containing disaccharides was previously reported by Polfer *et al.* with 7-11 µm photons from a free electron laser.[160] That work was able to assign both linkage position and sugar anomeric configuration.

During IR activation, multiple photons are absorbed and the corresponding energy is redistributed over all precursor ion vibrational modes.[158] Therefore, multiple fragmentation events may take place. One of the major advantages of IRMPD in FT-ICR MS is that no collision gas needs to be introduced to the ICR cell.[161] In addition, IRMPD provides on-axis fragmentation, thus there is no loss of resolution.

Lebrilla and co-workers have compared IRMPD fragmentation patterns to those from CAD of model oligosaccharides, N-linked glycans, and O-linked glycans ionized with alkali metals in FT-ICR MS.[30,46,79,162] Similar to CAD, IRMPD favors low energy dissociation pathways, thus mostly glycosidic cleavages but also some cross-ring

cleavages are observed in IRMPD spectra. However, contrary to CAD, IRMPD fragmentation efficiency increases with increasing glycan size: for large *O*-glycans, single-stage IRMPD resulted in cleavage of all glycosidic bonds.[162] Moreover, IRMPD of alkali metal-adducted oligosaccharides generates different fragmentation patterns compared to those from SORI-CAD, e.g., IRMPD readily yields monosaccharide residues, whereas multiple MS/MS stages of CAD are required to achieve similar results.[46,79] Therefore, IRMPD is not only a fast and efficient MS/MS method but it can also potentially serve as a complementary technique to CAD for structural characterization of glycans.

1.4.2 Ion-electron Reactions

ECD. ECD is performed by irradiating at least doubly positively charged precursor ions with low energy (<1 eV) electrons, generating charge-reduced radical species from electron capture and product ions from radical-driven fragmentation.[105,139,141,163] Since its first introduction in 1998,[105] the application of ECD for biomolecular structural analysis has been rapidly expanding due to its complementary nature compared to CAD and IRMPD.[104] For example, ECD shows unique analytical utility in PTM characterization because labile PTMs are retained and can thus be localized within a molecule. ECD has been successfully utilized in this manner for characterizing, e.g., protein *N*-glycosylation,[37,164] *O*-glycosylation,[137] and phosphorylation.[138,165]

While ECD has been widely applied to peptides and proteins, its application towards carbohydrates has just begun to emerge. Due to the lack of basic groups in carbohydrates and their frequent relatively small size, it is often difficult to obtain multiply protonated precursor ions (multiple positive charges are required for ECD). The

first application of ECD towards carbohydrate analysis circumvented this issue by involving aminoglycans, which can easily be multiply protonated. However, this work reported only glycosidic cleavages from ECD.[123] Our group utilized alkali, alkaline earth, and transition metals to generate multiply positively charged ions for model oligosaccharides and observed complementary fragmentation patterns from IRMPD and ECD of these species.[80] O'Connor and co-workers explored the application of CAD and hot ECD (i.e., ECD with ~10 eV electrons) towards permethylated oligosaccharides.[166] For linear oligosaccharides, CAD and hot ECD resulted in similar product ions. In contrast, CAD generated A-, B-, and Y-type ions for branched *N*-glycans, while hot ECD generated C-, Z- and complementary A- and X-type cross-ring fragment pairs. All these studies show that ECD has great potential to serve as a glycan structural analysis technique.

EDD. EDD was first introduced for the characterization of peptide anions in 2001.[106] In EDD, polyanions are irradiated with >10 eV electrons to yield electron detachment, forming radical anions which undergo further radical-driven fragmentation. EDD has been applied to peptides,[106,140,167] oligonucleotides,[168,169] gangliosides,[170] model oligosaccharides,[171] and GAG-derived oligosaccharides.[172-178] Our work demonstrated that EDD of neutral and sialylated oligosaccharides results in fragments complementary to those from IRMPD and CAD, including extensive cross-ring product ions such as ^{1,5}A, ^{3,5}A, ^{1,5}X and ^{3,5}X ions.[171] The extensive work by Amster and co-workers on EDD of GAGs has shown that extensive glycosidic and cross-ring cleavages are generated. In contrast, IRMPD and CAD of GAGs mainly generate glycosidic cleavages. EDD was also shown to be able to differentiate the isomers glucuronic acid and iduronic acid.[173]

The complementarity of EDD and IRMPD/CAD makes them highly promising approaches for structural characterization of carbohydrates, particularly acidic carbohydrates in negative-ion mode.

ETD.   ETD was first introduced in a radio-frequency linear quadruple ion trap to characterize peptides,[107] and later applied in orbitrap and FT-ICR instruments.[115] In ETD events, anion radicals transfer electrons to polycations, and induce fragmentation similar to that observed in ECD. Similar to ECD, ETD of PTM-modified peptides typically generates extensive peptide backbone cleavages while leaving the labile PTMs intact. Therefore, ETD is particularly powerful in analyzing protein PTMs, such as phosphorylation, glycosylation, methylation, acetylation, and disulfide bonds.[113,143]

1.5 Dissertation Overview

The research presented in the dissertation has focused on the utilization of various tandem mass spectrometric techniques for structural characterization of glycans and glycopeptides.   LC-MS methods were also developed to separate and identify oligosaccharides and N-linked glycans. Ion-electron reactions such as ECD, ETD, and EDD has been previously applied to characterize protein PTMs, however, application towards glycans and glycoconjugates still remains to be investigated. In the following Chapters, ion-electron reactions of metal-adducted glycans cations (Chapters 2 and 3), native sialylated glycans (Chapter 4), derivatized oligosaccharide anions (Chapter 5), and N- and O-linked glycopeptides (Chapter 6) will be described. Chapter 7 focuses on method development using hydrophilic interaction liquid chromatography (HILIC) and graphitized carbon LC-MS for *N*-glycan profiling.

Chapter 2 investigates ECD of metal-adducted sulfated *N*-glycans. Sulfated glycans have been associated with cancer metastasis processes.[179] However, sulfated glycans are highly challenging to analyze in mass spectrometry due to the labile sulfate groups. Previous work has shown that metal cations can help stabilize sulfate groups in the gas phase.[180] In Chapter 2, we show that ECD of metal-adducted sulfated *N*-glycans generate complementary structural information compared to IRMPD, while preserving the labile sulfate groups in all the product ions. At the time this work was conducted, it was the first time ECD had been applied to N-linked glycans released from glycoproteins.

Chapter 3 compares the fragmentation behaviors of metal-adducted oligosaccharides following ECD and ETD, and also compares such dissociation with that from CAD. ECD and ETD of peptides has demonstrated similar fragmentation patterns,[181] however, ECD and ETD of oligosaccharides have not previously been directly compared. For doubly charged oligosaccharide precursors, ECD typically generates similar but more extensive fragmentation compared to ETD.

Chapter 4 utilizes ion-electron reactions to characterize sialylated N-linked glycans both in positive- and negative-ion modes. GAGs and model oligosaccharides undergo extensive fragmentation in EDD, however, EDD of N-linked glycans released from glycoproteins had not been studied before. In Chapter 4, we compare the fragmentation patterns from IRMPD and ECD of metal-adducted sialylated glycans, and also IRMPD and EDD of sialylated glycan anions. Negative ion mode IRMPD and EDD both produced extensive glycosidic and cross-ring cleavages, and the cross-ring fragments from the two approaches are completely complementary. When the precursor

ion charge state increases, improved fragmentation efficiency is observed in both positive- and negative-ion mode.

Chapter 5 examines EDD and IRMPD of fluorescently labeled oligosaccharides. Reductive amination of oligosaccharides using fluorescent labels has been widely used to allow UV detection in HPLC and to increase hydrophobicity of oligosaccharides in MS.[49,62,64] However, fragmentation studies of such derivatized oligosaccharides using ion-electron reactions, had not been previously conducted. In Chapter 5, we compare EDD and IRMPD fragmentation patterns of derivatized oligosaccharides, and also compare the influence of different fluorescent labels.

Chapter 6 investigates structural characterization methods of N-linked and O-linked glycopeptides using negative ion mode IRMPD and EDD. We used the non-specific enzyme pronase, combined with EDD to characterize the structure of glycopeptides. For N-linked glycopeptides, EDD fragmentation efficiency decreases with increased peptide lengths. For O-linked glycopeptides, EDD is able to yield peptide backbone, glycosidic, and cross-ring cleavages in the same spectrum, thus being a very promising tool for structural analysis of *O*-glycopeptides.

Chapter 7 focuses on LC-MS method development using HILIC and porous graphitized carbon (PGC) columns to separate and identify *N*-glycans released from glycoproteins. The HILIC column was able to separate neutral and acidic *N*-glycans, while reproducibility is an issue. PGC LC-MS also achieved *N*-glycan profiling with good resolution, and potential separation of glycan isomers. Online PGC LC-MS/MS provided structural information both regarding monosaccharide composition and linkage type.

A summary of all results in this dissertation is given in Chapter 8. Finally, one appendix is included. We examined sulfated and sialylated glycan enrichment using ZrO_2 and TiO_2 microtips. Both sulfated and sialylated glycans are enriched from mixtures of acidic and neutral glycans.

1.6 References

1. Varki, A. Biological roles of oligosaccharides - All of the theories are correct. *Glycobiol.* **1993**, *3*, 97-130.
2. Rudd, P. M.; Elliott, T.; Cresswell, P.; Wilson, I. A.; Dwek, R. A. Glycosylation and the immune system. *Science* **2001**, *291*, 2370-2376.
3. Bertozzi, C. R.; Kiessling, L. L. Chemical glycobiology. *Science* **2001**, *291*, 2357-2364.
4. Krishnamoorthy, L.; Mahal, L. K. Glycomic analysis: an array of technologies. *ACS Chem. Biol.* **2009**, *4*, 715-732.
5. Dwek, R. A. Glycobiology: Toward understanding the function of sugars. *Chem. Rev.* **1996**, *96*, 683-720.
6. Dube, D. H.; Bertozzi, C. R. Glycans in cancer and inflammation. Potential for therapeutics and diagnostics. *Nat. Rev. Drug Discov.* **2005**, *4*, 477-488.
7. Zhao, Y. Y.; Takahashi, M.; Gu, J. G.; Miyoshi, E.; Matsumoto, A.; Kitazume, S.; Taniguchi, N. Functional roles of N-glycans in cell signaling and cell adhesion in cancer. *Cancer Sci.* **2008**, *99*, 1304-1310.
8. Ohtsubo, K.; Marth, J. D. Glycosylation in cellular mechanisms of health and disease. *Cell* **2006**, *126*, 855-867.
9. Brown, J. R.; Crawford, B. E.; Esko, J. D. Glycan antagonists and inhibitors: A fount for drug discovery. *Crit. Rev. Biochem. Mol. Biol.* **2007**, *42*, 481-515.
10. Raman, R.; Raguram, S.; Venkataraman, G.; Paulson, J. C.; Sasisekharan, R. Glycomics: an integrated systems approach to structure-function relationships of glycans. *Nat. Methods* **2005**, *2*, 817-824.
11. Shriver, Z.; Raguram, S.; Sasisekharan, R. Glycomics: A pathway to a class of new and improved therapeutics. *Nat. Rev. Drug Discov.* **2004**, *3*, 863-873.
12. Mechref, Y.; Novotny, M. V. Structural investigations of glycoconjugates at high sensitivity. *Chem. Rev.* **2002**, *102*, 321-369.
13. Zaia, J. Mass spectrometry and the emerging field of glycomics. *Chem. Biol.* **2008**, *15*, 881-892.
14. Harvey, D. J. Proteomic analysis of glycosylation: structural determination of N- and O-linked glycans by mass spectrometry. *Expert Rev. Proteomics* **2005**, *2*, 87-101.
15. Marshall, A. G.; Hendrickson, C. L. High-resolution mass spectrometers. *Annu. Rev. Anal. Chem.* **2008**, *1*, 579-599.

16.   Harvey, D. J. Matrix-assisted laser desorption/ionization mass spectrometry of carbohydrates. *Mass Spectrom. Rev.* **1999**, *18*, 349-450.

17.   Zaia, J. Mass spectrometry of oligosaccharides. *Mass Spectrom. Rev.* **2004**, *23*, 161-227.

18.   Park, Y. M.; Lebrilla, C. B. Application of Fourier transform ion cyclotron resonance mass spectrometry to oligosaccharides. *Mass Spectrom. Rev.* **2005**, *24*, 232-264.

19.   Zhou, W.; Håkansson, K. Structural characterization of carbohydrates by Fourier transform tandem mass spectrometry. *Curr. Proteomics* **2011**, *in press*.

20.   Morelle, W.; Michalski, J. C. Glycomics and mass spectrometry. *Curr. Pharm. Des.* **2005**, *11*, 2615-2645.

21.   Morelle, W.; Michalski, J. C. The mass spectrometric analysis of glycoproteins and their glycan structures. *Curr. Anal. Chem.* **2005**, *1*, 29-57.

22.   Morelle, W.; Canis, K.; Chirat, F.; Faid, V.; Michalski, J. C. The use of mass spectrometry for the proteomic analysis of glycosylation. *Proteomics* **2006**, *6*, 3993-4015.

23.   Zaia, J. Mass spectrometry and glycomics. *Omics* **2010**, *14*, 401-418.

24.   Dodds, E. D.; Seipert, R. R.; Clowers, B. H.; German, J. B.; Lebrilla, C. B. Analytical performance of immobilized pronase for glycopeptide footprinting and implications for surpassing reductionist glycoproteomics. *J. Proteome Res.* **2009**, *8*, 502-512.

25.   Tretter, V.; Altmann, F.; Marz, L. Peptide-N4-(N-acetyl-beta-glycosaminyl)asparagine amidase-F cannot release glycans with fucose attached alpha-1-3 to the asparagine-linked N-acetylglucosamine residue *Eur. J. Biochem.* **1991**, *199*, 647-652.

26.   Khoshnoodi, J.; Hill, S.; Tryggvason, K.; Hudson, B.; Friedman, D. B. Identification of N-linked glycosylation sites in human nephrin using mass spectrometry. *J. Mass Spectrom.* **2007**, *42*, 370-379.

27.   Liu, T.; Qian, W. J.; Gritsenko, M. A.; Camp, D. G.; Monroe, M. E.; Moore, R. J.; Smith, R. D. Human plasma N-glycoproteome analysis by immunoaffinity subtraction, hydrazide chemistry, and mass spectrometry. *J. Proteome Res.* **2005**, *4*, 2070-2080.

28.   An, H. J.; Peavy, T. R.; Hedrick, J. L.; Lebrilla, C. B. Determination of N-glycosylation sites and site heterogeneity in glycoproteins. *Anal. Chem.* **2003**, *75*, 5628-5637.

29.   Xie, Y. M.; Liu, J.; Zhang, J. H.; Hedrick, J. L.; Lebrilla, C. B. Method for the comparative glycomic analyses of O-linked, mucin-type oligosaccharides. *Anal. Chem.* **2004**, *76*, 5186-5197.

30.   An, H. J.; Miyamoto, S.; Lancaster, K. S.; Kirmiz, C.; Li, B. S.; Lam, K. S.; Leiserowitz, G. S.; Lebrilla, C. B. Profiling of glycans in serum for the discovery of potential biomarkers for ovarian cancer. *J. Proteome Res.* **2006**, *5*, 1626-1635.

31.   Zhao, J.; Qiu, W. L.; Simeone, D. M.; Lubman, D. M. N-linked glycosylation profiling of pancreatic cancer serum using capillary liquid phase separation coupled with mass spectrometric analysis. *J. Proteome Res.* **2007**, *6*, 1126-1138.

32.   Thomsson, K. A.; Backstrom, M.; Larsson, J. M. H.; Hansson, G. C.; Karlsson, H. Enhanced detection of sialylated and sulfated glycans with negative ion mode

nanoliquid chromatography/mass spectrometry at high pH. *Anal. Chem.* **2010**, *82*, 1470-1477.

33. Clowers, B. H.; Dodds, E. D.; Seipert, R. R.; Lebrilla, C. B. Site determination of protein glycosylation based on digestion with immobilized nonspecific proteases and Fourier transform ion cyclotron resonance mass spectrometry. *J. Proteome Res.* **2007**, *6*, 4032-4040.

34. Nwosu, C. C.; Strum, J. S.; An, H. J.; Lebrilla, C. B. Enhanced detection and identification of glycopeptides in negative ion mode mass spectrometry. *Anal. Chem.* **2010**, *82*, 9654-9662.

35. Zauner, G.; Koeleman, C. A. M.; Deelder, A. M.; Wuhrer, M. Protein glycosylation analysis by HILIC-LC-MS of Proteinase K-generated N- and O-glycopeptides. *J. Sep. Sci.* **2010**, *33*, 903-910.

36. Medzihradszky, K. F.; GilleceCastro, B. L.; Townsend, R. R.; Burlingame, A. L.; Hardy, M. R. Structural elucidation of O-linked glycopeptides by high energy collision-induced dissociation. *J. Am. Soc. Mass. Spectrom.* **1996**, *7*, 319-328.

37. Hakansson, K.; Chalmers, M. J.; Quinn, J. P.; McFarland, M. A.; Hendrickson, C. L.; Marshall, A. G. Combined electron capture and infrared multiphoton dissociation for multistage MS/MS in a Fourier transform ion cyclotron resonance mass spectrometer. *Anal. Chem.* **2003**, *75*, 3256-3262.

38. Adamson, J. T.; Hakansson, K. Infrared multiphoton dissociation and electron capture dissociation of high-mannose type glycopeptides. *J. Proteome Res.* **2006**, *5*, 493-501.

39. Deguchi, K.; Ito, H.; Takegawa, Y.; Shinji, N.; Nakagawa, H.; Nishimura, S. I. Complementary structural information of positive- and negative-ion MSn spectra of glycopeptides with neutral and sialylated N-glycans. *Rapid Commun. Mass Spectrom.* **2006**, *20*, 741-746.

40. Seipert, R. R.; Dodds, E. D.; Clowers, B. H.; Beecroft, S. M.; German, J. B.; Lebrilla, C. B. Factors that influence fragmentation behavior of N-linked glycopeptide ions. *Anal. Chem.* **2008**, *80*, 3684-3692.

41. Seipert, R. R.; Dodds, E. D.; Lebrilla, C. B. Exploiting differential dissociation chemistries of O-linked glycopeptide ions for the localization of mucin-type protein glycosylation. *J. Proteome Res.* **2009**, *8*, 493-501.

42. Alley, W. R.; Mechref, Y.; Novotny, M. V. Characterization of glycopeptides by combining collision-induced dissociation and electron-transfer dissociation mass spectrometry data. *Rapid Commun. Mass Spectrom.* **2009**, *23*, 161-170.

43. Zhang, L.; Reilly, J. P. Extracting both peptide sequence and glycan structural information by 157 nm photodissociation of N-linked glycopeptides. *J. Proteome Res.* **2009**, *8*, 734-742.

44. Segu, Z. M.; Mechref, Y. Characterizing protein glycosylation sites through higher-energy C-trap dissociation. *Rapid Commun. Mass Spectrom.* **2010**, *24*, 1217-1225.

45. Huberty, M. C.; Vath, J. E.; Yu, W.; Martin, S. A. Site-specific carbohydrate identification in recombinant proteins using MALDI-TOF MS. *Anal. Chem.* **1993**, *65*, 2791-2800.

46. Lancaster, K. S.; An, H. J.; Li, B. S.; Lebrilla, C. B. Interrogation of N-linked oligosaccharides using infrared multiphoton dissociation in FT-ICR mass spectrometry. *Anal. Chem.* **2006**, *78*, 4990-4997.

47. Karas, M.; Bahr, U.; Dulcks, T. Nano-electrospray ionization mass spectrometry: addressing analytical problems beyond routine. *Fresenius J. Anal. Chem.* **2000**, *366*, 669-676.

48. Kebarle, P.; Verkerk, U. H. Electrospray: from ions in solution to ions in the gas phase, what we know now. *Mass Spectrom. Rev.* **2009**, *28*, 898-917.

49. Pabst, M.; Kolarich, D.; Poltl, G.; Dalik, T.; Lubec, G.; Hofinger, A.; Altmann, F. Comparison of fluorescent labels for oligosaccharides and introduction of a new postlabeling purification method. *Anal. Biochem.* **2009**, *384*, 263-273.

50. Yoshino, K.; Takao, T.; Murata, H.; Shimonishi, Y. Use of the derivatizing agent 4-aminobenzoic acid 2-(diethylamino)ethyl ester for high-sensitivity detection of oligosaccharides by electrospray-ionization mass-spectrometry. *Anal. Chem.* **1995**, *67*, 4028-4031.

51. Bahr, U.; Pfenninger, A.; Karas, M.; Stahl, B. High sensitivity analysis of neutral underivatized oligosaccharides by nanoelectrospray mass spectrometry. *Anal. Chem.* **1997**, *69*, 4530-4535.

52. Bereman, M. S.; Williams, T. I.; Muddiman, D. C. Development of a nanoLC LTQ orbitrap mass spectrometric method for profiling glycans derived from plasma from healthy, benign tumor control, and epithelial ovarian cancer patients. *Anal. Chem.* **2009**, *81*, 1130-1136.

53. Luo, Q. Z.; Rejtar, T.; Wu, S. L.; Karger, B. L. Hydrophilic interaction 10 mu m ID porous layer open tubular columns for ultratrace glycan analysis by liquid chromatography-mass spectrometry. *J. Chromatogr. A* **2009**, *1216*, 1223-1231.

54. Wohlgemuth, J.; Karas, M.; Jiang, W.; Hendriks, R.; Andrecht, S. Enhanced glyco-profiling by specific glycopeptide enrichment and complementary monolithic nano-LC (ZIC-HILIC/RP18e)/ESI-MS analysis. *J. Sep. Sci.* **2010**, *33*, 880-890.

55. Tarentin.Al; Plummer, T. H.; Maley, F. Release of intact oligosaccharides from specfic glycoproteins by endo-beta-N-acetylglucosaminidase H *J. Biol. Chem.* **1974**, *249*, 818-824.

56. Adolf, G. R.; Kalsner, I.; Ahorn, H.; Maurerfogy, I.; Cantell, K. Natural human interferon-alpha-2 is O-glycosylated. *Biochem. J* **1991**, *276*, 511-518.

57. Patel, T.; Bruce, J.; Merry, A.; Bigge, C.; Wormald, M.; Jaques, A.; Parekh, R. Use of hydrazine to release in intact and unreduced form both N-linked and O-linked oligosaccharides from glycoproteins. *Biochemistry (Mosc).* **1993**, *32*, 679-693.

58. Harvey, D. J. Electrospray mass spectrometry and collision-induced fragmentation of 2-aminobenzamide-labelled neutral N-linked glycans. *Analyst* **2000**, *125*, 609-617.

59. Wheeler, S. F.; Harvey, D. J. Extension of the in-gel release method for structural analysis of neutral and sialylated N-linked glycans to the analysis of sulfated glycans: Application to the glycans from bovine thyroid-stimulating hormone. *Anal. Biochem.* **2001**, *296*, 92-100.

60. Harvey, D. J. Identification of protein-bound carbohydrates by mass spectrometry. *Proteomics* **2001**, *1*, 311-328.

61. Maniatis, S.; Zhou, H.; Reinhold, V. Rapid de-O-glycosylation concomitant with peptide labeling using microwave radiation and an alkyl amine base. *Anal. Chem.* **2010**, *82*, 2421-2425.

62. Anumula, K. R. Advances in fluorescence derivatization methods for high-performance liquid chromatographic analysis of glycoprotein carbohydrates. *Anal. Biochem.* **2006**, *350*, 1-23.

63. Goetz, J. A.; Novotny, M. V.; Mechref, Y. Enzymatic/chemical release of O-glycans allowing MS analysis at high sensitivity. *Anal. Chem.* **2009**, *81*, 9546-9552.

64. Ruhaak, L. R.; Zauner, G.; Huhn, C.; Bruggink, C.; Deelder, A. M.; Wuhrer, M. Glycan labeling strategies and their use in identification and quantification. *Anal. Bioanal. Chem.* **2010**, *397*, 3457-3481.

65. Mechref, Y.; Kang, P.; Novotny, M. V. Differentiating structural isomers of sialylated glycans by matrix-assisted laser desorption/ionization time-of-flight/time-of-flight tandem mass spectrometry. *Rapid Commun. Mass Spectrom.* **2006**, *20*, 1381-1389.

66. Sheeley, D. M.; Reinhold, V. N. Structural characterization of carbohydrate sequence, linkage, and branching in a quadrupole ion trap mass spectrometer: Neutral oligosaccharides and N-linked glycans. *Anal. Chem.* **1998**, *70*, 3053-3059.

67. Ciucanu, I.; Kerek, F. A simple and rapid method for the permethylation of carbohydrates. *Carbohydr. Res.* **1984**, *131*, 209-217.

68. Kang, P.; Mechref, Y.; Klouckova, I.; Novotny, M. V. Solid-phase permethylation of glycans for mass spectrometric analysis. *Rapid Commun. Mass Spectrom.* **2005**, *19*, 3421-3428.

69. Kang, P.; Mechref, Y.; Novotny, M. V. High-throughput solid-phase permethylation of glycans prior to mass spectrometry. *Rapid Commun. Mass Spectrom.* **2008**, *22*, 721-734.

70. Lei, M.; Mechref, Y.; Novotny, M. V. Structural analysis of sulfated glycans by sequential double-permethylation using methyl iodide and deuteromethyl iodide. *J. Am. Soc. Mass. Spectrom.* **2009**, *20*, 1660-1671.

71. Wilson, J. J.; Brodbelt, J. S. Ultraviolet photodissociation at 355 nm of fluorescently labeled oligosaccharides. *Anal. Chem.* **2008**, *80*, 5186-5196.

72. Wuhrer, M.; Deelder, A. M. Negative-mode MALDI-TOF/TOF-MS of oligosaccharides labeled with 2-aminobenzamide. *Anal. Chem.* **2005**, *77*, 6954-6959.

73. Harvey, D. J. Collision-induced fragmentation of negative ions from N-linked glycans derivatized with 2-aminobenzoic acid. *J. Mass Spectrom.* **2005**, *40*, 642-653.

74. Wuhrer, M.; Koeleman, C. A. M.; Deelder, A. M. Hexose rearrangements upon fragmentation of N-glycopeptides and reductively aminated N-glycans. *Anal. Chem.* **2009**, *81*, 4422-4432.

75. Hofmeister, G. E.; Zhou, Z.; Leary, J. A. Linkage position determination in lithium-cationized disaccharides - tandem mass-sepctrometry and semiempirical calculations *J. Am. Chem. Soc.* **1991**, *113*, 5964-5970.

76. Sible, E. M.; Brimmer, S. P.; Leary, J. A. Interaction of first row transition metals with alpha 1-3, alpha 1-6 mannotriose and conserved trimannosyl core oligosaccharides: A comparative electrospray ionization study of doubly and singly charged complexes. *J. Am. Soc. Mass. Spectrom.* **1997**, *8*, 32-42.

77. Konig, S.; Leary, J. A. Evidence for linkage position determination in cobalt coordinated pentasaccharides using ion trap mass spectrometry. *J. Am. Soc. Mass. Spectrom.* **1998**, *9*, 1125-1134.

78. Cancilla, M. T.; Penn, S. G.; Carroll, J. A.; Lebrilla, C. B. Coordination of alkali metals to oligosaccharides dictates fragmentation behavior in matrix assisted laser desorption ionization Fourier transform mass spectrometry. *J. Am. Chem. Soc.* **1996**, *118*, 6736-6745.

79. Xie, Y. M.; Lebrilla, C. B. Infrared multiphoton dissociation of alkali metal-coordinated oligosaccharides. *Anal. Chem.* **2003**, *75*, 1590-1598.

80. Adamson, J. T.; Hakansson, K. Electron capture dissociation of oligosaccharides ionized with alkali, alkaline earth, and transition metals. *Anal. Chem.* **2007**, *79*, 2901-2910.

81. Harvey, D. J. Ionization and collision-induced fragmentation of N-linked and related carbohydrates using divalent canons. *J. Am. Soc. Mass. Spectrom.* **2001**, *12*, 926-937.

82. Liu, H. C.; Hakansson, K. Divalent metal ion-peptide interactions probed by electron capture dissociation of trications. *J. Am. Soc. Mass. Spectrom.* **2006**, *17*, 1731-1741.

83. Liu, H.; Hakansson, K. Analysis of sulfated oligosaccharides with combination of divalent metal complexation and electron capture dissociation. *Int. J. Mass spectrom.* **2011**, In press.

84. Harvey, D. J.; Mattu, T. S.; Wormald, M. R.; Royle, L.; Dwek, R. A.; Rudd, P. M. "Internal residue loss": Rearrangements occurring during the fragmentation of carbohydrates derivatized at the reducing terminus. *Anal. Chem.* **2002**, *74*, 734-740.

85. Franz, A. H.; Lebrilla, C. B. Evidence for long-range glycosyl transfer reactions in the gas phase. *J. Am. Soc. Mass. Spectrom.* **2002**, *13*, 325-337.

86. Ernst, B.; Muller, D. R.; Richter, W. J. False sugar sequence ions in electrospray tandem mass spectrometry of underivatized sialyl-Lewis-type oligosaccharides. *Int. J. Mass Spectrom. Ion Processes* **1997**, *160*, 283-290.

87. Wuhrer, M.; Koeleman, C. A. M.; Hokke, C. H.; Deelder, A. M. Mass spectrometry of proton adducts of fucosylated N-glycans: fucose transfer between antennae gives rise to misleading fragments. *Rapid Commun. Mass Spectrom.* **2006**, *20*, 1747-1754.

88. Harvey, D. J. Fragmentation of negative ions from carbohydrates: Part 1. Use of nitrate and other anionic adducts for the production of negative ion electrospray spectra from N-linked carbohydrates. *J. Am. Soc. Mass. Spectrom.* **2005**, *16*, 622-630.

89. Zhu, J. H.; Cole, R. B. Ranking of gas-phase acidities and chloride affinities of monosaccharides and linkage specificity in collision-induced decompositions of negative ion electrospray-generated chloride adducts of oligosaccharides. *J. Am. Soc. Mass. Spectrom.* **2001**, *12*, 1193-1204.

90. Cai, Y.; Jiang, Y. J.; Cole, R. B. Anionic adducts of oligosaccharides by matrix-assisted laser desorption/ionization time-of-flight mass spectrometry. *Anal. Chem.* **2003**, *75*, 1638-1644.

91. Jiang, Y. J.; Cole, R. B. Oligosaccharide analysis using anion attachment in negative mode electrospray mass spectrometry. *J. Am. Soc. Mass. Spectrom.* **2005**, *16*, 60-70.

92. Marshall, A. G.; Hendrickson, C. L.; Jackson, G. S. Fourier transform ion cyclotron resonance mass spectrometry: A primer. *Mass Spectrom. Rev.* **1998**, *17*, 1-35.

93. Perry, R. H.; Cooks, R. G.; Noll, R. J. Orbitrap mass spectrometry : instrumentation, ion motion and applications *Mass Spectrom. Rev.* **2008**, *27*, 661-699.

94. Hu, Q. Z.; Noll, R. J.; Li, H. Y.; Makarov, A.; Hardman, M.; Cooks, R. G. The Orbitrap: a new mass spectrometer. *J. Mass Spectrom.* **2005**, *40*, 430-443.

95. Yates, J. R.; Ruse, C. I.; Nakorchevsky, A. Proteomics by mass spectrometry: approaches, advances, and applications. *Annu. Rev. Biomed. Eng.* **2009**, *11*, 49-79.

96. Scigelova, M.; Makarov, A. Orbitrap mass analyzer - Overview and applications in proteomics. *Proteomics* **2006**, 16-21.

97. Hakansson, K.; Cooper, H. J.; Hudgins, R. R.; Nilsson, C. L. High resolution tandem mass spectrometry for structural biochemistry. *Curr. Org. Chem.* **2003**, *7*, 1503-1525.

98. Arnaud, C. H. High-res mass spec. *Chemical & Engineering News* **2010**, *88*, 10-+.

99. Marshall, A.; Guan, S. Advantages of high magnetic field for Fourier transform ion cyclotron resonance mass spectrometry. *Rapid Commun. Mass Spectrom.* **1996**, *10*, 1819-1823.

100. Packer, N. H.; Karlsson, N. G. There are no facts, only interpretations. *J. Proteome Res.* **2006**, *5*, 1291-1292.

101. Sleno, L.; Volmer, D. A.; Marshall, A. G. Assigning product ions from complex MS/MS spectra: The importance of mass uncertainty and resolving power. *J. Am. Soc. Mass. Spectrom.* **2005**, *16*, 183-198.

102. Atwood, J. A.; Cheng, L.; Alvarez-Manilla, G.; Warren, N. L.; York, W. S.; Orlando, R. Quantitation by isobaric labeling: Applications to glycomics. *J. Proteome Res.* **2008**, *7*, 367-374.

103. Botelho, J. C.; Atwood, J. A.; Cheng, L.; Alvarez-Manilla, G.; York, W. S.; Orlando, R. Quantification by isobaric labeling (QUIBL) for the comparative glycomic study of O-linked glycans. *Int. J. Mass spectrom.* **2008**, *278*, 137-142.

104. Cooper, H. J.; Hakansson, K.; Marshall, A. G. The role of electron capture dissociation in biomolecular analysis. *Mass Spectrom. Rev.* **2005**, *24*, 201-222.

105. Zubarev, R. A.; Kelleher, N. L.; McLafferty, F. W. Electron capture dissociation of multiply charged protein cations. A nonergodic process. *J. Am. Chem. Soc.* **1998**, *120*, 3265-3266.

106. Budnik, B. A.; Haselmann, K. F.; Zubarev, R. A. Electron detachment dissociation of peptide di-anions: an electron-hole recombination phenomenon. *Chem. Phys. Lett.* **2001**, *342*, 299-302.

107. Syka, J. E. P.; Coon, J. J.; Schroeder, M. J.; Shabanowitz, J.; Hunt, D. F. Peptide and protein sequence analysis by electron transfer dissociation mass spectrometry. *Proc. Natl. Acad. Sci. U. S. A.* **2004**, *101*, 9528-9533.

108. Bushey, J. M.; Baba, T.; Glish, G. L. Simultaneous collision induced dissociation of the charge reduced parent ion during electron capture dissociation. *Anal. Chem.* **2009**, *81*, 6156-6164.

109. Silivra, O. A.; Kjeldsen, F.; Ivonin, I. A.; Zubarev, R. A. Electron capture dissociation of polypeptides in a three-dimensional quadrupole ion trap: Implementation and first results. *J. Am. Soc. Mass. Spectrom.* **2005**, *16*, 22-27.

110. Baba, T.; Hashimoto, Y.; Hasegawa, H.; Hirabayashi, A.; Waki, I. Electron capture dissociation in a radio frequency ion trap. *Anal. Chem.* **2004**, *76*, 4263-4266.

111. Ding, L.; Brancia, F. L. Electron capture dissociation in a digital ion trap mass spectrometer. *Anal. Chem.* **2006**, *78*, 1995-2000.

112. McCullough, B. J.; Entwistle, A.; Konishi, I.; Buffey, S.; Hasnain, S. S.; Brancia, F. L.; Grossmann, J. G.; Gaskell, S. J. Digital ion trap mass spectrometer for probing the structure of biological macromolecules by gas phase X-ray scattering. *Anal. Chem.* **2009**, *81*, 3392-3397.

113. Wiesner, J.; Premsler, T.; Sickmann, A. Application of electron transfer dissociation (ETD) for the analysis of posttranslational modifications. *Proteomics* **2008**, *8*, 4466-4483.

114. McAlister, G. C.; Berggren, W. T.; Griep-Raming, J.; Horning, S.; Makarov, A.; Phanstiel, D.; Stafford, G.; Swaney, D. L.; Syka, J. E. P.; Zabrouskov, V.; Coon, J. J. A proteomics grade electron transfer dissociation-enabled hybrid linear ion trap-orbitrap mass spectrometer. *J. Proteome Res.* **2008**, *7*, 3127-3136.

115. McAlister, G. C.; Phanstiel, D.; Good, D. M.; Berggren, W. T.; Coon, J. J. Implementation of electron-transfer dissociation on a hybrid linear ion trap-orbitrap mass spectrometer. *Anal. Chem.* **2007**, *79*, 3525-3534.

116. Kelly, R. T.; Tolmachev, A. V.; Page, J. S.; Tang, K. Q.; Smith, R. D. The ion funnel: theory, implementations, and applications. *Mass Spectrom. Rev.* **2010**, *29*, 294-312.

117. Tang, K.; Tolmachev, A.; Nikolaev, E.; Zhang, R.; Belov, M.; Udseth, H. Independent control of ion transmission in a jet disrupter dual-channel ion funnel electrospray ionization MS interface. *Anal. Chem.* **2002**, *74*, 5431-5437.

118. Guan, S. H.; Pasatolic, L.; Marshall, A. G.; Xiang, X. Z. Off-axis injection into an ICR ion-trap - a means for efficient capture of a continuous beam of externally generated ions. *Int. J. Mass spectrom.* **1994**, *139*, 75-86.

119. McLafferty, F. W., *Tandem mass spectrometry*. Wiley: New York, 1983.

120. Hunt, D. F.; Yates, J. R.; Shabanowitz, J.; Winston, S.; Hauer, C. R. Protein sequencing by tandem mass-spectrometry *Proc. Natl. Acad. Sci. U. S. A.* **1986**, *83*, 6233-6237.

121. Gauthier, J. W.; Trautman, T. R.; Jacobson, D. B. Sustained off-resonance irradiation for collision-activated dissociation involving Fourier-transform mass spectrometry - collision-activated dissociation technique that emulates infrared multiphoton dissociation *Anal. Chim. Acta* **1991**, *246*, 211-225.

122. Mirgorodskaya, E.; O'Connor, P. B.; Costello, C. E. A general method for precalculation of parameters for sustained off resonance irradiation/collision-induced dissociation. *J. Am. Soc. Mass. Spectrom.* **2002**, *13*, 318-324.

123. Budnik, B. A.; Haselmann, K. F.; Elkin, Y. N.; Gorbach, V. I.; Zubarev, R. A. Applications of electron-ion dissociation reactions for analysis of polycationic chitooligosaccharides in Fourier transform mass spectrometry. *Anal. Chem.* **2003**, *75*, 5994-6001.

124. Leavell, M. D.; Kruppa, G. H.; Leary, J. A. Determination of phosphate position in hexose monosaccharides using an FTICR mass spectrometer: ion/molecule reactions, labeling studies, and dissociation mechanisms. *Int. J. Mass spectrom.* **2003**, *222*, 135-153.

125. Aguilan, J. T.; Dayrit, F. M.; Zhang, J. H.; Ninonuevo, M. R.; Lebrilla, C. B. Structural analysis of alpha-carrageenan sulfated oligosaccharides by positive mode nano-ESI-FTICR-MS and MS/MS by SORI-CID. *J. Am. Soc. Mass. Spectrom.* **2006**, *17*, 96-103.

126. Liu, H. C.; Hakansson, K.; Lee, J. Y.; Sherman, D. H. Collision-activated dissociation, infrared multiphoton dissociation, and electron capture dissociation of the Bacillus anthracis siderophore petrobactin and its metal ion complexes. *J. Am. Soc. Mass. Spectrom.* **2007**, *18*, 842-849.

127. Liu, H.; Yoo, H. J.; Hakansson, K. Characterization of phosphate-containing metabolites by calcium adduction and electron capture dissociation. *J. Am. Soc. Mass. Spectrom.* **2008**, *19*, 799-808.

128. Little, D. P.; Speir, J. P.; Senko, M. W.; Oconnor, P. B.; McLafferty, F. W. Infrared multiphoton dissociation of large multiply-charged ions for biomolecule sequencing. *Anal. Chem.* **1994**, *66*, 2809-2815.

129. Goolsby, B. J.; Broadbelt, J. S. Analysis of protonated and alkali metal cationized aminoglycoside antibiotics by collision-activated dissociation and infrared multi-photon dissociation in the quadrupole ion trap. *J. Mass Spectrom.* **2000**, *35*, 1011-1024.

130. Brodbelt, J. S.; Wilson, J. J. Infrared multiphoton dissciation in quadrupole ion traps. *Mass Spectrom. Rev.* **2009**, *28*, 390-424.

131. Schnier, P. D.; Price, W. D.; Jockusch, R. A.; Williams, E. R. Blackbody infrared radiative dissociation of bradykinin and its analogues: Energetics, dynamics, and evidence for salt-bridge structures in the gas phase. *J. Am. Chem. Soc.* **1996**, *118*, 7178-7189.

132. Price, W. D.; Schnier, P. D.; Williams, E. R. Tandem mass spectrometry of large biomolecule ions by blackbody infrared radiative dissociation. *Anal. Chem.* **1996**, *68*, 859-866.

133. Jockusch, R. A.; Schnier, P. D.; Price, W. D.; Strittmatter, E. F.; Demirev, P. A.; Williams, E. R. Effects of charge state on fragmentation pathways, dynamics, and activation energies of ubiquitin ions measured by blackbody infrared radiative dissociation. *Anal. Chem.* **1997**, *69*, 1119-1126.

134. Williams, E. R.; Henry, K. D.; McLafferty, F. W.; Shabanowitz, J.; Hunt, D. F. Surface-induced dissociation of peptide ions in Fourier-transform mass-spectrometry. *J. Am. Soc. Mass. Spectrom.* **1990**, *1*, 413-416.

135.   Jones, J. L.; Dongre, A. R.; Somogyi, A.; Wysocki, V. H. Sequence dependence of peptide fragmentation efficiency curves determined by electrospray-ionization surface-induced dissociation mass-spectrometry *J. Am. Chem. Soc.* **1994**, *116*, 8368-8369.

136.   Dongre, A. R.; Somogyi, A.; Wysocki, V. H. Surface-induced dissociation: An effective tool to probe structure, energetics and fragmentation mechanisms of protonated peptides. *J. Mass Spectrom.* **1996**, *31*, 339-350.

137.   Mirgorodskaya, E.; Roepstorff, P.; Zubarev, R. A. Localization of O-glycosylation sites in peptides by electron capture dissociation in a fourier transform mass spectrometer. *Anal. Chem.* **1999**, *71*, 4431-4436.

138.   Stensballe, A.; Jensen, O. N.; Olsen, J. V.; Haselmann, K. F.; Zubarev, R. A. Electron capture dissociation of singly and multiply phosphorylated peptides. *Rapid Commun. Mass Spectrom.* **2000**, *14*, 1793-1800.

139.   Zubarev, R. A.; Horn, D. M.; Fridriksson, E. K.; Kelleher, N. L.; Kruger, N. A.; Lewis, M. A.; Carpenter, B. K.; McLafferty, F. W. Electron capture dissociation for structural characterization of multiply charged protein cations. *Anal. Chem.* **2000**, *72*, 563-573.

140.   Haselmann, K. F.; Budnik, B. A.; Kjeldsen, F.; Nielsen, M. L.; Olsen, J. V.; Zubarev, R. A. Electronic excitation gives informative fragmentation of polypeptide cations and anions. *Eur. J. Mass Spectrom.* **2002**, *8*, 117-121.

141.   Zubarev, R. A. Reactions of polypeptide ions with electrons in the gas phase. *Mass Spectrom. Rev.* **2003**, *22*, 57-77.

142.   Coon, J. J.; Syka, J. E. P.; Schwartz, J. C.; Shabanowitz, J.; Hunt, D. F. Anion dependence in the partitioning between proton and electron transfer in ion/ion reactions. *Int. J. Mass spectrom.* **2004**, *236*, 33-42.

143.   Mikesh, L. M.; Ueberheide, B.; Chi, A.; Coon, J. J.; Syka, J. E. P.; Shabanowitz, J.; Hunt, D. F. The utility of ETD mass spectrometry in proteomic analysis. *BBA-Proteins Proteomics* **2006**, *1764*, 1811-1822.

144.   Yoo, H. J.; Liu, H. C.; Hakansson, K. Infrared multiphoton dissociation and electron-induced dissociation as alternative MS/MS strategies for metabolite identification. *Anal. Chem.* **2007**, *79*, 7858-7866.

145.   Yoo, H. J.; Hakansson, K. Determination of double bond location in fatty acids by manganese adduction and electron induced dissociation. *Anal. Chem.* **2010**, *82*, 6940-6946.

146.   Domon, B.; Costello, C. E. A systematic nomenclature for carbohydrate fragmentations in FAB-MS MS spectra of glycoconjugates *Glycoconj. J.* **1988**, *5*, 397-409.

147.   Carroll, J. A.; Ngoka, L.; Beggs, C. G.; Lebrilla, C. B. Liquid secondary-ion mass-spectrometry Fourier-transform mass-spectrometry of oligosaccharide anions. *Anal. Chem.* **1993**, *65*, 1582-1587.

148.   Harvey, D. J. Fragmentation of negative ions from carbohydrates: Part 2. Fragmentation of high-mannose N-linked glycans. *J. Am. Soc. Mass. Spectrom.* **2005**, *16*, 631-646.

149.   Harvey, D. J. Fragmentation of negative ions from carbohydrates: Part 3. Fragmentation of hybrid and complex N-linked glycans. *J. Am. Soc. Mass. Spectrom.* **2005**, *16*, 647-659.

150. Seymour, J. L.; Costello, C. E.; Zaia, J. The influence of sialylation on glycan negative ion dissociation and energetics. *J. Am. Soc. Mass. Spectrom.* **2006**, *17*, 844-854.

151. Harvey, D. J.; Bateman, R. H.; Green, M. R. High-energy collision-induced fragmentation of complex oligosaccharides ionized by matrix-assisted laser desorption/ionization mass spectrometry. *J. Mass Spectrom.* **1997**, *32*, 167-187.

152. Mechref, Y.; Novotny, M. V.; Krishnan, C. Structural characterization of oligosaccharides using MALDI-TOF/TOF tandem mass spectrometry. *Anal. Chem.* **2003**, *75*, 4895-4903.

153. Yu, S. Y.; Wu, S. W.; Khoo, K. H. Distinctive characteristics of MALDI-Q/TOF and TOF/TOF tandem mass spectrometry for sequencing of permethylated complex type N-glycans. *Glycoconj. J.* **2006**, *23*, 355-369.

154. Maslen, S. L.; Goubet, F.; Adam, A.; Dupree, P.; Stephens, E. Structure elucidation of arabinoxylan isomers by normal phase HPLC-MALDI-TOF/TOF-MS/MS. *Carbohydr. Res.* **2007**, *342*, 724-735.

155. Solouki, T.; Reinhold, B. B.; Costello, C. E.; O'Malley, M.; Guan, S. H.; Marshall, A. G. Electrospray ionization and matrix-assisted laser desorption/ionization Fourier transform ion cyclotron resonance mass spectrometry of permethylated oligosaccharides. *Anal. Chem.* **1998**, *70*, 857-864.

156. Cancilla, M. T.; Wang, A. W.; Voss, L. R.; Lebrilla, C. B. Fragmentation reactions in the mass spectrometry analysis of neutral oligosaccharides. *Anal. Chem.* **1999**, *71*, 3206-3218.

157. Vala, M.; Szczepanski, J.; Oomens, J.; Steill, J. D. H-2 Ejection from Polycyclic Aromatic Hydrocarbons: Infrared Multiphoton Dissociation Study of Protonated 1,2-Dihydronaphthalene. *J. Am. Chem. Soc.* **2009**, *131*, 5784-5791.

158. Stefan, S. E.; Eyler, J. R. Differentiation of methyl-glucopyranoside anomers by infrared multiple photon dissociation with a tunable CO2 laser. *Anal. Chem.* **2009**, *81*, 1224-1227.

159. Vala, M.; Szczepanski, J.; Dunbar, R.; Oomens, J.; Steill, J. D. Infrared multiphoton dissociation spectrum of isolated protonated 1-azapyrene. *Chem. Phys. Lett.* **2009**, *473*, 43-48.

160. Polfer, N. C.; Valle, J. J.; Moore, D. T.; Oomens, J.; Eyler, J. R.; Bendiak, B. Differentiation of isomers by wavelength-tunable infrared multiple-photon dissociation-mass spectrometry: Application to glucose-containing disaccharides. *Anal. Chem.* **2006**, *78*, 670-679.

161. Hakansson, K.; Klassen, J. S., Ion activation methods for tandem mass spectrometry. In *Electrospray and MALDI Mass Spectrometry: Fundamentals, Instrumentation, Practicalities, and Biological Applications, 2nd Edition*, 2nd ed.; Cole, R. B., Ed. John Wiley & Sons, Inc., Hoboken, New Jersey: 2010.

162. Zhang, J. H.; Schubothe, K.; Li, B. S.; Russell, S.; Lebrilla, C. B. Infrared multiphoton dissociation of O-linked mucin-type oligosaccharides. *Anal. Chem.* **2005**, *77*, 208-214.

163. McLafferty, F. W.; Horn, D. M.; Breuker, K.; Ge, Y.; Lewis, M. A.; Cerda, B.; Zubarev, R. A.; Carpenter, B. K. Electron capture dissociation of gaseous multiply charged ions by Fourier-transform ion cyclotron resonance. *J. Am. Soc. Mass. Spectrom.* **2001**, *12*, 245-249.

164. Hakansson, K.; Cooper, H. J.; Emmett, M. R.; Costello, C. E.; Marshall, A. G.; Nilsson, C. L. Electron capture dissociation and infrared multiphoton dissociation MS/MS of an N-glycosylated tryptic peptide to yield complementary sequence information. *Anal. Chem.* **2001**, *73*, 4530-4536.

165. Shi, S. D. H.; Hemling, M. E.; Carr, S. A.; Horn, D. M.; Lindh, I.; McLafferty, F. W. Phosphopeptide/phosphoprotein mapping by electron capture dissociation mass spectrometry. *Anal. Chem.* **2001**, *73*, 19-22.

166. Zhao, C.; Xie, B.; Chan, S. Y.; Costello, C. E.; O'Connor, P. B. Collisionally activated dissociation and electron capture dissociation provide complementary structural information for branched permethylated oligosaccharides. *J. Am. Soc. Mass. Spectrom.* **2008**, *19*, 138-150.

167. Kalli, A.; Hakansson, K. Preferential cleavage of S-S and C-S bonds in electron detachment dissociation and infrared multiphoton dissociation of disulfide-linked peptide anions. *Int. J. Mass spectrom.* **2007**, *263*, 71-81.

168. Yang, J.; Mo, J. J.; Adamson, J. T.; Hakansson, K. Characterization of oligodeoxynucleotides by electron detachment dissociation Fourier transform ion cyclotron resonance mass spectrometry. *Anal. Chem.* **2005**, *77*, 1876-1882.

169. Yang, J.; Hakansson, K. Fragmentation of oligoribonucleotides from gas-phase ion-electron reactions. *J. Am. Soc. Mass. Spectrom.* **2006**, *17*, 1369-1375.

170. McFarland, M. A.; Marshall, A. G.; Hendrickson, C. L.; Nilsson, C. L.; Fredman, P.; Mansson, J. E. Structural characterization of the GM1 ganglioside by infrared multiphoton dissociation/electron capture dissociation, and electron detachment dissociation electrospray ionization FT-ICR MS/MS. *J. Am. Soc. Mass. Spectrom.* **2005**, *16*, 752-762.

171. Adamson, J. T.; Hakansson, K. Electron detachment dissociation of neutral and sialylated oligosaccharides. *J. Am. Soc. Mass. Spectrom.* **2007**, *18*, 2162-2172.

172. Wolff, J. J.; Amster, I. J.; Chi, L. L.; Linhardt, R. J. Electron detachment dissociation of glycosaminoglycan tetrasaccharides. *J. Am. Soc. Mass. Spectrom.* **2007**, *18*, 234-244.

173. Wolff, J. J.; Chi, L. L.; Linhardt, R. J.; Amster, I. J. Distinguishing glucuronic from iduronic acid in glycosaminoglycan tetrasaccharides by using electron detachment dissociation. *Anal. Chem.* **2007**, *79*, 2015-2022.

174. Wolff, J. J.; Laremore, T. N.; Busch, A. M.; Linhardt, R. J.; Amster, I. J. Electron detachment dissociation of dermatan sulfate oligosaccharides. *J. Am. Soc. Mass. Spectrom.* **2008**, *19*, 294-304.

175. Wolff, J. J.; Laremore, T. N.; Busch, A. M.; Linhardt, R. J.; Amster, I. J. Influence of charge state and sodium cationization on the electron detachment dissociation and infrared multiphoton dissociation of glycosaminoglycan oligosaccharides. *J. Am. Soc. Mass. Spectrom.* **2008**, *19*, 790-798.

176. Wolff, J. J.; Laremore, T. N.; Leach, F. E.; Linhardt, R. J.; Amster, I. J. Electron capture dissociation, electron detachment dissociation and infrared multiphoton dissociation of sucrose octasulfate. *Eur. J. Mass Spectrom.* **2009**, *15*, 275-281.

177. Chi, L. L.; Wolff, J. J.; Laremore, T. N.; Restaino, O. F.; Xie, J.; Schiraldi, C.; Toida, T.; Amster, I. J.; Linhardt, R. J. Structural analysis of bikunin glycosaminoglycan. *J. Am. Chem. Soc.* **2008**, *130*, 2617-2625.

178. Wolff, J. J.; Laremore, T. N.; Aslam, H.; Linhardt, R. J.; Amster, I. J. Electron-induced dissociation of glycosaminoglycan tetrasaccharides. *J. Am. Soc. Mass. Spectrom.* **2008**, *19*, 1449-1458.

179. Kim, Y. J.; Varki, A. Perspectives on the significance of altered glycosylation of glycoproteins in cancer. *Glycoconj. J.* **1997**, *14*, 569-576.

180. Liu, H.; Hakansson, K. Electron capture dissociation of tyrosine O-sulfated peptides complexed with divalent metal cations. *Anal. Chem.* **2006**, *78*, 7570-7576.

181. Zubarev, R. A.; Zubarev, A. R.; Savitski, M. M. Electron capture/transfer versus collisionally activated/induced dissociations: Solo or duet? *J. Am. Soc. Mass. Spectrom.* **2008**, *19*, 753-761.

Chapter 2

Electron Capture Dissociation of Divalent Metal-adducted N-linked Glycans Released from Bovine Stimulating Hormone

2.1 Introduction

Glycosylation is a prevalent protein post-translational modification (PTM), playing key roles in various cellular processes, such as metastasis, cell adhesion, molecular trafficking and clearance, and receptor activation.[1-8] Glycans are assembled in a step-wise fashion by the sequential actions of glycosyltransferases and glycosidases,[1] a process which results in highly diverse glycan structures. This structural complexity makes glycan characterization more challenging than the characterization of other linear biomolecules, such as peptides or oligonucleotides. In addition to the sequence of monosaccharides, linkages between the monosaccharides, degrees of branching, and stereochemistry (α vs. β) must be determined to achieve complete characterization of glycans. Mass spectrometry has been widely applied for the structural determination of glycans due to its ability to offer accurate results, analytical versatility, and high sensitivity (attomole to fentomole range).[9-12] In particular, Fourier transform ion cyclotron resonance (FT-ICR) mass spectrometry[13,14] is a powerful technique due to its high resolution and high mass accuracy,[15] and its ability to apply various tandem mass spectrometric (MS/MS) techniques.

Structural characterization of sulfated oligosaccharides has been a challenging task due to the high lability of the sulfate group. Most MS/MS analysis of sulfated oligosaccharides has been performed in negative ion mode because of the acidity of sulfate. In particular, collision activated dissociation (CAD) has been extensively applied to investigate sulfated oligosaccharide anions.[16-21] Loss of SO_3 or H_2SO_4 is a dominant fragmentation process in CAD and thus localization of sulfate groups is challenging. Choosing a precursor ion of higher charge state for CAD analysis can reduce sulfate elimination.[18,19] While CAD provides mostly glycosidic cleavages (B-, C-, Y-, and Z-type[22] ions) and some cross-ring cleavages (A- and X-type[22] ions),[16-20] infrared multiphoton dissociation (IRMPD), electron detachment dissociation (EDD)[23-25], and negative electron transfer dissociation (NETD)[26] have been shown to generate extensive cross-ring and glycosidic cleavages in negative ion mode analysis for sulfated glycans and glycosaminoglycans (GAGs).[27-33] Compared to IRMPD, EDD produces more abundant product ions and reduced sulfate elimination.[29] However, sulfate loss is still competing with other fragmentation pathways, and therefore remains an issue in sulfated oligosaccharide characterization.

In positive ion mode analysis, it has been demonstrated that sulfate groups can be stabilized by forming adducts with alkali and divalent metal cations.[34,35] It has also been reported that biomolecules coordinated to metal cations provide additional structural information in tandem mass spectrometry compared to their protonated species. For example, CAD of metal-adducted oligosaccharides yielded more extensive cross-ring cleavages than the corresponding protonated species.[36-40] However, the efficiency of CAD decreases with increasing glycan mass.[41] Alternative tandem mass spectrometric

techniques have also been applied for positive ion mode glycan structural analysis, including IRMPD,[37,42-45] high-energy CAD,[46-48] 157 nm photodissociation,[41,49,50] and electron capture dissociation (ECD),[51-55]   The first application of ECD to protonated carbohydrates mainly generated glycosidic cleavages.[51]   O'Connor and co-workers observed that ECD of permethylated glycans yielded some unique product ions compared to CAD of the same species,[54] illustrating the complementary nature of these two MS/MS techniques in glycan analysis.

The utilization of metals to ionize sulfated glycans has two main advantages: first, divalent metals can stabilize the labile sulfate group.[35,55]   Moreover, divalent metals facilitate the formation of at least doubly positively charged species, which are required for ECD.   Our group has previously demonstrated the application of ECD to model oligosaccharides ionized with alkali and divalent metals, and found that complementary structural information was obtained from ECD as compared to IRMPD.[53] We also found that ECD of sulfated oligosaccharides ionized with divalent metals provides information about the location of sulfate groups.[55]   However, previous work mainly focused on model oligosaccharides.   Here, our objective is to explore the applicability of ECD towards metal-adducted sulfated N-linked glycans released from a glycoprotein, and to compare ECD fragmentation patterns from such branched molecules to those from IRMPD.   Divalent metal cations including Ca^{2+}, Co^{2+}, and Mg^{2+} were selected as cationizing agents and comparisons were made to determine which metal cation provides the most structural information from IRMPD and ECD.   N-linked glycans from bovine thyroid stimulating hormone (bTSH) were released and investigated.

2.2 Experimental

2.2.1 Reagents

Bovine thyroid stimulating hormone and peptide-N-glycosidase F (PNGase F) were purchased from Sigma Chemical Co. (St. Louis, MO). $CaCl_2$, $CoBr_2$, $MgBr_2$, NH_4HCO_3, and formic acid were obtained from Fisher (Fair Lawn, NJ). SPE graphitized carbon column was purchased from Alltech Associates Inc. (Deerfield, IL). ZrO_2 microtips were obtained from Glygen Corp. (Columbia, MD).

2.2.2 Preparation of N-linked Glycans

Bovine thyroid stimulating hormone was denatured at 100 ^{o}C for 5 min, then digested with PNGase F (2U) in 50 mM NH_4HCO_3 (pH 8) overnight at 37 ^{o}C. The reaction was halted by heating at 100 ^{o}C for 5 min.

2.2.3 Purification and Enrichment of *N*-glycans

The released glycans were purified by SPE graphitized carbon column, and then enriched using ZrO_2 microtips. For each sample, a carbon cartridge was washed with 0.1% (v/v) formic acid in 80% acetonitrile/H_2O (v/v), followed by deionized water. The solution containing *N*-glycans was then loaded followed by washing with deionized water to remove salts and other contaminants. The glycans were eluted with 0.1% formic acid (v/v) in 20% acetonitrile/H_2O (v/v), the resulting solution was dried down in a vacuum concentrator (Eppendorf, Hamberg, Germany), reconstituted in 3.3% formic acid (binding solution), and loaded onto ZrO_2 microtips equilibrated with the same binding solution. Unbound glycans were removed with H_2O (washing solution), and bound sulfated glycans were eluted with 1% piperidine. The eluted solution was dried down and mixed with $CaCl_2$, $CoBr_2$, or $MgBr_2$ (final concentration 30-40 μM) in 50%

methanol/H_2O (v/v) for mass spectrometry analysis.

2.2.4 Mass Spectrometry

All mass spectra were collected with an actively shielded 7-T FT-ICR mass spectrometer with a quadrupole front-end (APEX-Q, Bruker Daltonics, Billerica, MA), as previously described.[56] An indirectly heated hollow dispenser cathode was used to perform ECD.[57] IRMPD was performed with a vertically mounted 25 W, 10.6 μM CO_2 laser (Synrad, Mukilteo, WA). Samples were infused via an Apollo II electrospray ion source at a flow rate of 70 μL/h with the assistance of N_2 nebulizing gas. Following ion accumulation in the first hexapole for 0.05 s, ions were mass selectively accumulated in the second hexapole for 1-4 s. Ions were then transferred through high voltage ion optics and captured with dynamic trapping in an Infinity ICR cell.[58] The accumulation sequence up to the ICR cell fill was looped 4-6 times to optimize precursor ion signal to noise (S/N) ratio. For ECD, the cathode heating current was kept constant at 1.8 A and the cathode voltage was pulsed during the ECD event to a bias voltage of - 0.1 to - 1.0 V for 50 ms to generate low energy electrons. IRMPD was performed with a laser power of 10 W and with firing times ranging from 40-100 ms. For activated-ion ECD (AI-ECD), *N*-glycan ions were heated with a 10 W, 20-25 ms IR laser pulse prior to electron irradiation to destroy intramolecular non-covalent interactions.[59]

2.2.5 Data Analysis

All mass spectra were acquired with XMASS software (Bruker Daltonics) with 256 data points from *m/z* 100 to 2000 and summed over 40-64 scans. Data processing was performed with MIDAS software.[60] Data were zero filled once, Hanning apodized, and exported to Microsoft Excel for internal frequency-to-mass calibration with a

two-term calibration equation.[61]   Product ion spectra were interpreted with the aid of the web application GlycoFragment (www.dkfz.de/spec/projekte/fragments/).[62]   Product ions were not assigned unless the S/N ratio was at least 3.

2.3 Results and Discussion

All product ions are labeled according to the Domon and Costello nomenclature.[22] Subscript numerals indicate where cleavage occurred and superscript numerals indicate where cross-ring cleavage occurred.   When more than one product assignment was possible, all assignments are listed.   Internal fragments are indicated by parentheses (e.g., $Z_{4\beta}/C_5$).   For branched oligosaccharides, the letter α represents the largest branch, the letter β represents the second largest branch, and the letter γ represents the third largest branch.   N-linked oligosaccharides on bovine TSH were previously examined by Green and co-workers by NMR.[63]   The three N-linked glycans investigated here, indicated as glycan 1, glycan 2 and glycan 3, respectively, are shown in Figure 2.1.   Product ions bearing a calcium cation as charge carrier are denoted with a superscript Ca (e.g., C_4^{Ca}). Product ions which underwent sulfate loss are underlined (e.g., $\underline{Y_{3\alpha}^{Ca}}$).   All three glycans are sulfated hybrid-type[11] *N*-glycans.
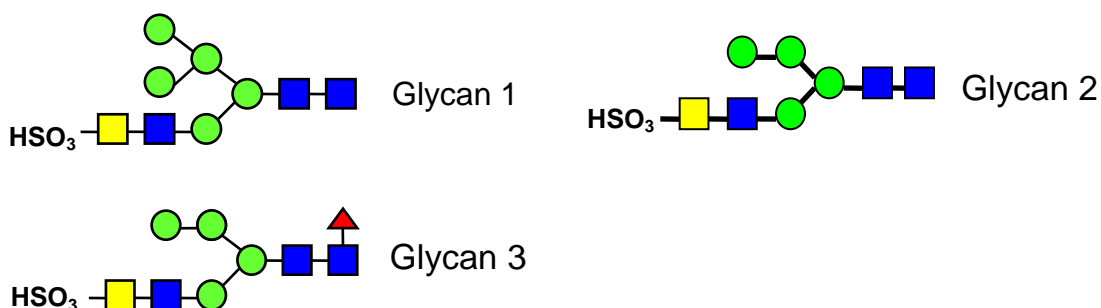
Figure 2.1.   N-linked glycans released from bovine thyroid stimulating hormone.   ● : mannose, ▢ : N-acetylglucosamine (GlcNAc), ▲ : fucose, ◼ : N-acetylgalactosamine (GalNAc).

2.3.1 Fragmentation Behavior of Glycan 1 with Different Metal Adducts in IRMPD and ECD

All selected precursor ions were triply charged with two divalent metal cations (Ca^{2+}, Co^{2+}, or Mg^{2+}) binding to the glycan. Fragmentation patterns of metal-adducted glycan 1 were shown in Figure 2.2.

Abundant signals were observed for calcium-adducted glycans $(M + 2Ca - H)^{3+}$, indicating that calcium salt is highly effective in ionizing carbohydrates.[36,38] IRMPD of Ca^{2+}-adducted glycan 1 (Figure 2.2a) generated glycosidic cleavages between every neighboring monosaccharide, providing rich information regarding sequence and monosaccharide composition. Sulfate loss was commonly observed in the spectrum (Figure 2.3a), thus information regarding sulfate location was absent. Several ions cannot be distinguished based on their accurate masses, such as $Z_{4\alpha}$ or $(B_4 - SO_3)$ and $Y_{4\alpha}$ or $(C_4 - SO_3)$. Therefore, both possibilities are included in Figure 2.3a. Several internal fragments resulting from more than one glycosidic cleavage were also generated, such as $\underline{(Man)_4(GlcNAc)^{Ca}}$. Such internal fragments provide additional structural information, but also complicate the spectra. Five cross-ring cleavages were observed following IRMPD, including $^{2,4}A_{2\alpha}$, $^{0,4}A_3$, $^{0,2}A_4$, $^{1,4}A_4$, and $^{0,2}X_1$. $^{0,2}A$, $^{0,4}A$, and $^{2,4}A$-type ions were previously found in CAD and IRMPD (low-energy fragmentation techniques) spectra of glycans.[34,42,43,53] The $^{0,2}A_4$ and $^{1,4}A_4$ fragments at the branching point aid the determination of the positions of the glycan antennae. X-type ions can be generated by high-energy CAD[46-48] and 157 nm photodissociation[41,49,50] of oligosaccharides, but are not commonly seen following IRMPD.
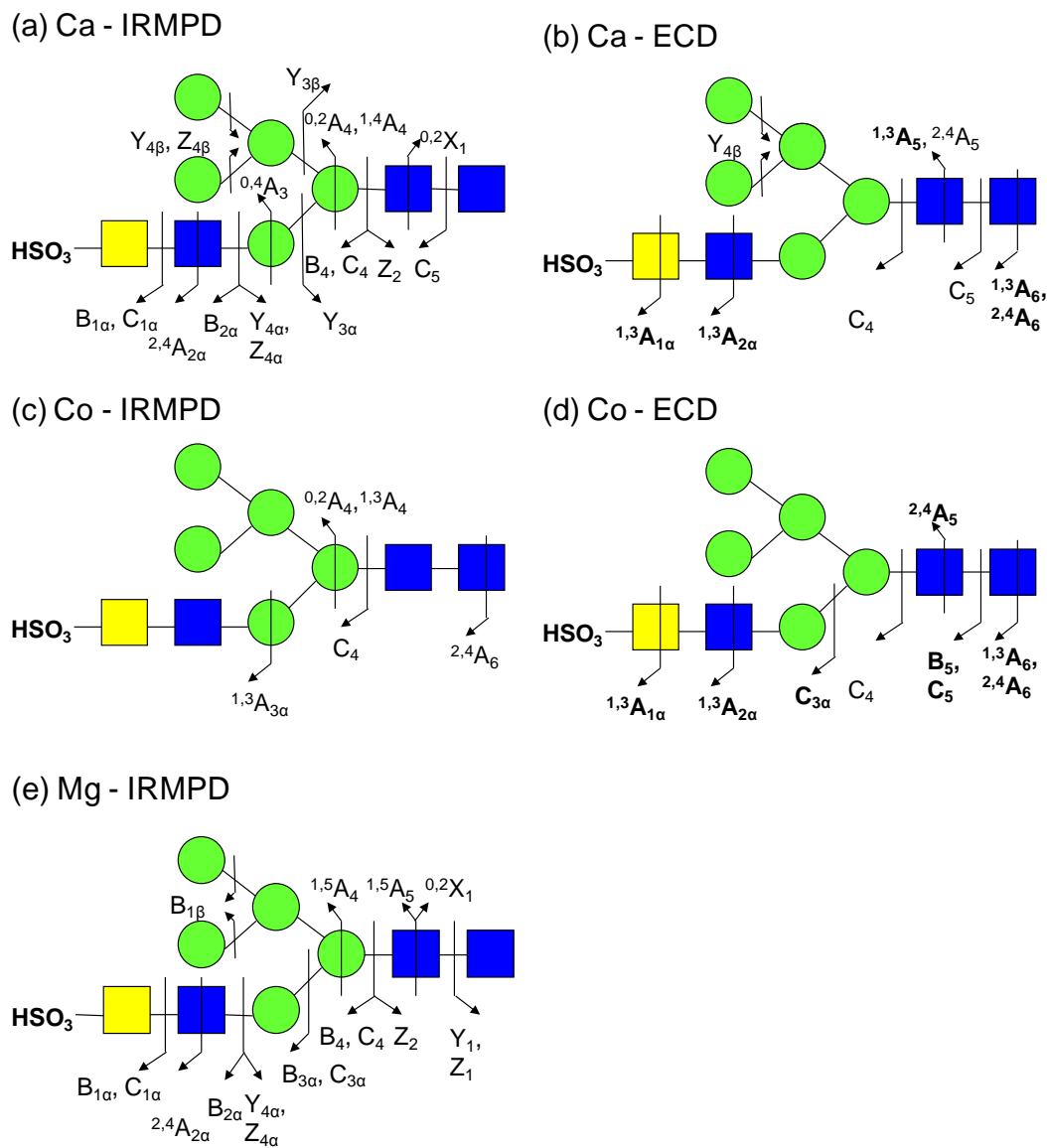
Figure 2.2. Fragmentation patterns of metal-adducted N-linked glycan 1: (a) IRMPD of calcium adduct (40 scans, 50 ms irradiation, 10 W laser power); (b) ECD of calcium adduct (40 scans, 80 ms electron irradiation with a bias voltage of – 0.2 V); (c) IRMPD of cobalt adduct (40 scans, 40 ms irradiation, 10 W laser power); (d) AI-ECD of cobalt adduct (40 scans, 15 ms irradiation with 10 W laser power, 80 ms electron irradiation with a bias voltage of – 0.15 V); (e) IRMPD of magnesium adduct (40 scans, 50 ms irradiation, 10 W laser power).

(a)

B$_{1\alpha}$^{Ca} (^{2,4}**A$_{2\alpha}$**^{2Ca}) − H$_2$O

C$_{1\alpha}$^{Ca} (^{2,4}**A$_{2\alpha}$**^{2Ca})

Z$_{3\alpha}$/Y$_{4\beta}$/C$_5$^{Ca}

^{1,4}**A$_4$**^{2Ca}

Y$_{3\alpha}$/Y$_{4\beta}$/C$_5$^{Ca}

(Z$_2$^{Ca} (B$_{2\alpha}$)^{Ca}

(Man)$_4$(GlcNAc)$_1$^{Ca}

(Man)$_5$(GlcNAc)$_1$^{Ca}

B$_{2\alpha}$^{Ca}

C$_5$^{2Ca}

Y$_{4\beta}$^{2Ca}

Y$_{3\alpha}$^{Ca}

*

^{0,4}**A$_3$**^{Ca}

Z$_{4\alpha}$^{Ca} (B$_4$)^{Ca}

Y$_{4\alpha}$^{Ca}(C$_4$)^{Ca}

Y$_{3\beta}$^{2Ca}

^{0,2}**A$_4$**^{2Ca}

C$_4$^{2Ca}

Z$_{4\beta}$/C$_5$^{2Ca}

Y$_{4\beta}$/C$_5$^{2Ca}

^{2,4}**A$_6$/Y$_{4\beta}$**^{2Ca}

C$_5$^{2Ca}

Z$_{4\beta}$^{2Ca}

Y$_{4\beta}$^{2Ca}

*

(M^{2Ca})$^{3+}$

(M^{2Ca})$^{2+}$

Abundance

25

20

15

10

5

300   400   500   600   700   800   900

m/z

(b)

(M^{2Ca})$^{3+}$

(M^{2Ca})$^{2+}$

(M^{2Ca} − 42)$^{2+}$

C$_5$^{2Ca}

C$_4$^{2Ca}

Y$_{4\beta}$^{2Ca}

^{2,4}**A$_6$**^{2Ca}

(M^{2Ca} − 101)$^{2+}$

^{2,4}**A$_5$**^{2Ca}

C$_5$^{2Ca}

^{2,4}**A$_6$**^{2Ca}

Abundance

25

20

15

10

5

600   700   800   900   1,000   1,100   1,200   1,300   1,400   1,500   1,600   1,700

m/z

(c)

C_4^{2Co}

$^{2,4}A_6^{2Co} - 3Man$

$^{2,4}A_6^{2Co}$

$^{1,3}A_4^{Co}$

$^{0,2}A_4^{Co} / ^{1,3}A_{3\alpha}^{Co}$

$(M^{2Co})^{3+}$

$(M^{2Co})^{3+}$

$(M^{2Co} - 101)^{3+}$

$^{2,4}A_6^{2Co}$

$^{2,4}A_5^{2Co}$

C_3^{Co}

C_4^{2Co}

$(B_5 - 57)^{2Co}$

B_5^{2Co}

C_5^{2Co}

$(M^{2Co})^{2+}$

(d)

(e)

$(M^{2Mg})^{3+}$

$\underline{B}_{1\beta}$

$\underline{Z}_1 (B_{1\alpha})- 2H_2O$

$\underline{Z}_1 (B_{1\alpha})- H_2O$

$\underline{Z}_1 (B_{1\alpha})$

$\underline{Z}_2 (B_{2\alpha})$

$\underline{Z}_2{}^{Mg} (B_{2\alpha})^{Mg}$

$\mathbf{{}^{1,5}A_4{}^{2Mg}} - H_2O$

$(M^{2Mg})^{2+}$

$\underline{Y}_1 (C_{1\alpha})$

$\underline{Y}_1{}^{Mg} (C_{1\alpha})^{Mg}$

$\mathbf{{}^{2,4}\underline{A}_{2\alpha}{}^{Mg}}$

$\mathbf{{}^{1,5}\underline{A}_5{}^{2Mg}}$

$B_{2\alpha}{}^{Mg}$

$C_{1\alpha}$

$\underline{C}_{3\alpha}{}^{Mg}$

$B_{1\alpha}{}^{Mg}$

$C_{1\alpha}{}^{Mg}$

$\underline{B}_4{}^{Mg}(Z_{4\alpha})^{Mg}$

$\underline{C}_4{}^{Mg} (Y_{4\alpha})^{Mg}$

$B_{3\alpha}{}^{Mg}$

Abundance

m/z
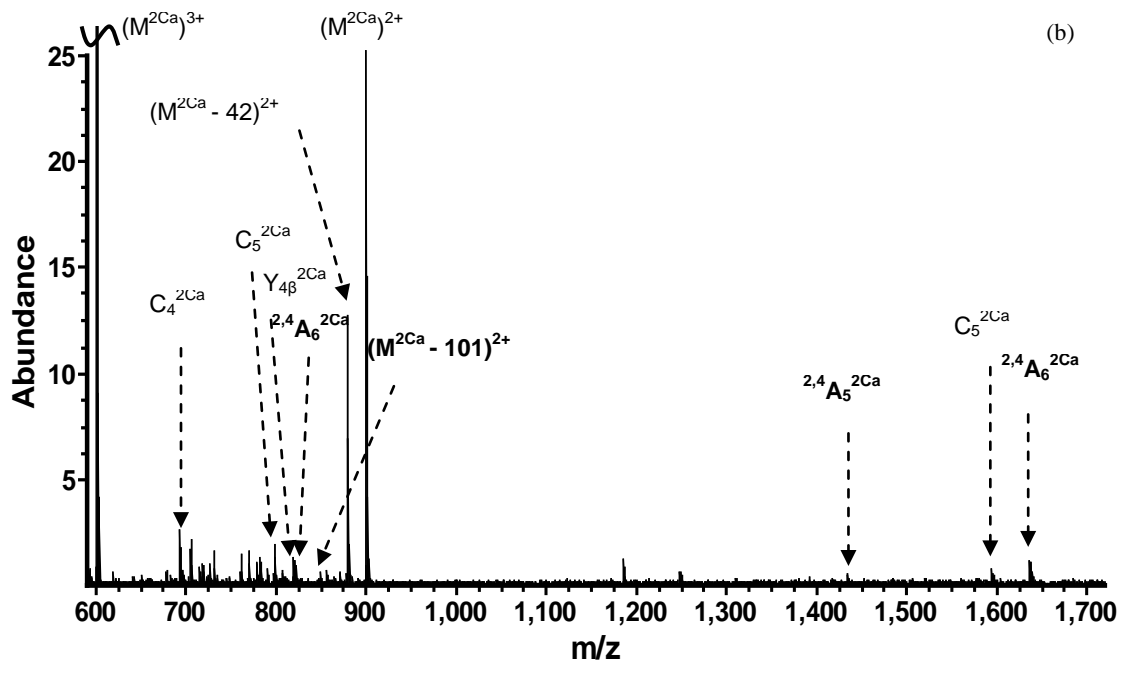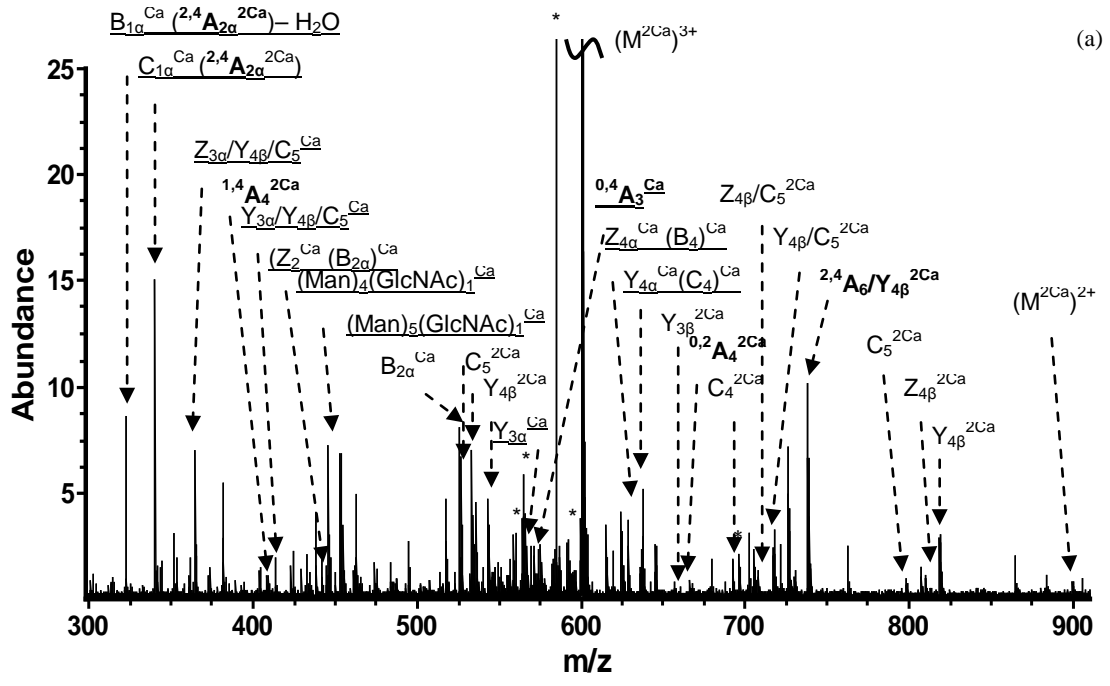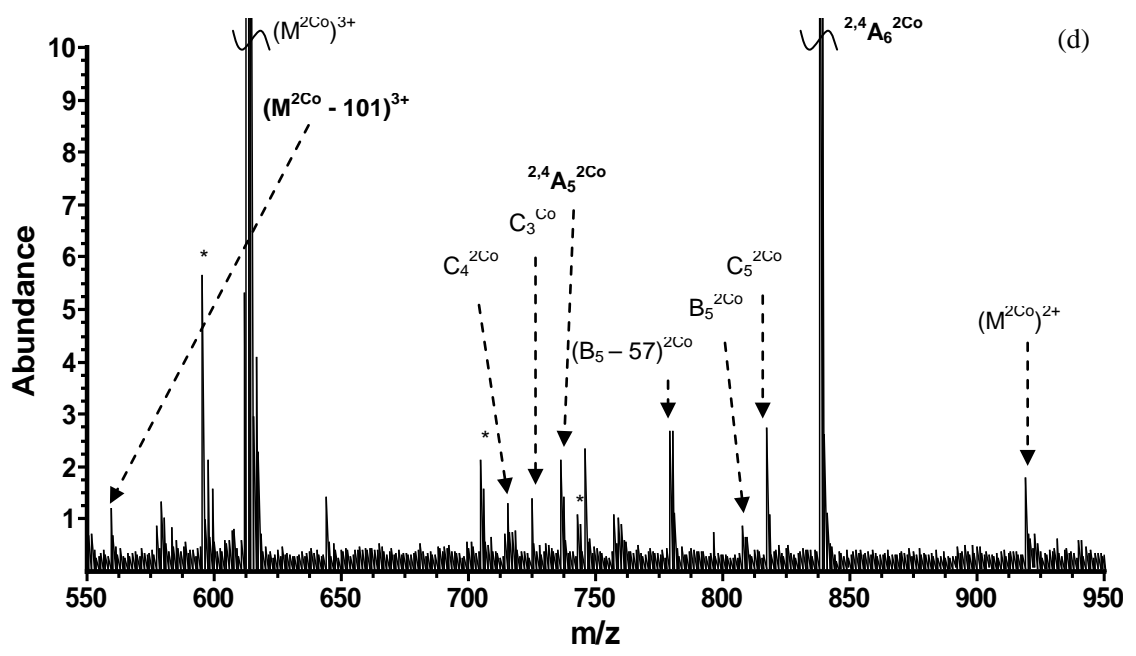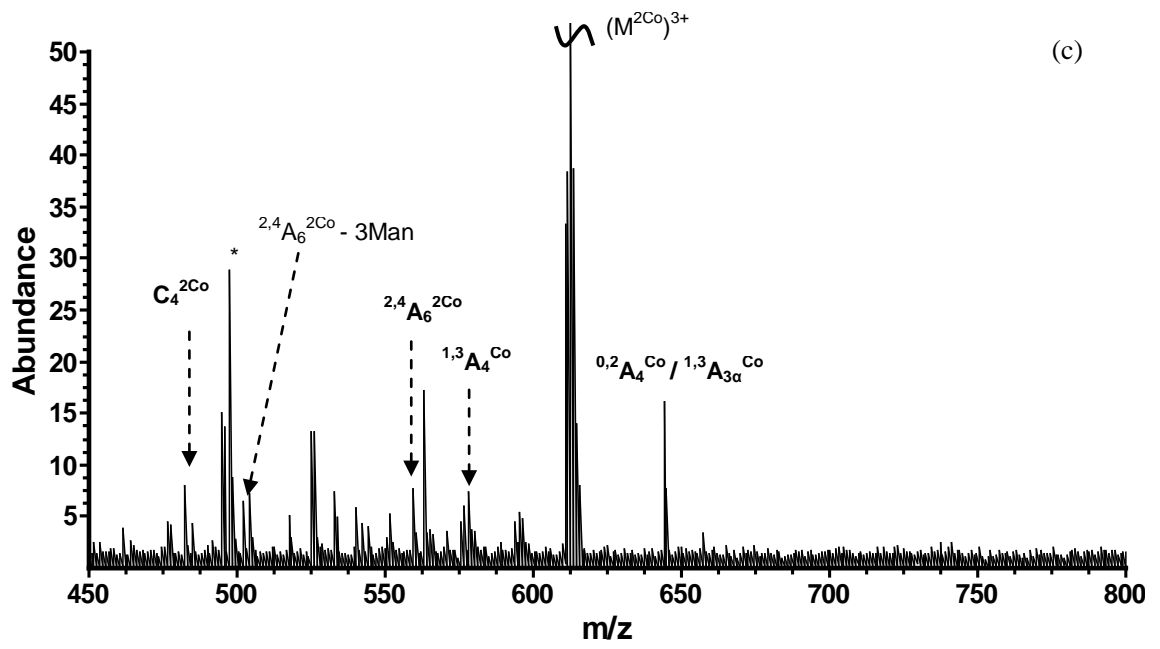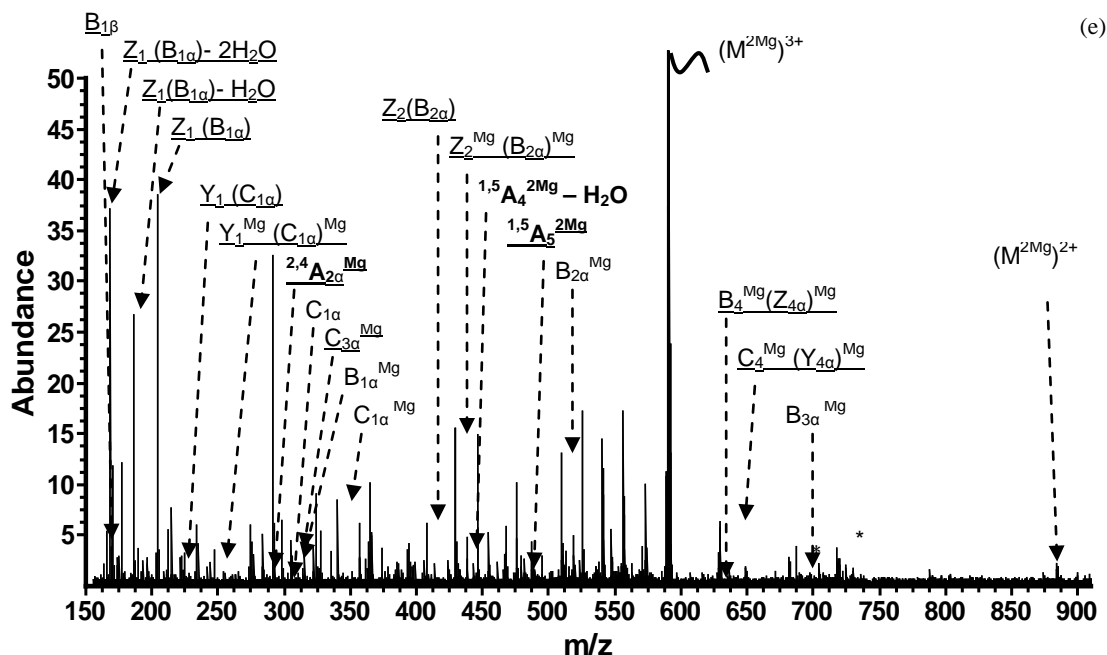
Figure 2.3. FT-ICR tandem mass spectra of metal-adducted N-linked glycan 1: (a) IRMPD of calcium adduct (40 scans, 50 ms irradiation, 10 W laser power); (b) ECD of calcium adduct (40 scans, 80 ms electron irradiation with a bias voltage of – 0.2 V); (c) IRMPD of cobalt adduct (40 scans, 40 ms irradiation, 10 W laser power); (d) AI-ECD of cobalt adduct (40 scans, 15 ms irradiation with 10 W laser power, 80 ms electron irradiation with a bias voltage of – 0.15 V); (e) IRMPD of magnesium adduct (40 scans, 50 ms irradiation, 10 W laser power).   Product ions are underlined if they underwent sulfate loss.   Assignments indicated in bold are cross-ring product ions.   * denotes electronic noise.

Figure 2.2b shows the fragmentation pattern of sulfated glycan 1 following ECD. All product ions were even-electron ions.   Charge-reduced species were not detected, instead proton-stripped species were observed, resulting from gain of an electron by precursor ions and loss of hydrogen.   Product ions corresponding to proton-stripped species and neutral loss from the proton-stripped species were the most abundant peaks in the spectrum.   The sulfate group was retained in all product ions, demonstrating the ability of ECD to retain labile groups.   ECD is well-known to have the ability to retain labile PTMs, including phosphorylation, sulfation, and glycosylaton.[35,64-67]   Compared

to IRMPD, several additional cross-ring cleavages were observed. The product ion at $m/z = 848.7$, labeled as loss of 101 Da from the proton-stripped species, can be assigned to several ^{1,3}A-type ions sharing the same m/z, including $^{1,3}A_{1\alpha}$, $^{1,3}A_{2\alpha}$, $^{1,3}A_5$, or $^{1,3}A_6$. The combination of ^{1,3}A and ^{2,4}A-type ions from both IRMPD and ECD determines the linkage position of the non-reducing end GlcNAc as the C4-position ($^{1,3}A_{2\alpha}$ and $^{2,4}A_{2\alpha}$). Overall, the combination of IRMPD and ECD of the calcium-adducted N-glycan provided extensive structural information.

The IRMPD and ECD fragmentation patterns of the $(M + 2Co - H)^{3+}$ form of glycan 1 are shown in Figures 2.2c and 2.2d, respectively. Compared to the calcium-adducted species, cobalt adducts generated weaker signal and only one glycosidic cleavage was observed following IRMPD. However, several diagnostic cross-ring cleavage product ions were found only from the cobalt-adducted precursor ion, such as $^{1,3}A_{3\alpha}$, $^{1,3}A_4$, and $^{2,4}A_6$. The two product ions ($^{0,2}A_4$ and $^{1,3}A_4$) at the branching point of the tri-mannose core aid determination of the position of the 3-antenna. This fragmentation pattern is in accordance with an earlier study by Leary and co-workers, who examined the dissociation pathways of Ca^{2+}-, Co^{2+}-, and Mn^{2+}-coordinated oligosaccharides, and found that Co^{2+}-coordinated species exhibited unique fragmentation patterns.[38] In ECD, cobalt adducts yielded three additional glycosidic cleavages ($C_{3\alpha}$, B_5, and C_5) and several additional cross-ring cleavages compared to IRMPD. The peak denoted as $B_5 - 57$ Da ($m/z = 779.2$) likely corresponds to loss of C_2H_3NO from N-acetylglucosamine (supplementary Figure 2.1d). Similar to the calcium adducts, loss of 101 Da from the precursor ion was also observed. The combination of $^{1,3}A_6$ and $^{2,4}A_6$ from ECD of cobalt-adducted glycan 1 determines the

linkage position of the GlcNAc at the reducing end. Cross-ring product ions are helpful in linkage type determination, particularly the ones occurring at the branching points. However, the lack of sufficient glycosidic cleavages made the sequencing of this glycan difficult. Therefore, cobalt adducts are not as effective as calcium adducts in achieving extensive structural characterization of sulfated N-glycan 1 from IRMPD and ECD.

IRMPD and ECD were also performed for magnesium-adducted glycan 1 $(M + 2Mg - H)^{3+}$. Following IRMPD, glycosidic cleavages between every neighboring monosaccharide, and five cross-ring cleavages were observed (Figure 2.2e). Among the five cross-ring cleavages, three were unique in the IRMPD spectrum of Mg^{2+}-adducted glycan 1 with one of them at the branching point of the tri-mannose core. When product ions cannot be distinguished based on their m/z ratio, all possible assignments are included. For example, Z_1 and $B_{1\alpha}$ without a sulfate attached both correspond to the mass of a HexNAc. Such ambiguous assignments are often a consequence of sulfate loss from B or C-type ions. The latter loss was common in product ions generated by IRMPD. However, all assignments in ECD spectra were unambiguous, because all product ions in ECD spectra retained the sulfate group.

In contrast to calcium and cobalt adducts, ECD of Mg^{2+}-adducted glycan 1 provided very little structural information (data not shown). Only the proton stripped species $(M + 2Mg - 2H)^{2+}$ and loss of 42 Da from the proton stripped species were observed. Loss of 42 Da likely corresponds to loss of a ketene molecule (CH_2CO) from N-acetylglucosamine, as previously reported.[51,53] We observed retention of the sulfate group in calcium and cobalt adducted N-glycans following ECD, while IRMPD of metal-adducted glycan 1 showed extensive sulfate loss (see supplementary Figures 2.1c

and 2.1e).   Therefore, magnesium adduction is not favored for glycan 1 due to the difficulty in achieving sulfate localization and unambiguous fragment assignments.

We also attempted to ionize the *N*-glycan with other metal cations, such as Mn^{2+}, Zn^{2+}, Ba^{2+}, and Al^{3+}.   However, no metal-adducted glycan was observed in positive ion mode.   The lack of adduct formation may be attributed to the ionic radii and coordination numbers of different metal cations.[38]   In general, larger metal ions are not favored for glycan fragmentation, probably because it is difficult for large metal cations to assist charge-induced fragmentation.[37,42]   Harvey investigated the ability of divalent metal ions for ionizing carbohydrates, and found that calcium is most effective with magnesium and cobalt being somewhat less effective,[36] in accordance with our observation.   Although cobalt-coordinated oligosaccharides have shown unique fragmentation pathways in CAD,[38,39]   it is not straightforward to form cobalt adducts with the sulfated *N*-glycan examined here compared to calcium adducts.   Also, few glycosidic cleavages were observed in both IRMPD and ECD spectra of the cobalt-adducted glycan.   Therefore, we focused on calcium adducts, due to the higher available signal, and the ability to generate extensive glycosidic and cross-ring cleavages in IRMPD and ECD.

2.3.2 Fragmentation Behavior of Ca^{2+}-adducted Glycan 2 in IRMPD and ECD

IRMPD was performed of Ca^{2+}-adducted sulfated glycan 2 $(M + 2Ca - H)^{3+}$ (Figure 2.4a).   Glycosidic cleavages were generated between every neighboring monosaccharide unit with only one exception.   Most of the glycosidic cleavages resulted in B- and C-type ions with low molecular weight, indicating that fragmentation may occur from the non-reducing end of the *N*-glycan.   Four cross-ring fragments were seen

($^{0,2}A_{2\alpha}$, $^{2,4}A_{2\alpha}$, $^{0,2}A_{2\beta}$, and $^{0,4}A_4$) with one ($^{0,4}A_4$) at the tri-mannose core branching site, aiding determination of the branch position.   Sulfate loss was observed in most of the product ions, which precluded localization of the labile sulfate group.   It is difficult to localize where the two Ca^{2+} ions bind based on the product ion assignments.   Lebrilla and co-workers investigated the coordination of alkali metal ions to oligosaccharides by calculating multicollision dissociation threshold (MCDT) values and by molecular dynamics, and predicted that metal ions coordinate at or near glycosidic oxygen(s).[37] Most product ions bearing two calcium cations retained the sulfate group, whereas most product ions that lost the sulfate group bore only one calcium cation.   Therefore, we believe one of the Ca^{2+} ions likely binds to the acidic sulfate group, while the other one coordinates with one or more glycosidic oxygen(s).

In the ECD spectrum of $(M + 2Ca - H)^{3+}$ (Figure 2.4b), fewer fragments were observed compared to IRMPD, due to the lower fragmentation efficiency of ECD.[57] However, two product ions unique to ECD provided additional structural information compared to IRMPD.   In order to break non-covalent interactions within this *N*-glycan and thus improve fragmentation efficiency, AI-ECD[59] was applied.   Following AI-ECD (Figure 2.4c), three additional product ions (B_5, $C_{2\alpha}$, and $^{2,4}A_5$) were detected compared to ECD alone, demonstrating improved fragmentation efficiency.   In contrast to IRMPD, ECD mainly produced large fragments containing the reducing end, indicating that charge neutralization occurs remote from the reducing end of the *N*-glycan.   Our previous study on model oligosaccharides showed similar fragmentation behavior.[53] Moreover, all product ions from AI-ECD were completely different from the ones observed in IRMPD, thereby generating complementary structural information (Schemes

2.1a and 2.1b).   The complementary capabilities of IRMPD and ECD for biomolecular structural analysis have previously been applied to a variety of biomolecules, including peptides,[57,64] proteins,[68] oligosaccharides,[53-55] and oligonucleotides.[24,69]   Our results demonstrated that the combination of IRMPD and ECD is also a promising tool for structural characterization of released sulfated *N*-glycans.
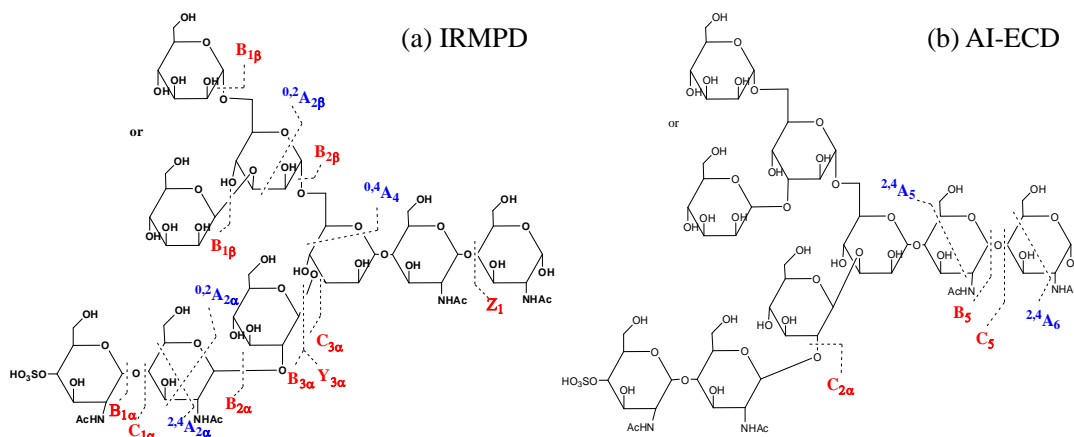
Scheme 2.1.   Fragmentation patterns of Ca^{2+}-adducted *N*-glycan 2: (a) IRMPD and (b) AI-ECD.   Glycosidic cleavages are labeled in red.   Cross-ring cleavages are labeled in blue.
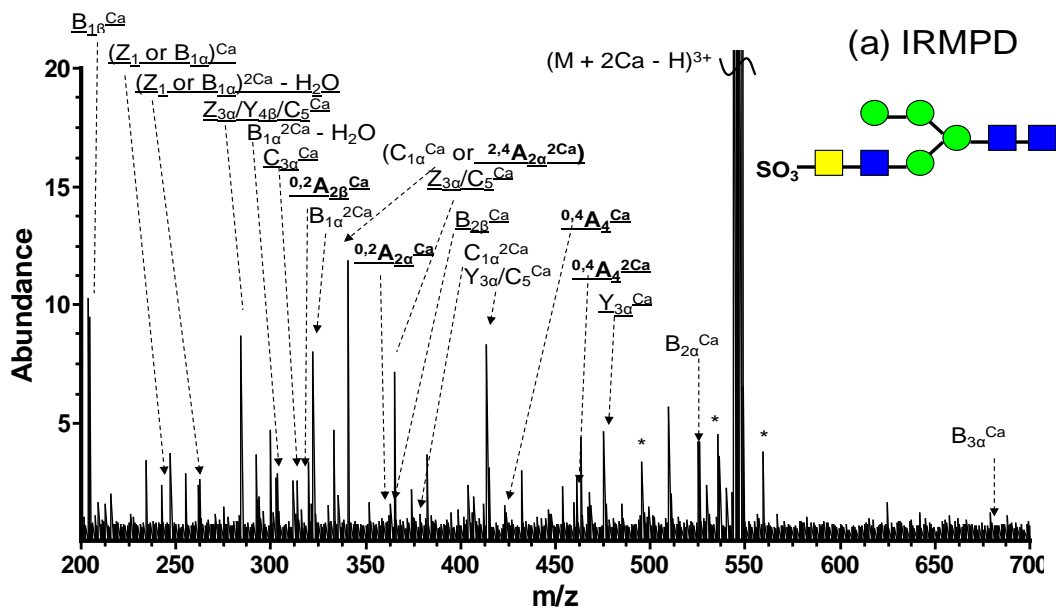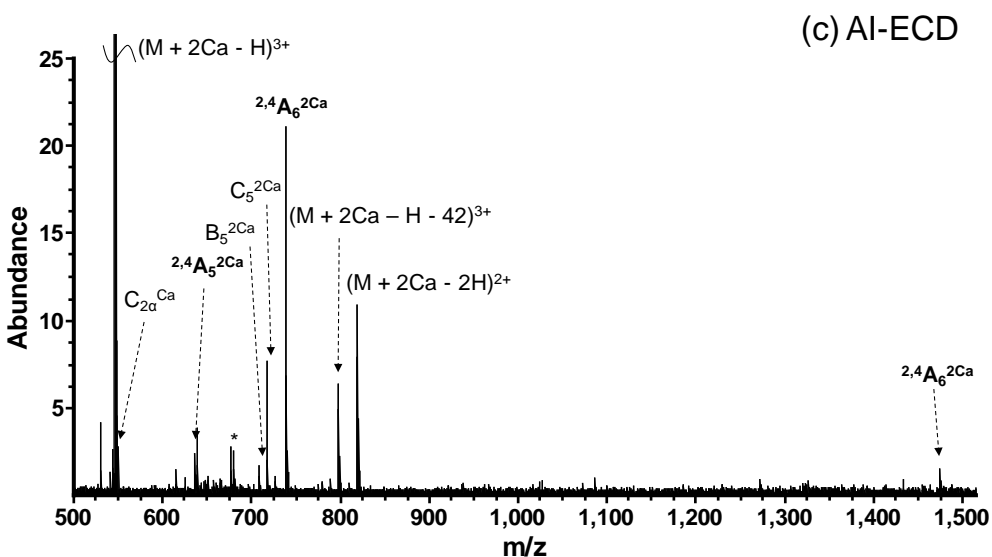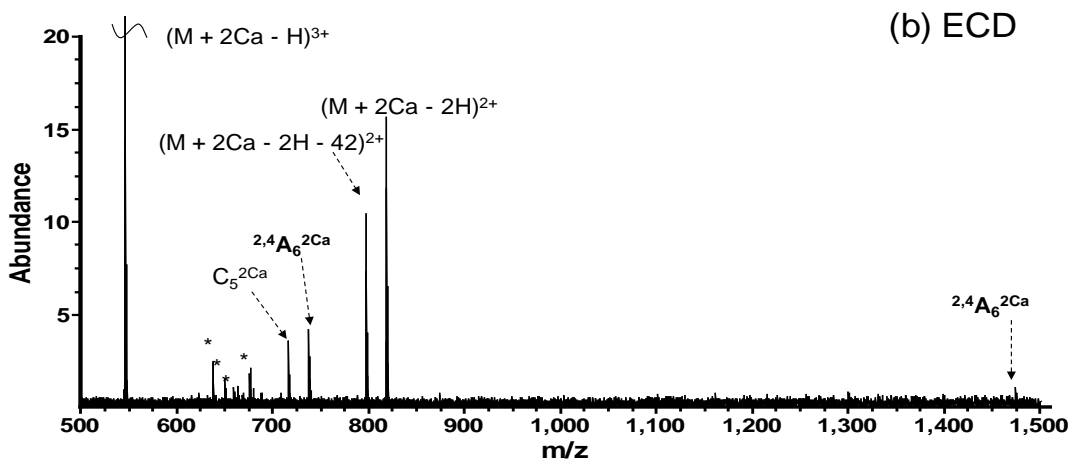
Figure 2.4. FT-ICR tandem mass spectra of Ca^{2+}-adducted N-linked glycan 2. (a) IRMPD (40 scans, 80 ms irradiation, 10 W laser power); (b) ECD (50 scans, 50 ms electron irradiation with a bias voltage of – 0.2 V); (c) AI-ECD (40 scans, 20 ms irradiation with 10 W laser power, 100 ms electron irradiation with a bias voltage of – 0.25 V). Product ions are underlined if they underwent sulfate loss. The superscript 'Ca' indicates product ions bearing a calcium cation. Assignments indicated in bold are cross-ring product ions. * denotes electronic noise.

2.3.3 Fragmentation Behavior of Ca^{2+}-adducted Glycan 3 in IRMPD and ECD

IRMPD and ECD fragmentation patterns of calcium-adducted glycan 3 are shown in Figures 2.5a and 2.5b, respectively. In the IRMPD spectrum, the most abundant fragment is assigned as Y_γ^{2Ca} (m/z = 545.8), corresponding to loss of a fucose residue

from the core structure. The fucose glycosidic bond is highly labile. Dominant fucose loss has been previously observed.[70] Except for Y_{γ}^{2Ca}, all other glycosidic cleavages resulted in B and C-type ions. In addition to six glycosidic cleavages, three cross-ring cleavages were found, with one of them ($^{0,4}A_4$) occurring at the tri-mannose branching site. This result verifies that IRMPD of sulfated *N*-glycans can provide rich structural information.

Following ECD, the fragment corresponding to fucose loss was not detected. In addition, sulfate loss from the product ions was absent. The preservation of labile bonds demonstrates that ECD proceeds through a different mechanism compared to IRMPD and thus provides complementary structural information. Similar to ECD of glycan 2, no charge-reduced species was found. Instead, proton-stripped species and loss of 42 Da from the proton-stripped species were observed with high relative abundance. Compared to IRMPD, fewer product ions were observed. However, the fragment at *m/z* 737.7 ($^{2,4}A_6^{2Ca}$) was only found following ECD, demonstrating the ability of ECD to provide additional information in comparison to IRMPD.
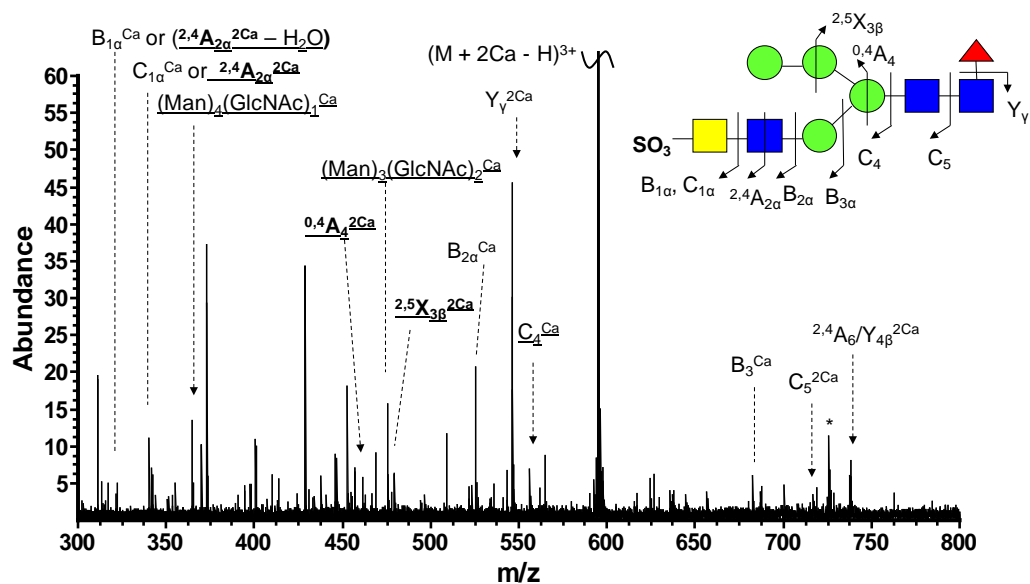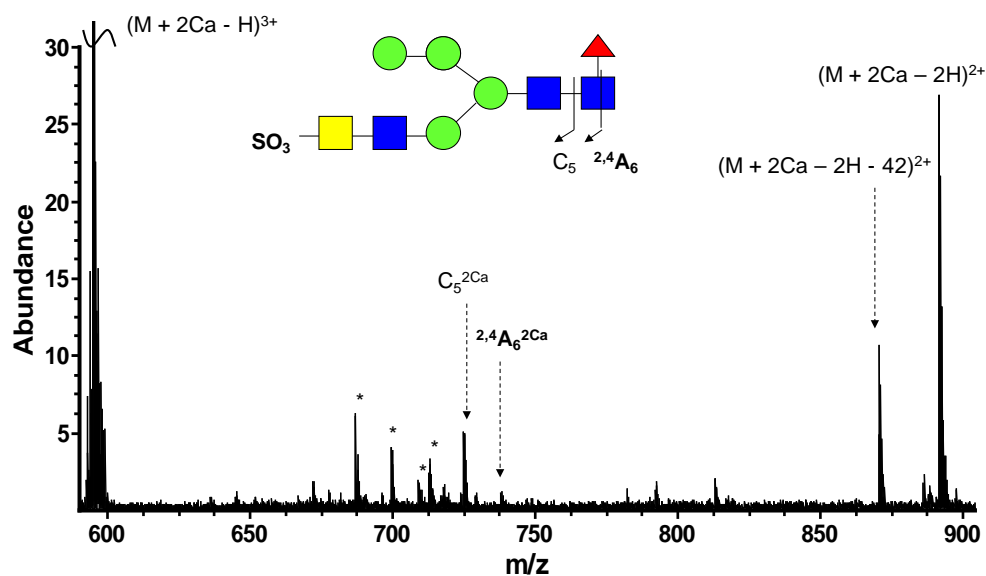
Figure 2.5. FT-ICR tandem mass spectra and fragmentation patterns of Ca^{2+}-adducted N-linked glycan 3: (a) IRMPD of calcium adduct (30 scans, 50 ms irradiation, 10 W laser power); (b) ECD of calcium adduct (64 scans, 50 ms electron irradiation with a bias voltage of – 0.3 V). Product ions are underlined if they underwent sulfate loss. Assignments indicated in bold are cross-ring product ions. * denotes electronic noise.

2.4 Conclusions

We have demonstrated the first application of metal-assisted ECD towards sulfated N-linked glycans released from glycoproteins. Influence of different divalent metal cations such as Ca^{2+}, Mg^{2+}, and Co^{2+} was investigated, and calcium adducts were found as the most promising species, due to high signal abundance and ability to provide extensive glycosidic and cross-ring cleavages following both IRMPD and ECD. Co^{2+}-adducted glycans generated some unique product ions. However, in both IRMPD and ECD of cobalt-adducted species, cross-ring fragments were predominant and the lack of glycosidic cleavages significantly increased the difficulty of glycan sequencing. Mg^{2+}-adducted glycans provided rich structural information following IRMPD, including both glycosidic cleavages and some cross-ring cleavages. However, ECD of magnesium-adducted glycans generated few fragments, thus making sulfate localization difficult. Therefore, we believe that calcium-assisted IRMPD and ECD provide the most structural information of sulfated *N*-glycans.

IRMPD and ECD were applied to several sulfated N-linked glycans released from bTSH. IRMPD of Ca^{2+}-adducted glycans produced extensive glycosidic cleavages and several cross-ring cleavages at the branching point. However, most product ions underwent sulfate loss. Therefore, it is difficult to determine the position of the sulfate group. ECD of Ca^{2+}-adducted glycans yielded unique product ions in comparison to IRMPD, thus providing complementary structural information. Moreover, all product ions observed in ECD spectra retained the sulfate group, which is crucial to sulfate localization. The complementary ability of IRMPD and ECD makes the combination of these two MS/MS techniques a powerful tool in sulfated *N*-glycan structural analysis.

2.5 References

1.   Bertozzi, C. R.; Kiessling, L. L. Chemical glycobiology. *Science* **2001**, *291*, 2357-2364.
2.   Rudd, P. M.; Elliott, T.; Cresswell, P.; Wilson, I. A.; Dwek, R. A. Glycosylation and the immune system. *Science* **2001**, *291*, 2370-2376.
3.   Ohtsubo, K.; Marth, J. D. Glycosylation in cellular mechanisms of health and disease. *Cell* **2006**, *126*, 855-867.
4.   Dube, D. H.; Bertozzi, C. R. Glycans in cancer and inflammation. Potential for therapeutics and diagnostics. *Nature Reviews Drug Discovery* **2005**, *4*, 477-488.
5.   Lowe, J. B.; Marth, J. D. A genetic approach to mammalian glycan function. *Annu. Rev. Biochem* **2003**, *72*, 643-691.
6.   Pilobello, K. T.; Mahal, L. K. Deciphering the glycocode: the complexity and analytical challenge of glycomics. *Curr. Opin. Chem. Biol.* **2007**, *11*, 300-305.
7.   Zhao, Y. Y.; Takahashi, M.; Gu, J. G.; Miyoshi, E.; Matsumoto, A.; Kitazume, S.; Taniguchi, N. Functional roles of N-glycans in cell signaling and cell adhesion in cancer. *Cancer Sci.* **2008**, *99*, 1304-1310.
8.   Varki, A. Biological roles of oligosaccharides - All of the theories are correct. *Glycobiol.* **1993**, *3*, 97-130.
9.   Zaia, J. Mass spectrometry of oligosaccharides. *Mass Spectrom. Rev.* **2004**, *23*, 161-227.
10.   Harvey, D. J. Matrix-assisted laser desorption/ionization mass spectrometry of carbohydrates. *Mass Spectrom. Rev.* **1999**, *18*, 349-450.
11.   Mechref, Y.; Novotny, M. V. Structural investigations of glycoconjugates at high sensitivity. *Chem. Rev.* **2002**, *102*, 321-369.
12.   Perry, R. H.; Cooks, R. G.; Noll, R. J. Orbitrap mass spectrometry : instrumentation, ion motion and applications *Mass Spectrom. Rev.* **2008**, *27*, 661-699.
13.   Marshall, A. G.; Hendrickson, C. L.; Jackson, G. S. Fourier transform ion cyclotron resonance mass spectrometry: A primer. *Mass Spectrom. Rev.* **1998**, *17*, 1-35.
14.   Marshall, A. G.; Hendrickson, C. L. High-resolution mass spectrometers. *Annu. Rev. Anal. Chem.* **2008**, *1*, 579-599.
15.   Park, Y. M.; Lebrilla, C. B. Application of Fourier transform ion cyclotron resonance mass spectrometry to oligosaccharides. *Mass Spectrom. Rev.* **2005**, *24*, 232-264.
16.   Zaia, J.; McClellan, J. E.; Costello, C. E. Tandem mass spectrometric determination of the 4S/6S sulfation sequence in chondroitin sulfate oligosaccharides. *Anal. Chem.* **2001**, *73*, 6030-6039.
17.   Wheeler, S. F.; Harvey, D. J. Extension of the in-gel release method for structural analysis of neutral and sialylated N-linked glycans to the analysis of sulfated glycans: Application to the glycans from bovine thyroid-stimulating hormone. *Anal. Biochem.* **2001**, *296*, 92-100.
18.   Zaia, J.; Li, X. Q.; Chan, S. Y.; Costello, C. E. Tandem mass spectrometric strategies for determination of sulfation positions and uronic acid epimerization in chondroitin sulfate oligosaccharides. *J. Am. Soc. Mass. Spectrom.* **2003**, *14*,

1270-1281.

19. Naggar, E. F.; Costello, C. E.; Zaia, J. Competing fragmentation processes in tandem mass spectra of heparin-like Glycosaminoglycans. *J. Am. Soc. Mass. Spectrom.* **2004**, *15*, 1534-1544.

20. Yu, G. L.; Zhao, X.; Yang, B.; Ren, S. M.; Guan, H. S.; Zhang, Y. B.; Lawson, A. M.; Chai, W. G. Sequence determination of sulfated carrageenan-derived oligosaccharides by high-sensitivity negative-ion electrospray tandem mass spectrometry. *Anal. Chem.* **2006**, *78*, 8499-8505.

21. Desaire, H.; Leary, J. A. Detection and quantification of the sulfated disaccharides in chondroitin sulfate by electrospray tandem mass spectrometry. *J. Am. Soc. Mass. Spectrom.* **2000**, *11*, 916-920.

22. Domon, B.; Costello, C. E. A systematic nomenclature for carbohydrate fragmentations in FAB-MS MS spectra of glycoconjugates *Glycoconj. J.* **1988**, *5*, 397-409.

23. Budnik, B. A.; Haselmann, K. F.; Zubarev, R. A. Electron detachment dissociation of peptide di-anions: an electron-hole recombination phenomenon. *Chem. Phys. Lett.* **2001**, *342*, 299-302.

24. Yang, J.; Hakansson, K. Fragmentation of oligoribonucleotides from gas-phase ion-electron reactions. *J. Am. Soc. Mass. Spectrom.* **2006**, *17*, 1369-1375.

25. Adamson, J. T.; Hakansson, K. Electron detachment dissociation of neutral and sialylated oligosaccharides. *J. Am. Soc. Mass. Spectrom.* **2007**, *18*, 2162-2172.

26. Huzarska, M.; Ugalde, I.; Kaplan, D. A.; Hartmer, R.; Easterling, M. L.; Polfer, N. C. Negative electron transfer dissociation of deprotonated phosphopeptide anions: choice of radical cation reagent and competition between electron and proton transfer. *Anal. Chem.* **2010**, *82*, 2873-2878.

27. Zhang, J. H.; Schubothe, K.; Li, B. S.; Russell, S.; Lebrilla, C. B. Infrared multiphoton dissociation of O-linked mucin-type oligosaccharides. *Anal. Chem.* **2005**, *77*, 208-214.

28. Wolff, J. J.; Chi, L. L.; Linhardt, R. J.; Amster, I. J. Distinguishing glucuronic from iduronic acid in glycosaminoglycan tetrasaccharides by using electron detachment dissociation. *Anal. Chem.* **2007**, *79*, 2015-2022.

29. Wolff, J. J.; Laremore, T. N.; Busch, A. M.; Linhardt, R. J.; Amster, I. J. Electron detachment dissociation of dermatan sulfate oligosaccharides. *J. Am. Soc. Mass. Spectrom.* **2008**, *19*, 294-304.

30. Wolff, J. J.; Laremore, T. N.; Busch, A. M.; Linhardt, R. J.; Amster, I. J. Influence of charge state and sodium cationization on the electron detachment dissociation and infrared multiphoton dissociation of glycosaminoglycan oligosaccharides. *J. Am. Soc. Mass. Spectrom.* **2008**, *19*, 790-798.

31. Wolff, J. J.; Laremore, T. N.; Leach, F. E.; Linhardt, R. J.; Amster, I. J. Electron capture dissociation, electron detachment dissociation and infrared multiphoton dissociation of sucrose octasulfate. *Eur. J. Mass Spectrom.* **2009**, *15*, 275-281.

32. Wolff, J. J.; Amster, I. J.; Chi, L. L.; Linhardt, R. J. Electron detachment dissociation of glycosaminoglycan tetrasaccharides. *J. Am. Soc. Mass. Spectrom.* **2007**, *18*, 234-244.

33. Wolff, J. J.; Leach, F. E.; Laremore, T. N.; Kaplan, D. A.; Easterling, M. L.; Linhardt, R. J.; Amster, I. J. Negative electron transfer dissociation of

glycosaminoglycans. *Anal. Chem.* **2010**, *82*, 3460-3466.

34. Aguilan, J. T.; Dayrit, F. M.; Zhang, J. H.; Ninonuevo, M. R.; Lebrilla, C. B. Structural analysis of alpha-carrageenan sulfated oligosaccharides by positive mode nano-ESI-FTICR-MS and MS/MS by SORI-CID. *J. Am. Soc. Mass. Spectrom.* **2006**, *17*, 96-103.

35. Liu, H.; Hakansson, K. Electron capture dissociation of tyrosine O-sulfated peptides complexed with divalent metal cations. *Anal. Chem.* **2006**, *78*, 7570-7576.

36. Harvey, D. J. Ionization and collision-induced fragmentation of N-linked and related carbohydrates using divalent canons. *J. Am. Soc. Mass. Spectrom.* **2001**, *12*, 926-937.

37. Cancilla, M. T.; Wang, A. W.; Voss, L. R.; Lebrilla, C. B. Fragmentation reactions in the mass spectrometry analysis of neutral oligosaccharides. *Anal. Chem.* **1999**, *71*, 3206-3218.

38. Sible, E. M.; Brimmer, S. P.; Leary, J. A. Interaction of first row transition metals with alpha 1-3, alpha 1-6 mannotriose and conserved trimannosyl core oligosaccharides: A comparative electrospray ionization study of doubly and singly charged complexes. *J. Am. Soc. Mass. Spectrom.* **1997**, *8*, 32-42.

39. Konig, S.; Leary, J. A. Evidence for linkage position determination in cobalt coordinated pentasaccharides using ion trap mass spectrometry. *J. Am. Soc. Mass. Spectrom.* **1998**, *9*, 1125-1134.

40. Hofmeister, G. E.; Zhou, Z.; Leary, J. A. Linkage position determination in lithium-cationized disaccharides - tandem mass-sepctrometry and semiempirical calculations *J. Am. Chem. Soc.* **1991**, *113*, 5964-5970.

41. Devakumar, A.; Mechref, Y.; Kang, P.; Novotny, M. V.; Reilly, J. P. Identification of isomeric N-glycan structures by mass spectrometry with 157 nm laser-induced photofragmentation. *J. Am. Soc. Mass. Spectrom.* **2008**, *19*, 1027-1040.

42. Xie, Y. M.; Lebrilla, C. B. Infrared multiphoton dissociation of alkali metal-coordinated oligosaccharides. *Anal. Chem.* **2003**, *75*, 1590-1598.

43. Lancaster, K. S.; An, H. J.; Li, B. S.; Lebrilla, C. B. Interrogation of N-linked oligosaccharides using infrared multiphoton dissociation in FT-ICR mass spectrometry. *Anal. Chem.* **2006**, *78*, 4990-4997.

44. An, H. J.; Miyamoto, S.; Lancaster, K. S.; Kirmiz, C.; Li, B. S.; Lam, K. S.; Leiserowitz, G. S.; Lebrilla, C. B. Profiling of glycans in serum for the discovery of potential biomarkers for ovarian cancer. *Journal of Proteome Research* **2006**, *5*, 1626-1635.

45. Pikulski, M.; Hargrove, A.; Shabbir, S. H.; Anslyn, E. V.; Brodbelt, J. S. Sequencing and characterization of oligosaccharides using infrared multiphoton dissociation and boronic acid derivatization in a quadrupole ion trap. *J. Am. Soc. Mass. Spectrom.* **2007**, *18*, 2094-2106.

46. Harvey, D. J.; Naven, T. J. P.; Kuster, B.; Bateman, R. H.; Green, M. R.; Critchley, G. Comparison of fragmentation modes for the structural determination of complex oligosaccharides ionized by matrix-assisted laser desorption/ionization mass spectrometry. *Rapid Commun. Mass Spectrom.* **1995**, *9*, 1556-1561.

47. Harvey, D. J.; Bateman, R. H.; Green, M. R. High-energy collision-induced fragmentation of complex oligosaccharides ionized by matrix-assisted laser

desorption/ionization mass spectrometry. *J. Mass Spectrom.* **1997**, *32*, 167-187.

48.   Yu, S. Y.; Wu, S. W.; Khoo, K. H. Distinctive characteristics of MALDI-Q/TOF and TOF/TOF tandem mass spectrometry for sequencing of permethylated complex type N-glycans. *Glycoconjugate J.* **2006**, *23*, 355-369.

49.   Devakumar, A.; Thompson, M. S.; Reilly, J. P. dFragmentation of oligosaccharide ions with 157 nm vacuum ultraviolet light. *Rapid Commun. Mass Spectrom.* **2005**, *19*, 2313-2320.

50.   Devakumar, A.; Mechref, Y.; Kang, P.; Novotny, M. V.; Reilly, J. P. Laser-induced photofragmentation of neutral and acidic glycans inside an ion-trap mass spectrometer. *Rapid Commun. Mass Spectrom.* **2007**, *21*, 1452-1460.

51.   Budnik, B. A.; Haselmann, K. F.; Elkin, Y. N.; Gorbach, V. I.; Zubarev, R. A. Applications of electron-ion dissociation reactions for analysis of polycationic chitooligosaccharides in Fourier transform mass spectrometry. *Anal. Chem.* **2003**, *75*, 5994-6001.

52.   McFarland, M. A.; Marshall, A. G.; Hendrickson, C. L.; Nilsson, C. L.; Fredman, P.; Mansson, J. E. Structural characterization of the GM1 ganglioside by infrared multiphoton dissociation/electron capture dissociation, and electron detachment dissociation electrospray ionization FT-ICR MS/MS. *J. Am. Soc. Mass. Spectrom.* **2005**, *16*, 752-762.

53.   Adamson, J. T.; Hakansson, K. Electron capture dissociation of oligosaccharides ionized with alkali, alkaline earth, and transition metals. *Anal. Chem.* **2007**, *79*, 2901-2910.

54.   Zhao, C.; Xie, B.; Chan, S. Y.; Costello, C. E.; O'Connor, P. B. Collisionally activated dissociation and electron capture dissociation provide complementary structural information for branched permethylated oligosaccharides. *J. Am. Soc. Mass. Spectrom.* **2008**, *19*, 138-150.

55.   Liu, H.; Hakansson, K. Analysis of sulfated oligosaccharides with combination of divalent metal complexation and electron capture dissociation. *Int. J. Mass spectrom.* **2011**, In press.

56.   Yang, J.; Mo, J. J.; Adamson, J. T.; Hakansson, K. Characterization of oligodeoxynucleotides by electron detachment dissociation Fourier transform ion cyclotron resonance mass spectrometry. *Anal. Chem.* **2005**, *77*, 1876-1882.

57.   Tsybin, Y. O.; Witt, M.; Baykut, G.; Kjeldsen, F.; Hakansson, P. Combined infrared multiphoton dissociation and electron capture dissociation with a hollow electron beam in Fourier transform ion cyclotron resonance mass spectrometry. *Rapid Commun. Mass Spectrom.* **2003**, *17*, 1759-1768.

58.   Caravatti, P.; Allemann, M. The infinity cell - a new trapped-ion cell with radiofrequency covered trapping electrodes for Fourier-transform ion-cyclotron resonance mass-spectrometry. *Org. Mass Spectrom.* **1991**, *26*, 514-518.

59.   Horn, D. M.; Ge, Y.; McLafferty, F. W. Activated ion electron capture dissociation for mass spectral sequencing of larger (42 kDa) proteins. *Anal. Chem.* **2000**, *72*, 4778-4784.

60.   Senko, M. W.; Canterbury, J. D.; Guan, S. H.; Marshall, A. G. A high-performance modular data system for Fourier transform ion cyclotron resonance mass spectrometry. *Rapid Commun. Mass Spectrom.* **1996**, *10*, 1839-1844.

61.   Ledford, E. B.; Rempel, D. L.; Gross, M. L. Space-charge effects in

Fourier-transform mass-spectrometry - mass calibration *Anal. Chem.* **1984**, *56*, 2744-2748.

62.   Lohmann, K. K.; von der Lieth, C. W. GlycoFragment and GlycoSearchMS: web tools to support the interpretation of mass spectra of complex carbohydrates. *Nucleic Acids Res.* **2004**, *32*, W261-W266.

63.   Green, E. D.; Baenziger, J. U. Asparagine-linked oligosaccharides on lutropin, follitropin, and thyrotropin. 1. structural elucidation of the sulfated and sialylated oligosaccharides on bovine, ovine, and human pituitary glycoprotein hormones *J. Biol. Chem.* **1988**, *263*, 25-35.

64.   Hakansson, K.; Cooper, H. J.; Emmett, M. R.; Costello, C. E.; Marshall, A. G.; Nilsson, C. L. Electron capture dissociation and infrared multiphoton dissociation MS/MS of an N-glycosylated tryptic peptide to yield complementary sequence information. *Anal. Chem.* **2001**, *73*, 4530-4536.

65.   Stensballe, A.; Jensen, O. N.; Olsen, J. V.; Haselmann, K. F.; Zubarev, R. A. Electron capture dissociation of singly and multiply phosphorylated peptides. *Rapid Commun. Mass Spectrom.* **2000**, *14*, 1793-1800.

66.   Shi, S. D. H.; Hemling, M. E.; Carr, S. A.; Horn, D. M.; Lindh, I.; McLafferty, F. W. Phosphopeptide/phosphoprotein mapping by electron capture dissociation mass spectrometry. *Anal. Chem.* **2001**, *73*, 19-22.

67.   Hakansson, K.; Chalmers, M. J.; Quinn, J. P.; McFarland, M. A.; Hendrickson, C. L.; Marshall, A. G. Combined electron capture and infrared multiphoton dissociation for multistage MS/MS in a Fourier transform ion cyclotron resonance mass spectrometer. *Anal. Chem.* **2003**, *75*, 3256-3262.

68.   Cooper, H. J.; Tatham, M. H.; Jaffray, E.; Heath, J. K.; Lam, T. T.; Marshall, A. G.; Hay, R. T. Fourier transform ion cyclotron resonance mass spectrometry for the analysis of small ubiquitin-like modifier (SUMO) modification: Identification of lysines in RanBP2 and SUMO targeted for modification during the E3 AutoSUMOylation reaction. *Anal. Chem.* **2005**, *77*, 6310-6319.

69.   Hakansson, K.; Hudgins, R. R.; Marshall, A. G.; O'Hair, R. A. J. Electron capture dissociation and infrared multiphoton dissociation of oligodeoxynucleotide dications. *J. Am. Soc. Mass. Spectrom.* **2003**, *14*, 23-41.

70.   Penn, S. G.; Cancilla, M. T.; Lebrilla, C. B. Collision-induced dissociation of branched oligosaccharide ions with analysis and calculation of relative dissociation thresholds. *Anal. Chem.* **1996**, *68*, 2331-2339.

Chapter 3

Electron Transfer Dissociation (ETD) vs. Electron Capture Dissociation (ECD) of Metal-adducted Oligosaccharides

3.1 Introduction

Glycans and glycoconjugates are prevalent in biological systems. About 50% of the proteins in mammalian cells are glycosylated and their glycosylation has been linked to various biological activities, including cell-cell interactions, immune responses, and different disease states.[1-6] Despite the crucial roles glycosylation play, structural elucidation of glycans and glycoconjugates is underrepresented compared to linear biomolecules such as proteins, peptides, and nucleic acids due to the highly diverse structures of glycans. Glycans are synthesized by a variety of glycosyltransferases in a non-template driven manner. Complete characterization of glycans requires information regarding monosaccharide composition, linkage, degree of branching, and anomeric configuration. Traditionally, exoglycosidase digestion, nuclear magnetic resonance (NMR) spectroscopy, X-ray crystallography, and gas chromatography/mass spectrometry (GC/MS) have all been used for structural analysis of glycans.[7] However, the sensitivity of these methods does not fulfill the need of current glycomics and glycoproteomics.

Mass spectrometry (MS) is an important tool to characterize glycans due to its high sensitivity and ability to provide accurate results.[7-10] Particularly, Fourier transform ion cyclotron resonance mass spectrometry (FT-ICR MS)[11,12] offers ultrahigh mass accuracy and high resolution, and the availability of various tandem mass spectrometric techniques (MS/MS).[13] Even though oligosaccharide profiling can be achieved by MS with high mass accuracy, detailed structural information of oligosaccharides still requires MS/MS due to their structural complexity. A variety of MS/MS approaches have been applied for oligosaccharide structural characterization, including collision activated dissociation (CAD),[14-16] infrared multiphoton dissociation (IRMPD),[17-19] high energy CAD (HeCAD),[20-22] electron capture dissociation (ECD),[23-27] electron detachment dissociation (EDD),[28-33] negative electron transfer dissociation (NETD),[34] 157 nm laser photodissociation,[35-37] and electron induced dissociation (EID).[38]

There are two types of cleavages in MS/MS of oligosaccharides.[39] Glycosidic cleavages occur between monosaccharides and provide information regarding monosaccharide composition and sequence. Cross-ring cleavages occur across sugar rings, and provide information indicating linkage type. Collision activated dissociation is the most widely used MS/MS technique. In positive-ion mode, CAD of protonated oligosaccharides mostly generates glycosidic cleavages such as B- and Y-type ions.[8,9] CAD of metal-adducted oligosaccharides has been investigated both by experimental and computational approaches, and the results demonstrated that metal-adducted oligosaccharides undergo different dissociation pathways compared to their protonated counterparts, generating more A-type cross-ring cleavages.[40-46] In particular, divalent metal cations such as Ca^{2+}, Co^{2+}, and Mg^{2+} have received increasing attention due to the

high efficiency in aiding ionization of oligosaccharides and the ability to provide more cross-ring cleavages.[41,43-45] However, CAD is a "slow-heating" technique, which preferably cleaves the weakest bonds in the gas phase. Therefore, CAD of acidic oligosaccharides such as sulfated and sialylated species, often generate product ions with loss of labile acidic groups, thus providing insufficient glycan sequence information.

ECD[47] and ETD[48] are more recently developed dissociation techniques, which can provide complementary information compared to traditionally used CAD.[49-54] In ECD, at least doubly positively charged precursor ions are irradiated with low energy (<1 eV) electrons, generating charge-reduced radical species from electron capture and product ions from radical-driven fragmentation.[47] ETD was first introduced in a radio-frequency linear quadruple ion trap to characterize peptides,[48] and later implemented on orbitrap and FT-ICR instruments.[55,56] In ETD, anion radicals transfer electrons to polycations, and induce fragmentation similar to that observed in ECD.

ECD and ETD have been widely utilized to analyze proteins and peptides, and are particularly powerful for characterization of protein post-translational modifications, such as phosphorylation, glycosylation, methylation, acetylation, and disulfide bonds.[54,57-70] However, the application of ion-electron and ion-ion reactions towards structural characterization of oligosaccharides has just begun to emerge. ECD was first applied to analyze aminoglycans, which could easily form multiply positively charged precursor ions.[25] Several groups have utilized metal cations to aid the generation of multiply charged precursor ions, which are required for ECD.[23,24] Our group examined complexes formed between model oligosaccharides and alkali, alkaline earth, and transition metals by ECD and IRMPD (CAD) and observed complementary fragmentation patterns from

those species.[24] O'Connor and co-workers explored CAD and hot ECD (i.e., ECD with

~10 eV electrons)[71] of sodiated permethylated oligosaccharides, and observed

complementary fragmentation patterns for branched N-linked glycans.[23] Here, we

investigate ECD and ETD of metal-adducted oligosaccharides, and compare the

fragmentation behaviors of these two approaches.

3.2 Experimental

3.2.1 Sample Preparation

2 µM p-lacto-N-hexaose (pLNH), or lacto-N-difucohexaose (LNDFH), or an

asialo N-linked glycan (NA2) (V-labs Inc, Covington, LA), were mixed with 8 µM cobalt

bromide (Fisher, Fair Lawn, NJ) in 50% methanol/H_2O (v/v) for mass spectrometry

analysis.

3.2.2 FT-ICR Mass Spectrometry

All mass spectra were collected with an actively shielded 7-T FT-ICR mass

spectrometer with a quadrupole front-end (Solarix, Bruker Daltonics, Billerica, MA). An

indirectly heated hollow dispenser cathode was used to perform ECD.[72] Samples were

infused via an electrospray ion source at a flow rate of 70 µL/h with the assistance of N_2

nebulizing gas. Following ion accumulation in the front octopole for 0.05 s, ions were

mass selectively accumulated in a hexapole collision cell for 0.5 - 1 s. Ions were then

transferred through a transfer hexapole and captured with sidekick trapping in an Infinity

ICR cell.[73] The accumulation sequence up to the ICR cell fill was looped 3 times to

optimize precursor ion signal to noise (S/N) ratio. External CAD was performed in the

hexapole collision cell following mass selective ion accumulation with argon as collision

gas. For ECD, the cathode heating current was kept constant at 1.6 A and the cathode

voltage was pulsed during the ECD event to a bias voltage of - 1.0 V for 200 - 300 ms to generate low energy electrons. For ETD, ETD reagent (fluoranthene, Sigma-Aldrich, St. Louis, WO) anions were produced externally in the CI source, admitted to the collision cell for 300 - 500 ms, and allowed to react with the precursor ions for 300 - 500 ms.

3.2.3 Data Analysis

All mass spectra were acquired with SolarixControl software (Bruker Daltonics) with 256 data points from m/z 100 to 2000 and summed over 50 - 80 scans. Data processing was performed with Data Analysis software (Bruker Daltonics). Calibration was performed by the Internal Calibration function in Data Analysis software. Product ion spectra were interpreted with the aid of GlycoWorkbench software.[74] Product ions were not assigned unless the S/N ratio was at least 3.

3.3 Results and Discussion

MS/MS spectra were assigned based on the Domon and Costello nomenclature.[39] Glycosidic cleavages generate B-, C-, Y-, Z-type ions and cross-ring cleavages yield A- and X-type ions. When more than one product assignment was possible based on the m/z value, all assignments are listed. For branched oligosaccharides, the letter α represents the largest branch and the letter β represents the second largest branch.

3.3.1 MS/MS of *p*LNH

*p*LNH   is   a   linear   oligosaccharide   with   the   composition Galβ3GlcNAcβ3Galβ4GlcNAcβ3Galβ4Glc. Figure 3.1 displays ECD, ETD, and CAD spectra of cobalt-adducted *p*LNH. Doubly charged *p*LNH ((M + Co)$^{2+}$) underwent extensive fragmentation in ECD (Figure 3.1a), generating five glycosidic and nine cross-ring cleavages, including ^{0,2}A-, ^{0,3}A-, ^{1,4}A-, ^{2,4}A-, and ^{3,5}A-type ions. Leary and co-

workers investigated the influence of cobalt adducts in CAD fragmentation and found that cobalt cations promoted cross-ring fragmentation.[41,45] In ECD, all product ions were singly charged (as expected), and most of them bore the cobalt cation. The charge-reduced species was not observed. Instead, the "proton-stripped" species $(M + Co - H)^+$ was detected, which has been previously reported for ECD of metal-adducted oligosaccharides.[24] The Y_4 ion (m/z = 765.17) was the most abundant species in the spectrum.

ETD of cobalt-adducted pLNH showed similar fragmentation pathways compared to ECD (Figure 3.1b): almost all product ions detected in ETD were also observed in ECD, with C_4 ions constituting an exception. It is noteworthy that the proton-stripped species $(M + Co - H)^+$ in the ETD spectrum had a relative abundance of 80%, which is comparable to the precursor ion $(M + Co)^{2+}$, while the same species in ECD was only 2.5%. Three glycosidic cleavages and three cross-ring cleavages were observed in ETD but the most abundant product ion was $Y_4 - 16$ Da (or $Z_4 + 2H$)[33] instead of Y_4. This ion was unique to ETD of pLNH. Y – 16 Da fragments have previously been reported in EDD spectra of oligosaccharides and glycosaminoglycans (GAGs), but they are not frequently observed in ECD.[28-33,75] Several peaks in the ETD spectrum could not be assigned. Those peaks were not present in the ECD spectrum, suggesting unique dissociation pathways in ETD.
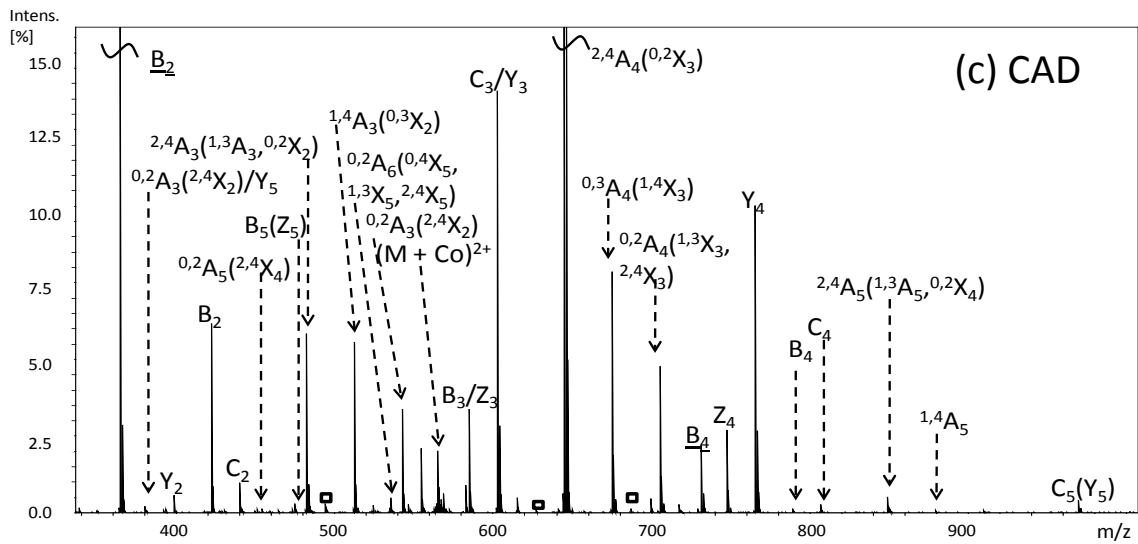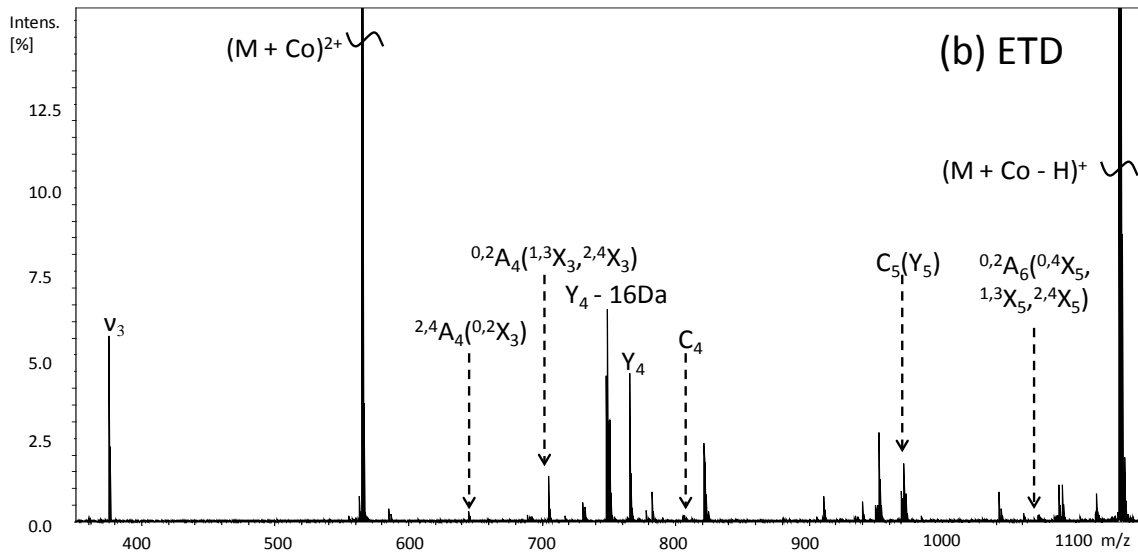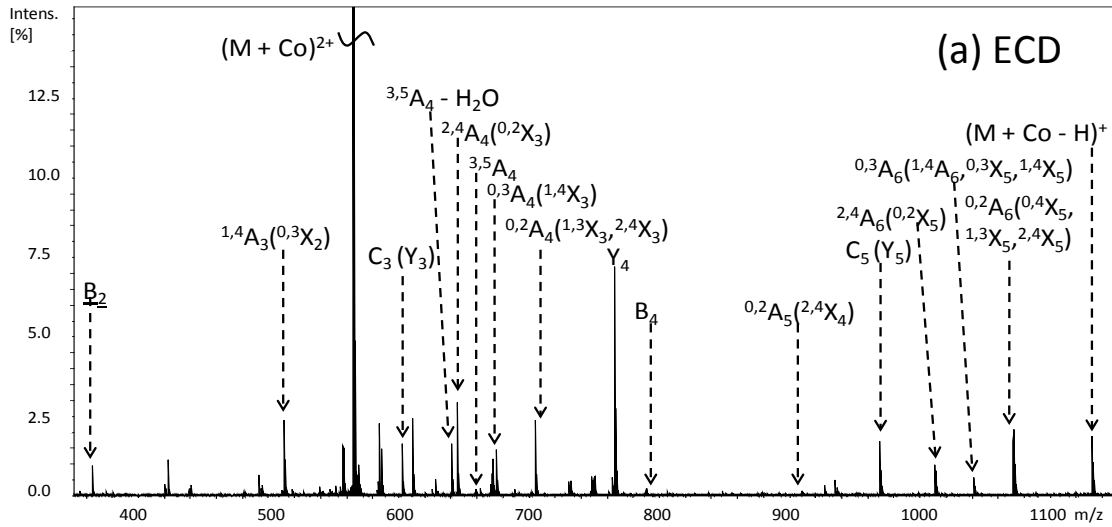
Figure 3.1. FT-ICR tandem mass spectra of Co^{2+}-adducted pLNH. (a) ECD (60 scans, 80 ms electron irradiation with a bias voltage of $-$ 1.0 V); (b) ETD (60 scans, 400 ms reagent accmulation time and 400 ms reaction time); (c) CAD (60 scans, collision voltage 6.0 V). Product ions are underlined if they lack a cobalt cation. Fragmentation patterns from ECD, ETD, and CAD are summarized at the bottom. If more than one assignment was possible, the alternative one is indicated in brackets (for spectra only). Squares indicate water loss from the adjacent product ion. v_3 indicates the third harmonic peak of the precursor ion.

The fragmentation behavior in CAD of the same species was significantly different from ECD and ETD. Eleven glycosidic and eleven cross-ring fragments were observed, including several doubly charged species. Series of B-, C-, ^{0,2}A-, and ^{2,4}A-type ions were observed, providing rich structural information both regarding oligosaccharide sequence and linkage type. Compared to CAD, ECD yielded several unique cross-ring fragment ions, including ^{3,5}A_4, ^{2,4}A_6, and ^{0,3}A_6 ions. In all three dissociation techniques, ETD provided the least structural information for pLNH.

3.3.2 MS/MS of LNDFH

LNDFH is a branched oligosaccharide with the composition Galβ3(Fucα4)GlcNAcβ3Galβ4Glc. ECD and ETD fragmentation patterns are compared in Figure 3.2. ECD of cobalt-adducted doubly charged LNDFH yielded seven glycosidic cleavages and four cross-ring cleavages. Glycosidic fragments between every neighboring monosaccharide were observed, providing extensive structural information regarding monosaccharide composition and sequence. All product ions were singly charged and contained the cobalt cation. Fucose losses from the precursor ion, glycosidic fragments, and cross-ring fragments were abundant in the ECD spectrum.[76] This observation may be attributed to the high secondary ionization potential of cobalt.[43]

ETD of the same species is displayed in Figure 3.2b. Again, the fragmentation patterns from ETD and ECD are similar, yielding seven glycosidic and two cross-ring cleavages. Most product ions were observed between m/z 500 and 1000, and only one product ion was observed in the low m/z range (400 - 500) in the ETD spectrum. In contrast, more product ions from ECD fragmentation were detected between m/z 400 and 500, most of which were unique to ECD, such as $^{1,3}A_3$, $^{1,4}X_2$, B_3 – fucose, and C_3 – fucose. This phenomenon may be attributed to the time-of-flight effect in FT-ICR MS,[77,78] which arises from the fact that ions generated in the hexapole collision cell need to travel a certain distance prior to entering the detector, while those generated in the ICR cell do not. Similar to MS/MS of pLNH, the proton-stripped species of LNDFH was of low abundance in ECD, while the same species had a relative abundance of 45 % in ETD. This observation indicates that additional activation may be required for successful ETD to enhance the generated structural information.
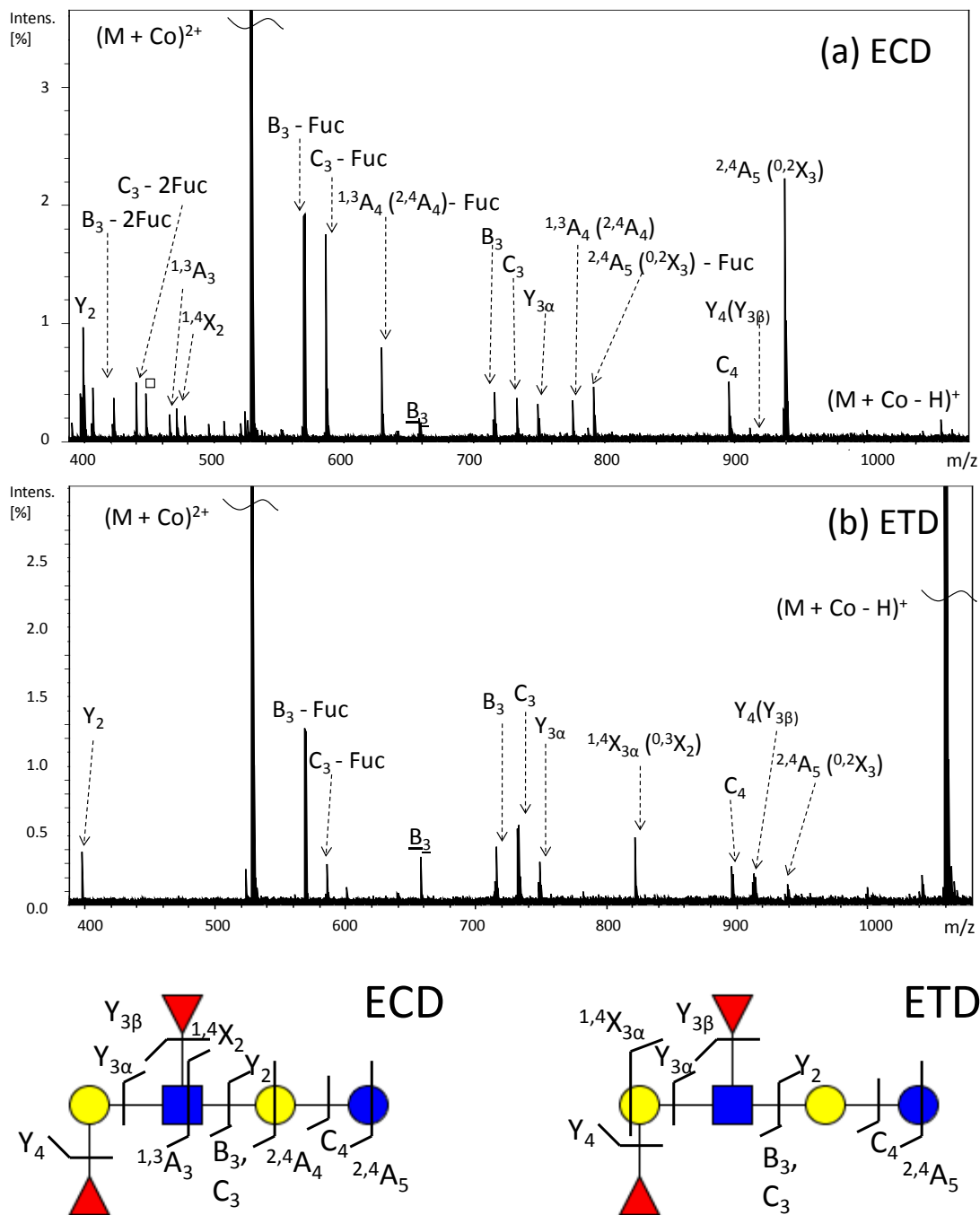
Figure 3.2. FT-ICR tandem mass spectra of Co^{2+}-adducted LNDFH. (a) ECD (50 scans, 200 ms electron irradiation with a bias voltage of $-$ 1.0 V); (b) ETD (50 scans, 500 ms reagent accmulation time and 500 ms reaction time). Product ions are underlined if they lack a cobalt cation. Fragmentation patterns from ECD and ETD are summarized at the bottom. If more than one assignment was possible, the alternative one is indicated in brackets (for spectra only). Squares indicate water loss from the adjacent product ion.

71

3.3.3 MS/MS of NA2

NA2 is a branched asialo N-linked glycan (see Figure 3.3 for structure). ECD and ETD demonstrated drastically different fragmentation behaviors. ECD of cobalt-adducted doubly charged NA2 induced extensive fragmentation, and produced nine glycosidic and four cross-ring product ions (Figure 3.3a). Glycosidic cleavages between every adjacent monosaccharide provided extensive information regarding glycan sequence, and cross-ring cleavages aided the determination of linkage types. In addition, $Y - 16$ Da $(Z + 2H)$ ions, loss of 42 Da from glycosidic fragments, and internal fragments were observed in the ECD spectrum. Loss of 42 Da likely corresponds to loss of a ketene molecule (CH_2CO) from N-acetylglucosamine, as previously reported.[24,25] ETD of the same species only yielded one glycosidic fragment (Y_4, $m/z = 1333.39$), demonstrating a significantly different fragmentation pattern (Figure 3.3b). When increasing the ETD reagent accumulation time and ETD reaction time, the abundance of the proton-stripped species increased, however, no additional fragments were observed. This phenomenon is further discussed below.

For comparison, CAD of the same species was also investigated and the fragmentation pattern is displayed in Figure 3.3. CAD generated ten glycosidic and five cross-ring cleavages. Compared to CAD, ECD yielded three unique product ions, including Y_5, $^{0,2}A_5$, and $^{1,4}X_3$ ions. The Y_5 ion determined the glycan sequence to be (Hex)(HexNAc) rather than (HexNAc)(Hex) from the non-reducing end, and the two cross-ring cleavages aided the determination of glycan linkage type. Therefore, ECD is a valuable tool for glycan structural analysis due to its ability to provide complementary structural information compared to CAD.
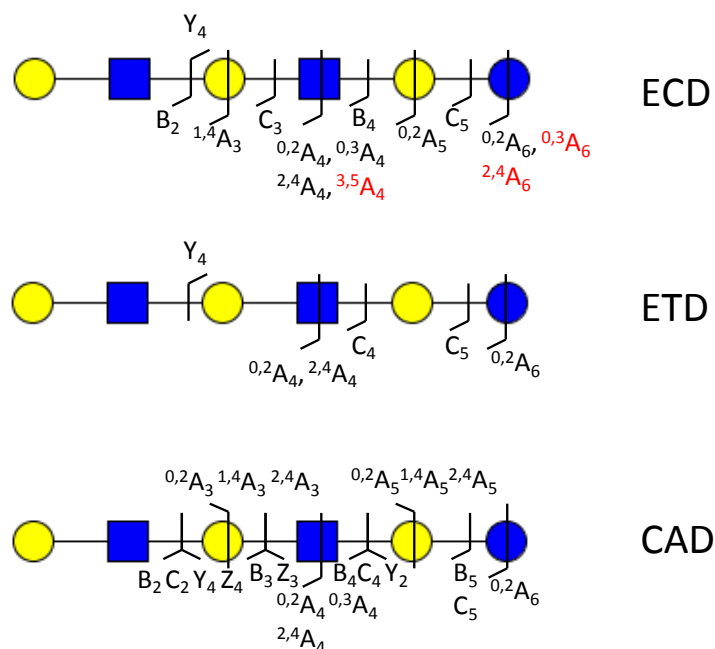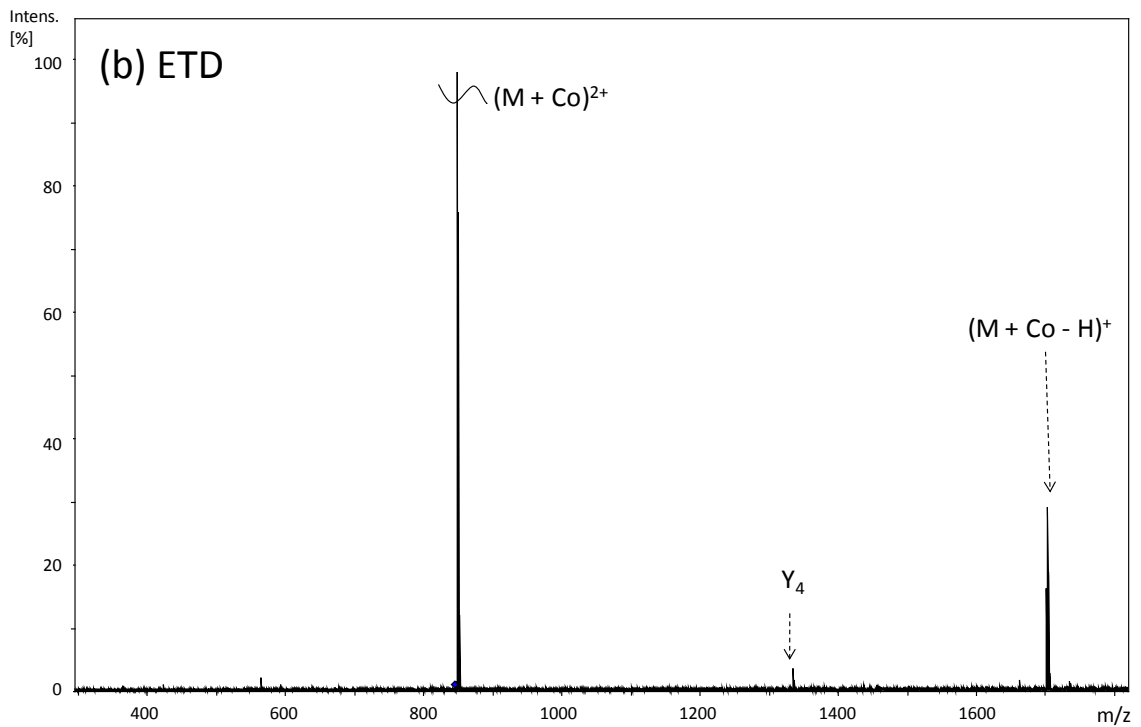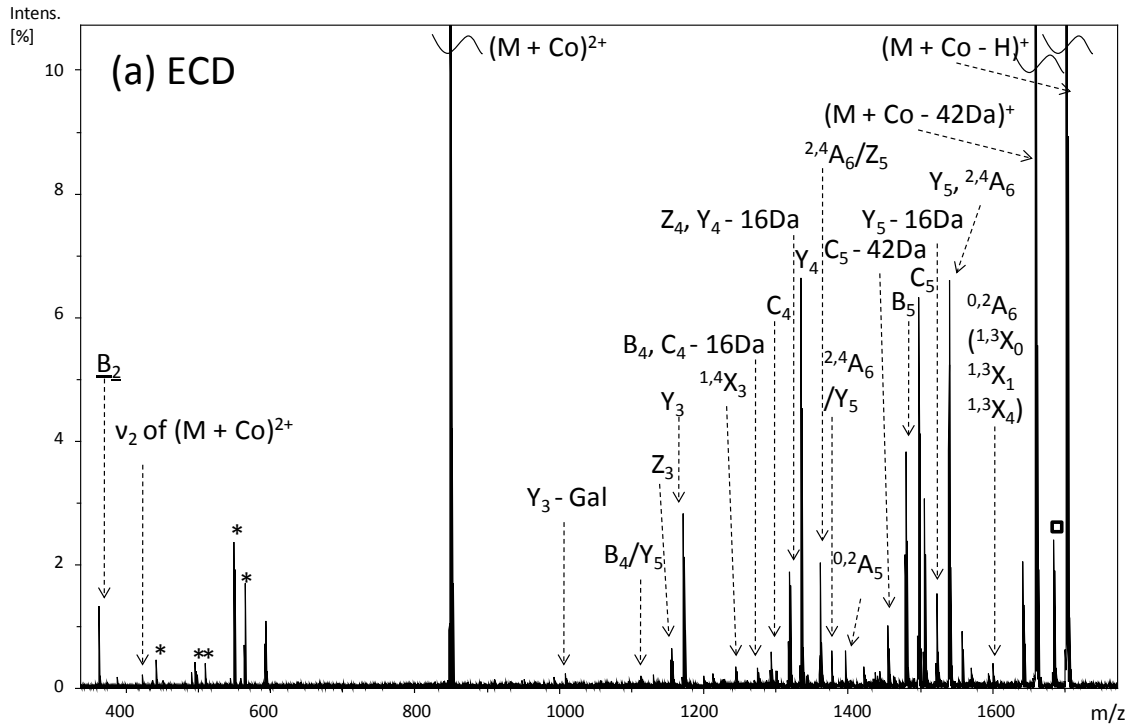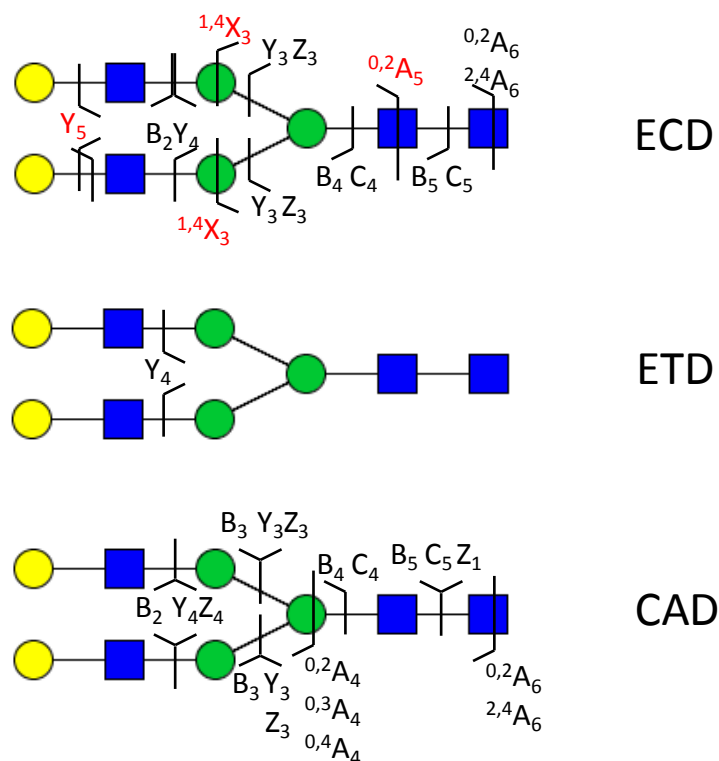
Figure 3.3. FT-ICR tandem mass spectra of Co^{2+}-adducted NA2. (a) ECD (80 scans, 300 ms electron irradiation with a bias voltage of – 1.0 V); (b) ETD (80 scans, 500 ms reagent accmulation time and 500 ms reaction time). Product ions are underlined if they lack a cobalt cation. Fragmentation patterns from ECD, ETD, and CAD are summarized at the bottom. If more than one assignment was possible, the alternative one is indicated in brackets (for spectra only). Squares indicate water loss from adjacent product ions. Fragments highlighted in red are unique to ECD.

3.3.4 ECD vs. ETD of Metal-adducted Oligosaccharides

In general, ECD and ETD of proteins and peptides result in similar fragmentation pathways.[49-54] Both ECD and ETD fragmentation efficiency improve with higher precursor ion charge state.[79-82] Furthermore, due to generation of fewer backbone c and z$^{\bullet}$ ions, lower charge state precursor ions tend to yield more non-dissociative electron capture or electron transfer species for proteins and peptides.[81] This phenomenon is in accordance with our observation for the cobalt-adducted oligosaccharides. For all three

oligosaccharides examined, abundant proton-stripped species were observed in ETD without further dissociation. For smaller oligosaccharides, the difference between ECD and ETD fragmentation patterns was less distinct. For the larger oligosaccharide NA2, ECD generated extensive fragmentation while ETD only generated the non-dissociated electron transfer species. This behavior may be attributed to the different pressure during ECD and ETD events. ECD occurs at ultrahigh vacuum in the ICR cell, at a pressure of less than 10^{-9} Torr. ETD occurs at relativity high pressure ($\sim 10^{-3}$ Torr), and thus the precursor ions are in a less "activated" state than in ECD due to pressure cooling effects. Therefore, the energy deposited through Coulomb relaxation upon electron capture/transfer may not be sufficient to fragment large oligosaccharides such as NA2. In contrast, because the precursor ions in ECD are more "activated" due to lack of a cooling mechanism in the ICR cell, dissociation of the oligosaccharide can still occur.

3.4 Conclusions

We investigated ECD and ETD of metal-adducted oligosaccharides, and compared the fragmentation patterns from these two radical-driven dissociation techniques. For doubly charged small oligosaccharides, ECD and ETD fragmentation patterns were similar, both generating glycosidic and cross-ring cleavages. For a doubly charged N-linked glycan, ECD yielded extensive fragment, providing rich structural information regarding glycan sequence and linkage type. In contrast, ETD only generated extensive proton-stripped species and one glycosidic cleavage with low abundance. The significant difference in fragmentation behaviors may be attributed to the conditions under which ECD and ETD occur.

3.5 References

1. Varki, A. Biological roles of oligosaccharides - All of the theories are correct. *Glycobiol.* **1993**, *3*, 97-130.
2. Dwek, R. A. Glycobiology: Toward understanding the function of sugars. *Chem. Rev.* **1996**, *96*, 683-720.
3. Bertozzi, C. R.; Kiessling, L. L. Chemical glycobiology. *Science* **2001**, *291*, 2357-2364.
4. van den Steen, P.; Rudd, P. M.; Dwek, R. A.; Opdenakker, G. Concepts and principles of O-linked glycosylation. *Crit. Rev. Biochem. Mol. Biol.* **1998**, *33*, 151-208.
5. Hakomori, S. Glycosylation defining cancer malignancy: New wine in an old bottle. *Proc. Natl. Acad. Sci. U. S. A.* **2002**, *99*, 10231-10233.
6. Dube, D. H.; Bertozzi, C. R. Glycans in cancer and inflammation. Potential for therapeutics and diagnostics. *Nat. Rev. Drug Discov.* **2005**, *4*, 477-488.
7. Mechref, Y.; Novotny, M. V. Structural investigations of glycoconjugates at high sensitivity. *Chem. Rev.* **2002**, *102*, 321-369.
8. Harvey, D. J. Matrix-assisted laser desorption/ionization mass spectrometry of carbohydrates. *Mass Spectrom. Rev.* **1999**, *18*, 349-450.
9. Zaia, J. Mass spectrometry of oligosaccharides. *Mass Spectrom. Rev.* **2004**, *23*, 161-227.
10. Zaia, J. Mass spectrometry and the emerging field of glycomics. *Chem. Biol.* **2008**, *15*, 881-892.
11. Marshall, A. G.; Hendrickson, C. L.; Jackson, G. S. Fourier transform ion cyclotron resonance mass spectrometry: A primer. *Mass Spectrom. Rev.* **1998**, *17*, 1-35.
12. Marshall, A. G.; Hendrickson, C. L. High-resolution mass spectrometers. *Annu. Rev. Anal. Chem.* **2008**, *1*, 579-599.
13. Park, Y. M.; Lebrilla, C. B. Application of Fourier transform ion cyclotron resonance mass spectrometry to oligosaccharides. *Mass Spectrom. Rev.* **2005**, *24*, 232-264.
14. Harvey, D. J. Collision-induced fragmentation of negative ions from N-linked glycans derivatized with 2-aminobenzoic acid. *J. Mass Spectrom.* **2005**, *40*, 642-653.
15. Sagi, D.; Peter-Katalinic, J.; Conradt, H. S.; Nimtz, M. Sequencing of tri- and tetraantennary N-glycans containing sialic acid by negative mode ESI QTOF tandem MS. *J. Am. Soc. Mass. Spectrom.* **2002**, *13*, 1138-1148.
16. Zaia, J.; Miller, M. J. C.; Seymour, J. L.; Costello, C. E. The role of mobile protons in negative ion CID of oligosaccharides. *J. Am. Soc. Mass. Spectrom.* **2007**, *18*, 952-960.
17. Lancaster, K. S.; An, H. J.; Li, B. S.; Lebrilla, C. B. Interrogation of N-linked oligosaccharides using infrared multiphoton dissociation in FT-ICR mass spectrometry. *Anal. Chem.* **2006**, *78*, 4990-4997.
18. Xie, Y. M.; Lebrilla, C. B. Infrared multiphoton dissociation of alkali metal-coordinated oligosaccharides. *Anal. Chem.* **2003**, *75*, 1590-1598.

19. Zhang, J. H.; Schubothe, K.; Li, B. S.; Russell, S.; Lebrilla, C. B. Infrared multiphoton dissociation of O-linked mucin-type oligosaccharides. *Anal. Chem.* **2005**, *77*, 208-214.

20. Harvey, D. J.; Naven, T. J. P.; Kuster, B.; Bateman, R. H.; Green, M. R.; Critchley, G. Comparison of fragmentation modes for the structural determination of complex oligosaccharides ionized by matrix-assisted laser desorption/ionization mass spectrometry. *Rapid Commun. Mass Spectrom.* **1995**, *9*, 1556-1561.

21. Harvey, D. J.; Bateman, R. H.; Green, M. R. High-energy collision-induced fragmentation of complex oligosaccharides ionized by matrix-assisted laser desorption/ionization mass spectrometry. *J. Mass Spectrom.* **1997**, *32*, 167-187.

22. Lewandrowski, U.; Resemann, A.; Sickmann, A. Laser-induced dissociation/high-energy collision-induced dissociation fragmentation using MALDI-TOF/TOF-MS instrumentation for the analysis of neutral and acidic oligosaccharides. *Anal. Chem.* **2005**, *77*, 3274-3283.

23. Zhao, C.; Xie, B.; Chan, S. Y.; Costello, C. E.; O'Connor, P. B. Collisionally activated dissociation and electron capture dissociation provide complementary structural information for branched permethylated oligosaccharides. *J. Am. Soc. Mass. Spectrom.* **2008**, *19*, 138-150.

24. Adamson, J. T.; Hakansson, K. Electron capture dissociation of oligosaccharides ionized with alkali, alkaline earth, and transition metals. *Anal. Chem.* **2007**, *79*, 2901-2910.

25. Budnik, B. A.; Haselmann, K. F.; Elkin, Y. N.; Gorbach, V. I.; Zubarev, R. A. Applications of electron-ion dissociation reactions for analysis of polycationic chitooligosaccharides in Fourier transform mass spectrometry. *Anal. Chem.* **2003**, *75*, 5994-6001.

26. McFarland, M. A.; Marshall, A. G.; Hendrickson, C. L.; Nilsson, C. L.; Fredman, P.; Mansson, J. E. Structural characterization of the GM1 ganglioside by infrared multiphoton dissociation/electron capture dissociation, and electron detachment dissociation electrospray ionization FT-ICR MS/MS. *J. Am. Soc. Mass. Spectrom.* **2005**, *16*, 752-762.

27. Liu, H.; Hakansson, K., Analysis of Sulfated Oligosaccharides with Combination of Divalent Metal Complexation and Electron Capture Dissociation. In *Int. J. Mass spectrom.*, 2010.

28. Wolff, J. J.; Chi, L. L.; Linhardt, R. J.; Amster, I. J. Distinguishing glucuronic from iduronic acid in glycosaminoglycan tetrasaccharides by using electron detachment dissociation. *Anal. Chem.* **2007**, *79*, 2015-2022.

29. Wolff, J. J.; Laremore, T. N.; Busch, A. M.; Linhardt, R. J.; Amster, I. J. Electron detachment dissociation of dermatan sulfate oligosaccharides. *J. Am. Soc. Mass. Spectrom.* **2008**, *19*, 294-304.

30. Wolff, J. J.; Laremore, T. N.; Busch, A. M.; Linhardt, R. J.; Amster, I. J. Influence of charge state and sodium cationization on the electron detachment dissociation and infrared multiphoton dissociation of glycosaminoglycan oligosaccharides. *J. Am. Soc. Mass. Spectrom.* **2008**, *19*, 790-798.

31. Wolff, J. J.; Amster, I. J.; Chi, L. L.; Linhardt, R. J. Electron detachment dissociation of glycosaminoglycan tetrasaccharides. *J. Am. Soc. Mass. Spectrom.* **2007**, *18*, 234-244.

32. Wolff, J. J.; Laremore, T. N.; Leach, F. E.; Linhardt, R. J.; Amster, I. J. Electron capture dissociation, electron detachment dissociation and infrared multiphoton dissociation of sucrose octasulfate. *Eur. J. Mass Spectrom.* **2009**, *15*, 275-281.

33. Adamson, J. T.; Hakansson, K. Electron detachment dissociation of neutral and sialylated oligosaccharides. *J. Am. Soc. Mass. Spectrom.* **2007**, *18*, 2162-2172.

34. Wolff, J. J.; Leach, F. E.; Laremore, T. N.; Kaplan, D. A.; Easterling, M. L.; Linhardt, R. J.; Amster, I. J. Negative electron transfer dissociation of glycosaminoglycans. *Anal. Chem.* **2010**, *82*, 3460-3466.

35. Devakumar, A.; Thompson, M. S.; Reilly, J. P. dFragmentation of oligosaccharide ions with 157 nm vacuum ultraviolet light. *Rapid Commun. Mass Spectrom.* **2005**, *19*, 2313-2320.

36. Devakumar, A.; Mechref, Y.; Kang, P.; Novotny, M. V.; Reilly, J. P. Identification of isomeric N-glycan structures by mass spectrometry with 157 nm laser-induced photofragmentation. *J. Am. Soc. Mass. Spectrom.* **2008**, *19*, 1027-1040.

37. Devakumar, A.; Mechref, Y.; Kang, P.; Novotny, M. V.; Reilly, J. P. Laser-induced photofragmentation of neutral and acidic glycans inside an ion-trap mass spectrometer. *Rapid Commun. Mass Spectrom.* **2007**, *21*, 1452-1460.

38. Gao, D.; Zhou, W.; Hakansson, K. In *Electron induced dissociation (EID) of singly protonated glycans*, 58th ASMS Conference on Mass Spectrometry and Allied Topics, Salt Lake City, UT, 2010.

39. Domon, B.; Costello, C. E. A systematic nomenclature for carbohydrate fragmentations in FAB-MS MS spectra of glycoconjugates *Glycoconj. J.* **1988**, *5*, 397-409.

40. Cancilla, M. T.; Penn, S. G.; Carroll, J. A.; Lebrilla, C. B. Coordination of alkali metals to oligosaccharides dictates fragmentation behavior in matrix assisted laser desorption ionization Fourier transform mass spectrometry. *J. Am. Chem. Soc.* **1996**, *118*, 6736-6745.

41. Sible, E. M.; Brimmer, S. P.; Leary, J. A. Interaction of first row transition metals with alpha 1-3, alpha 1-6 mannotriose and conserved trimannosyl core oligosaccharides: A comparative electrospray ionization study of doubly and singly charged complexes. *J. Am. Soc. Mass. Spectrom.* **1997**, *8*, 32-42.

42. Cancilla, M. T.; Wang, A. W.; Voss, L. R.; Lebrilla, C. B. Fragmentation reactions in the mass spectrometry analysis of neutral oligosaccharides. *Anal. Chem.* **1999**, *71*, 3206-3218.

43. Harvey, D. J. Ionization and collision-induced fragmentation of N-linked and related carbohydrates using divalent canons. *J. Am. Soc. Mass. Spectrom.* **2001**, *12*, 926-937.

44. Hofmeister, G. E.; Zhou, Z.; Leary, J. A. Linkage position determination in lithium-cationized disaccharides - tandem mass-sepctrometry and semiempirical calculations *J. Am. Chem. Soc.* **1991**, *113*, 5964-5970.

45. Konig, S.; Leary, J. A. Evidence for linkage position determination in cobalt coordinated pentasaccharides using ion trap mass spectrometry. *J. Am. Soc. Mass. Spectrom.* **1998**, *9*, 1125-1134.

46. Suzuki, H.; Kameyama, A.; Tachibana, K.; Narimatsu, H.; Fukui, K. Computationally and experimentally derived general rules for fragmentation of various glycosyl bonds in sodium adduct oligosaccharides. *Anal. Chem.* **2009**, *81*, 1108-1120.

47. Zubarev, R. A.; Kelleher, N. L.; McLafferty, F. W. Electron capture dissociation of multiply charged protein cations. A nonergodic process. *J. Am. Chem. Soc.* **1998**, *120*, 3265-3266.

48. Syka, J. E. P.; Coon, J. J.; Schroeder, M. J.; Shabanowitz, J.; Hunt, D. F. Peptide and protein sequence analysis by electron transfer dissociation mass spectrometry. *Proc. Natl. Acad. Sci. U. S. A.* **2004**, *101*, 9528-9533.

49. Zubarev, R. A. Reactions of polypeptide ions with electrons in the gas phase. *Mass Spectrom. Rev.* **2003**, *22*, 57-77.

50. Hakansson, K.; Cooper, H. J.; Hudgins, R. R.; Nilsson, C. L. High resolution tandem mass spectrometry for structural biochemistry. *Curr. Org. Chem.* **2003**, *7*, 1503-1525.

51. Cooper, H. J.; Hakansson, K.; Marshall, A. G. The role of electron capture dissociation in biomolecular analysis. *Mass Spectrom. Rev.* **2005**, *24*, 201-222.

52. McLuckey, S. A.; Stephenson, J. L. Ion ion chemistry of high-mass multiply charged ions. *Mass Spectrom. Rev.* **1998**, *17*, 369-407.

53. Mikesh, L. M.; Ueberheide, B.; Chi, A.; Coon, J. J.; Syka, J. E. P.; Shabanowitz, J.; Hunt, D. F. The utility of ETD mass spectrometry in proteomic analysis. *BBA-Proteins Proteomics* **2006**, *1764*, 1811-1822.

54. Wiesner, J.; Premsler, T.; Sickmann, A. Application of electron transfer dissociation (ETD) for the analysis of posttranslational modifications. *Proteomics* **2008**, *8*, 4466-4483.

55. McAlister, G. C.; Phanstiel, D.; Good, D. M.; Berggren, W. T.; Coon, J. J. Implementation of electron-transfer dissociation on a hybrid linear ion trap-orbitrap mass spectrometer. *Anal. Chem.* **2007**, *79*, 3525-3534.

56. Kaplan, D. A.; Hartmer, R.; Speir, J. P.; Stoermer, C.; Gumerov, D.; Easterling, M. L.; Brekenfeld, A.; Kim, T.; Laukien, F.; Park, M. A. Electron transfer dissociation in the hexapole collision cell of a hybrid quadrupole-hexapole Fourier transform ion cyclotron resonance mass spectrometer. *Rapid Commun. Mass Spectrom.* **2008**, *22*, 271-278.

57. Mirgorodskaya, E.; Roepstorff, P.; Zubarev, R. A. Localization of O-glycosylation sites in peptides by electron capture dissociation in a fourier transform mass spectrometer. *Anal. Chem.* **1999**, *71*, 4431-4436.

58. Stensballe, A.; Jensen, O. N.; Olsen, J. V.; Haselmann, K. F.; Zubarev, R. A. Electron capture dissociation of singly and multiply phosphorylated peptides. *Rapid Commun. Mass Spectrom.* **2000**, *14*, 1793-1800.

59. Hakansson, K.; Cooper, H. J.; Emmett, M. R.; Costello, C. E.; Marshall, A. G.; Nilsson, C. L. Electron capture dissociation and infrared multiphoton dissociation MS/MS of an N-glycosylated tryptic peptide to yield complementary sequence information. *Anal. Chem.* **2001**, *73*, 4530-4536.

60. Shi, S. D. H.; Hemling, M. E.; Carr, S. A.; Horn, D. M.; Lindh, I.; McLafferty, F. W. Phosphopeptide/phosphoprotein mapping by electron capture dissociation mass spectrometry. *Anal. Chem.* **2001**, *73*, 19-22.

61. Hakansson, K.; Emmett, M. R.; Hendrickson, C. L.; Marshall, A. G. High-sensitivity electron capture dissociation tandem FTICR mass spectrometry of microelectrosprayed peptides. *Anal. Chem.* **2001**, *73*, 3605-3610.

62. Hakansson, K.; Chalmers, M. J.; Quinn, J. P.; McFarland, M. A.; Hendrickson, C. L.; Marshall, A. G. Combined electron capture and infrared multiphoton dissociation for multistage MS/MS in a Fourier transform ion cyclotron resonance mass spectrometer. *Anal. Chem.* **2003**, *75*, 3256-3262.

63. Mormann, M.; Paulsen, H.; Peter-Katalinic, J. Electron capture dissociation of O-glycosylated peptides: radical site-induced fragmentation of glycosidic bonds. *Eur. J. Mass Spectrom.* **2005**, *11*, 497-511.

64. Hogan, J. M.; Pitteri, S. J.; Chrisman, P. A.; McLuckey, S. A. Complementary structural information from a tryptic N-linked glycopeptide via electron transfer ion/ion reactions and collision-induced dissociation. *J. Proteome Res.* **2005**, *4*, 628-632.

65. Adamson, J. T.; Hakansson, K. Infrared multiphoton dissociation and electron capture dissociation of high-mannose type glycopeptides. *J. Proteome Res.* **2006**, *5*, 493-501.

66. Liu, H.; Hakansson, K. Electron capture dissociation of tyrosine O-sulfated peptides complexed with divalent metal cations. *Anal. Chem.* **2006**, *78*, 7570-7576.

67. Liu, H. C.; Hakansson, K.; Lee, J. Y.; Sherman, D. H. Collision-activated dissociation, infrared multiphoton dissociation, and electron capture dissociation of the Bacillus anthracis siderophore petrobactin and its metal ion complexes. *J. Am. Soc. Mass. Spectrom.* **2007**, *18*, 842-849.

68. Catalina, M. I.; Koeleman, C. A. M.; Deelder, A. M.; Wuhrer, M. Electron transfer dissociation of N-glycopeptides: loss of the entire N-glycosylated asparagine side chain. *Rapid Commun. Mass Spectrom.* **2007**, *21*, 1053-1061.

69. Sihlbom, C.; Hard, I. V.; Lidell, M. E.; Noll, T.; Hansson, G. C.; Backstrom, M. Localization of O-glycans in MUC1 glycoproteins using electron-capture dissociation fragmentation mass spectrometry. *Glycobiol.* **2009**, *19*, 375-381.

70. Alley, W. R.; Mechref, Y.; Novotny, M. V. Characterization of glycopeptides by combining collision-induced dissociation and electron-transfer dissociation mass spectrometry data. *Rapid Commun. Mass Spectrom.* **2009**, *23*, 161-170.

71. Haselmann, K. F.; Budnik, B. A.; Kjeldsen, F.; Nielsen, M. L.; Olsen, J. V.; Zubarev, R. A. Electronic excitation gives informative fragmentation of polypeptide cations and anions. *Eur. J. Mass Spectrom.* **2002**, *8*, 117-121.

72. Tsybin, Y. O.; Witt, M.; Baykut, G.; Kjeldsen, F.; Hakansson, P. Combined infrared multiphoton dissociation and electron capture dissociation with a hollow electron beam in Fourier transform ion cyclotron resonance mass spectrometry. *Rapid Commun. Mass Spectrom.* **2003**, *17*, 1759-1768.

73. Caravatti, P.; Allemann, M. The infinity cell - a new trapped-ion cell with radiofrequency covered trapping electrodes for Fourier-transform ion-cyclotron resonance mass-spectrometry. *Org. Mass Spectrom.* **1991**, *26*, 514-518.

74. Ceroni, A.; Maass, K.; Geyer, H.; Geyer, R.; Dell, A.; Haslam, S. M. GlycoWorkbench: A tool for the computer-assisted annotation of mass spectra of Glycans. *J. Proteome Res.* **2008**, *7*, 1650-1659.

75. Wolff, J. J.; Laremore, T. N.; Aslam, H.; Linhardt, R. J.; Amster, I. J. Electron-induced dissociation of glycosaminoglycan tetrasaccharides. *J. Am. Soc. Mass. Spectrom.* **2008**, *19*, 1449-1458.

76. Penn, S. G.; Cancilla, M. T.; Lebrilla, C. B. Collision-induced dissociation of branched oligosaccharide ions with analysis and calculation of relative dissociation thresholds. *Anal. Chem.* **1996**, *68*, 2331-2339.

77. Sze, T. P. E.; Chan, T. W. D. Time-of-flight effects in matrix-assisted laser desorption/ionization Fourier transform mass spectrometry. *Rapid Commun. Mass Spectrom.* **1999**, *13*, 398-406.

78. Chan, T. W. D.; Duan, L.; Sze, T. P. E. Accurate mass measurements for peptide and protein mixtures by using matrix-assisted laser desorption/ionization Fourier transform mass spectrometry. *Anal. Chem.* **2002**, *74*, 5282-5289.

79. Kalli, A.; Hakansson, K. Comparison of the electron capture dissociation fragmentation behavior of doubly and triply protonated peptides from trypsin, Glu-C, and chymotrypsin digestion. *J. Proteome Res.* **2008**, *7*, 2834-2844.

80. Kalli, A.; Hakansson, K. Electron capture dissociation of highly charged proteolytic peptides from Lys N, Lys C and Glu C digestion. *Molecular bioSystems* **2010**, *6*, 1668-1681.

81. Swaney, D. L.; McAlister, G. C.; Wirtala, M.; Schwartz, J. C.; Syka, J. E. P.; Coon, J. J. Supplemental activation method for high-efficiency electron-transfer dissociation of doubly protonated peptide precursors. *Anal. Chem.* **2007**, *79*, 477-485.

82. Ledvina, A. R.; Beauchene, N. A.; McAlister, G. C.; Syka, J. E. P.; Schwartz, J. C.; Griep-Raming, J.; Westphall, M. S.; Coon, J. J. Activated-ion electron transfer dissociation improves the ability of electron transfer dissociation to identify peptides in a complex mixture. *Anal. Chem.* **2010**, *82*, 10068-10074.

Chapter 4

Ion-electron Reactions of Sialylated N-linked Glycans Released from Glycoproteins

4.1 Introduction

The biological significance of glycoproteins and glycoconjugates is well established. Glycosylation plays important roles in protein folding, cell adhesion, cell signaling, molecular trafficking, and receptor activation.[1-6] Aberrant protein glycosylation and alterations of glycan structures have been demonstrated to correlate with cancer and other diseases.[7-9] However, structural characterization of an oligosaccharide on a specific glycoconjugate is still far from routine. Because oligosaccharides are assembled in a non-template driven, step-wise manner by various glycosyltransferases and glycosidases,[7] highly diverse structures are frequently observed for oligosaccharides. Mass spectrometry (MS) has become an indispensable tool for glycan structural elucidation based on tandem mass spectrometry (MS/MS).[10-15] MS/MS spectra of oligosaccharides mainly consist of two types of product ions: glycosidic cleavages between monosaccharides and cross-ring cleavages across sugar rings.[16] Glycosidic cleavages provide information regarding monosaccharide composition, while cross-ring cleavages aid the determination of saccharide linkage type, particularly when occurring at branching residues.

Many N-linked glycans contain sialic acids (e.g., N-acetyl neuraminic acid, NeuAc), which carry a carboxylic acid group at the C-1 position. Due to the negative charge of this acidic group, sialic acids are labile,[17] particularly in positive-ion mode matrix-assisted laser desorption/ionization (MALDI).[18,19] Chemical derivatization (such as permethylation, methylesterification, and amidation) of sialylated oligosaccharides have been shown to aid the retention of the labile acidic group, and also enable differentiation of structural isomers.[20-24] However, derivatization approaches may suffer from sample loss and nonspecific modification at sites other than sialic acids.[23] It has been demonstrated that oligosaccharides ionized with alkali, alkaline earth, and transition metals often generate more cross-ring cleavages than their protonated counterparts following collision activated dissociation (CAD).[25-28] Metal cations and metal ligands also help stabilize acidic groups, such as sulfate groups and sialic acids in glycans and peptides.[29-33]

Compared to cations, fragmentation of oligosaccharide anions is not as frequently employed in mass spectrometry. The acidic group makes native sialylated glycans highly suitable for negative ion mode analysis. Abundant signal is often observed and differentiation of structural isomers has also been reported.[34-36] Zaia and co-workers explored the influence of sialylation in CAD of glycan anions, and found that more energy was required to fragment native sialylated glycans compared to the corresponding asialo species and to nitrate adducts.[37]

Fourier transform ion cyclotron resonance mass spectrometry (FT-ICR MS) has become widely practiced due to its high resolution and high mass accuracy, and its ability to apply various MS/MS techniques.[38,39] In addition to conventional vibrational

excitation (i.e.,CAD), infrared multiphoton dissociation (IRMPD),[18,40,41] high energy CAD,[42-44] electron capture dissociation (ECD),[24,31,32,45,46] electron detachment dissociation (EDD),[47-52] negative electron transfer dissociation (NETD),[53] 157 nm laser photodissociation,[54-56] and electron induced dissociation (EID)[57] have been utilized for glycan structural characterization. IRMPD has a higher fragmentation efficiency compared to CAD because multiple fragmentation events may occur during the IRMPD process.[18] IRMPD is particularly advantageous for fragmenting large ions, because IRMPD fragmentation efficiency increases with increasing glycan size.[41] High energy CAD and 157 nm laser photodissociation yield extensive cross-ring cleavages.[43,55] However, application of high energy CAD is limited to MALDI TOF/TOF and sector instruments. In addition, significant ion scattering occurs, which limits sensitivity. ECD was first applied to protonated aminoglycans, and yielded mostly glycosidic cleavages.[45] In Chapter 2, we explored the application of metal-assisted ECD to model oligosaccharides and to sulfated glycans released from a glycoprotein, and found that ECD generates complementary structural information compared to IRMPD.[31,32] The ability of ECD and CAD to provide complementary results for branched permethylated oligosaccharides was also demonstrated by O'Connor and co-workers.[24]

EDD is a relatively new fragmentation technique, introduced in 2001.[58] In EDD, polyanions are irradiated by high energy electrons (>10 eV) to form electron deficient radical ions, followed by subsequent fragmentation. EDD has been applied to neutral and sialylated oligosaccharides as well as to glycosaminoglycans (GAGs),[47-51] and shown to generate extensive glycosidic and cross-ring cleavages, with some product ions being unique to EDD. Compared to IRMPD, EDD produces more extensive fragmentation,

and has been used to distinguish the isomeric glucuronic from iduronic acid in GAGs.[48] However, previous work mainly focused on model oligosaccharides and shorter GAGs. Here, we investigate the first application of EDD and metal-assisted ECD towards sialylated N-linked glycans released from glycoproteins, and compare the fragmentation patterns to those from IRMPD in both positive- and negative-ion mode.

4.2 Experimental

4.2.1 Reagents

Human apo-transferrin, fetuin from fetal calf serum, α1-acid glycoprotein from human plasma, 1,4-dithio-DL-threitol (DTT), iodoacetamide and SPE graphitized carbon columns were purchased from Sigma Chemical Co. (St. Louis, MO). Peptide-N-glycosidase F (PNGase F) was purchased from EMD Chemicals, Inc. (Gibbstown, NJ). $CaCl_2$, NH_4HCO_3, and formic acid were obtained from Fisher (Fair Lawn, NJ).

4.2.2 Preparation of N-linked Glycans

Glycoproteins were reduced in 5 mM DTT at $56\,^{o}C$ for 45 min, alkylated with 15 mM iodoacetamide in the dark at room temperature for 1 h, and digested with PNGase F (2 U) in 50 mM NH_4HCO_3 (pH 8) overnight at $37\,^{o}C$.

4.2.3 Purification and Enrichment of *N*-glycans

Released glycans were purified by SPE graphitized carbon columns. For each sample, a carbon cartridge was washed with 0.1% (v/v) formic acid in 80% acetonitrile/H_2O (v/v), followed by deionized water. The solution containing *N*-glycans was slowly loaded. The cartridge was then washed by deionized water to remove salts and other contaminants. The glycans were eluted with 0.1% formic acid (v/v) in 20%

acetonitrile/H_2O (v/v). The solution was then dried down in a vacuum concentrator (Eppendorf, Hamberg, Germany). For positive-ion mode analysis, the glycans were mixed with $CaCl_2$ (final concentration 20-40 μM) in a 50% methanol/H_2O (v/v) solution. For negative ion mode analysis, the glycans were reconstituted in 50% methanol, 0.1% NH_4OH (v/v) solution.

4.2.4 Mass Spectrometry

All mass spectra were collected with an actively shielded 7 T FT-ICR mass spectrometer with a quadrupole front-end (APEX-Q, Bruker Daltonics, Billerica, MA), as previously described.[59] An indirectly heated hollow dispenser cathode was used to perform ECD.[60] IRMPD was performed with a vertically mounted 25 W, 10.6 μM CO_2 laser (Synrad, Mukilteo, WA). Samples were infused via an Apollo II electrospray ion source at a flow rate of 70 μL/h with the assistance of N_2 nebulizing gas. Following ion accumulation in the first hexapole for 0.05 s, ions were mass selectively accumulated in the second hexapole for 1-6 s. Ions were then transferred through high voltage ion optics and captured with dynamic trapping in an Infinity ICR cell.[61] The accumulation sequence up to the ICR cell fill was looped 3 times to optimize precursor ion signal to noise (S/N) ratio. For regular ECD and hot ECD, the cathode heating current was kept at 1.8 A, and the cathode voltage was pulsed during the ECD event to a bias voltage of - 0.1 to - 1.0 V for 50 ms to generate low energy electrons, and to a bias voltage of - 10.0 V for 45 ms to generate high energy electrons. For EDD, the cathode heating current was kept at 2.0 A, and the cathode voltage was pulsed to - 30 to - 35 V for 1 s. IRMPD was performed with a laser power of 10 W and with firing times ranging from 40-180 ms.

For activated-ion ECD (AI-ECD), ions were heated with a 10 W, 20-25 ms IR laser pulse prior to electron capture to destroy intramolecular non-covalent interactions. [62]

4.2.5 Data Analysis

All mass spectra were acquired with XMASS software (Bruker Daltonics) with 256 data points from m/z 100 to 2000 and summed over 60 - 100 scans. Data processing was performed with MIDAS software.[63] Data were zero filled once, Hanning apodized, and exported to Microsoft Excel for internal frequency-to-mass calibration with a two-term calibration equation.[64] Product ion spectra were interpreted with the aid of the web application GlycoFragment (www.dkfz.de/spec/projekte/fragments/).[65] Product ions were not assigned unless they were at least 3x the noise level.

4.3 Results and Discussion

All product ions were labeled according to the Domon and Costello nomenclature.[16] Subscript numerals indicate between which residues cleavage occurred, and superscript numerals indicate where cross-ring cleavage occurred.   When more than one product assignment was possible, all assignments are listed.   Internal fragments are indicated by parentheses (e.g., $Z_{4\beta}/C_5$). For branched oligosaccharides, the letter α represents the largest branch, the letter β represents the second largest branch, and the letter γ represents the third largest branch.   Product ions bearing a calcium cation as a charge carrier are denoted with a superscript Ca (e.g., C_4^{Ca}).

4.3.1 Positive Ion Mode Analysis: Calcium-adducted *N*-glycan Cations

N-linked sialylated glycans released from human transferrin, bovine fetuin and α1-acid glycoprotein (AGP) were ionized with Ca^{2+} in positive ion mode electrospray (ESI).   Oligosaccharides ionized with alkali, alkaline earth and transition metals often

yield more cross-ring cleavages compared to their protonated counterparts following CAD, IRMPD, and ECD.[25-28,31] Fragmentation patterns of metal-coordinated oligosaccharides are highly dependent on the metal cations chosen.[27,31] Harvey compared the ionization and CAD fragmentation patterns of oligosaccharides ionized with different divalent metal cations, such as Ca^{2+}, Co^{2+}, Mg^{2+}, Cu^{2+}, and Mn^{2+}, and found that calcium adducts yielded the highest sensitivity and provided rich structural information.[27] In addition, Ca^{2+} has been shown to stabilize acidic groups in peptides and oligosaccharides, and to aid generation of precursor ions with more than one charge, which are required for ECD.[31,32] Therefore, we chose to investigate IRMPD and ECD of Ca^{2+}-adducted N-linked glycans.

IRMPD of a triply charged calcium-adducted tri-antennary *N*-glycan (mass 3170.1060) generated 19 glycosidic cleavages, including almost complete series of B-, Y-, and Z-ions (Figure 4.1), demonstrating the high fragmentation efficiency of IRMPD. However, no cross-ring cleavages were observed, preventing acquisition of linkage information. When applying ECD to the same precursor ions, fewer glycosidic cleavages were found, with loss of sialic acids constituting dominating fragmentation pathways. The lower fragmentation efficiency in ECD may be attributed to intramolecular non-covalent interactions of the *N*-glycan,[31] which may be partially compensated by activating the precursor ions before ECD with laser irradiation (AI-ECD),[60,66] or by applying higher voltages during ECD (so called hot ECD).[67,68] Hot ECD yielded more product ions compared to regular ECD and AI-ECD (nine glycosidic cleavages from hot ECD compared to four from regular ECD and AI-ECD). However, cross-ring cleavages were still not found following hot ECD, and no complementary

structural information was generated compared to IRMPD. When applying IRMPD, regular ECD, and AI-ECD to other sialylated *N*-glycans, similar trends were observed, as summarized in Table 4.1.
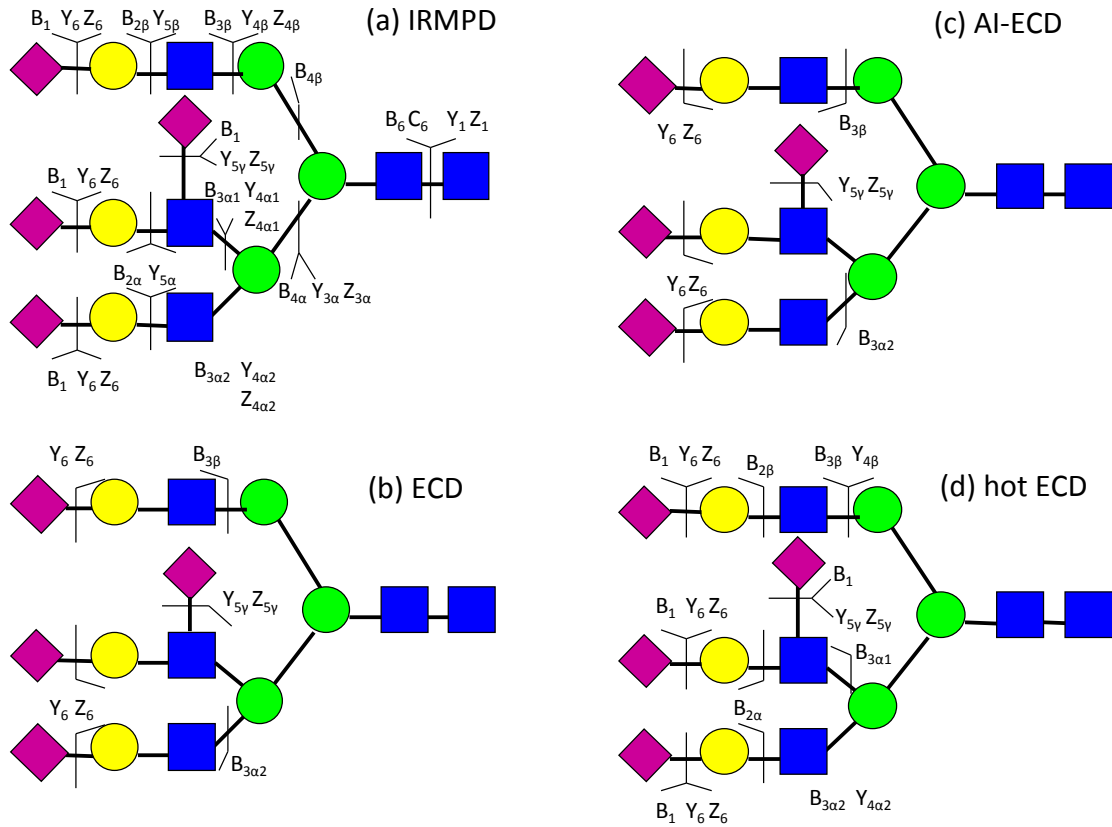
Figure 4.1. (a) IRMPD, (b) ECD, (c) AI-ECD, and (d) hot ECD fragmentation patterns from a calcium-adducted sialylated *N*-glycan released from bovine fetuin.
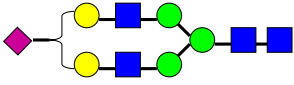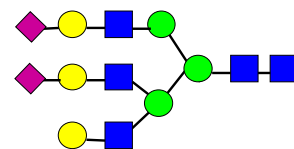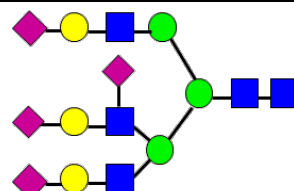
Glycan	IRMPD	ECD	AI-ECD
	$B_{3\alpha}$, $B_{4\alpha}$, $B_{2\beta}$, B_6, C_6, $Y_{4\alpha}$, $Y_{3\beta}$, $Y_{4\beta}$, Y_6, Z_1, Z_6	Y_6	$B_{2\beta}$, $B_{3\alpha}$, C_6, $Y_{4\alpha}$, Y_6
	$B_{1\alpha1}$, $B_{2\alpha2}$, $B_{3\alpha1}$, $B_{4\alpha}$, $B_{1\beta}$, $B_{2\beta}$, $B_{3\beta}$, $B_{4\beta}$, B_6, C_6, Y_1, $Y_{3\alpha}$, $Y_{4\alpha1}$, $Y_{4\alpha2}$, $Y_{5\alpha1}$, $Y_{5\alpha2}$, $Y_{3\beta}$, $Y_{4\beta}$, $Y_{5\beta}$, Y_6, Z_1, $Z_{3\alpha}$, $Z_{4\alpha1}$, $Z_{4\alpha2}$, $Z_{5\alpha1}$, $Z_{5\alpha2}$, $Z_{4\beta}$, $Z_{5\beta}$, Z_6	$B_{2\alpha2}$, $B_{3\alpha1}$, $B_{3\beta}$, C_6, $Y_{4\alpha1}$, $Y_{4\alpha2}$, Y_6, Z_6	$B_{1\alpha1}$, $B_{3\alpha1}$, $B_{1\beta}$, $B_{3\beta}$, $C_{2\beta}$, $Y_{4\alpha1}$, $Y_{3\beta}$, Y_6, Z_6
	B_1, B_2, $B_{3\alpha1}$, $B_{3\alpha2}$, $B_{4\alpha}$, $B_{3\beta}$, $B_{4\beta}$, B_6, C_6, Y_1, $Y_{3\alpha}$, $Y_{4\alpha1}$, $Y_{4\alpha2}$, $Y_{4\beta}$, $Y_{5\alpha}$, $Y_{5\beta}$, $Y_{5\gamma}$, Y_6, Z_1, $Z_{3\alpha}$, $Z_{4\alpha1}$, $Z_{4\alpha2}$, $Z_{4\beta}$, $Z_{5\gamma}$, Z_6	$B_{3\alpha2}$, $B_{3\beta}$, $Y_{5\gamma}$, Y_6, $Z_{5\gamma}$, Z_6	$B_{3\alpha2}$, $B_{3\beta}$, $Y_{5\gamma}$, Y_6, $Z_{5\gamma}$, Z_6

Table 4.1. Summary of product ions observed for calcium-adducted sialylated *N*-glycans following positive-ion mode IRMPD, ECD, and AI-ECD. IRMPD yielded the most glycosidic cleavages in all cases.

Another possible approach for overcoming the low fragmentation efficiency of ECD is to increase the precursor ion charge state. When precursor ions contain more charge, Coulomb repulsion between charges may result in more extended structures in the gas phase, which contain less intramolecular interactions.[69-71] To examine the charge state effect of glycans, we increased the final concentration of Ca^{2+} from 20 μM to 40 μM in the electrospray solution, thereby obtaining higher charge species as precursor ions, which were subjected to IRMPD, ECD, and AI-ECD. Figure 4.2 shows the fragmentation patterns from a doubly $(M + Ca)^{2+}$ and triply $(M + Ca + H)^{3+}$ charged di-antennary *N*-glycan (mass 2222.7830). For doubly charged precursor ions, ECD yielded no fragments other than the charge-reduced species, whereas triply charged precursor ions generated significantly more product ions, including glycosidic cleavages

between every neighboring monosaccharide. Similar trends were observed in both AI-ECD and IRMPD spectra, where higher precursor charge states resulted in higher fragmentation efficiency. However, cross-ring cleavages were still not generated in ECD, which lead us to explore alternative MS/MS approaches in negative ion mode.
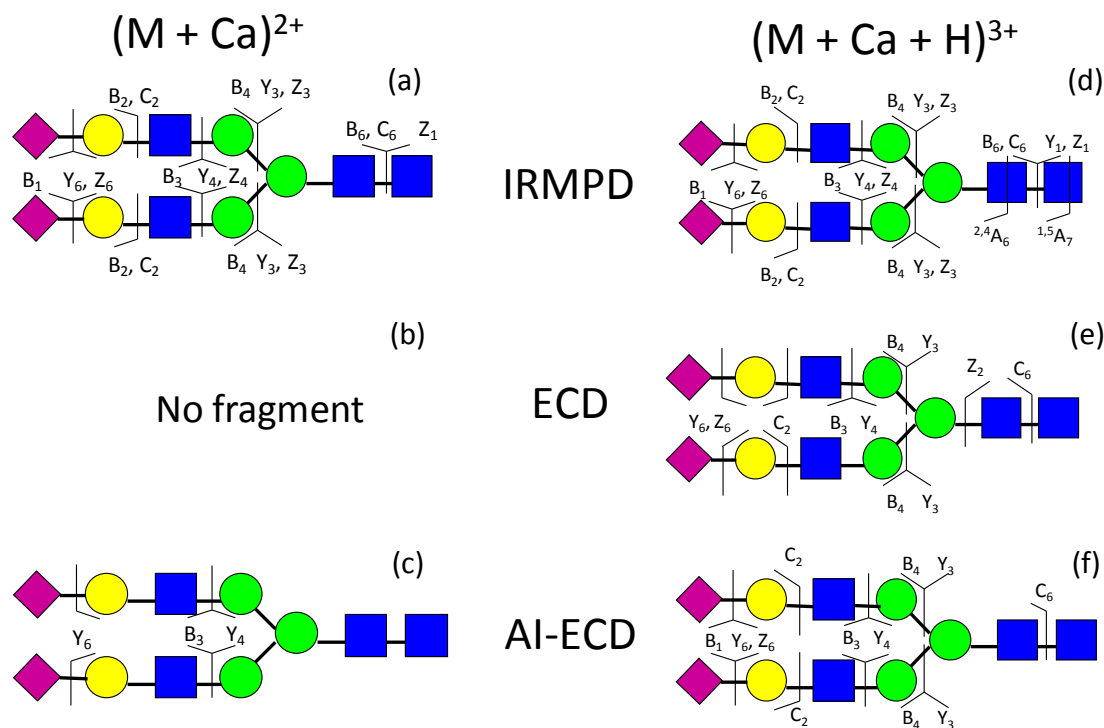
Figure 4.2. MS/MS fragmentation patterns from a calcium-adducted di-antennary N-glycan released from human transferrin. (a) IRMPD, (b) ECD, and (c) AI-ECD from doubly charged precursor ions. (d) IRMPD, (e) ECD, and (f) AI-ECD from triply charged precursor ions.

4.3.2 Negative Ion Mode Analysis: Native *N*-glycan Anions

Due to the acidity of sialic acids, negative ion mode is highly suitable for sialylated glycan analysis. Not only is negative-ion mode more advantageous for detection of molecular ions compared to positive ion mode, it is also less likely for sialylated glycans to undergo in-source sialic acid loss prior to MS/MS.[35,37] Low energy CAD of native oligosaccharides tends to produce abundant C-type ions, and A-type ions

are commonly observed for (1-4) and (1-6) linked monosaccharides.[72-75] Another main feature of negative ion mode CAD is the generation of characteristic D-type ions, for residues that are either (1-3) linked, or have a substituted 3-position carbon.[36,76] IRMPD was applied to native sialylated oligosaccharide anions by Lebrilla and co-workers, but only product ions corresponding to deprotonated sialic acid residues were observed.[41] We previously reported IRMPD of model sialylated oligosaccharide anions, and observed extensive fragmentation behavior for both linear and branched species.[31] Because the efficiency of IRMPD increases with increasing glycan size, whereas CAD does not work efficiently for high mass ions,[41] IRMPD was primarily chosen to examine sialylated glycan anions in this study. Comparison of the fragmentation patterns between IRMPD and CAD is shown in Figure 4.3, where IRMPD produced more unique product ions compared to CAD, although the fragmentation behaviors in these two vibrational activation techniques are generally similar. For the di-antennary N-glycan, seven unique product ions were observed following IRMPD compared to CAD, two of which were cross-ring fragments ($^{0,2}A_3$ and $^{1,5}A_2$). CAD generated three unique fragments (Z_4, Z_6, and B_5), but none of these are cross-ring fragments.

Figure 4.4 displays IRMPD and EDD spectra as well as fragmentation patterns for the same di-antennary N-glycan (mass 2222.7830) shown in Figure 4.2. Extensive glycosidic and cross-ring cleavages were generated in both IRMPD and EDD. IRMPD mainly produced A-, B-, and C-type ions containing the non-reducing end, while EDD yielded abundant X-, Y-, and Z-type ions containing the reducing end. The B_1 ion was the most abundant product ion, similar to observations by Zaia and co-workers from
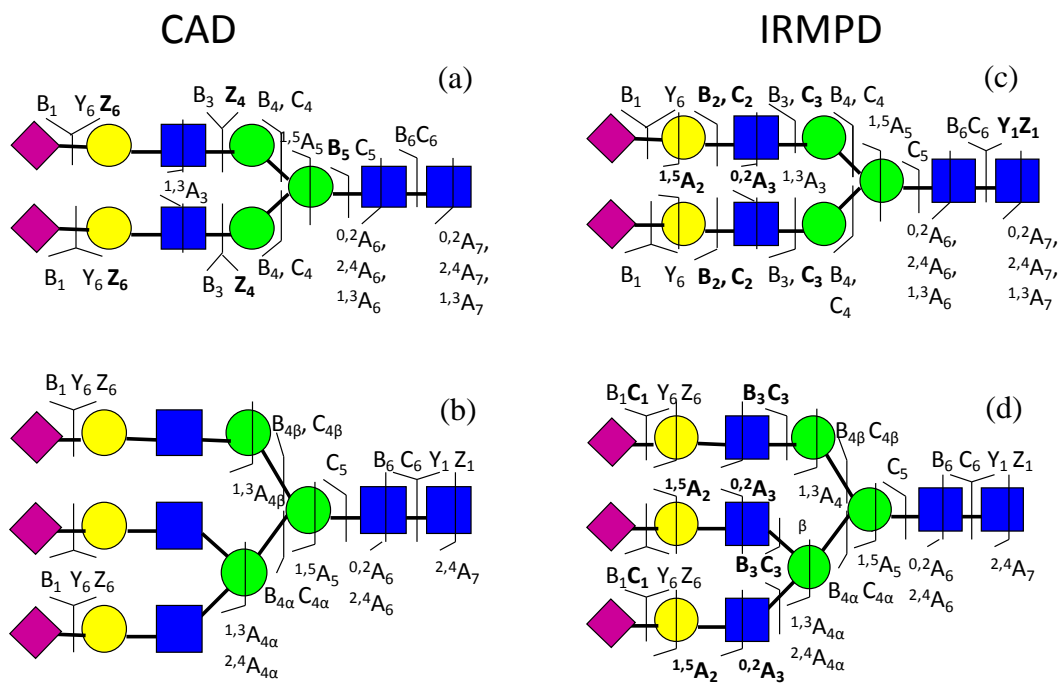
Figure 4.3. Fragmentation patterns for a di-antennary *N*-glycan following negative-ion mode (a) CAD and (c) IRMPD, and fragmentation patterns for a tri-antennary *N*-glycan following (b) CAD and (d) IRMPD. Product ions unique to each fragmentation method are highlighted in bold.

CAD of the same *N*-glycan.[37]   Seven unique A-type ions were found in IRMPD spectra,

including ^{0,2}A-, ^{1,3}A-, ^{2,4}A-, and ^{1,5}A-type ions.   The ^{1,5}A$_5$ fragment from the branching

mannose of the chitobiose core aided determination of the positions of the antennae.   In

EDD, two ^{1,5}A-type and three ^{1,5}X-type ions were observed.   These product ions are

completely complementary to those found following IRMPD. ^{1,5}X-type ions have

previously been reported in positive mode high-energy CAD, and also in EDD of

glycosaminoglycans.[48-51]   In addition to cross-ring cleavages, several unique product

ions were observed, including C – 2H, Y – 2H, and neutral loss (H$_2$O, CH$_3$O) from the

charge-reduced species in the EDD spectrum.   Glycosidic cleavages accompanied by

satellite peaks such as C$_3$ – 2H, C$_4$ – 2H and Y$_4$ – 2H, have been previously reported by

Wolff et al. in EDD of GAGs, and such products were used as diagnostic ions to distinguish IdoA and GlcA.[48]

IRMPD and EDD of a doubly deprotonated tri-antennary *N*-glycan (mass 2879.0106) was also examined (Figure 4.5). As expected, both glycosidic and cross-ring cleavages were observed in both IRMPD and EDD spectra. Similar to the fragmentation behavior of the di-antennary *N*-glycan, IRMPD preferably generated A-, B-, and C-type product ions, whereas EDD mostly generated X-, Y-, and Z-type ions. In IRMPD, ten glycosidic cleavages and seven cross-ring cleavages were observed. Y_6 (m/z = 1292.96, loss of sialic acid from precursor ions) and B_1 (m/z = 290.09, deprotonated sialic acid) fragments corresponded to the most abundant product ion species, in accordance with previous results.[41] $^{1,5}A_5$ at the branching mannose residue aided linkage determination. Water loss and internal fragments were also prevalent, which complicated the IRMPD spectrum. Notably, EDD of the same *N*-glycan produced completely different product ions (both glycosidic and cross-ring) compared to those from IRMPD, implicating very different mechanisms between these two MS/MS techniques. In addition to $^{1,5}A$- and $^{1,5}X$-type ions, previously observed from EDD, $^{1,4}A$- and $^{2,5}X$-type ions were observed. Series of Y – 2H, C – 2H products, and neutral loss from the charge reduced species were also generated. The EDD fragmentation efficiency of this tri-sialylated glycan was not as good as the di-sialylated one, presumably due to the larger glycan size and increased precursor ion *m/z*.
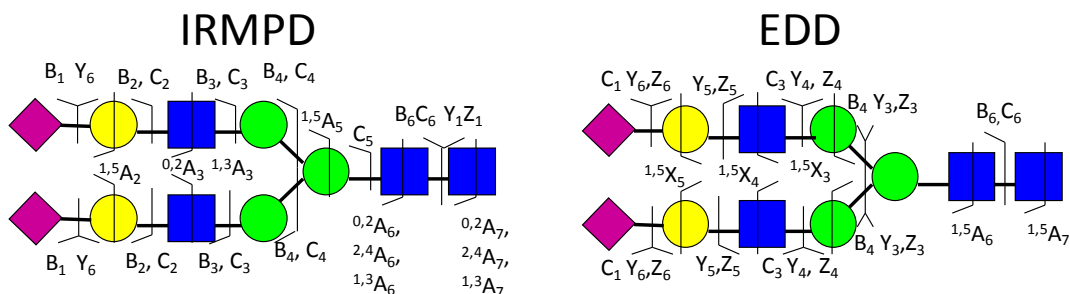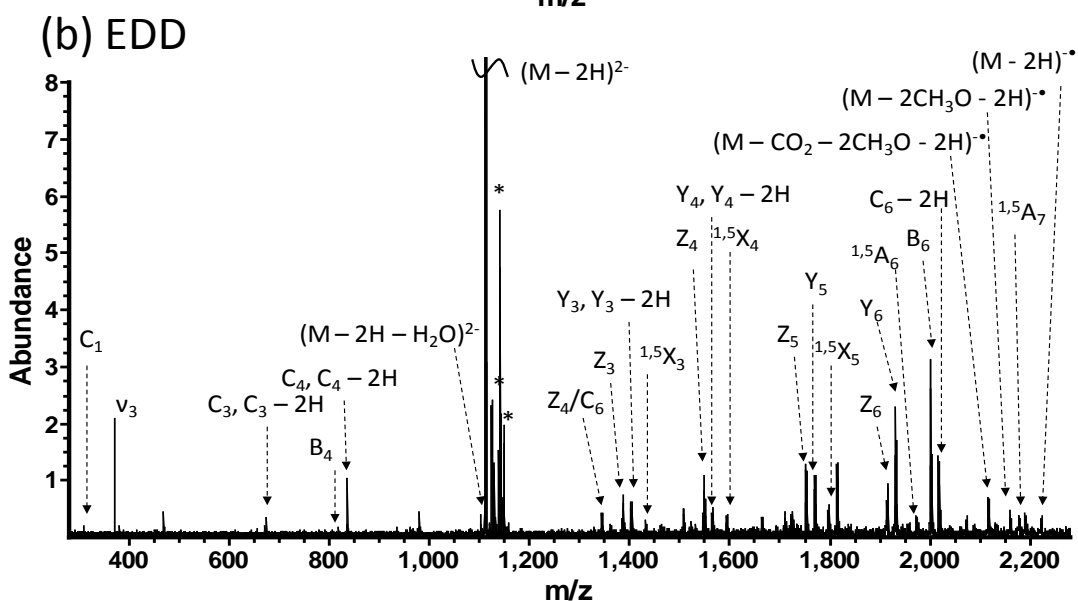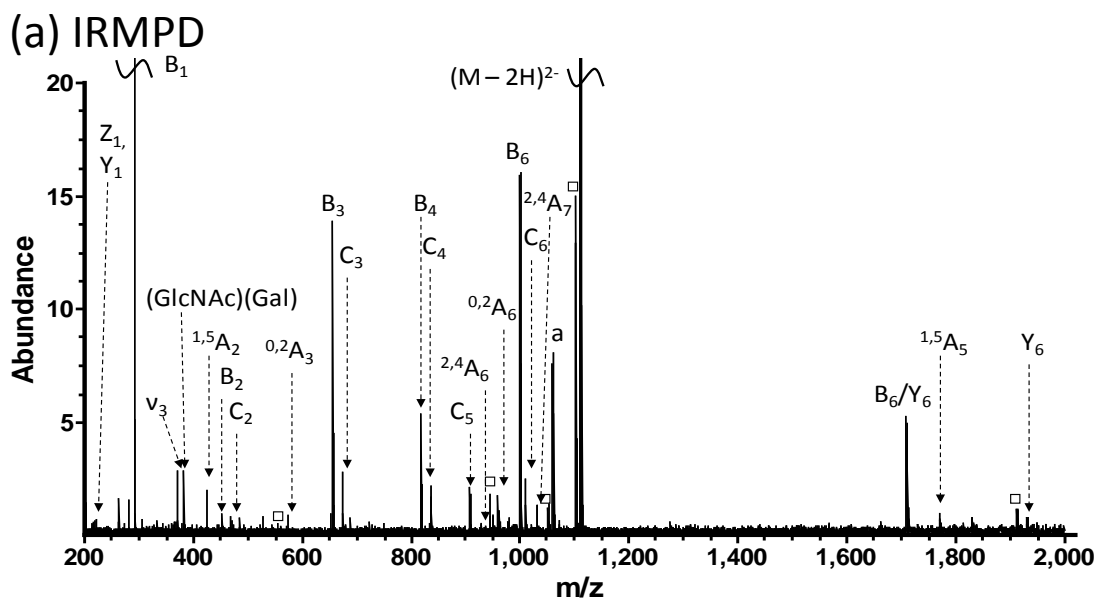
Figure 4.4. (a) IRMPD (80 scans, 170 ms at 10 W) and (b) EDD (80 scans, 1s irradiation, cathode bias – 35 V) spectra of a doubly deprotonated di-sialylated *N*-glycan released from transferrin. Squares indicate water loss from the adjacent product ion. a = $^{1,3}A_6$, $^{1,3}A_3$, $^{0,2}A_7$ or $^{1,3}A_7$ (these ions share the same *m/z*). Fragmentation patterns from IRMPD and EDD are summarized at the bottom.
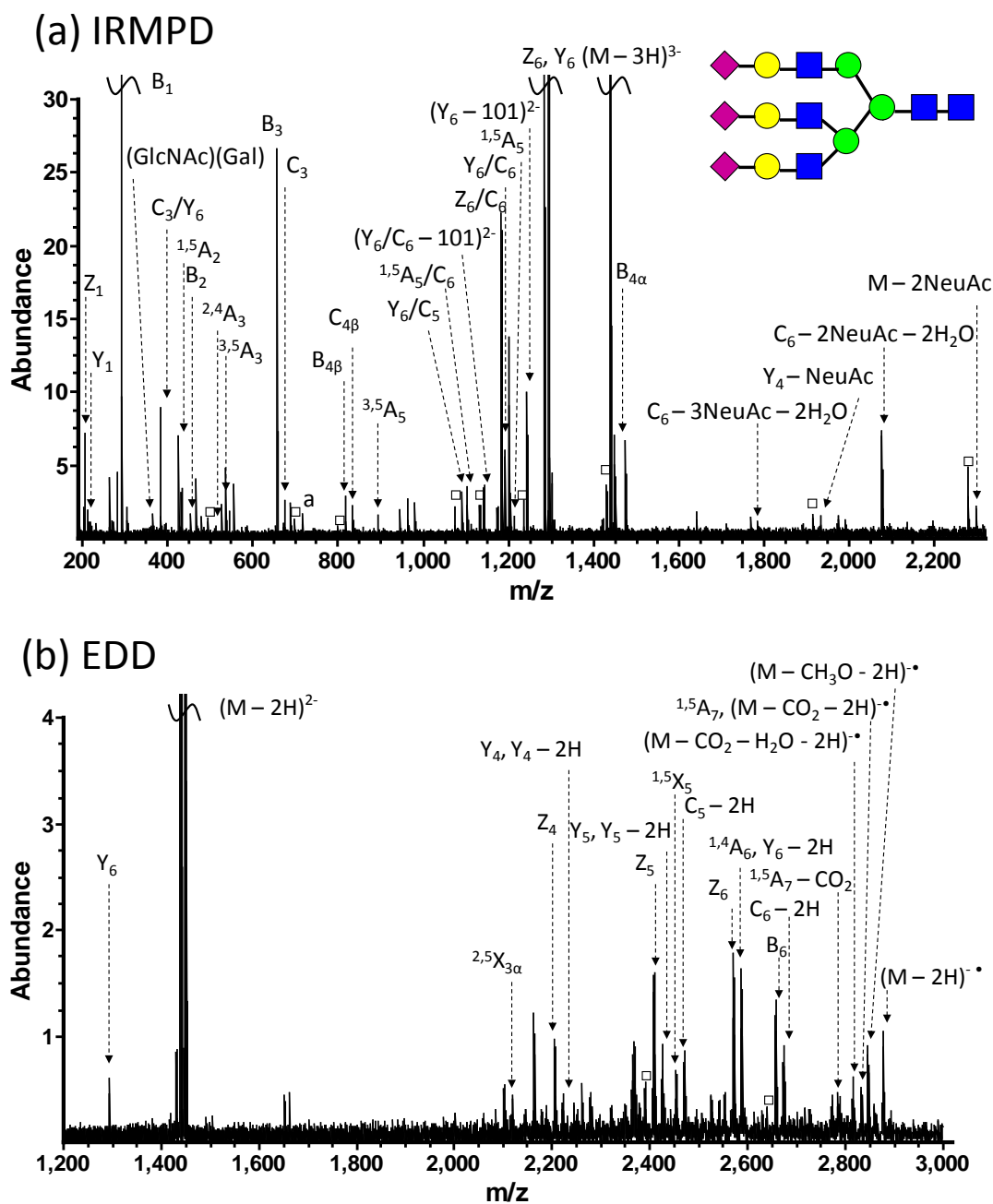
Figure 4.5. (a) IRMPD (80 scans, 150 ms at 10 W) and (b) EDD (80 scans, 1s irradiation, cathode bias – 35 V) spectra from a doubly deprotonated tri-sialylated *N*-glycan released from bovine fetuin. Squares indicate water loss from adjacent product ions.

Figure 4.6 shows IRMPD and EDD of the triply charged species of the same glycan as in Figure 4.5. IRMPD of $(M - 3H)^{3-}$ yielded 15 glycosidic and 13 cross-ring cleavages, most of which were A- and C-type ions, demonstrating improved fragmentation efficiency compared to 10 glycosidic and 7 cross-ring cleavages from $(M - 2H)^{2-}$. This observation is in accordance with previous findings reporting that negative-ion mode CAD tends to produce A- and C-type ions, unlike the B- and Y-type product ions found following positive-ion mode CAD.[74] The improved fragmentation efficiency of the higher charge state may be attributed to: (1) more "unfolded" gas-phase structure resulting from Coulomb repulsion, and (2) improved probability of generating a deprotonated hydroxyl in the precursor ions. Harvey investigated the fragmentation mechanism of negatively charged glycan ions, and proposed that deprotonated hydroxyl is a prerequisite for forming cross-ring cleavages in CAD.[72,75] When precursor ion charge state is increased, it is more likely for deprotonation to occur on hydroxyl groups. Unlike EDD of the doubly charged N-glycan, EDD of $(M - 3H)^{3-}$ yielded more product ions containing the non-reducing end (e.g., B_1, C_1, B_2, C_2, B_3, and C_3), indicating that charges were more evenly distributed across the glycan. Several unique product ions, such as C – 2H ions and neutral loss from the charge-reduced species were also generated following EDD of the higher charge state. 15 glycosidic and 4 cross-ring fragments were observed from $(M - 3H)^{3-}$, whereas 7 glycosidic and 4 cross-ring fragments were observed from $(M - 2H)^{2-}$, demonstrating a significant improvement in fragmentation yield. The influence of the precursor charge state of this glycan is summarized in Table 4.2.
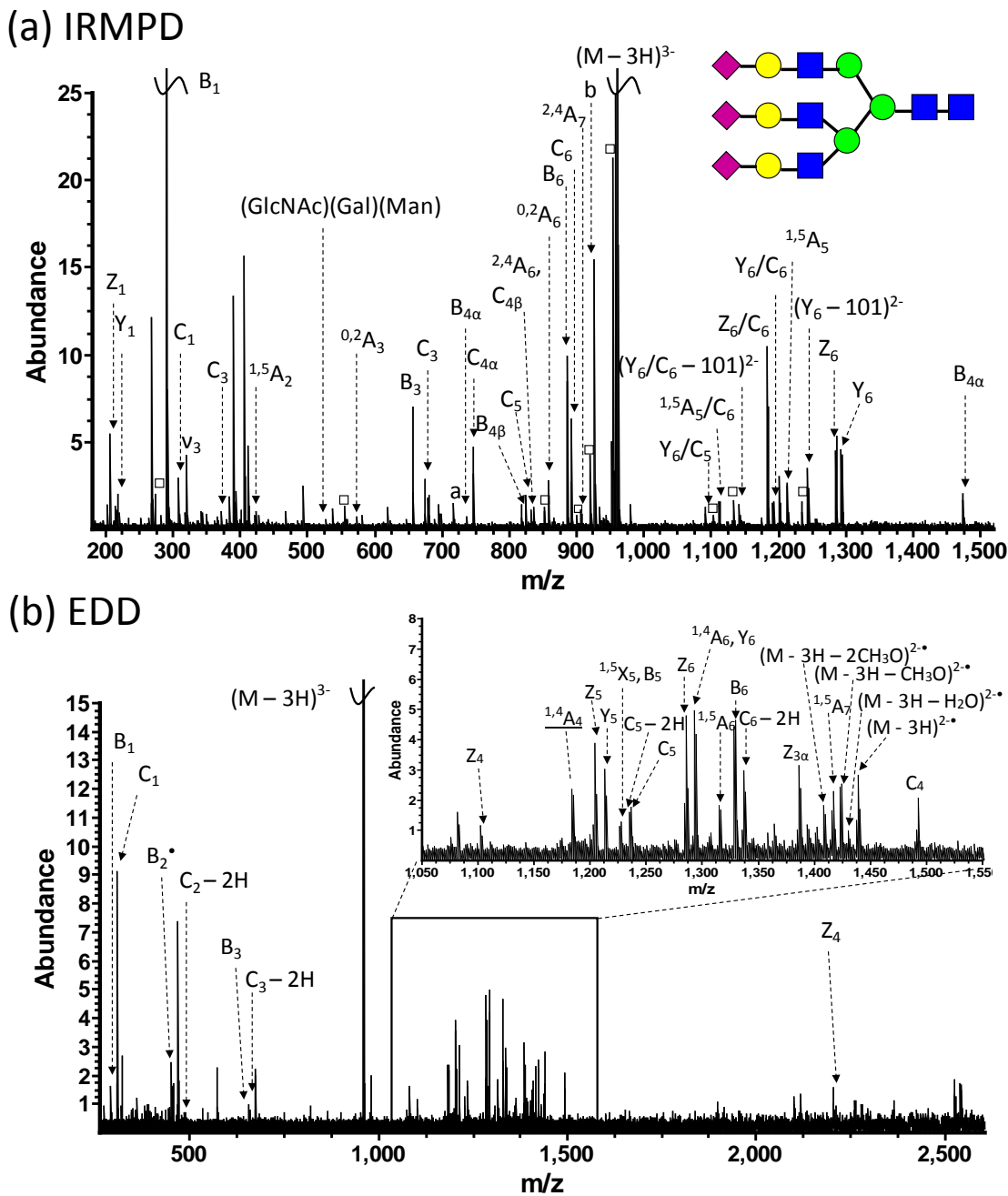
Figure 4.6. (a) IRMPD (80 scans, 120 ms at 10 W) and (b) EDD (80 scans, 1s irradiation, cathode bias – 35 V) spectra from a triply deprotonated tri-sialylated *N*-glycan released from bovine fetuin. Squares indicate water loss from adjacent product ions. a = $^{1,3}A_6$, $^{1,3}A_3$, $^{0,2}A_7$ or $^{1,3}A_7$ (these ions share the same *m/z*).

	IRMPD (2-)	IRMPD (3-)
Glycosidic cleavages	B_1, B_2, B_3, B_4, C_3, C_4	B_1, B_3, $B_{4\alpha}$, $B_{4\beta}$, B_6, C_1, C_3, $C_{4\alpha}$, $C_{4\beta}$, C_5, C_6, Y_1, Z_1
Cross-ring cleavages	$^{1,5}A_2$, $^{2,4}A_3$, $^{1,3}A_{4\alpha}$, $^{2,4}A_{2\alpha}$, $^{1,3}A_{4\beta}$, $^{1,5}A_5$	$^{1,5}A_2$, $^{0,2}A_3$, $^{1,3}A_{4\alpha}$, $^{2,4}A_{2\alpha}$, $^{1,3}A_{4\beta}$, $^{1,5}A_5$, $^{0,2}A_6$, $^{2,4}A_6$, $^{2,4}A_7$
	EDD (2-)	EDD (3-)
Glycosidic cleavages	B_5, B_6, Y_4, Y_6, Z_4, Z_5, Z_6	B_1, B_2, B_3, B_6, C_1, C_2, C_3, $C_{4\alpha}$, C_5, C_6, Y_4, Y_5, Y_6, $Z_{3\alpha}$, Z_4, Z_5, Z_6
Cross-ring cleavages	$^{1,4}A_6$, $^{2,5}X_3$, $^{1,5}X_5$	$^{1,4}A_6$, $^{1,5}A_6$, $^{1,5}A_7$, $^{1,5}X_5$

Table 4.2. Charge state effect in IRMPD and EDD of a tri-sialylated *N*-glycan released from bovine fetuin.

IRMPD and EDD fragmentation patterns of a di-sialylated tri-antennary *N*-glycan from bovine fetuin are shown in Figure 4.7. Similar to previous results, both IRMPD and EDD generated extensive fragmentation including both glycosidic and cross-ring fragments. In IRMPD, glycosidic cleavages between almost every neighboring monosaccharide were produced, providing rich structural information. Four cross-ring cleavages were also observed, two of which ($^{0,2}A_5$ and $^{1,5}A_5$) occurred at the branching mannose, thus aiding linkage determination. EDD of the same species resulted in six glycosidic and three cross-ring cleavages, with all cross-ring cleavages being different from those from IRMPD, thus providing additional structural information about the glycan.
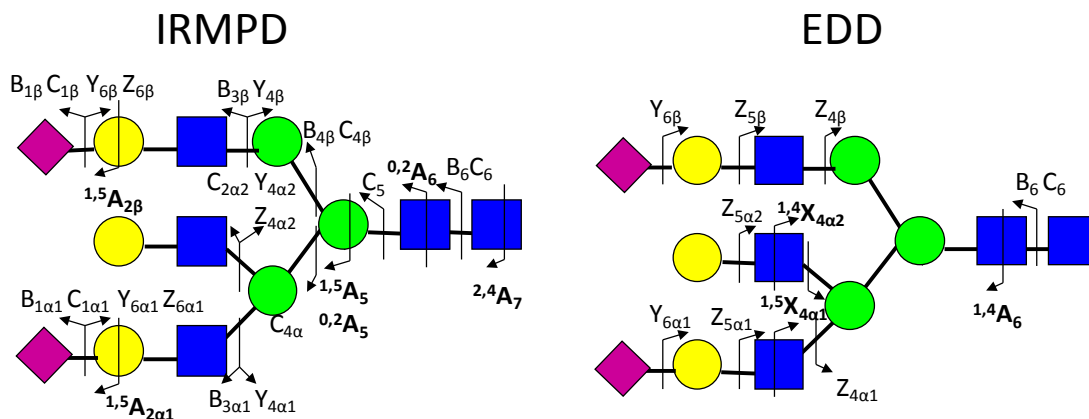
Figure 4.7. Fragmentation patterns for a tri-antennary *N*-glycan following negative-ion mode IRMPD and EDD. Cross-ring cleavages from IRMPD and EDD are completely complementary.

4.4 Conclusions

We investigated the application of ion-electron reactions towards sialylated N-linked glycans released from glycoproteins in both positive- and negative-ion mode. ECD and IRMPD of calcium-adducted glycan cations mostly resulted in glycosidic cleavages. Compared to regular ECD, AI-ECD and hot ECD showed improved fragmentation efficiency. Acidic glycan analysis in negative-ion mode benefits from more abundant signal and less ion suppression from neutral species compared to positive-ion mode. When applying EDD and IRMPD to glycan anions, extensive fragmentation including both glycosidic and cross-ring cleavages was observed. The large number of glycosidic cleavages provided important "sequence" information, and the complementary cross-ring cleavages from the two techniques aided determination of linkage type. Charge state effects were also examined. When precursor charge states were increased, IRMPD, ECD, and EDD all demonstrated improved fragmentation. This behavior is likely due to more extended glycan gas-phase structures and/or less

stable precursor ions as a result of intramolecular Coulomb repulsion. Overall, the combination of EDD and negative-ion mode IRMPD appears to constitute a highly powerful and promising approach for structural characterization of sialylated *N*-glycans.

4.5 References

1. Rudd, P. M.; Elliott, T.; Cresswell, P.; Wilson, I. A.; Dwek, R. A. Glycosylation and the immune system. *Science* **2001**, *291*, 2370-2376.
2. Bertozzi, C. R.; Kiessling, L. L. Chemical glycobiology. *Science* **2001**, *291*, 2357-2364.
3. Ohtsubo, K.; Marth, J. D. Glycosylation in cellular mechanisms of health and disease. *Cell* **2006**, *126*, 855-867.
4. Lowe, J. B.; Marth, J. D. A genetic approach to mammalian glycan function. *Annu. Rev. Biochem* **2003**, *72*, 643-691.
5. Pilobello, K. T.; Mahal, L. K. Deciphering the glycocode: the complexity and analytical challenge of glycomics. *Curr. Opin. Chem. Biol.* **2007**, *11*, 300-305.
6. Varki, A. Biological roles of oligosaccharides - All of the theories are correct. *Glycobiol.* **1993**, *3*, 97-130.
7. Dube, D. H.; Bertozzi, C. R. Glycans in cancer and inflammation. Potential for therapeutics and diagnostics. *Nature Reviews Drug Discovery* **2005**, *4*, 477-488.
8. Hakomori, S. Glycosylation defining cancer malignancy: New wine in an old bottle. *Proc. Natl. Acad. Sci. U. S. A.* **2002**, *99*, 10231-10233.
9. Zhao, Y. Y.; Takahashi, M.; Gu, J. G.; Miyoshi, E.; Matsumoto, A.; Kitazume, S.; Taniguchi, N. Functional roles of N-glycans in cell signaling and cell adhesion in cancer. *Cancer Sci.* **2008**, *99*, 1304-1310.
10. Mechref, Y.; Novotny, M. V. Structural investigations of glycoconjugates at high sensitivity. *Chem. Rev.* **2002**, *102*, 321-369.
11. Zaia, J. Mass spectrometry of oligosaccharides. *Mass Spectrom. Rev.* **2004**, *23*, 161-227.
12. Park, Y. M.; Lebrilla, C. B. Application of Fourier transform ion cyclotron resonance mass spectrometry to oligosaccharides. *Mass Spectrom. Rev.* **2005**, *24*, 232-264.
13. Harvey, D. J. Matrix-assisted laser desorption/ionization mass spectrometry of carbohydrates. *Mass Spectrom. Rev.* **1999**, *18*, 349-450.
14. Harvey, D. J. Proteomic analysis of glycosylation: structural determination of N- and O-linked glycans by mass spectrometry. *Expert Rev. Proteomics* **2005**, *2*, 87-101.
15. Zaia, J. Mass spectrometry and the emerging field of glycomics. *Chem. Biol.* **2008**, *15*, 881-892.
16. Domon, B.; Costello, C. E. A systematic nomenclature for carbohydrate fragmentations in FAB-MS MS spectra of glycoconjugates *Glycoconj. J.* **1988**, *5*, 397-409.
17. Wheeler, S. F.; Domann, P.; Harvey, D. J. Derivatization of sialic acids for stabilization in matrix-assisted laser desorption/ionization mass spectrometry and

concomitant differentiation of alpha(2 -> 3)- and alpha(2 -> 6)-isomers. *Rapid Commun. Mass Spectrom.* **2009**, *23*, 303-312.

18. Lancaster, K. S.; An, H. J.; Li, B. S.; Lebrilla, C. B. Interrogation of N-linked oligosaccharides using infrared multiphoton dissociation in FT-ICR mass spectrometry. *Anal. Chem.* **2006**, *78*, 4990-4997.

19. Huberty, M. C.; Vath, J. E.; Yu, W.; Martin, S. A. Site-specific carbohydrate identification in recombinant proteins using MALDI-TOF MS. *Anal. Chem.* **1993**, *65*, 2791-2800.

20. Sheeley, D. M.; Reinhold, V. N. Structural characterization of carbohydrate sequence, linkage, and branching in a quadrupole ion trap mass spectrometer: Neutral oligosaccharides and N-linked glycans. *Anal. Chem.* **1998**, *70*, 3053-3059.

21. Mechref, Y.; Kang, P.; Novotny, M. V. Differentiating structural isomers of sialylated glycans by matrix-assisted laser desorption/ionization time-of-flight/time-of-flight tandem mass spectrometry. *Rapid Commun. Mass Spectrom.* **2006**, *20*, 1381-1389.

22. Sekiya, S.; Wada, Y.; Tanaka, K. Derivatization for stabilizing sialic acids in MALDI-MS. *Anal. Chem.* **2005**, *77*, 4962-4968.

23. Toyoda, M.; Ito, H.; Matsuno, Y. K.; Narimatsu, H.; Kameyama, A. Quantitative derivatization of sialic acids for the detection of sialoglycans by MALDI MS. *Anal. Chem.* **2008**, *80*, 5211-5218.

24. Zhao, C.; Xie, B.; Chan, S. Y.; Costello, C. E.; O'Connor, P. B. Collisionally activated dissociation and electron capture dissociation provide complementary structural information for branched permethylated oligosaccharides. *J. Am. Soc. Mass. Spectrom.* **2008**, *19*, 138-150.

25. Sible, E. M.; Brimmer, S. P.; Leary, J. A. Interaction of first row transition metals with alpha 1-3, alpha 1-6 mannotriose and conserved trimannosyl core oligosaccharides: A comparative electrospray ionization study of doubly and singly charged complexes. *J. Am. Soc. Mass. Spectrom.* **1997**, *8*, 32-42.

26. Cancilla, M. T.; Wang, A. W.; Voss, L. R.; Lebrilla, C. B. Fragmentation reactions in the mass spectrometry analysis of neutral oligosaccharides. *Anal. Chem.* **1999**, *71*, 3206-3218.

27. Harvey, D. J. Ionization and collision-induced fragmentation of N-linked and related carbohydrates using divalent canons. *J. Am. Soc. Mass. Spectrom.* **2001**, *12*, 926-937.

28. Hofmeister, G. E.; Zhou, Z.; Leary, J. A. Linkage position determination in lithium-cationized disaccharides - tandem mass-sepctrometry and semiempirical calculations *J. Am. Chem. Soc.* **1991**, *113*, 5964-5970.

29. Von Seggern, C.; Zarek, P.; Cotter, R. Fragmentation of sialylated carbohydrates using infrared atmospheric pressure MALDI ion trap mass spectrometry from cation-doped liquid matrixes. *Anal. Chem.* **2003**, *75*, 6523-6530.

30. Liu, H.; Hakansson, K. Electron capture dissociation of tyrosine O-sulfated peptides complexed with divalent metal cations. *Anal. Chem.* **2006**, *78*, 7570-7576.

31.   Adamson, J. T.; Hakansson, K. Electron capture dissociation of oligosaccharides ionized with alkali, alkaline earth, and transition metals. *Anal. Chem.* **2007**, *79*, 2901-2910.

32.   Liu, H.; Hakansson, K., Analysis of Sulfated Oligosaccharides with Combination of Divalent Metal Complexation and Electron Capture Dissociation. In *Int. J. Mass spectrom.*, 2010.

33.   Leavell, M. D.; Leary, J. A. Stabilization and linkage analysis of metal-ligated sialic acid containing oligosaccharides. *J. Am. Soc. Mass. Spectrom.* **2001**, *12*, 528-536.

34.   Wheeler, S. F.; Harvey, D. J. Negative ion mass spectrometry of sialylated carbohydrates: Discrimination of N-acetylneuraminic acid linkages by MALDI-TOF and ESI-TOF mass spectrometry. *Anal. Chem.* **2000**, *72*, 5027-5039.

35.   Sagi, D.; Peter-Katalinic, J.; Conradt, H. S.; Nimtz, M. Sequencing of tri- and tetraantennary N-glycans containing sialic acid by negative mode ESI QTOF tandem MS. *J. Am. Soc. Mass. Spectrom.* **2002**, *13*, 1138-1148.

36.   Chai, W.; Piskarev, V. E.; Mulloy, B.; Liu, Y.; Evans, P. G.; Osborn, H. M. I.; Lawson, A. M. Analysis of chain and blood group type and branching pattern of sialylated oligosaccharides by negative ion electrospray tandem mass spectrometry. *Anal. Chem.* **2006**, *78*, 1581-1592.

37.   Seymour, J. L.; Costello, C. E.; Zaia, J. The influence of sialylation on glycan negative ion dissociation and energetics. *J. Am. Soc. Mass. Spectrom.* **2006**, *17*, 844-854.

38.   Marshall, A. G.; Hendrickson, C. L.; Jackson, G. S. Fourier transform ion cyclotron resonance mass spectrometry: A primer. *Mass Spectrom. Rev.* **1998**, *17*, 1-35.

39.   Marshall, A. G.; Hendrickson, C. L. High-resolution mass spectrometers. *Annu. Rev. Anal. Chem.* **2008**, *1*, 579-599.

40.   Xie, Y. M.; Lebrilla, C. B. Infrared multiphoton dissociation of alkali metal-coordinated oligosaccharides. *Anal. Chem.* **2003**, *75*, 1590-1598.

41.   Zhang, J. H.; Schubothe, K.; Li, B. S.; Russell, S.; Lebrilla, C. B. Infrared multiphoton dissociation of O-linked mucin-type oligosaccharides. *Anal. Chem.* **2005**, *77*, 208-214.

42.   Harvey, D. J.; Naven, T. J. P.; Kuster, B.; Bateman, R. H.; Green, M. R.; Critchley, G. Comparison of fragmentation modes for the structural determination of complex oligosaccharides ionized by matrix-assisted laser desorption/ionization mass spectrometry. *Rapid Commun. Mass Spectrom.* **1995**, *9*, 1556-1561.

43.   Harvey, D. J.; Bateman, R. H.; Green, M. R. High-energy collision-induced fragmentation of complex oligosaccharides ionized by matrix-assisted laser desorption/ionization mass spectrometry. *J. Mass Spectrom.* **1997**, *32*, 167-187.

44.   Lewandrowski, U.; Resemann, A.; Sickmann, A. Laser-induced dissociation/high-energy collision-induced dissociation fragmentation using MALDI-TOF/TOF-MS instrumentation for the analysis of neutral and acidic oligosaccharides. *Anal. Chem.* **2005**, *77*, 3274-3283.

45.   Budnik, B. A.; Haselmann, K. F.; Elkin, Y. N.; Gorbach, V. I.; Zubarev, R. A. Applications of electron-ion dissociation reactions for analysis of polycationic chitooligosaccharides in Fourier transform mass spectrometry. *Anal. Chem.* **2003**, *75*, 5994-6001.

46.   McFarland, M. A.; Marshall, A. G.; Hendrickson, C. L.; Nilsson, C. L.; Fredman, P.; Mansson, J. E. Structural characterization of the GM1 ganglioside by infrared multiphoton dissociation/electron capture dissociation, and electron detachment dissociation electrospray ionization FT-ICR MS/MS. *J. Am. Soc. Mass. Spectrom.* **2005**, *16*, 752-762.

47.   Adamson, J.; Adamson Electron detachment dissociation of neutral and sialylated oligosaccharides. *J. Am. Soc. Mass. Spectrom.* **2007**, *18*, 2162-2172.

48.   Wolff, J. J.; Chi, L. L.; Linhardt, R. J.; Amster, I. J. Distinguishing glucuronic from iduronic acid in glycosaminoglycan tetrasaccharides by using electron detachment dissociation. *Anal. Chem.* **2007**, *79*, 2015-2022.

49.   Wolff, J. J.; Laremore, T. N.; Busch, A. M.; Linhardt, R. J.; Amster, I. J. Electron detachment dissociation of dermatan sulfate oligosaccharides. *J. Am. Soc. Mass. Spectrom.* **2008**, *19*, 294-304.

50.   Wolff, J. J.; Laremore, T. N.; Busch, A. M.; Linhardt, R. J.; Amster, I. J. Influence of charge state and sodium cationization on the electron detachment dissociation and infrared multiphoton dissociation of glycosaminoglycan oligosaccharides. *J. Am. Soc. Mass. Spectrom.* **2008**, *19*, 790-798.

51.   Wolff, J. J.; Amster, I. J.; Chi, L. L.; Linhardt, R. J. Electron detachment dissociation of glycosaminoglycan tetrasaccharides. *J. Am. Soc. Mass. Spectrom.* **2007**, *18*, 234-244.

52.   Wolff, J. J.; Laremore, T. N.; Leach, F. E.; Linhardt, R. J.; Amster, I. J. Electron capture dissociation, electron detachment dissociation and infrared multiphoton dissociation of sucrose octasulfate. *Eur. J. Mass Spectrom.* **2009**, *15*, 275-281.

53.   Wolff, J. J.; Leach, F. E.; Laremore, T. N.; Kaplan, D. A.; Easterling, M. L.; Linhardt, R. J.; Amster, I. J. Negative electron transfer dissociation of glycosaminoglycans. *Anal. Chem.* **2010**, *82*, 3460-3466.

54.   Devakumar, A.; Thompson, M. S.; Reilly, J. P. dFragmentation of oligosaccharide ions with 157 nm vacuum ultraviolet light. *Rapid Commun. Mass Spectrom.* **2005**, *19*, 2313-2320.

55.   Devakumar, A.; Mechref, Y.; Kang, P.; Novotny, M. V.; Reilly, J. P. Identification of isomeric N-glycan structures by mass spectrometry with 157 nm laser-induced photofragmentation. *J. Am. Soc. Mass. Spectrom.* **2008**, *19*, 1027-1040.

56.   Devakumar, A.; Mechref, Y.; Kang, P.; Novotny, M. V.; Reilly, J. P. Laser-induced photofragmentation of neutral and acidic glycans inside an ion-trap mass spectrometer. *Rapid Commun. Mass Spectrom.* **2007**, *21*, 1452-1460.

57.   Gao, D.; Zhou, W.; Hakansson, K. In *Electron induced dissociation (EID) of singly protonated glycans*, 58th ASMS Conference on Mass Spectrometry and Allied Topics, Salt Lake City, UT, 2010.

58.   Budnik, B. A.; Haselmann, K. F.; Zubarev, R. A. Electron detachment dissociation of peptide di-anions: an electron-hole recombination phenomenon. *Chem. Phys. Lett.* **2001**, *342*, 299-302.

59. Yang, J.; Mo, J. J.; Adamson, J. T.; Hakansson, K. Characterization of oligodeoxynucleotides by electron detachment dissociation Fourier transform ion cyclotron resonance mass spectrometry. *Anal. Chem.* **2005**, *77*, 1876-1882.

60. Tsybin, Y. O.; Witt, M.; Baykut, G.; Kjeldsen, F.; Hakansson, P. Combined infrared multiphoton dissociation and electron capture dissociation with a hollow electron beam in Fourier transform ion cyclotron resonance mass spectrometry. *Rapid Commun. Mass Spectrom.* **2003**, *17*, 1759-1768.

61. Caravatti, P.; Allemann, M. The infinity cell - a new trapped-ion cell with radiofrequency covered trapping electrodes for Fourier-transform ion-cyclotron resonance mass-spectrometry. *Org. Mass Spectrom.* **1991**, *26*, 514-518.

62. Horn, D. M.; Ge, Y.; McLafferty, F. W. Activated ion electron capture dissociation for mass spectral sequencing of larger (42 kDa) proteins. *Anal. Chem.* **2000**, *72*, 4778-4784.

63. Senko, M. W.; Canterbury, J. D.; Guan, S. H.; Marshall, A. G. A high-performance modular data system for Fourier transform ion cyclotron resonance mass spectrometry. *Rapid Commun. Mass Spectrom.* **1996**, *10*, 1839-1844.

64. Ledford, E. B.; Rempel, D. L.; Gross, M. L. Space-charge effects in Fourier-transform mass-spectrometry - mass calibration *Anal. Chem.* **1984**, *56*, 2744-2748.

65. Lohmann, K. K.; von der Lieth, C. W. GlycoFragment and GlycoSearchMS: web tools to support the interpretation of mass spectra of complex carbohydrates. *Nucleic Acids Res.* **2004**, *32*, W261-W266.

66. Cooper, H. J.; Tatham, M. H.; Jaffray, E.; Heath, J. K.; Lam, T. T.; Marshall, A. G.; Hay, R. T. Fourier transform ion cyclotron resonance mass spectrometry for the analysis of small ubiquitin-like modifier (SUMO) modification: Identification of lysines in RanBP2 and SUMO targeted for modification during the E3 AutoSUMOylation reaction. *Anal. Chem.* **2005**, *77*, 6310-6319.

67. Haselmann, K. F.; Budnik, B. A.; Kjeldsen, F.; Nielsen, M. L.; Olsen, J. V.; Zubarev, R. A. Electronic excitation gives informative fragmentation of polypeptide cations and anions. *Eur. J. Mass Spectrom.* **2002**, *8*, 117-121.

68. Kjeldsen, F.; Haselmann, K. F.; Sorensen, E. S.; Zubarev, R. A. Distinguishing of Ile/Leu amino acid residues in the PP3 protein by (hot) electron capture dissociation in Fourier transform ion cyclotron resonance mass spectrometry. *Anal. Chem.* **2003**, *75*, 1267-1274.

69. Sze, S. K.; Ge, Y.; Oh, H.; McLafferty, F. W. Top-down mass spectrometry of a 29-kDa protein for characterization of any posttranslational modification to within one residue. *Proc. Natl. Acad. Sci. U. S. A.* **2002**, *99*, 1774-1779.

70. Kalli, A.; Hakansson, K. Comparison of the electron capture dissociation fragmentation behavior of doubly and triply protonated peptides from trypsin, Glu-C, and chymotrypsin digestion. *J. Proteome Res.* **2008**, *7*, 2834-2844.

71. Kalli, A.; Hakansson, K. Electron capture dissociation of highly charged proteolytic peptides from Lys N, Lys C and Glu C digestion. *Molecular bioSystems* **2010**, *6*, 1668-1681.

72. Harvey, D. J. Fragmentation of negative ions from carbohydrates: Part 2. Fragmentation of high-mannose N-linked glycans. *J. Am. Soc. Mass. Spectrom.* **2005**, *16*, 631-646.

73. Carroll, J. A.; Ngoka, L.; Beggs, C. G.; Lebrilla, C. B. Liquid secondary-ion mass-spectrometry Fourier-transform mass-spectrometry of oligosaccharide anions. *Anal. Chem.* **1993**, *65*, 1582-1587.

74. Harvey, D. J. Fragmentation of negative ions from carbohydrates: Part 1. Use of nitrate and other anionic adducts for the production of negative ion electrospray spectra from N-linked carbohydrates. *J. Am. Soc. Mass. Spectrom.* **2005**, *16*, 622-630.

75. Harvey, D. J. Fragmentation of negative ions from carbohydrates: Part 3. Fragmentation of hybrid and complex N-linked glycans. *J. Am. Soc. Mass. Spectrom.* **2005**, *16*, 647-659.

76. Chai, W. G.; Piskarev, V.; Lawson, A. M. Negative ion electrospray mass spectrometry of neutral underivatized oligosaccharides. *Anal. Chem.* **2001**, *73*, 651-657.

Chapter 5

Electron Detachment Dissociation (EDD) of Fluorescently Labeled Sialylated Oligosaccharides

5.1 Introduction

Glycosylation plays essential roles in a variety of cellular processes, including tumor growth and metastasis, immune response, and cell-cell communication.[1-6] Sialic acids (e.g., N-acetyl neuraminic acid, NeuAc) are an important family of sugars that contains a carboxylic acid at the C-1 position of the six-member sugar ring. Sialic acids are often found at the terminal positions of glycans and glycoconjugates, and they are involved in a large number of protein-glycan and glycan-glycan interactions in cellular processes, including intercellular adhesion, signaling, and microbial attachment.[7] Compared to proteomics and genomics, glycomics analysis faces unique challenges due to the non-template driven biosynthesis and the highly diverse structures of glycans. In order to achieve thorough structural elucidation of glycans, monosaccharide composition, degree of branching (for branched glycans), linkage type, and anomeric configuration all need to be determined.

Mass spectrometry (MS) based approaches for structural characterization of glycans have become an emerging field due to its high sensitivity and ability to perform

high-throughput analysis.[8-11]   Fourier transform ion cyclotron resonance mass spectrometry (FT-ICR MS) is a powerful tool for the structural analysis of glycans benefiting from ultra-high mass accuracy, high resolution, and compatibility with various MS/MS techniques.[12-14] While mass profiling of glycans can be obtained by MS, detailed structures are difficult to assign without tandem mass spectrometry (MS/MS). Collision activated dissociation (CAD),[15-17] infrared multiphoton dissociation (IRMPD),[18-20] high energy CAD (HeCAD),[21-23] electron capture dissociation (ECD),[24-28] electron detachment dissociation (EDD),[29-34] negative electron transfer dissociation (NETD),[35] 157 nm laser photodissociation,[36-38] and electron induced dissociation (EID)[39] have all been applied for glycan structural characterization.

During IRMPD, precursor ions are irradiated by an IR laser (typically 10.6 µm CO_2 laser). Multiple photons are absorbed and the corresponding energy is redistributed over all precursor ion vibrational modes.[40,41]   Compared to CAD, IRMPD is more advantageous for glycan structural analysis because of its ability to readily generate secondary fragmentation, which provides higher fragmentation efficiency, particularly for large glycans.[18] EDD was first introduced to characterize peptide anions in 2001.[42] During EDD, polyanions are irradiated with >10 eV energy electrons. Electron detachment occurs and generates charge-reduced species, followed by subsequent fragmentation.[43]   Our lab previously showed that EDD provides complementary structural information of model oligosaccharides and sialylated *N*-glycans compared to IRMPD.[34,44] Amster and co-workers investigated the fragmentation behavior in EDD of GAGs, and found that EDD yielded extensive glycosidic and cross-ring cleavages, whereas CAD and IRMPD mostly resulted in glycosidic cleavages.[29-33,45] EDD could

also be utilized to differentiate the isomers glucuronic acid and iduronic acid.[29] The combination of EDD and IRMPD/CAD is a highly valuable tool for structural characterization of carbohydrates, particularly acidic carbohydrates in negative-ion mode, due to the ability to provide complementary structural information.

Fluorescent labeling of glycans is frequently employed prior to MS for several reasons. First, introducing a hydrophobic label to the hydrophilic glycans helps improve sensitivity in the mass spectrometer.[46] Second, fluorescent labels enable UV or fluorescence detection in high-performance liquid chromatography (HPLC), and also enhance glycan retention on reverse phase (C_{18}) columns.[47-50] Native glycans often exhibit poor retention, while derivatized glycans can be separated and identified using C_{18} columns.[51] In addition, recent studies have demonstrated that quantitation of glycans can be obtained by utilizing stable isotopic labeling.[52-54] The most commonly used labeling method is reductive amination. The primary amine of the label reacts with the aldehyde group of the glycan to generate a Schiff base intermediate, which is then stabilized through reduction to form a secondary amine.[55] 2-aminobenzoic acid (2-AA), 2-aminobenzamide (2-AB), 2-aminopyridine (2-AP), and 5-amino-2-naphthalenesulfonic acid (ANSA) are some of the commonly utilized fluorescent labels.[56-68]

It has been previously reported that labels may change fragmentation behaviors of glycans.[48,50,69] For neutral glycans and labeled glycans which do not contain acidic groups, positive-ion mode analysis is frequently employed. 2-AB tagged oligosaccharides were examined in both protonated and sodiated forms by CAD, HeCAD, post-source decay (PSD), and ultraviolet photodissociation (UVPD).[59-61,64,70,71] Harvey reported that 2-AB labeling at the reducing end did not significantly alter fragmentation

behavior of *N*-glycans in CAD.[59] The protonated species mostly produced B- and Y-type glycosidic cleavages, whereas the sodiated species generated additional C-, and Y-type as well as cross-ring fragments.[60,71] 355 nm UVPD of fluorescently labeled sodiated oligosaccharides resulted in efficient fragmentation, generating series of A- and C-ions, complementary to CAD.[70] 2-AB labeled oligosaccharides were also analyzed in negative-ion mode MALDI-TOF/TOF-MS, demonstrating considerably different fragmentation patterns compared to positive-ion mode.[63] Various cross-ring fragments such as [1,3]A-type ions were observed, providing linkage information. In addition, fucose residues were stabilized in negative-ion mode analysis, which allowed improved fucosylation site determination.[63] Acidic glycans (e.g., sialylated glycans) or glycans with acidic labels (e.g., 2-AA) tend to produce abundant signals in negative-ion mode, which makes negative-ion mode analysis a highly favorable choice. 2-AA labeled *N*-glycans mostly generates Y-ions containing the reducing end, and also some A-type cross-ring cleavages in negative-ion mode CAD.[15] Here, we investigate the fragmentation behaviors of fluorescently labeled sialylated oligosaccharides by EDD and IRMPD, and compare those to the fragmentation patterns of underivatized species.

5.2 Experimental

5.2.1 Reagents

Disialyl-lacto-*N*-tetraose (DSLNT) and LS-tetrasaccharide b (LSTb) were purchased from V-labs Inc (Covington, LA). Human apo-transferrin, 1,4-dithio-DL-threitol (DTT), iodoacetamide2-AA, 2-AB, boric acid, sodium acetate, and sodium cyanoborohydride (NaCNBH$_3$) were obtained from Sigma Chemical Co. (St. Louis, MO). NH$_4$HCO$_3$, NH$_4$OH, methanol, acetonitrile, glacial acetic acid, dimethyl sulfoxide

(DMSO), and formic acid were obtained from Fisher (Fair Lawn, NJ). Peptide-*N*-glycosidase F (PNGase F) was purchased from Calbiochem (Gibbstown, NJ).

5.2.2 Preparation of N-linked Glycans

The glycoprotein was reduced in 5 mM DTT at 56 $^{\circ}$C for 45 min, alkylated by 15 mM iodoacetamide in the dark at room temperature for 1 h, and digested with PNGase F (2 U) in 50 mM NH_4HCO_3 (pH 8) overnight at 37 $^{\circ}$C.

5.2.3 Fluorescent Labeling of Oligosaccharides

Oligosaccharides (2 nmol) were first dried down, reconstituted in 60 µL freshly prepared labeling reagent, and incubated at 80 $^{\circ}$C for 1h (2-AA) or 65 $^{\circ}$C for 2h (2-AB). For 2-AA labeling, labeling reagent was prepared by dissolving 30 mg 2-AA and 30 mg $NaCNBH_3$ in 1 mL methanol containing 4% sodium acetate (w/v) and 2% boric acid (w/v). For 2-AB labeling, labeling reagent was 0.35 M 2-AB and 1 M $NaCNBH_3$ in a DMSO/glacial acetic acid mixture (7:3 (v/v)).

5.2.4 Purification of Oligosaccharides

The fluorescently labeled oligosaccharides were purified by SPE graphitized carbon cartridge. For each sample, a carbon cartridge was washed with 0.1% (v/v) formic acid in 80% acetonitrile/H_2O (v/v), followed by deionized water. The solution containing labeled oligosaccharides was loaded. The cartridge was then washed by deionized water to remove salts and other contaminants. The glycans were eluted with 0.1% formic acid (v/v) in 20% or 40% acetonitrile/H_2O (v/v). The solution was then dried down in a vacuum concentrator (Eppendorf, Hamberg, Germany), and reconstituted in 50% methanol, 0.1% NH_4OH (v/v) solution for MS analysis.

5.2.5 Mass Spectrometry

All mass spectra were collected with an actively shielded 7 T FT-ICR mass spectrometer with a quadrupole front-end (APEX-Q, Bruker Daltonics, Billerica, MA), as previously described.[72] An indirectly heated hollow dispenser cathode was used to perform EDD.[73] IRMPD was performed with a vertically mounted 25 W, 10.6 μM CO_2 laser (Synrad, Mukilteo, WA). Samples were infused via an Apollo II electrospray ion source at a flow rate of 70 μL/h with the assistance of N_2 nebulizing gas. Following ion accumulation in the first hexapole for 0.05 s, ions were mass selectively accumulated in the second hexapole for 1-6 s. Ions were then transferred through high voltage ion optics and captured with dynamic trapping in an Infinity ICR cell.[74] The accumulation sequence up to the ICR cell fill was looped 3 times to optimize precursor ion signal to noise (S/N) ratio. For EDD, the cathode heating current was kept at 2.0 A, and the cathode voltage was pulsed to a bias voltage of - 30 to - 35 V for 1 s. IRMPD was performed with a laser power of 10 W with firing times ranging from 0.25-1 s.

5.2.6 Data Analysis

All mass spectra were acquired with XMASS software (Bruker Daltonics) with 256 data points from *m*/*z* 100 to 2000 and summed over 60-100 scans. Data processing was performed with MIDAS software.[75] Data were zero filled once, Hanning apodized, and exported to Microsoft Excel for internal frequency-to-mass calibration with a two-term calibration equation.[76] Product ion spectra were interpreted with the aid of the web application GlycoFragment (www.dkfz.de/spec/projekte/fragments/).[77] Product ions were not assigned unless they were at least 3x the noise level.

5.3 Results and Discussion

MS/MS spectra of oligosaccharides mainly contain two types of bond cleavages: glycosidic cleavages which occur between monosaccharide residues, and cross-ring cleavages occurring across sugar rings.[78] Glycosidic cleavages provide structural information regarding monosaccharide composition, whereas cross-ring cleavages aid the determination of linkage type. EDD and IRMPD fragmentation patterns of the 2-AA and 2-AB labeled sialylated oligosaccharides DSLNT and LSTb, and an *N*-glycan released from human transferrin were investigated. Structures of 2-AA and 2-AB are shown in Figure 5.1.

2-aminobenzoic acid (2-AA)   2-aminobenzamide (2-AB)
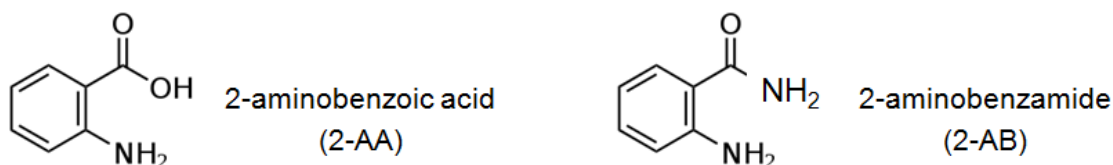
Figure 5.1. Structures of 2-aminobenzoic acid (2-AA) and 2-aminobenzamide (2-AB).

5.3.1 DSLNT

DSLNT is a branched di-sialylated oligosaccharide with the composition Neu5Acβ3Galβ3(Neu5Acβ6)GlcNAcβ3Galβ4Glc. Negative-ion mode IRMPD of 2-AB labeled DSLNT resulted in an almost complete series of Y-ions, all containing the fluorescent label (Figure 5.2a), similar to the fragmentation patterns from MALDI-PSD of 2-AB labeled oligosaccharides.[61] $Y_{4\alpha(3\beta)}$ (m/z = 1117.4) corresponding to sialic acid loss was the most abundant species among the product ions, illustrating the gas-phase lability of sialic acids. No cross-ring fragments were found, thus precluding acquisition of linkage information. EDD of doubly deprotonated 2-AB labeled DSLNT resulted in

extensive fragmentation (Figure 5.2b). All product ions were singly charged, which may arise from two different fragmentation mechanisms, either via direct fragmentation of activated precursor ions, or via the charged reduced radical ions generated after electron detachment.[32] Glycosidic cleavages between every neighboring monosaccharide were observed, along with five cross-ring cleavages, including ^{0,2}A-, ^{1,5}A-, ^{0,2}X-, and ^{1,5}X-type ions. ^{0,2}X- and ^{1,5}X-type ions are generally not present in CAD/IRMPD spectra, but they have been observed from high-energy CAD, laser induced dissociation (LID) of sodiated fluorescently labeled oligosaccharides,[63,69] and EDD of underivatized oligosaccharides and GAGs.[30,32,34] Among all the product ions, $C_{1\alpha(1\beta)}$ ($m/z = 308.1$) corresponding to sialic acid loss was the most abundant species. CO_2 loss from the charge reduced species, glycosidic fragments, and cross-ring fragments was frequently observed, presumably originating from the carboxylic acid of the sialic acids and complicating the spectrum. Several satellite peaks, such as C – 2H, Y – 2H, and Y – 16 Da (or Z + 2H)[34] were also found in the spectra. Those ions were only observed in EDD, indicating that such ions may arise from radical driven fragmentation pathways.[30] Compared to IRMPD, EDD produced additional structural information including both glycosidic and cross-ring cleavages, rendering EDD a highly valuable and promising tool for structural characterization of fluorescently labeled oligosaccharides in negative-ion mode.
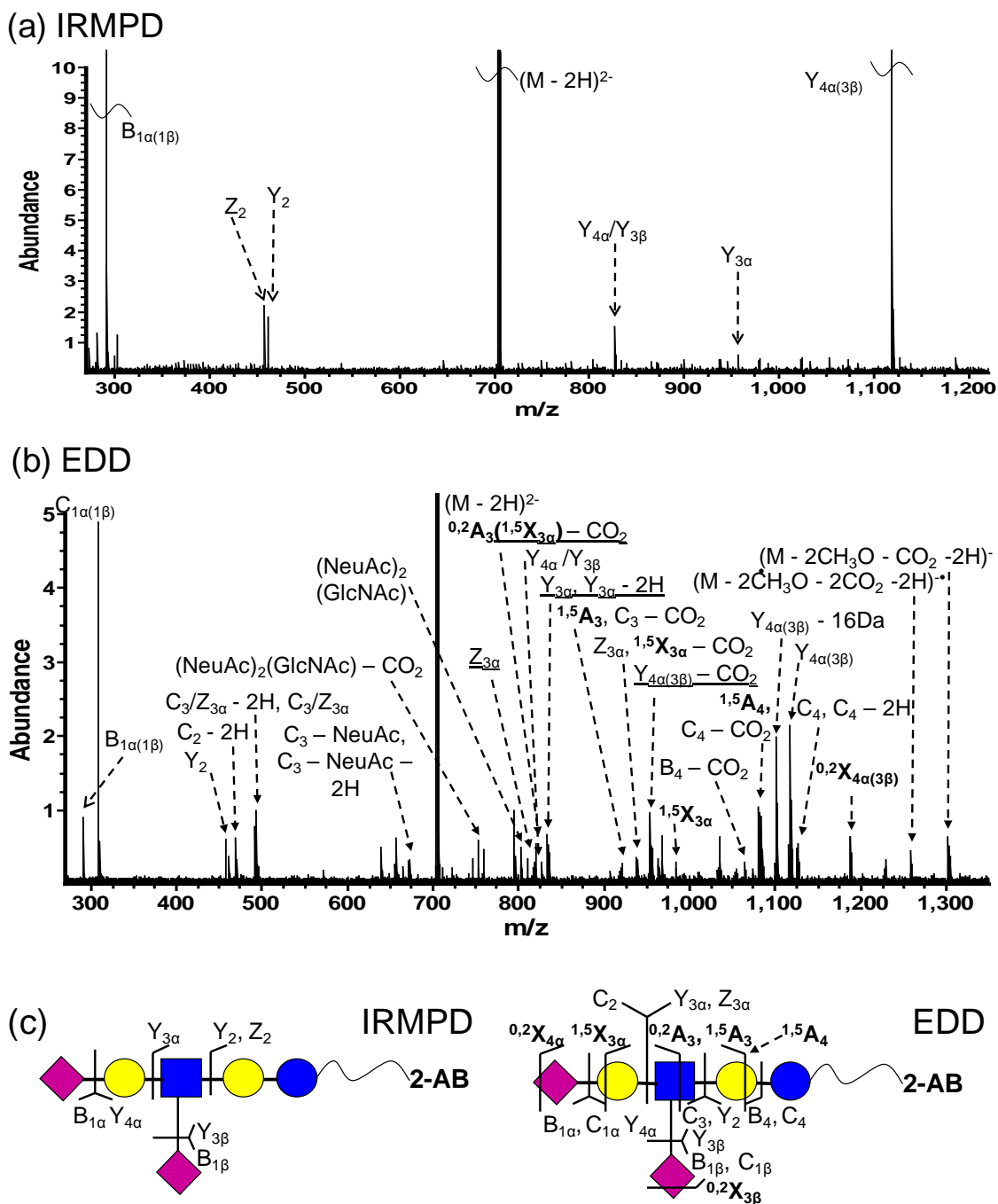
Figure 5.2. (a) IRMPD (80 scans, 0.8 s at 10 W) and (b) EDD (80 scans, 1s irradiation, cathode bias – 30 V) spectra of 2-AB labeled DSLNT. Cross-ring fragments are highlighted in bold. Reducing end product ions lacking 2-AB are underlined in the spectra. Fragmentation patterns from IRMPD and EDD are summarized in Figure 5.2c.

115

MS/MS of 2-AA labeled DSLNT is shown in Figure 5.3. Compared to 2-AB labeled species, 2-AA labeled DSLNT readily generated abundant signal in negative-ion mode. In order to compare the fragmentation behaviors, shorter ion accumulation time was chosen for 2-AA tagged species to yield the same precursor ion abundance. IRMPD of 2-AA labeled DSLNT mostly resulted in Y-ions containing the fluorescent tag, which could aid determination of monosaccharide composition and "sequence" of the oligosaccharide (Figure 5.3a). Again, no cross-ring cleavages were produced. EDD of 2-AA labeled DSLNT demonstrated similar fragmentation compared to the 2-AB labeled species (Figure 5.3b). Thirteen glycosidic and four cross-ring cleavages were observed, including ^{1,5}A-, ^{0,2}X-, ^{1,3}X- and ^{1,5}X-type ions. All product ions were singly charged. Extensive neutral loss (CO_2, CH_3O, and H_2O) from the charged reduced species and glycosidic fragments, and internal fragments were observed in the EDD spectrum. Similar to Figure 5.2b, satellite ions such as $C_4 - 2H$ were found. Their absence in the IRMPD spectrum of the same species suggests that those ions may originate from radical-driven fragmentation, or from electronic excitation. Compared to 2-AB labeled species, 2-AA labeled DSLNT generated fewer cross-ring fragments (four compared to five), suggesting that the nature of the reducing end substitute affects EDD fragmentation behavior.
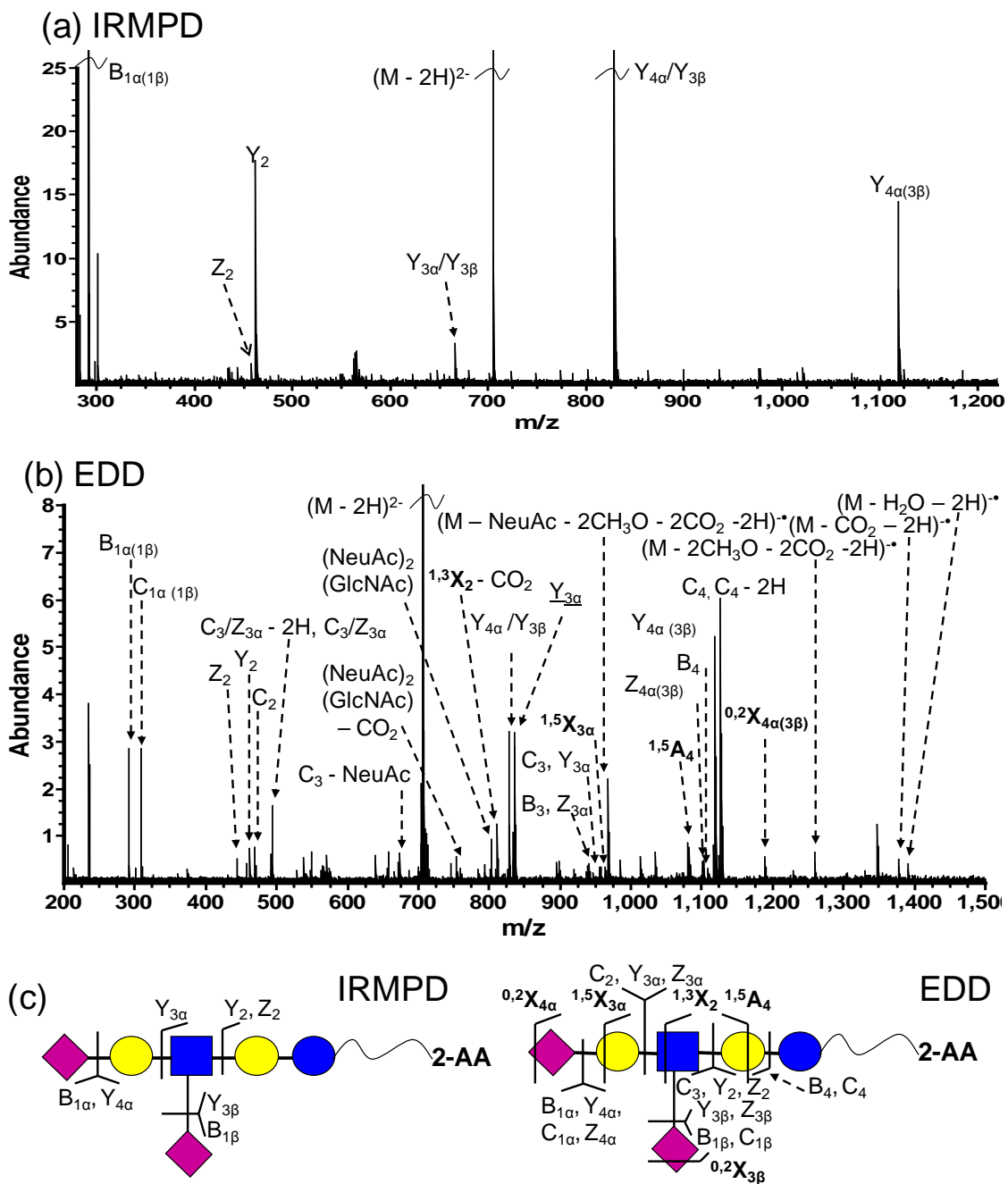
Figure 5.3. (a) IRMPD (80 scans, 1 s at 10 W) and (b) EDD (80 scans, 1s irradiation, cathode bias – 30 V) spectra of 2-AA labeled DSLNT. Cross-ring fragments are highlighted in bold. Reducing end fragment ions lacking 2-AA are underlined in the spectra. Fragmentation patterns from IRMPD and EDD are summarized in Figure 5.3c.

5.3.2 Sialylated *N*-glycan

IRMPD and EDD of the fluorescently labeled di-sialylated *N*-glycan from human transferrin were also examined (see Figure 5.4). Most product ions from IRMPD of the 2-AB labeled glycan (Figure 5.4a) were singly charged, while one product from cross-ring cleavage (*m/z* = 1110.9) was doubly charged. Most glycosidic fragments were B- and C-type ions contained the non-reducing end. EDD of the 2-AB labeled *N*-glycan produced a large number of glycosidic and cross-ring fragments, which provided rich structural information (Figure 5.4b). In addition to glycosidic cleavages between every neighboring monosaccharide, three cross-ring cleavages were observed, including ^{1,3}A-, ^{1,5}A-, and ^{0,2}A-type ions. ^{0,2}A-, ^{1,3}A-, and ^{1,5}A-type ions have been previously reported from MS/MS of deprotonated 2-AB labeled neutral *N*-glycans in MALDI-TOF/TOF-MS,[63] and they are also commonly observed in negative-ion mode CAD of glycans.[79-81] The ^{1,5}A$_5$ ion (*m/z* = 1769.6) at the branching mannose of the chitobiose core aided determination of the positions of the two antenna. Unlike EDD of 2-AA and 2-AB labeled DSLNT, no X-type ions were found.

MS/MS of the 2-AA tagged *N*-glycan showed somewhat different fragmentation behaviors compared to the 2-AB tagged species. IRMPD of the 2-AA labeled *N*-glycan resulted in efficient fragmentation, generating eleven glycosidic and two cross-ring cleavages (Figure 5.4c). It is interesting to note that ^{2,4}X$_1$ containing the fluorescent tag (*m/z* = 484.2) was observed. Typically, X-type ions are absent in CAD/IRMPD of *N*-glycans.[18,82] The observation of X-type ions following derivatization may indicate that the charge locations are different in the 2-AA labeled *N*-glycan compared to the underivatized glycan. Introduction of the acidic tag 2-AA adds an additional likely site

for deprotonation. EDD of the 2-AA labeled *N*-glycan resulted in only glycosidic cleavages (Figure 5.4d). All observed Y- and Z-type ions contained the fluorescent label 2-AA, suggesting that one negative charge is located on 2-AA. Compared to EDD of the 2-AB labeled *N*-glycan, the most distinct difference was the absence of cross-ring fragments. This difference may be explained by the altered charge location (as further discussed below).
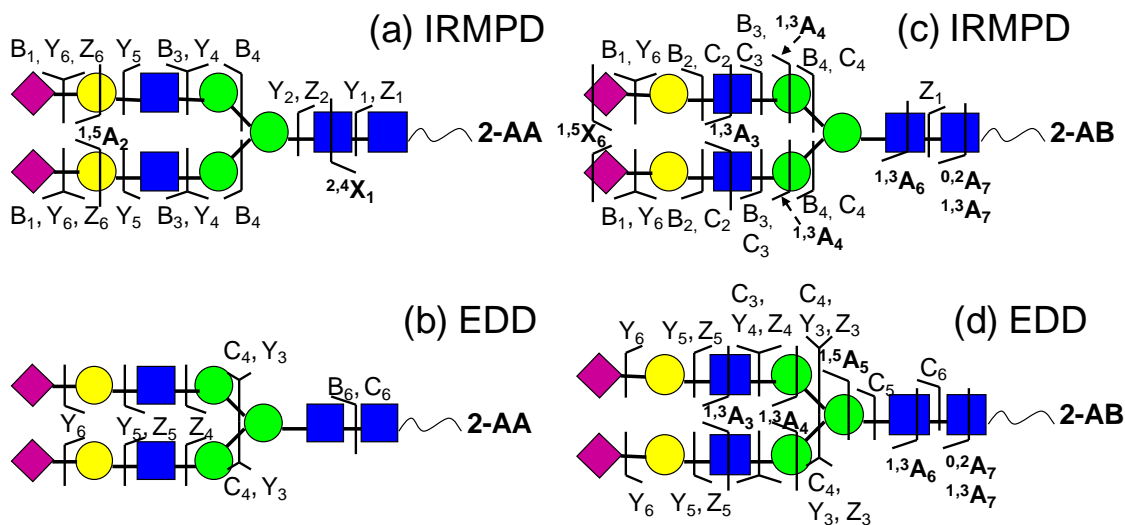
Figure 5.4. MS/MS of a 2-AA (a), (b) and 2-AB (c), (d) derivatized N-linked glycan released from human transferrin. Fragmentation patterns from IRMPD (a), (c) and EDD (b), (d) are shown.

5.3.3 LSTb

LSTb is a branched mono-sialylated oligosaccharide with the composition Galβ3(Neu5Acβ6)GlcNAcβ3Galβ4Glc. Negative-ion mode IRMPD and EDD of 2-AA labeled LSTb were investigated and the results are summarized in Figure 5.5. IRMPD of 2-AA labeled LSTb yielded a complete series of Y- and Z-ions, and also one cross-ring fragment ($^{0,2}X_{3\alpha}$). Again, all the Y- and Z-type ions contained the fluorescent tag. EDD of 2-AA labeled LSTb produced six additional glycosidic and two additional cross-ring

fragments, including $^{1,5}X_2$, and $^{1,5}X_{3\beta}$ ions. $^{0,2}X$- and $^{1,5}X$-type ions have also been reported in positive-ion mode high-energy CAD, LID of sodiated 2-AB labeled oligosaccharides, and EDD of sialylated oligosaccharides.[34,63,69] Similar to EDD of 2-AA labeled DSLNT and the *N*-glycan, unique product ions such as neutral loss (H_2O and CH_3O) from the charge reduced species and C – 2H type satellite ions were observed in the EDD spectrum.

2-AB labeling of LSTb was also conducted and the labeling reaction was successful, however, even with careful tuning of the instrument parameters, the signal abundance of doubly charged species was too low for EDD. Therefore, we were not able to investigate EDD of 2-AB labeled LSTb. In EDD, at least two precursor ion charges are required. In addition, due to the low efficiency of EDD,[27] abundant precursor ion signal is a prerequisite to observe product ions. LSTb has only one acidic site, which is the carboxylic acid on the sialic acid and 2-AB is a neutral tag that does not enhance ionization in negative-ion mode. In contrast, 2-AA labeled LSTb readily generated abundant signal in MS due to the acidity of 2-AA, thus EDD fragmentation could easily be achieved. These observations suggest that the chosen fluorescent tag for derivatization has a strong influence on whether EDD will be successful.
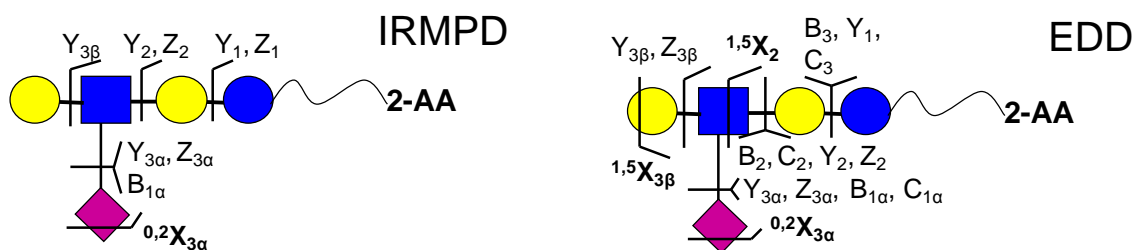
Figure 5.5. IRMPD and EDD fragmentation patterns of 2-AA labeled LSTb.

5.3.4 Influence of Reducing End Derivatization on EDD Fragmentation

EDD fragmentation patterns of DSLNT, LSTb, and the N-linked glycan released from human transferrin with and without fluorescent labels are summarized in Table 5.1. Although product ions resulting from glycosidic and cross-ring cleavages were observed in almost all cases, the degree of fragmentation was different, particularly for the number of observed cross-ring cleavages. Underivatized oligosaccharides provided the most cross-ring fragments in all three sialylated oligosaccharides investigated, followed by 2-AB labeled oligosaccharides. This result is similar to previous studies reported by Harvey and co-workers in positive-ion mode.[69] They compared the effects of reducing end substituent in high-energy CAD of N-linked oligosaccharides, including underivatized and 2-AB labeled oligosaccharides, and *N*-glycopeptides with one and four amino acids. Compared to 2-AB derivatized oligosaccharides, the native species generated a more complete series of glycosidic fragments and also more cross-ring fragments due to the open nature of the reducing terminus ring.[69]

2-AA labeling enhances signal abundance of oligosaccharides in negative-ion mode, however, the 2-AA derivatized oligosaccharides generated the smallest number of cross-ring cleavages. Particularly, no cross-ring fragments were observed for the 2-AA labeled *N*-glycan (compared to three from the 2-AB labeled species and five from the native glycan), which makes 2-AA labeling less favorable in EDD of derivatized oligosaccharides. One possible explanation of this observation is that the introduction of a fluorescent tag at the reducing end of oligosaccharides alters the locations of the negative charges. It has been previously reported that deprotonated hydroxyl is required to obtain cross-ring cleavages in negative-ion mode.[79-81] Without derivatization, it is

most favorable for the negative charges to be located on the sialic acids, but also possible to have deprotonated hydroxyl groups. When 2-AA is introduced at the reducing end, the carboxylic acid on 2-AA is preferably deprotonated, which competes with deprotonation of hydroxyl groups, thus making cross-ring cleavages less likely to occur. 2-AB is a neutral fluorescent label; therefore introducing 2-AB does not cause a significant alteration of negative charges. However, for less acidic oligosaccharides, which are difficult to doubly deprotonate, 2-AB is less favorable due to the lack of an acidic moiety.

EDD FRAGMENTATION	DSLNT	LSTb	*N*-glycan from transferrin
Unlabeled	10 glycosidic 6 cross-ring	11 glycosidic 7 cross-ring	16 glycosidic 5 cross-ring
2-AA labeled	13 glycosidic 4 cross-ring	13 glycosidic 3 cross-ring	10 glycosidic 0 cross-ring
2-AB labeled	11 glycosidic 5 cross-ring	N/A	11 glycosidic 3 cross-ring

Table 5.1. EDD fragmentation summary of DSLNT, LSTb and an *N*-glycan released from transferrin with or without fluorescent labels.

5.4 Conclusions

We demonstrate that EDD of fluorescently labeled sialylated oligosaccharides results in extensive fragmentation, providing rich glycosidic and cross-ring fragments. We also show that complementary structural information can be obtained from EDD compared to IRMPD of the same species. When investigating the influence of introducing different fluorescent labels at the reducing end of oligosaccharides, we found that not only does the labels effect signal abundance, but they also have a strong

influence on the EDD fragmentation behavior. Native oligosaccharides showed the most extensive fragmentation compared to their 2-AA and 2-AB labeled counterparts. The acidic tag 2-AA promotes precursor ion signal abundance in negative-ion mode. However, it introduces another deprotonation site to compete with the sialic acids and hydroxyl groups, thus suggesting that deprotonated hydroxyls are important for cross-ring fragmentation in EDD, as in CAD.[79-81] The neutral label 2-AB does not significantly impede generation of cross-ring cleavages, but for small and less acidic glycans which are difficult to doubly deprotonate, 2-AB may not be the best choice.

5.5 References

1. Varki, A. Biological roles of oligosaccharides - All of the theories are correct. *Glycobiol.* **1993**, *3*, 97-130.
2. Kim, Y. J.; Varki, A. Perspectives on the significance of altered glycosylation of glycoproteins in cancer. *Glycoconj. J.* **1997**, *14*, 569-576.
3. Raman, R.; Raguram, S.; Venkataraman, G.; Paulson, J. C.; Sasisekharan, R. Glycomics: an integrated systems approach to structure-function relationships of glycans. *Nat. Methods* **2005**, *2*, 817-824.
4. Dube, D. H.; Bertozzi, C. R. Glycans in cancer and inflammation. Potential for therapeutics and diagnostics. *Nat. Rev. Drug Discov.* **2005**, *4*, 477-488.
5. Bertozzi, C. R.; Kiessling, L. L. Chemical glycobiology. *Science* **2001**, *291*, 2357-2364.
6. Finkelstein, J. Insight - glycochemistry & glycobiology. *Nature* **2007**, *446*, 999-999.
7. Varki, A. Glycan-based interactions involving vertebrate sialic-acid-recognizing proteins. *Nature* **2007**, *446*, 1023-1029.
8. Morelle, W.; Michalski, J. C. Glycomics and mass spectrometry. *Curr. Pharm. Des.* **2005**, *11*, 2615-2645.
9. Zaia, J. Mass spectrometry and the emerging field of glycomics. *Chem. Biol.* **2008**, *15*, 881-892.
10. Krishnamoorthy, L.; Mahal, L. K. Glycomic analysis: an array of technologies. *ACS Chem. Biol.* **2009**, *4*, 715-732.
11. Mechref, Y.; Novotny, M. V. Structural investigations of glycoconjugates at high sensitivity. *Chem. Rev.* **2002**, *102*, 321-369.
12. Marshall, A. G.; Hendrickson, C. L.; Jackson, G. S. Fourier transform ion cyclotron resonance mass spectrometry: A primer. *Mass Spectrom. Rev.* **1998**, *17*, 1-35.

13. Park, Y. M.; Lebrilla, C. B. Application of Fourier transform ion cyclotron resonance mass spectrometry to oligosaccharides. *Mass Spectrom. Rev.* **2005**, *24*, 232-264.

14. Marshall, A. G.; Hendrickson, C. L. High-resolution mass spectrometers. *Annu. Rev. Anal. Chem.* **2008**, *1*, 579-599.

15. Harvey, D. J. Collision-induced fragmentation of negative ions from N-linked glycans derivatized with 2-aminobenzoic acid. *J. Mass Spectrom.* **2005**, *40*, 642-653.

16. Sagi, D.; Peter-Katalinic, J.; Conradt, H. S.; Nimtz, M. Sequencing of tri- and tetraantennary N-glycans containing sialic acid by negative mode ESI QTOF tandem MS. *J. Am. Soc. Mass. Spectrom.* **2002**, *13*, 1138-1148.

17. Zaia, J.; Miller, M. J. C.; Seymour, J. L.; Costello, C. E. The role of mobile protons in negative ion CID of oligosaccharides. *J. Am. Soc. Mass. Spectrom.* **2007**, *18*, 952-960.

18. Lancaster, K. S.; An, H. J.; Li, B. S.; Lebrilla, C. B. Interrogation of N-linked oligosaccharides using infrared multiphoton dissociation in FT-ICR mass spectrometry. *Anal. Chem.* **2006**, *78*, 4990-4997.

19. Xie, Y. M.; Lebrilla, C. B. Infrared multiphoton dissociation of alkali metal-coordinated oligosaccharides. *Anal. Chem.* **2003**, *75*, 1590-1598.

20. Zhang, J. H.; Schubothe, K.; Li, B. S.; Russell, S.; Lebrilla, C. B. Infrared multiphoton dissociation of O-linked mucin-type oligosaccharides. *Anal. Chem.* **2005**, *77*, 208-214.

21. Harvey, D. J.; Naven, T. J. P.; Kuster, B.; Bateman, R. H.; Green, M. R.; Critchley, G. Comparison of fragmentation modes for the structural determination of complex oligosaccharides ionized by matrix-assisted laser desorption/ionization mass spectrometry. *Rapid Commun. Mass Spectrom.* **1995**, *9*, 1556-1561.

22. Harvey, D. J.; Bateman, R. H.; Green, M. R. High-energy collision-induced fragmentation of complex oligosaccharides ionized by matrix-assisted laser desorption/ionization mass spectrometry. *J. Mass Spectrom.* **1997**, *32*, 167-187.

23. Lewandrowski, U.; Resemann, A.; Sickmann, A. Laser-induced dissociation/high-energy collision-induced dissociation fragmentation using MALDI-TOF/TOF-MS instrumentation for the analysis of neutral and acidic oligosaccharides. *Anal. Chem.* **2005**, *77*, 3274-3283.

24. Zhao, C.; Xie, B.; Chan, S. Y.; Costello, C. E.; O'Connor, P. B. Collisionally activated dissociation and electron capture dissociation provide complementary structural information for branched permethylated oligosaccharides. *J. Am. Soc. Mass. Spectrom.* **2008**, *19*, 138-150.

25. Adamson, J. T.; Hakansson, K. Electron capture dissociation of oligosaccharides ionized with alkali, alkaline earth, and transition metals. *Anal. Chem.* **2007**, *79*, 2901-2910.

26. Budnik, B. A.; Haselmann, K. F.; Elkin, Y. N.; Gorbach, V. I.; Zubarev, R. A. Applications of electron-ion dissociation reactions for analysis of polycationic chitooligosaccharides in Fourier transform mass spectrometry. *Anal. Chem.* **2003**, *75*, 5994-6001.

27.	McFarland, M. A.; Marshall, A. G.; Hendrickson, C. L.; Nilsson, C. L.; Fredman, P.; Mansson, J. E. Structural characterization of the GM1 ganglioside by infrared multiphoton dissociation/electron capture dissociation, and electron detachment dissociation electrospray ionization FT-ICR MS/MS. *J. Am. Soc. Mass. Spectrom.* **2005**, *16*, 752-762.

28.	Liu, H.; Hakansson, K., Analysis of Sulfated Oligosaccharides with Combination of Divalent Metal Complexation and Electron Capture Dissociation. In *Int. J. Mass spectrom.*, 2010.

29.	Wolff, J. J.; Chi, L. L.; Linhardt, R. J.; Amster, I. J. Distinguishing glucuronic from iduronic acid in glycosaminoglycan tetrasaccharides by using electron detachment dissociation. *Anal. Chem.* **2007**, *79*, 2015-2022.

30.	Wolff, J. J.; Laremore, T. N.; Busch, A. M.; Linhardt, R. J.; Amster, I. J. Electron detachment dissociation of dermatan sulfate oligosaccharides. *J. Am. Soc. Mass. Spectrom.* **2008**, *19*, 294-304.

31.	Wolff, J. J.; Laremore, T. N.; Busch, A. M.; Linhardt, R. J.; Amster, I. J. Influence of charge state and sodium cationization on the electron detachment dissociation and infrared multiphoton dissociation of glycosaminoglycan oligosaccharides. *J. Am. Soc. Mass. Spectrom.* **2008**, *19*, 790-798.

32.	Wolff, J. J.; Amster, I. J.; Chi, L. L.; Linhardt, R. J. Electron detachment dissociation of glycosaminoglycan tetrasaccharides. *J. Am. Soc. Mass. Spectrom.* **2007**, *18*, 234-244.

33.	Wolff, J. J.; Laremore, T. N.; Leach, F. E.; Linhardt, R. J.; Amster, I. J. Electron capture dissociation, electron detachment dissociation and infrared multiphoton dissociation of sucrose octasulfate. *Eur. J. Mass Spectrom.* **2009**, *15*, 275-281.

34.	Adamson, J. T.; Hakansson, K. Electron detachment dissociation of neutral and sialylated oligosaccharides. *J. Am. Soc. Mass. Spectrom.* **2007**, *18*, 2162-2172.

35.	Wolff, J. J.; Leach, F. E.; Laremore, T. N.; Kaplan, D. A.; Easterling, M. L.; Linhardt, R. J.; Amster, I. J. Negative electron transfer dissociation of glycosaminoglycans. *Anal. Chem.* **2010**, *82*, 3460-3466.

36.	Devakumar, A.; Thompson, M. S.; Reilly, J. P. dFragmentation of oligosaccharide ions with 157 nm vacuum ultraviolet light. *Rapid Commun. Mass Spectrom.* **2005**, *19*, 2313-2320.

37.	Devakumar, A.; Mechref, Y.; Kang, P.; Novotny, M. V.; Reilly, J. P. Identification of isomeric N-glycan structures by mass spectrometry with 157 nm laser-induced photofragmentation. *J. Am. Soc. Mass. Spectrom.* **2008**, *19*, 1027-1040.

38.	Devakumar, A.; Mechref, Y.; Kang, P.; Novotny, M. V.; Reilly, J. P. Laser-induced photofragmentation of neutral and acidic glycans inside an ion-trap mass spectrometer. *Rapid Commun. Mass Spectrom.* **2007**, *21*, 1452-1460.

39.	Gao, D.; Zhou, W.; Hakansson, K. In *Electron induced dissociation (EID) of singly protonated glycans*, 58th ASMS Conference on Mass Spectrometry and Allied Topics, Salt Lake City, UT, 2010.

40.	Brodbelt, J. S.; Wilson, J. J. Infrared multiphoton dissciation in quadrupole ion traps. *Mass Spectrom. Rev.* **2009**, *28*, 390-424.

41.	Eyler, J. R. Infrared multiple photon dissociation spectroscopy of ions in Penning traps *Mass Spectrom. Rev.* **2009**, *28*, 448-467.

42. Budnik, B. A.; Haselmann, K. F.; Zubarev, R. A. Electron detachment dissociation of peptide di-anions: an electron-hole recombination phenomenon. *Chem. Phys. Lett.* **2001**, *342*, 299-302.

43. Zubarev, R. A. Reactions of polypeptide ions with electrons in the gas phase. *Mass Spectrom. Rev.* **2003**, *22*, 57-77.

44. Zhou, W.; Håkansson, K. In *Ion-electron reactions of sialylated N-linked glycans released from glycoproteins*, 57th ASMS Conference on Mass Spectrometry and Allied Topics, Philadelphia, PA, 2009.

45. Wolff, J. J.; Laremore, T. N.; Aslam, H.; Linhardt, R. J.; Amster, I. J. Electron-induced dissociation of glycosaminoglycan tetrasaccharides. *J. Am. Soc. Mass. Spectrom.* **2008**, *19*, 1449-1458.

46. Yoshino, K.; Takao, T.; Murata, H.; Shimonishi, Y. Use of the derivatizing agent 4-aminobenzoic acid 2-(diethylamino)ethyl ester for high-sensitivity detection of oligosaccharides by electrospray-ionization mass-spectrometry. *Anal. Chem.* **1995**, *67*, 4028-4031.

47. Lamari, F. N.; Kuhn, R.; Karamanos, N. K. Derivatization of carbohydrates for chromatographic, electrophoretic and mass spectrometric structure analysis. *Journal of Chromatography B-Analytical Technologies in the Biomedical and Life Sciences* **2003**, *793*, 15-36.

48. Lattova, E.; Snovida, S.; Perreault, H.; Krokhin, O. Influence of the labeling group on ionization and fragmentation of carbohydrates in mass spectrometry. *J. Am. Soc. Mass. Spectrom.* **2005**, *16*, 683-696.

49. Anumula, K. R. Advances in fluorescence derivatization methods for high-performance liquid chromatographic analysis of glycoprotein carbohydrates. *Anal. Biochem.* **2006**, *350*, 1-23.

50. Ruhaak, L. R.; Zauner, G.; Huhn, C.; Bruggink, C.; Deelder, A. M.; Wuhrer, M. Glycan labeling strategies and their use in identification and quantification. *Anal. Bioanal. Chem.* **2010**, *397*, 3457-3481.

51. Wuhrer, M.; Deelder, A. M.; Hokke, C. H. Protein glycosylation analysis by liquid chromatography-mass spectrometry. *Journal of Chromatography B-Analytical Technologies in the Biomedical and Life Sciences* **2005**, *825*, 124-133.

52. Bowman, M. J.; Zaia, J. Tags for the stable isotopic labeling of carbohydrates and quantitative analysis by mass spectrometry. *Anal. Chem.* **2007**, *79*, 5777-5784.

53. Xia, B. Y.; Feasley, C. L.; Sachdev, G. P.; Smith, D. F.; Cummings, R. D. Glycan reductive isotope labeling for quantitative glycomics. *Anal. Biochem.* **2009**, *387*, 162-170.

54. Prien, J. M.; Prater, B. D.; Qin, Q.; Cockrill, S. L. Mass spectrometric-based stable isotopic 2-aminobenzoic acid glycan mapping for rapid glycan screening of biotherapeutics. *Anal. Chem.* **2010**, *82*, 1498-1508.

55. Bigge, J. C.; Patel, T. P.; Bruce, J. A.; Goulding, P. N.; Charles, S. M.; Parekh, R. B. Nonselective and Efficient Fluorescent Labeling of Glycans using 2-amino Benzamide and Anthranilic Acid. *Anal. Biochem.* **1995**, *230*, 229-238.

56. Maslen, S.; Sadowski, P.; Adam, A.; Lilley, K.; Stephens, E. Differentiation of isomeric N-glycan structures by normal-phase liquid chromatography-MALDI-TOF/TOF tandem mass spectrometry. *Anal. Chem.* **2006**, *78*, 8491-8498.

57. Maslen, S. L.; Goubet, F.; Adam, A.; Dupree, P.; Stephens, E. Structure elucidation of arabinoxylan isomers by normal phase HPLC-MALDI-TOF/TOF-MS/MS. *Carbohydr. Res.* **2007**, *342*, 724-735.

58. Wuhrer, M.; Koeleman, C. A. M.; Deelder, A. M. Hexose rearrangements upon fragmentation of N-glycopeptides and reductively aminated N-glycans. *Anal. Chem.* **2009**, *81*, 4422-4432.

59. Harvey, D. J. Electrospray mass spectrometry and collision-induced fragmentation of 2-aminobenzamide-labelled neutral N-linked glycans. *Analyst* **2000**, *125*, 609-617.

60. Harvey, D. J. Electrospray mass spectrometry and fragmentation of N-linked carbohydrates derivatized at the reducing terminus. *J. Am. Soc. Mass. Spectrom.* **2000**, *11*, 900-915.

61. Sato, Y.; Suzuki, M.; Nirasawa, T.; Suzuki, A.; Endo, T. Microsequencing of glycans using 2-aminobenzamide and MALDI-TOF mass spectrometry: Occurrence of unique linkage-dependent fragmentation. *Anal. Chem.* **2000**, *72*, 1207-1216.

62. Wuhrer, M.; Koeleman, C. A. M.; Hokke, C. H.; Deelder, A. M. Nano-scale liquid chromatography-mass spectrometry of 2-aminobenzamide-labeled oligosaccharides at low femtomole sensitivity. *Int. J. Mass spectrom.* **2004**, *232*, 51-57.

63. Wuhrer, M.; Deelder, A. M. Negative-mode MALDI-TOF/TOF-MS of oligosaccharides labeled with 2-aminobenzamide. *Anal. Chem.* **2005**, *77*, 6954-6959.

64. Morelle, W.; Slomianny, M. C.; Diemer, H.; Schaeffer, C.; van Dorsselaer, A.; Michalski, J. C. Structural characterization of 2-aminobenzamide-derivatized oligosaccharides using a matrix-assisted laser desorption/ionization two-stage time-of-flight tandem mass spectrometer. *Rapid Commun. Mass Spectrom.* **2005**, *19*, 2075-2084.

65. Chen, X. Y.; Flynn, G. C. Gas-phase oligosaccharide nonreducing end (GONE) sequencing and structural analysis by reversed phase HPLC/mass spectrometry with polarity switching. *J. Am. Soc. Mass. Spectrom.* **2009**, *20*, 1821-1833.

66. Takegawa, Y.; Deguchi, K.; Ito, S.; Yoshioka, S.; Nakagawa, H.; Nishimura, S. I. Structural assignment of isomeric 2-aminopyridine-derivatized oligosaccharides using negative-ion MSn spectral matching. *Rapid Commun. Mass Spectrom.* **2005**, *19*, 937-946.

67. Deguchi, K.; Takegawa, Y.; Ito, H.; Miura, N.; Yoshioka, S.; Nagai, S.; Nakagawa, H.; Nishimura, S. I. Structural assignment of isomeric 2-aminopyridine-derivatized monosialylated biantennary N-linked oligosaccharides using negative-ion multistage tandem mass spectral matching. *Rapid Commun. Mass Spectrom.* **2006**, *20*, 412-418.

68. Briggs, J. B.; Keck, R. G.; Ma, S.; Lau, W. D.; Jones, A. J. S. An analytical system for the characterization of highly heterogeneous mixtures of N-linked oligosaccharides. *Anal. Biochem.* **2009**, *389*, 40-51.

69. Kuster, B.; Naven, T. J. P.; Harvey, D. J. Effect of the reducing-terminal substituents on the high energy collision-induced dissociation matrix-assisted

laser desorption/ionization mass spectra of oligosaccharides. *Rapid Commun. Mass Spectrom.* **1996**, *10*, 1645-1651.

70. Wilson, J. J.; Brodbelt, J. S. Ultraviolet photodissociation at 355 nm of fluorescently labeled oligosaccharides. *Anal. Chem.* **2008**, *80*, 5186-5196.

71. Morelle, W.; Page, A.; Michalski, J. C. Electrospray ionization ion trap mass spectrometry for structural characterization of oligosaccharides derivatized with 2-aminobenzamide. *Rapid Commun. Mass Spectrom.* **2005**, *19*, 1145-1158.

72. Yang, J.; Mo, J. J.; Adamson, J. T.; Hakansson, K. Characterization of oligodeoxynucleotides by electron detachment dissociation Fourier transform ion cyclotron resonance mass spectrometry. *Anal. Chem.* **2005**, *77*, 1876-1882.

73. Tsybin, Y. O.; Witt, M.; Baykut, G.; Kjeldsen, F.; Hakansson, P. Combined infrared multiphoton dissociation and electron capture dissociation with a hollow electron beam in Fourier transform ion cyclotron resonance mass spectrometry. *Rapid Commun. Mass Spectrom.* **2003**, *17*, 1759-1768.

74. Caravatti, P.; Allemann, M. The infinity cell - a new trapped-ion cell with radiofrequency covered trapping electrodes for Fourier-transform ion-cyclotron resonance mass-spectrometry. *Org. Mass Spectrom.* **1991**, *26*, 514-518.

75. Senko, M. W.; Canterbury, J. D.; Guan, S. H.; Marshall, A. G. A high-performance modular data system for Fourier transform ion cyclotron resonance mass spectrometry. *Rapid Commun. Mass Spectrom.* **1996**, *10*, 1839-1844.

76. Ledford, E. B.; Rempel, D. L.; Gross, M. L. Space-charge effects in Fourier-transform mass-spectrometry - mass calibration *Anal. Chem.* **1984**, *56*, 2744-2748.

77. Lohmann, K. K.; von der Lieth, C. W. GlycoFragment and GlycoSearchMS: web tools to support the interpretation of mass spectra of complex carbohydrates. *Nucleic Acids Res.* **2004**, *32*, W261-W266.

78. Domon, B.; Costello, C. E. A systematic nomenclature for carbohydrate fragmentations in FAB-MS MS spectra of glycoconjugates *Glycoconj. J.* **1988**, *5*, 397-409.

79. Harvey, D. J. Fragmentation of negative ions from carbohydrates: Part 1. Use of nitrate and other anionic adducts for the production of negative ion electrospray spectra from N-linked carbohydrates. *J. Am. Soc. Mass. Spectrom.* **2005**, *16*, 622-630.

80. Harvey, D. J. Fragmentation of negative ions from carbohydrates: Part 2. Fragmentation of high-mannose N-linked glycans. *J. Am. Soc. Mass. Spectrom.* **2005**, *16*, 631-646.

81. Harvey, D. J. Fragmentation of negative ions from carbohydrates: Part 3. Fragmentation of hybrid and complex N-linked glycans. *J. Am. Soc. Mass. Spectrom.* **2005**, *16*, 647-659.

82. Pikulski, M.; Hargrove, A.; Shabbir, S. H.; Anslyn, E. V.; Brodbelt, J. S. Sequencing and characterization of oligosaccharides using infrared multiphoton dissociation and boronic acid derivatization in a quadrupole ion trap. *J. Am. Soc. Mass. Spectrom.* **2007**, *18*, 2094-2106.

Chapter 6

Electron Detachment Dissociation (EDD) of Pronase-derived Sialylated N- and O-linked Glycopeptides

6.1 Introduction

Protein glycosylation is one of the most prevalent post-translational modifications (PTMs). It has been estimated that over 50% of proteins in mammalian proteomes are glycosylated.[1] Glycosylation plays vital roles in various cellular processes, such as cell-cell adhesion, cell-cell repulsion, molecular trafficking, and cancer metastasis.[2-5] Aberrant glycosylation has been associated with many diseases, such as cancer.[6-8] Investigating site-specific glycosylation is essential for further understanding of the functions and roles of glycans in biological systems. However, compared to other PTMs such as phosphorylation, glycosylation is often less understood, due to the structural complexity of glycans and the heterogeneity of glycoforms on a specific glycosylation site.[9-14] Based on the different sites in a polypeptide chain that glycans are attached to, glycosylation can be divided into N-linked and O-linked glycosylation.[9] In *N*-glycosylation, glycans are attached to asparagine residues via amide bonds in the consensus peptide sequence Asn-Xxx-Ser/Thr (Xxx cannot be proline) and share a pentasaccharide core structure. O-linked glycosylation does not have a consensus peptide

sequence or one single core structure for all O-linked glycans, which make *O*-glycosylation even more difficult to characterize.

Despite recent technological advances, it is still analytically challenging to characterize glycosylation by mass spectrometry (MS) based approaches. In order to fully characterize glycosylation, glycosylation site, glycan structures, and different glycoforms all need to be determined. Peptide-*N*-glycosidase F (PNGase F) has been widely applied to study *N*-glycosylation.[15] It can cleave the amide bond between the *N*-glycan and the asparagine residue to release glycans from glycoproteins, which allows further purification and structural analysis of the glycans. Meanwhile, the previously glycosylated asparagine residue is converted to an aspartic acid, introducing a mass difference of 1 Da in the peptide, which aids glycosylation site determination.[16-18] However, glycans and de-glycosylated peptides are often analyzed separately, which can be labor intensive for large scale analysis. It would be advantageous to develop novel methods which could provide glycosylation site and glycan structural information simultaneously. Therefore, structural characterization of glycopeptides has received increasing attention.[19-22]

Tandem mass spectrometry (MS/MS) has become an indispensable tool for structural analysis of biomolecules. A variety of MS/MS techniques have been employed to characterize glycopeptides, including collision activated dissociation (CAD),[23-27] high-energy CAD (HeCAD),[28] infrared multiphoton dissociation (IRMPD),[29-35] electron capture dissociation (ECD),[29,30,35-37] electron transfer dissociation (ETD),[38-42] 157 nm ultraviolet photon dissociation (UVPD),[43] high-energy C-trap dissociation (HCD),[44] and post source decay (PSD).[45,46] CAD and IRMPD are "slow-heating" techniques, in which

precursors ions are activated either by colliding with neutral gas molecules, or by absorbing photons, often resulting in rupture of the weakest bonds. IRMPD often demonstrates higher fragmentation efficiency compared to CAD, due to its ability to induce multiple fragmentation events.[47] When applying CAD/IRMPD to glycopeptides, glycosidic cleavages on the glycan moiety are frequently observed, whereas the peptides remain intact.[29,30,35] Monosaccharide composition can be determined by CAD/IRMPD, however, glycosylation site information is often absent. In ECD or ETD, precursor ions are irradiated with low energy electrons or reacted with radical anions to generate charge-reduced species via electron capture or transfer followed by subsequent radical-driven fragmentation. ECD and ETD typically provide more complete sequence information compared to CAD/IRMPD.[48-50] When applying ECD/ETD to glycopeptides, peptide backbone cleavages (c and z$^\bullet$ ions) are observed, while the glycan moiety is retained on the peptide backbone, providing information regarding glycosylation sites.[29,30,35-42] Due to the ability of CAD/IRMPD and ECD/ETD to yield complementary structural information, the slow-heating and radical-driven dissociation approaches are frequently combined to characterize glycopeptides in positive-ion mode.

Structural analysis of glycopeptides in negative-ion mode MS is not as widely utilized. However, acidic glycopeptides such as sialylated glycopeptides are readily deprotonated, which makes negative-ion mode analysis a logical choice due to the corresponding abundant signal. Lebrilla and co-workers investigated N- and O-linked glycopeptides by MS and MS/MS, and showed that negative-ion mode analysis of glycopeptides demonstrated unique advantages, including enhanced detection of glycopeptides, particularly for sialylated *O*-glycopeptides, and generation of more

peptide structural information in MS/MS.[51] Deguchi and co-workers compared negative-ion to positive-ion MS analysis of sialylated glycopeptides by MS[n] and also reported that more information about peptide sequence could be obtained from negative-ion mode.[24] Electron detachment dissociation (EDD) was recently introduced for structural characterization of peptide anions,[52] and also has been utilized to analyze oligonucleotides,[53,54] gangliosides,[55] model oligosaccharides,[56] and GAG-derived oligosaccharides.[57-63] In EDD, polyanions are irradiated with >10 eV electrons to yield electron detachment, forming radical anions which undergo further radical-driven fragmentation. EDD of sialylated oligosaccharides provided complementary structural information compared to negative-ion mode IRMPD, rendering EDD a promising tool for biomolecule structural elucidation.[56]

Pronase E is a non-specific enzyme which can cleave a peptide backbone at any amino acid, thus generating short peptides with as little as one, two, or several amino acids.[28] Compared to traditionally used trypsin, pronase has several advantages: due to the steric hindrance of glycans adjacent to the glycosylation site, the reactivity of the protease reaction is significantly reduced. Therefore, when short glycopeptides are produced via pronase digestion, non-glycosylated peptides are already digested into single amino acids or di-peptides, which decreases ion suppression from non-glycosylated peptides. In addition, compared to tryptic glycopeptides which often suffer from large sizes, the lengths of glycopeptides can be controlled by changing digestion time and protein/enzyme ratio. MS analysis combined with pronase digestion has shown significant potential of achieving comprehensive structural analysis of glycopeptides.[18,25,28,31-33,51,64-66] Here, we explore EDD and IRMPD of sialylated

glycopeptides from pronase digestion of human transferrin and bovine fetuin and compare the fragmentation behaviors from these two techniques. To the best of our knowledge, this work demonstrates the first application of EDD to acidic glycopeptides.

6.2 Experimental

6.2.1 Reagents

Human apo-transferrin, bovine fetuin, and protease E from Streptomyces griseus Type XIVin (pronase E) were purchased from Sigma Chemical Co. (St. Louis, MO). NH_4HCO_3, NH_4OH, H_2O, methanol, and acetonitrile were obtained from Fisher (Fair Lawn, NJ).

6.2.2 Pronase Digestion of Glycoproteins and Glycopeptide Purification

Glycoproteins were dissolved in 50 mM NH_4HCO_3 solution (pH 8), and incubated with pronase E at 37 ^oC from 2 h to overnight. The mass ratio of protein to enzyme varied from 1:1 to 50:1. The resulting mixtures were desalted with SPE graphitized carbon column (Supelco, Bellefonte, PA). For each sample, a carbon cartridge was washed with 0.1% (v/v) formic acid in 80% acetonitrile/H_2O (v/v), followed by deionized water. The solution containing glycopeptides was loaded, and the cartridge was then washed with deionized water to remove salts and other contaminants. The glycans were eluted with 0.1% formic acid (v/v) in 20%, 40% or 60% acetonitrile/H_2O (v/v). The solution was dried down in a vacuum concentrator (Eppendorf, Hamberg, Germany) and reconstituted in 50% methanol, 0.1% NH_4OH (v/v) solution for MS analysis.

6.2.3 Mass Spectrometry

All mass spectra were collected with an actively shielded 7 T FT-ICR mass spectrometer with a quadrupole front-end (APEX-Q, Bruker Daltonics, Billerica, MA), as

previously described.[53]   An indirectly heated hollow dispenser cathode was used to perform EDD.[67]   IRMPD was performed with a vertically mounted 25 W, 10.6 μM CO_2 laser (Synrad, Mukilteo, WA). Samples were infused via an Apollo II electrospray ion source at a flow rate of 70 μL/h with the assistance of N_2 nebulizing gas. Following ion accumulation in the first hexapole for 0.05 s, ions were mass selectively accumulated in the second hexapole for 1-6 s. Ions were then transferred through high voltage ion optics and captured with dynamic trapping in an Infinity ICR cell.[68]   The accumulation sequence up to the ICR cell fill was looped 3 times to optimize precursor ion signal to noise (S/N) ratio. For EDD, the cathode heating current was kept at 2.0 A, and the cathode voltage was pulsed to a bias voltage of - 30 to - 35 V for 1 s. IRMPD was performed with a laser power of 10 W with firing times ranging from 0.25–0.6 s.

6.2.4 Data Analysis

All mass spectra were acquired with XMASS software (Bruker Daltonics) with 256 data points from m/z 100 to 2000 and summed over 60-100 scans. Data processing was performed with MIDAS software.[69]   Data were zero filled once, Hanning apodized, and exported to Microsoft Excel for internal frequency-to-mass calibration with a two-term calibration equation.[70]   Product ion spectra were interpreted with the aid of the web application GlycoFragment (www.dkfz.de/spec/projekte/fragments/).[71]   Product ions were not assigned unless the S/N ratio was at least 3.

6.3 Results and Discussion

Protein glycosylation of human transferrin and bovine fetuin has been previously well studied.[72-74] In the MS/MS spectra, glycan fragments are labeled with capital letters using the Domon/Costello nomenclature, whereas peptide fragments are labeled with

lower case letters using Biemann's nomenclature.[75,76] MS/MS of glycans mainly results in two types of cleavages: glycosidic cleavages (B- and C-type ions) which occur between monosaccharide residues, and cross-ring cleavages (A- and X-type ions) across the sugar rings.[75] Glycosidic cleavages provide structural information regarding monosaccharide composition, while cross-ring cleavages aid the determination of linkage type.

6.3.1 An N-linked Glycopeptide with Only Asparagine

N-linked glycopeptides can be generated by incubating the glycoprotein with pronase E at $37^{o}C$ overnight. When the mass ratio of pronase/protein equaled 1, the most abundant species in the mixture were glycopeptides with only one amino acid attached, accompanied by some glycosylated di-peptides (data not shown). MS/MS of a glycopeptide with only asparagine from human transferrin is shown in Figure 6.1. Negative-ion mode IRMPD of this glycopeptide generated extensive fragments, including thirteen glycan glycosidic cleavages and eleven cross-ring cleavages, most of them being A-, B-, and C-type ions containing the non-reducing end (Figure 6.1a). The reducing end fragments (Z_5, Y_6, and Z_6) all retained the asparagine residue. B_1 (m/z = 290.09, deprotonated sialic acid) was the most abundant product ion species, in accordance with previous results.[77] Notably, the large number of cross-ring fragments significantly contributed to the determination of linkage types. The cross-ring fragments on the GlcNAc residue at the antenna ($^{0,2}A_3$, $^{1,3}A_3$ and $^{2,4}A_3$) determined the linkage of GlcNAc to be $\alpha1$-4. The cross-ring fragments on the GlcNAc residue attached to the amino acid ($^{0,2}A_7$, $^{1,3}A_7$ and $^{2,4}A_7$) determined the linkage of the neighboring GlcNAc to be $\alpha1$-4 as well. These results demonstrate that negative-ion mode IRMPD is a highly useful tool

135

for sialylated glycopeptide characterization, providing both monosaccharide composition and linkage information simultaneously.

As shown in Figure 6.1b, EDD of the same glycopeptide resulted in drastically different fragmentation pathways. Eleven glycosidic cleavages were observed while cross-ring cleavages were absent in the EDD spectrum. Most product ions were Y- and Z-type ions retaining the amino acid. Several fragments unique to EDD, such as C – 2H, and neutral losses (CO_2 and H_2O) from the charge-reduced species were also observed. C – 2H type ions have been previously reported in EDD of GAGs, standard oligosaccharides, and sialylated N-linked glycans, and some product ions generated from GAGs were used as diagnostic ions to distinguish IdoA and GlcA.[56,58,78]   EDD of the sialylated glycopeptide has a relatively simple fragmentation pattern compared to IRMPD, and the glycan "sequence" can be determined from the glycosidic cleavages between every neighboring monosaccharide. However, lack of cross-ring fragments renders linkage determination difficult.

(a) IRMPD
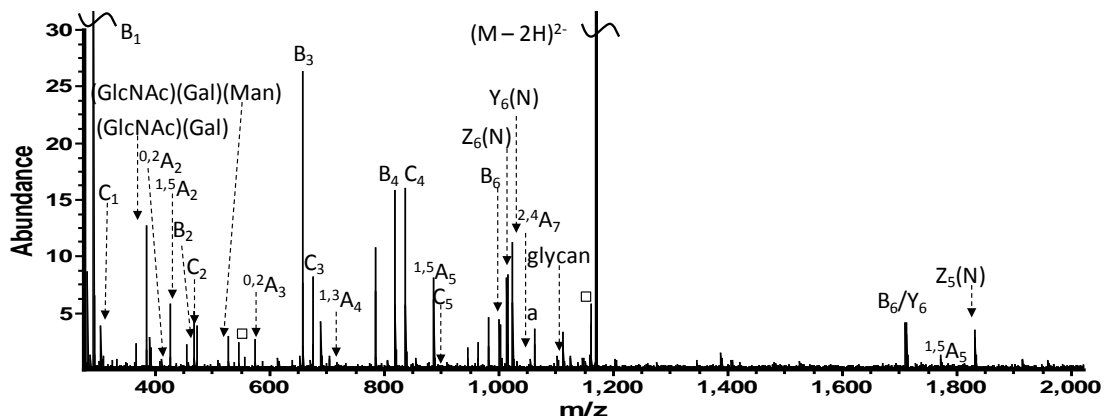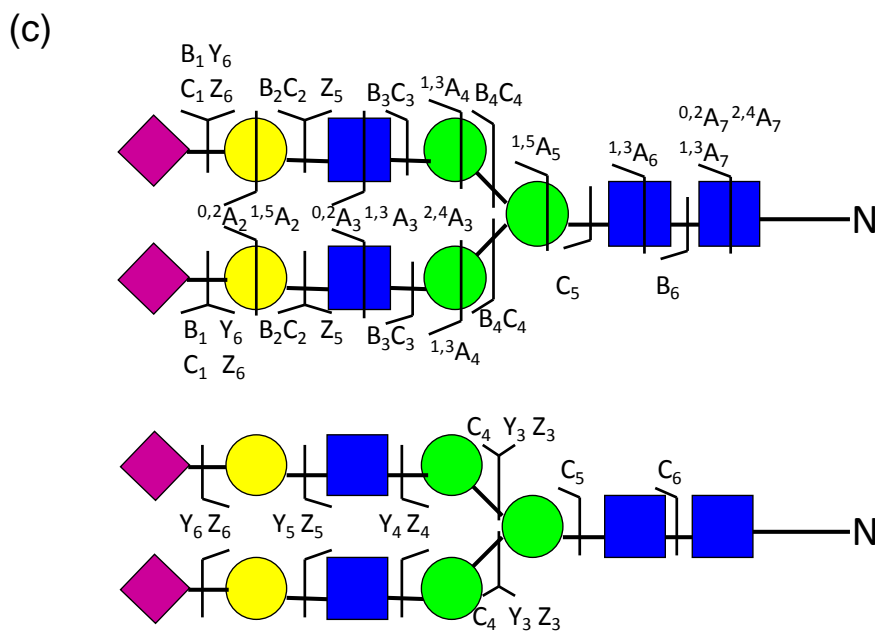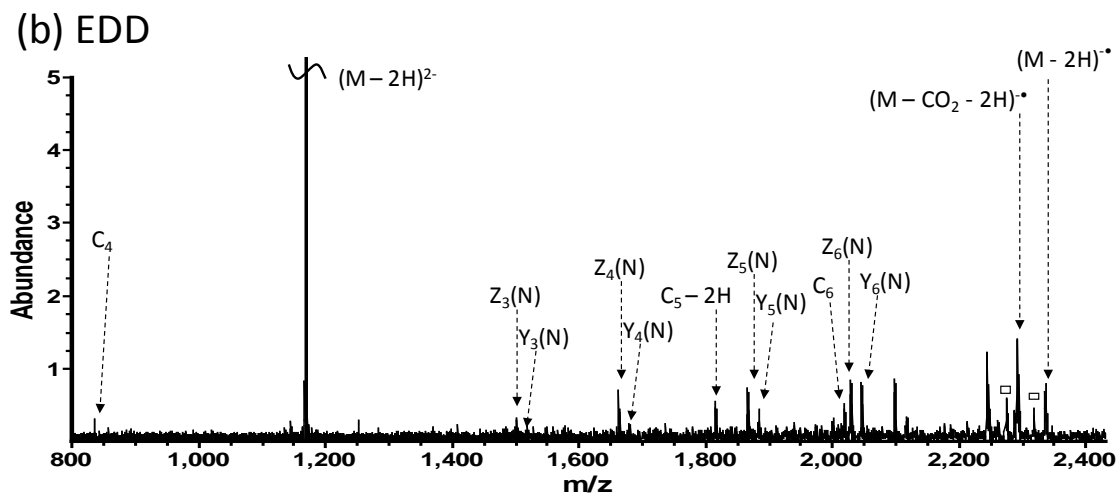
Figure 6.1. (a) IRMPD (80 scans, 0.35 s at 10 W) and (b) EDD (80 scans, 1s irradiation, cathode bias – 30 V) spectra of a doubly deprotonated *N*-glycopeptide with one amino acid from pronase digestion of human transferrin. Squares indicate water loss from the adjacent product ion. Fragments containing the asparagine residue are labeled as Y(N) or Z(N). a = $^{1,3}A_6$, $^{1,3}A_3$, $^{0,2}A_7$ or $^{1,3}A_7$ (these ions share the same *m/z*). Fragmentation patterns from IRMPD and EDD are summarized in Figure 6.1c.

137

6.3.2 N-linked Glycopeptides with Different Peptide Lengths

During pronase E digestion, the peptide lengths can be controlled by changing the ratios of pronase/protein, or by changing the incubation time.[31] We were able to obtain a series of glycopeptides with different peptide lengths but sharing the same N-linked glycan structure using mass ratios of pronase/protein from 1:1 to 1:50. Such related glycopeptides allow investigation of the influence of the peptide moiety on the fragmentation of glycopeptides.

Figure 6.2 displays the EDD fragmentation patterns of a released N-linked glycan and three N-linked glycopeptides (bearing the same *N*-glycan) with one, two, or three amino acid(s) from pronase digestion of transferrin. EDD of the N-linked glycan generated extensive fragmentation (Figure 6.2a), resulting in thirteen glycosidic cleavages and five cross-ring cleavages, including ^{1,5}A- and ^{1,5}X-type ions. EDD of the N-linked glycopeptide with only an asparagine residue attached, as discussed previously, yielded eleven glycosidic fragments and no cross-ring fragments (Figure 6.2b). It is interesting to note the absence of cross-ring fragments for the glycopeptide. The *m/z* difference of the doubly deprotonated glycan and glycopeptide species is not significant (1110 vs 1167). However, a drastic change in the fragmentation behavior was observed when one amino acid was present. When the peptide length was further increased to a di-peptide sharing the same glycan structure and subjected to EDD, only six glycosidic cleavages were observed and cross-ring cleavages were still absent (Figure 6.2c). EDD of a tri-peptide sharing the same glycan moiety yielded even fewer glycosidic cleavages (three compared to six and eleven) and no cross-ring cleavages (Figure 6.2d). One possible explanation is altered negative charge locations due to the presence of the

glycopeptide C-terminus. Harvey reported that deprotonated hydroxyl is required for glycan anions to generate cross-ring fragments in CAD.[79-81] Our results suggest that deprotonated hydroxyl groups may also be required for cross-ring fragmentation in EDD. Therefore, when a peptide portion is present, EDD fragmentation efficiency decreases, and less glycan structural information is obtained. In addition, when peptide length increases, further decrease in fragmentation efficiency may be explained by more folded gas-phase structures.
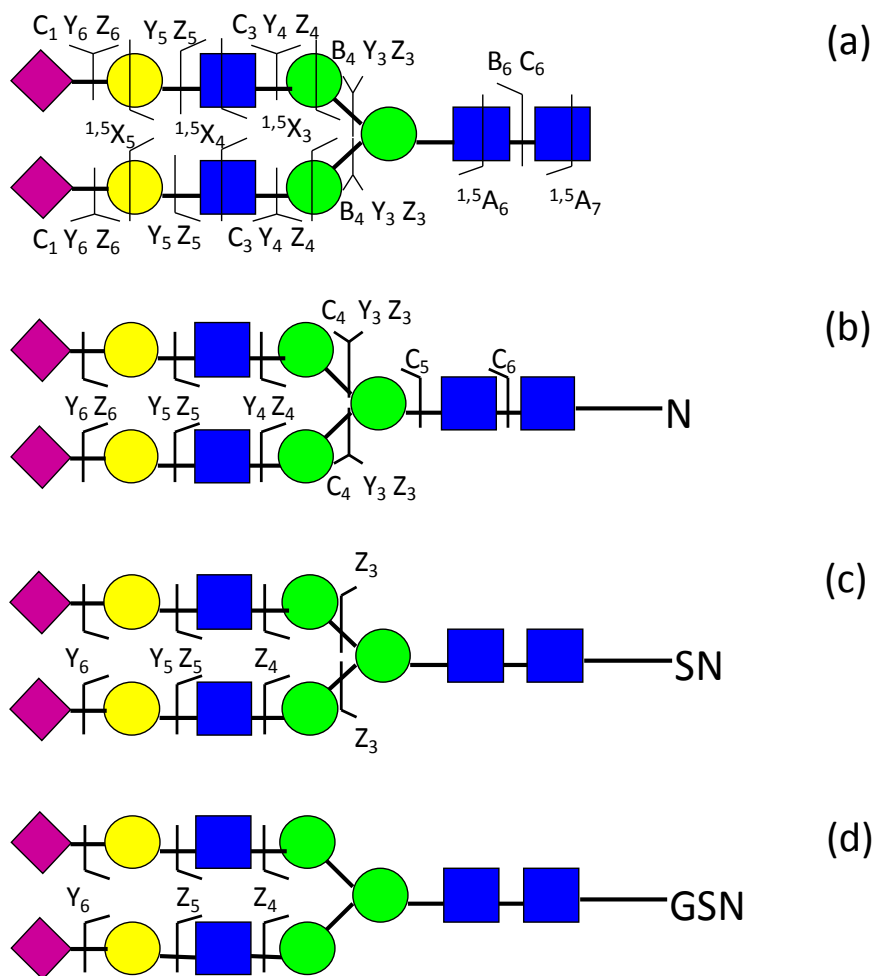
Figure 6.2. EDD fragmentation patterns of an N-linked glycan released from human transferrin (a), and of pronase-derived *N*-glycopeptides with one, two, and three amino acid(s) from human transferrin ((b), (c), and (d), respectively).
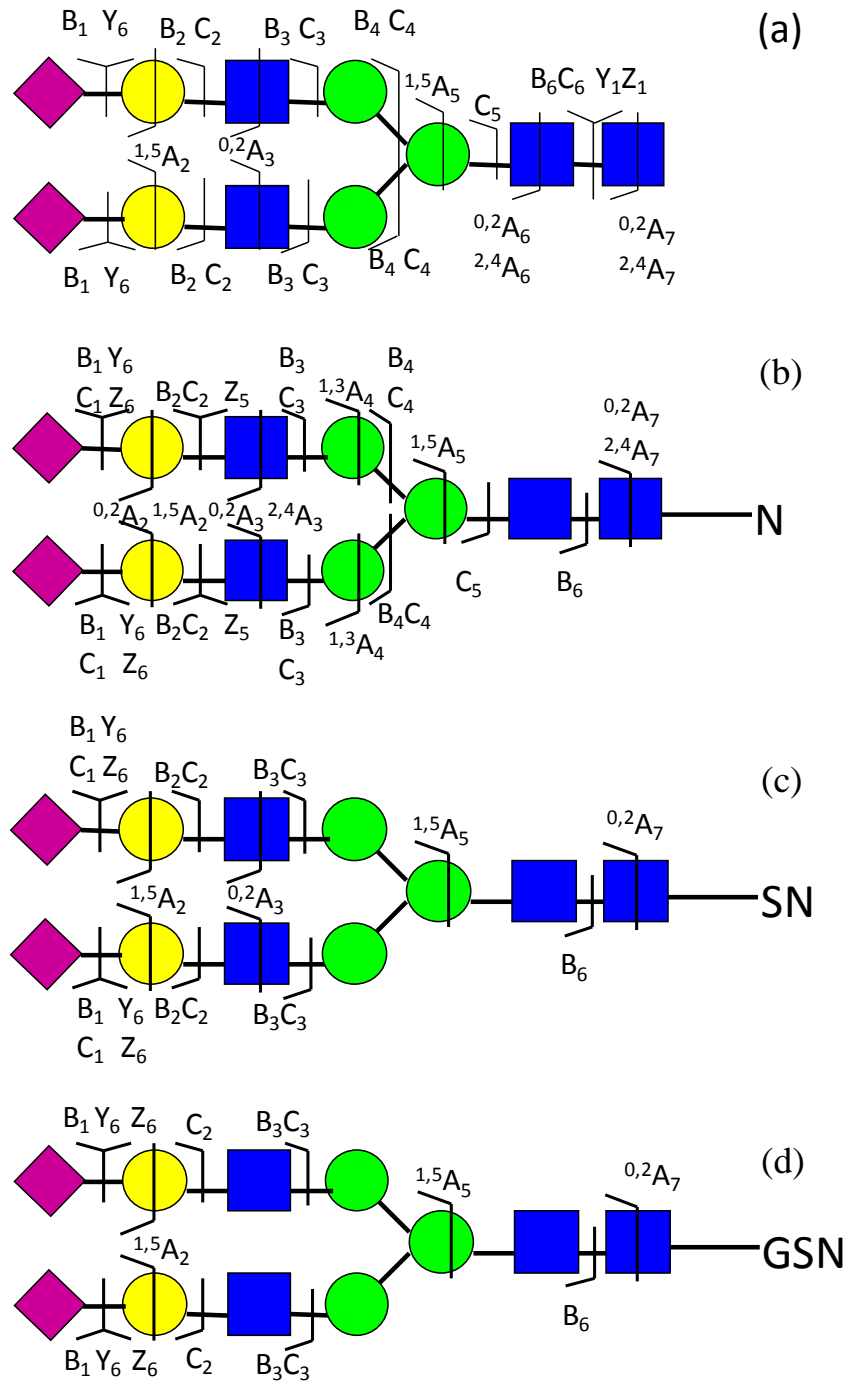
Figure 6.3. IRMPD fragmentation patterns of an N-linked glycan released from human transferrin (a), and pronase-derived *N*-glycopeptides with one, two, and three amino acid(s) from human transferrin ((b), (c), and (d), respectively). Increased peptide length decreases fragmentation for *N*-glycopeptides.

For IRMPD of N-linked glycopeptides, a similar but less dramatic trend was observed. IRMPD fragmentation patterns of the same N-linked glycan and N-linked glycopeptides are compared in Figure 6.3. When peptide lengths increased from zero (glycan) to four amino acids, the number of glycosidic cleavages decreased from thirteen to eight, and the number of cross-ring cleavages decreased from seven to three. In IRMPD spectra, most product ions contained the non-reducing end (A-, B-, and C-type), including ^{0,2}A-, ^{1,3}A-, ^{1,5}A-, and ^{2,4}A-type ions. ^{0,2}A- and ^{2,4}A-type ions are commonly observed in negative-ion mode CAD of glycans.[79-81] The doubly charged ^{1,5}A$_5$ ion (m/z = 884.3), present in all IRMPD spectra, aided antenna determination. Overall, EDD and IRMPD fragmentation efficiency decrease when glycopeptide lengths increase. The glycopeptide with only asparagine residue attached generated the most extensive glycan structural information among the glycopeptides investigated. However, with only one amino acid, it does not provide information on the N-glycosylation site within the protein. There seems to be a trade-off between glycosylation site determination and simultaneous abundant glycan structural information.

6.3.3 An O-linked Glycopeptide with One Glycosylation Site

O-glycosylation characterization is highly challenging because there is no consensus peptide sequence for O-glycosylation, and no single core structure for O-linked glycans. Compared to traditionally used amino acid specific enzymes such as trypsin and Glu C, pronase-derived O-glycopeptides are generally significantly smaller, often shorter than ten amino acids. However, with the same enzyme digestion time, it is interesting to note that the peptide lengths for O-glycopeptides were consistently longer

than for *N*-glycopeptides. This effect may be attributed to the more significant steric hindrance of *O*-glycans compared to *N*-glycans.[33]

Negative-ion mode CAD, IRMPD and EDD of an *O*-glycopeptide from bovine fetuin were investigated and the results are shown in Figure 6.4. Two peptide sequences are possible for this glycopeptide (APSAVPD or PSAVPDA), impossible to distinguish without MS/MS results. CAD of the doubly deprotonated glycopeptide yielded one glycosidic cleavage in the glycan moiety and one peptide backbone cleavage (Figure 6.4a). No cross-ring fragments were observed. The most abundant product ions corresponded to loss of one sialic acid (Y_2 or $Y_{1\beta}$), which is commonly observed in CAD/IRMPD of sialylated glycans or glycopeptides.[34,56,77] The peptide backbone cleavage occurred on the C-terminal side of proline, which appears unusual. Harrison and co-workers investigated deprotonated peptides containing proline using CAD, and observed substantial proline effect (cleaving the amide bond N-terminal to proline).[82] Internal fragments involving multiple bond cleavages and neutral loss (H_2O and CO_2) were also detected in the CAD spectrum. IRMPD of the same glycopeptide resulted in both glycan structural information (three glycosidic cleavages, complete coverage of monosaccharide composition) and peptide sequence information (three peptide backbone cleavages, i.e., partial coverage), demonstrating improved fragmentation efficiency compared to CAD (Figure 6.4b). However, cross-ring cleavage was still absent in the IRMPD spectrum. EDD of the same species generated five glycosidic cleavages and two cross-ring cleavages, including $^{0,2}X_2$ ($^{0,2}X_{1\beta}$) and $^{1,5}X_{1\alpha}$. $^{1,5}X$-type ions have previously been reported from EDD of sialylated oligosaccharides and GAGs.[56-59] Multiple CO_2 losses from the charge-reduced species were produced, presumably originating from the
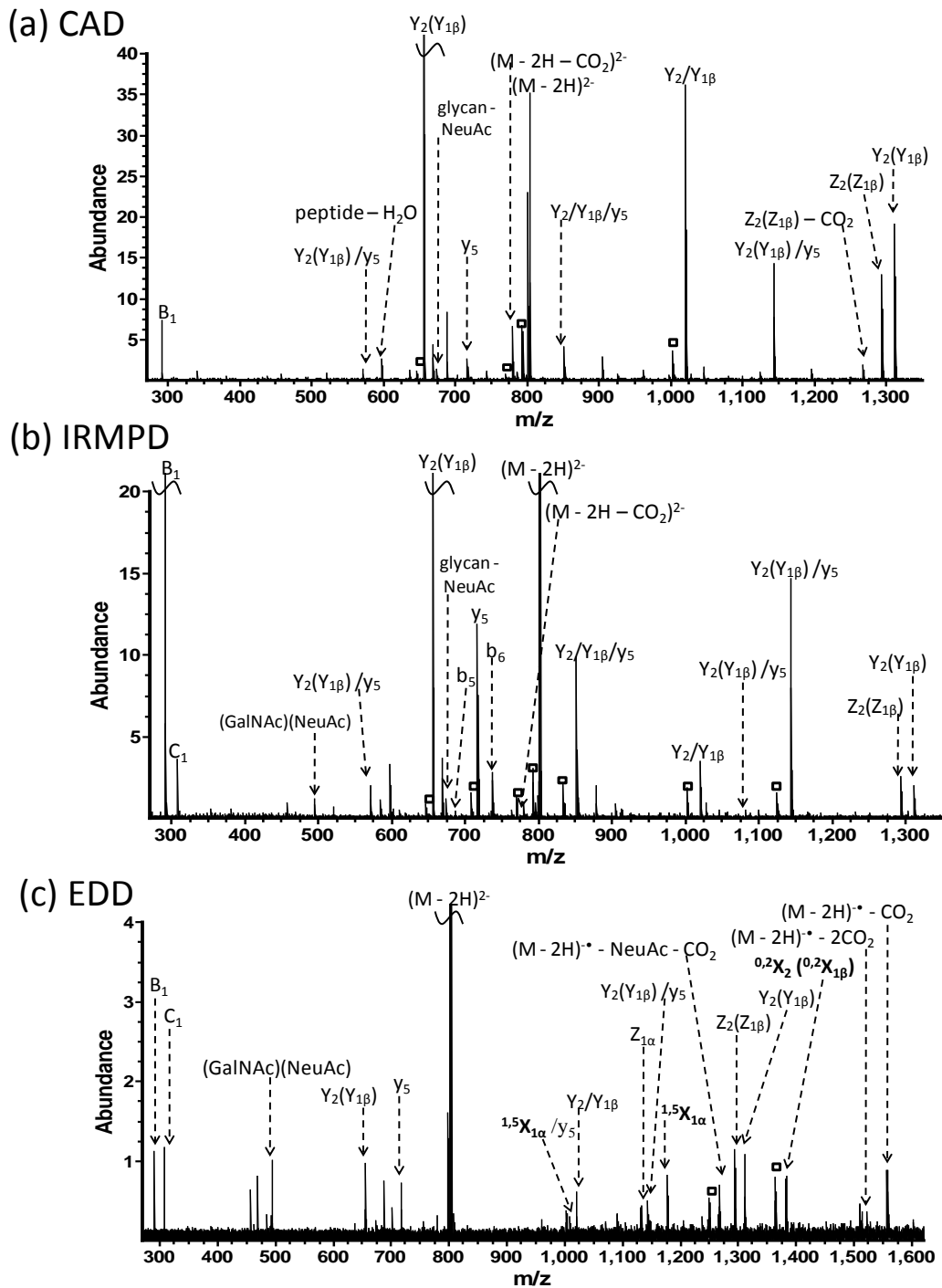
Figure 6.4. (a) CAD (80 scans, 12 V), (b) IRMPD (80 scans, 0.35 s at 10 W), and (c) EDD (80 scans, 1s irradiation, cathode bias – 30 V) spectra of a doubly deprotonated *O*-glycopeptide from bovine fetuin. Squares indicate water loss from the adjacent product ion. When multiple cleavages occurred, they are indicated by a slash. If multiple assignments are possible for one peak, the alternative assignment is indicated in the bracket.

143

sialic acids on the *O*-glycopeptide. Compared to CAD and IRMPD, EDD of this glycopeptide provided the most structural information of the glycan, whereas IRMPD had the highest peptide sequence coverage. Notably, only peptide backbone cleavages corresponding to the sequence APSAVPD were observed, suggesting that this sequence was dominant in the glycopeptide mixture.

Figure 6.5 demonstrates the influence of precursor ion charge state in CAD, IRMPD and EDD of the same *O*-glycopeptide as in Figure 6.4. Doubly deprotonated and triply deprotonated glycopeptide were examined. CAD and IRMPD fragmentation patterns of the triply deprotonated glycopeptide were analogous, providing structural information regarding both glycan and peptide sequence. CAD of the triply deprotonated glycopeptide yielded glycosidic cleavages between every neighboring monosaccharide and one cross-ring cleavage, demonstrating improved fragmentation efficiency compared to the doubly charged counterpart (one glycosidic and no cross-ring cleavage). IRMPD of the triply charged precursor ions generated the same peptide backbone fragments, but produced three additional glycosidic cleavages and one additional cross-ring cleavage compared to the doubly charged species. EDD of the $(M - 3H)^{3-}$ precursor ions resulted in efficient fragmentation, producing seven glycosidic, two cross-ring, and five peptide backbone fragments, while EDD of $(M - 2H)^{2-}$ yielded five glycosidic, two cross-ring, and one peptide backbone fragments. Almost all peptide backbone fragments were assigned to the peptide sequence AP**S**AVPD, again indicating that this sequence is the dominant species in the mixture. The improved fragmentation efficiency of the MS/MS approaches for the higher charge state may be attributed to a more "unfolded" gas-phase structure resulting from Coulomb repulsion. In addition, the peptide moiety with the

acidic C-terminus can effectively compete with sialic acids as the negative charge carrier.[34] When precursor ion charge state increases, it is more likely for the non-reducing end sialic acids to become deprotonated. Consistently, CAD, IRMPD, and EDD of $(M - 3H)^{3-}$ yielded more product ions containing the non-reducing end (e.g. B_1, C_1, and C_2 ions) compared to $(M - 2H)^{2-}$.

$(M - 2H)^{2-}$ $(M - 3H)^{3-}$

CAD

$Y_2 Z_2$ + APSAVPD (PSAVPDA) $Y_{1\beta} Z_{1\beta}$ y_5

$^{0,2}X_2$ $C_2 Z_{1\alpha}$ y_5 + APSAVPD (PSAVPDA) $B_1 Y_2$ $C_1 Z_2$ $Y_{1\beta} Z_{1\beta}$ b_5 $B_1 C_1$

IRMPD

$Z_{1\alpha}$ y_5 + APSAVPD (PSAVPDA) b_5 b_6 $Y_2 Z_2$ $Y_{1\beta} Z_{1\beta}$

$^{0,2}X_2$ $C_2 Z_{1\alpha}$ y_5 + APSAVPD (PSAVPDA) $B_1 Y_2$ $C_1 Z_2$ $Y_{1\beta} Z_{1\beta}$ b_5 b_6 $B_1 C_1$

EDD

$^{0,2}X_2$ $^{1,5}X_{1\alpha}$ $Z_{1\alpha}$ y_5 + APSAVPD (PSAVPDA) $B_1 Y_2$ $C_1 Z_2$ $Y_{1\beta} Z_{1\beta}$ $B_1 C_1$

$^{0,2}X_2$ $^{1,5}X_{1\alpha}$ $C_2 Y_{1\alpha} Z_{1\alpha}$ x_5 y_5 + APSAVPD (PSAVPDA) $B_1 Y_2$ $C_1 Z_2$ $Y_{1\beta} Z_{1\beta}$ b_5 b_6 a_5' $B_1 C_1$

Figure 6.5. CAD, IRMPD, and EDD (top to bottom) fragmentation patterns of an *O*-glycopeptide with different precursor ion charge states. Fragmentation patterns for the doubly deprotonated glycopeptide are shown on the left and those for the triply deprotonated species are shown on the right. The glycosylation site (serine) is labeled in red and cross-ring cleavages are labeled in bold. Peptide backbone cleavage corresponding to an alternative peptide sequence is labeled with an additional prime (such as a_5' instead of a_5).

6.3.4 An O-linked Glycopeptide with Multiple Potential Glycosylation Sites

Though pronase E is able to generate short glycopeptides, it is difficult to produce *O*-glycopeptides containing three or fewer amino acids. Ideally, if pronase can cleave between adjacent glycosylation sites and thus generate only singly glycosylated peptides, characterization of *O*-glycosylation would be less challenging. However, due to the steric hindrance of O-linked glycans, sometimes only multiply glycosylated peptides (i.e., with multiple glycosylation sites) are obtained even when very long digestion times are used (more than 48 h).

IRMPD and EDD were applied to an *O*-glycopeptide with different precursor ion charge states. The mass of this glycopeptide is 1840.72, corresponding to the peptide sequence AGPTPS (or GPTPSA) and the glycan moiety $(Hex)_2(HexNAc)_2(NeuAc)_2$. Both the serine and threonine can be *O*-glycosylated, and the glycan moiety can be either two trisaccharides or a hexasaccharide.[28,66,83] Without MS/MS results, it is impossible to determine the presence of a specific structure. Though most peaks in the MS/MS spectra can be assigned to multiple structures, we found that a doubly charged peak at m/z = 822.2997 could be exclusively assigned to the structure shown in Figure 6.6 (one hexasaccharide attached to threonine). Therefore, we use this structure as an example to illustrate the IRMPD and EDD fragmentation patterns of this *O*-glycopeptide.

IRMPD of $(M - 2H)^{2-}$ generated five glycosidic cleavages on the glycan and three peptide backbone cleavages. The B_1 ion (m/z = 290.09) corresponding to a deprotonated sialic acid residue was the most abundant product ion in the spectrum, which is common in CAD/IRMPD of sialylated oligosaccharides. All fragments observed resulted from single bond cleavage, i.e., either from glycosidic cleavage or peptide backbone cleavage.

Internal fragments were not observed. IRMPD of $(M - 3H)^{3-}$ yielded nine glycosidic cleavages and one peptide backbone cleavage, and also several internal fragments, providing more detail regarding glycan structures compared to its doubly charged counterpart. Glycosidic cleavages between every adjacent monosaccharide were detected, generating rich "glycan sequencing" information. However, no cross-ring fragments were observed in the IRMPD spectra, precluding linkage determination. Peptide backbone fragments which could be assigned to both peptide sequences were observed, indicating that both species were present in the mixture.

EDD of the *O*-glycopeptide induced extensive fragmentation, generating glycosidic, cross-ring, and peptide backbone cleavages simultaneously, and providing additional information compared to IRMPD. Seven glycosidic, five cross-ring, and six backbone fragments were observed from $(M - 2H)^{2-}$, and nine glycosidic, eight cross-ring, and nine backbone fragments were detected from $(M - 3H)^{3-}$ (see Figure 6.6). For structural elucidation of the glycan moiety, abundant glycosidic fragments resulting from cleavages between every adjacent monosaccharide were observed, whereas cross-ring fragments such as ^{1,5}X- and ^{3,5}X- type ions aid the determination of glycan linkage type. For glycosylation site determination, in addition to the a- and x-type ions which are common in EDD of peptides,[52,84] b- and y-ions often observed in CAD/IRMPD of peptides were also found. When considering the glycopeptide as AGPTPS + Hex, the sequence coverage obtained from $(M - 2H)^{2-}$ is 60%, and the sequence coverage from $(M - 3H)^{3-}$ is 100%. In both cases the glycosylation site can be unambiguously assigned to the threonine. When considering the glycopeptide as GPTPSA + Hex, the sequence coverage obtained from $(M - 2H)^{2-}$ is 40%, and that from $(M - 3H)^{3-}$ is 60%. Again, the

glycosylation site determination is exclusively based on the EDD results. Therefore, EDD is a highly valuable tool for *O*-glycopeptide structural characterization, due to its ability to generate rich glycan structural information, and to effectively determine glycosylation sites.
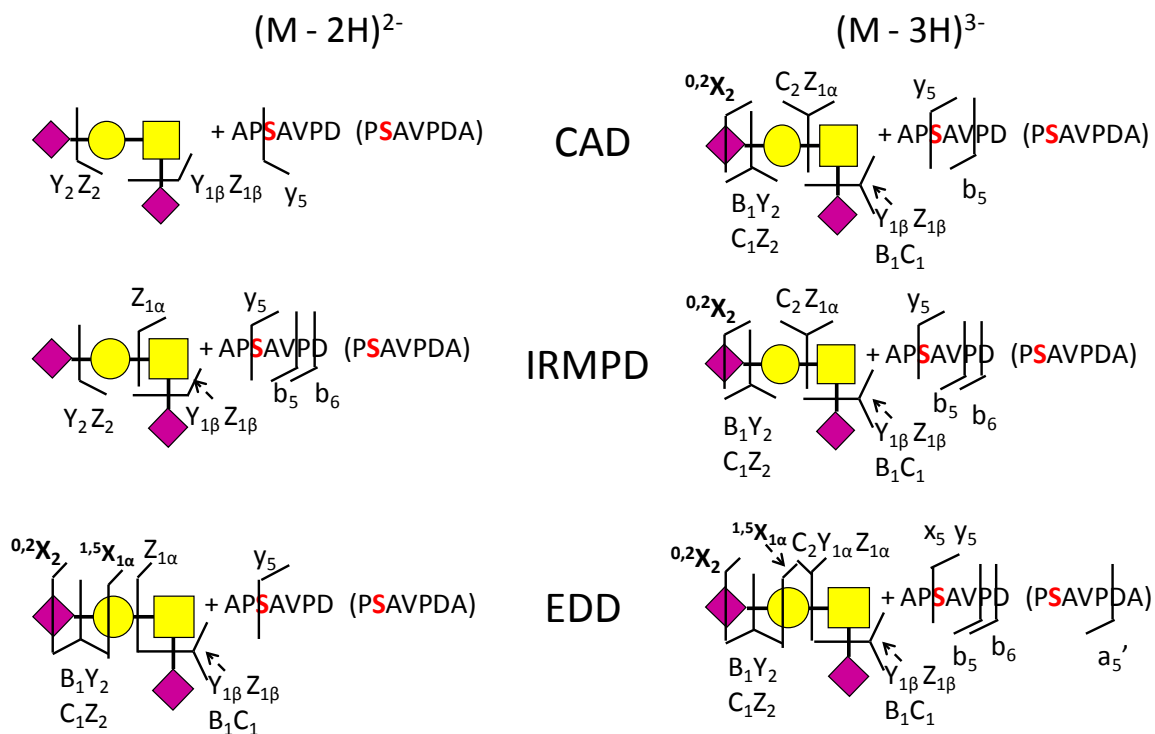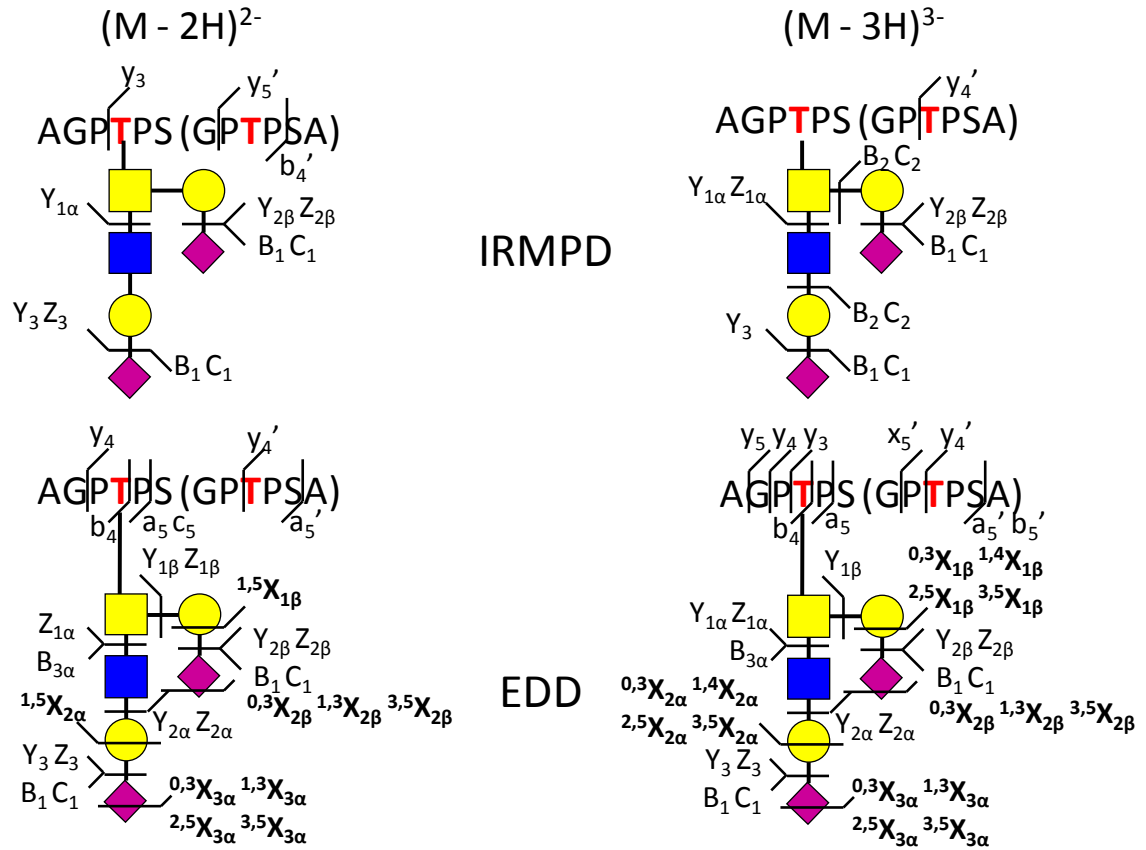

Figure 6.6. IRMPD and EDD (top to bottom) fragmentation patterns of an *O*-glycopeptide with different precursor ion charge states. Fragmentation patterns for the doubly deprotonated glycopeptide are shown on the left, and those for the triply deprotonated species are shown on the right. The glycosylation site (threonine) is labeled in red and cross-ring cleavages are labeled in bold. Peptide backbone cleavage corresponding to an alternative peptide sequence is labeled with an additional prime (such as a_5' instead of a_5).

6.4 Conclusions

EDD and IRMPD were utilized to characterize deprotonated N-linked and O-linked glycopeptides. Compared to specific enzymes such as trypsin and Glu C, the non-specific enzyme pronase E produced length-controllable glycopeptides, while significantly reducing ion suppression from non-glycosylated peptides. For *N*-glycopeptides sharing the same glycan structure, fragmentation efficiency of EDD and IRMPD decreased when peptide lengths increased. This effect may be attributed to competition between the acidic peptide C-terminus and sialic acids as negative charge carriers, resulting in altered charge locations, as well as different gas-phase structures. For *O*-glycopeptides, relatively longer glycopeptides were obtained compared to *N*-glycopeptides. EDD induced extensive fragmentation both on the peptide and glycan moieties. When fragmentation occurred on the peptide, a- and x-type ions (frequently observed in EDD of peptides) and b-/y-type ions (commonly seen in CAD/IRMPD of peptides) provided reasonably good sequence coverage, allowing glycosylation site determination. When fragmentation occurred on the glycan, both extensive glycosidic and cross-ring fragments were generated, providing information regarding both monosaccharide composition and linkage type. The fragmentation behavior in EDD was significantly different from the the vibrational activation technique IRMPD, which only yielded few peptide backbone fragments and some glycosidic fragments.

6.5 References

1. van den Steen, P.; Rudd, P. M.; Dwek, R. A.; Opdenakker, G. Concepts and principles of O-linked glycosylation. *Crit. Rev. Biochem. Mol. Biol.* **1998**, *33*, 151-208.
2. Varki, A. Biological roles of oligosaccharides - All of the theories are correct. *Glycobiol.* **1993**, *3*, 97-130.
3. Bertozzi, C. R.; Kiessling, L. L. Chemical glycobiology. *Science* **2001**, *291*, 2357-2364.
4. Dube, D. H.; Bertozzi, C. R. Glycans in cancer and inflammation. Potential for therapeutics and diagnostics. *Nat. Rev. Drug Discov.* **2005**, *4*, 477-488.
5. Dwek, R. A. Glycobiology: Toward understanding the function of sugars. *Chem. Rev.* **1996**, *96*, 683-720.
6. Barchi, J. J. Emerging roles of carbohydrates and glycomimetics in anticancer drug design. *Curr. Pharm. Des.* **2000**, *6*, 485-501.
7. Zhao, Y. Y.; Takahashi, M.; Gu, J. G.; Miyoshi, E.; Matsumoto, A.; Kitazume, S.; Taniguchi, N. Functional roles of N-glycans in cell signaling and cell adhesion in cancer. *Cancer Sci.* **2008**, *99*, 1304-1310.
8. Krishnamoorthy, L.; Mahal, L. K. Glycomic analysis: an array of technologies. *ACS Chem. Biol.* **2009**, *4*, 715-732.
9. Mechref, Y.; Novotny, M. V. Structural investigations of glycoconjugates at high sensitivity. *Chem. Rev.* **2002**, *102*, 321-369.
10. Harvey, D. J. Matrix-assisted laser desorption/ionization mass spectrometry of carbohydrates. *Mass Spectrom. Rev.* **1999**, *18*, 349-450.
11. Zaia, J. Mass spectrometry of oligosaccharides. *Mass Spectrom. Rev.* **2004**, *23*, 161-227.
12. Park, Y. M.; Lebrilla, C. B. Application of Fourier transform ion cyclotron resonance mass spectrometry to oligosaccharides. *Mass Spectrom. Rev.* **2005**, *24*, 232-264.
13. Harvey, D. J. Proteomic analysis of glycosylation: structural determination of N- and O-linked glycans by mass spectrometry. *Expert Rev. Proteomics* **2005**, *2*, 87-101.
14. Zaia, J. Mass spectrometry and the emerging field of glycomics. *Chem. Biol.* **2008**, *15*, 881-892.
15. Tretter, V.; Altmann, F.; Marz, L. Peptide-N4-(N-acetyl-beta-glycosaminyl)asparagine amidase-F cannot release glycans with fucose attached alpha-1-3 to the asparagine-linked N-acetylglucosamine residue *Eur. J. Biochem.* **1991**, *199*, 647-652.
16. Liu, T.; Qian, W. J.; Gritsenko, M. A.; Camp, D. G.; Monroe, M. E.; Moore, R. J.; Smith, R. D. Human plasma N-glycoproteome analysis by immunoaffinity subtraction, hydrazide chemistry, and mass spectrometry. *J. Proteome Res.* **2005**, *4*, 2070-2080.
17. Khoshnoodi, J.; Hill, S.; Tryggvason, K.; Hudson, B.; Friedman, D. B. Identification of N-linked glycosylation sites in human nephrin using mass spectrometry. *J. Mass Spectrom.* **2007**, *42*, 370-379.

18.   An, H. J.; Peavy, T. R.; Hedrick, J. L.; Lebrilla, C. B. Determination of N-glycosylation sites and site heterogeneity in glycoproteins. *Anal. Chem.* **2003**, *75*, 5628-5637.

19.   Geyer, H.; Geyer, R. Strategies for analysis of glycoprotein glycosylation. *BBA-Proteins Proteomics* **2006**, *1764*, 1853-1869.

20.   Wuhrer, M.; Catalina, M.; Deelder, A.; Hokke, C. Glycoproteomics based on tandem mass spectrometry of glycopeptides. *J. Chromatogr. B* **2007**, *849*, 115-128.

21.   Dalpathado, D. S.; Desaire, H. Glycopeptide analysis by mass spectrometry. *Analyst* **2008**, *133*, 731-738.

22.   North, S. J.; Hitchen, P. G.; Haslam, S. M.; Dell, A. Mass spectrometry in the analysis of N-linked and O-linked glycans. *Curr. Opin. Struct. Biol.* **2009**, *19*, 498-506.

23.   Huberty, M. C.; Vath, J. E.; Yu, W.; Martin, S. A. Site-specific carbohydrate identification in recombinant proteins using MALDI-TOF MS. *Anal. Chem.* **1993**, *65*, 2791-2800.

24.   Deguchi, K.; Ito, H.; Takegawa, Y.; Shinji, N.; Nakagawa, H.; Nishimura, S. I. Complementary structural information of positive- and negative-ion MSn spectra of glycopeptides with neutral and sialylated N-glycans. *Rapid Commun. Mass Spectrom.* **2006**, *20*, 741-746.

25.   Yu, Y. Q.; Fournier, J.; Gilar, M.; Gebler, J. C. Identification of N-linked glycosylation sites using glycoprotein digestion with pronase prior to MALDI tandem time-of-flight mass spectrometry. *Anal. Chem.* **2007**, *79*, 1731-1738.

26.   Wuhrer, M.; Koeleman, C. A. M.; Deelder, A. M. Hexose rearrangements upon fragmentation of N-glycopeptides and reductively aminated N-glycans. *Anal. Chem.* **2009**, *81*, 4422-4432.

27.   Prien, J. M.; Prater, B. D.; Qin, Q.; Cockrill, S. L. Mass spectrometric-based stable isotopic 2-aminobenzoic acid glycan mapping for rapid glycan screening of biotherapeutics. *Anal. Chem.* **2010**, *82*, 1498-1508.

28.   Medzihradszky, K. F.; GilleceCastro, B. L.; Townsend, R. R.; Burlingame, A. L.; Hardy, M. R. Structural elucidation of O-linked glycopeptides by high energy collision-induced dissociation. *J. Am. Soc. Mass. Spectrom.* **1996**, *7*, 319-328.

29.   Hakansson, K.; Chalmers, M. J.; Quinn, J. P.; McFarland, M. A.; Hendrickson, C. L.; Marshall, A. G. Combined electron capture and infrared multiphoton dissociation for multistage MS/MS in a Fourier transform ion cyclotron resonance mass spectrometer. *Anal. Chem.* **2003**, *75*, 3256-3262.

30.   Adamson, J. T.; Hakansson, K. Infrared multiphoton dissociation and electron capture dissociation of high-mannose type glycopeptides. *J. Proteome Res.* **2006**, *5*, 493-501.

31.   Clowers, B. H.; Dodds, E. D.; Seipert, R. R.; Lebrilla, C. B. Site determination of protein glycosylation based on digestion with immobilized nonspecific proteases and Fourier transform ion cyclotron resonance mass spectrometry. *J. Proteome Res.* **2007**, *6*, 4032-4040.

32.   Seipert, R. R.; Dodds, E. D.; Clowers, B. H.; Beecroft, S. M.; German, J. B.; Lebrilla, C. B. Factors that influence fragmentation behavior of N-linked glycopeptide ions. *Anal. Chem.* **2008**, *80*, 3684-3692.

33. Dodds, E. D.; Seipert, R. R.; Clowers, B. H.; German, J. B.; Lebrilla, C. B. Analytical performance of immobilized pronase for glycopeptide footprinting and implications for surpassing reductionist glycoproteomics. *J. Proteome Res.* **2009**, *8*, 502-512.

34. Seipert, R. R.; Dodds, E. D.; Lebrilla, C. B. Exploiting differential dissociation chemistries of O-linked glycopeptide ions for the localization of mucin-type protein glycosylation. *J. Proteome Res.* **2009**, *8*, 493-501.

35. Hakansson, K.; Cooper, H. J.; Emmett, M. R.; Costello, C. E.; Marshall, A. G.; Nilsson, C. L. Electron capture dissociation and infrared multiphoton dissociation MS/MS of an N-glycosylated tryptic peptide to yield complementary sequence information. *Anal. Chem.* **2001**, *73*, 4530-4536.

36. Mormann, M.; Paulsen, H.; Peter-Katalinic, J. Electron capture dissociation of O-glycosylated peptides: radical site-induced fragmentation of glycosidic bonds. *Eur. J. Mass Spectrom.* **2005**, *11*, 497-511.

37. Sihlbom, C.; Hard, I. V.; Lidell, M. E.; Noll, T.; Hansson, G. C.; Backstrom, M. Localization of O-glycans in MUC1 glycoproteins using electron-capture dissociation fragmentation mass spectrometry. *Glycobiol.* **2009**, *19*, 375-381.

38. Hogan, J. M.; Pitteri, S. J.; Chrisman, P. A.; McLuckey, S. A. Complementary structural information from a tryptic N-linked glycopeptide via electron transfer ion/ion reactions and collision-induced dissociation. *J. Proteome Res.* **2005**, *4*, 628-632.

39. Catalina, M. I.; Koeleman, C. A. M.; Deelder, A. M.; Wuhrer, M. Electron transfer dissociation of N-glycopeptides: loss of the entire N-glycosylated asparagine side chain. *Rapid Commun. Mass Spectrom.* **2007**, *21*, 1053-1061.

40. Han, H.; Xia, Y.; Yang, M.; McLuckey, S. A. Rapidly alternating transmission mode electron-transfer dissociation and collisional activation for the characterization of polypeptide ions. *Anal. Chem.* **2008**, *80*, 3492-3497.

41. Alley, W. R.; Mechref, Y.; Novotny, M. V. Characterization of glycopeptides by combining collision-induced dissociation and electron-transfer dissociation mass spectrometry data. *Rapid Commun. Mass Spectrom.* **2009**, *23*, 161-170.

42. Christiansen, M. N.; Kolarich, D.; Nevalainen, H.; Packer, N. H.; Jensen, P. H. Challenges of determining O-glycopeptide heterogeneity: a fungal glucanase model system. *Anal. Chem.* **2010**, *82*, 3500-3509.

43. Zhang, L.; Reilly, J. P. Extracting both peptide sequence and glycan structural information by 157 nm photodissociation of N-linked glycopeptides. *J. Proteome Res.* **2009**, *8*, 734-742.

44. Segu, Z. M.; Mechref, Y. Characterizing protein glycosylation sites through higher-energy C-trap dissociation. *Rapid Commun. Mass Spectrom.* **2010**, *24*, 1217-1225.

45. Tsarbopoulos, A.; Bahr, U.; Pramanik, B. N.; Karas, M. Glycoprotein analysis by delayed extraction and post-source decay MALDI-TOF-MS. *Int. J. Mass spectrom.* **1997**, *169*, 251-261.

46. Bezouska, K.; Sklenar, J.; Novak, P.; Halada, P.; Havlicek, V.; Kraus, M.; Ticha, M.; Jonakova, V. Determination of the complete covalent structure of the major glycoform of DQH sperm surface protein, a novel trypsin-resistant boar seminal plasma O-glycoprotein related to pB1 protein. *Protein Sci.* **1999**, *8*, 1551-1556.

47. Lancaster, K. S.; An, H. J.; Li, B. S.; Lebrilla, C. B. Interrogation of N-linked oligosaccharides using infrared multiphoton dissociation in FT-ICR mass spectrometry. *Anal. Chem.* **2006**, *78*, 4990-4997.

48. Zubarev, R. A. Reactions of polypeptide ions with electrons in the gas phase. *Mass Spectrom. Rev.* **2003**, *22*, 57-77.

49. Hakansson, K.; Cooper, H. J.; Hudgins, R. R.; Nilsson, C. L. High resolution tandem mass spectrometry for structural biochemistry. *Curr. Org. Chem.* **2003**, *7*, 1503-1525.

50. Wiesner, J.; Premsler, T.; Sickmann, A. Application of electron transfer dissociation (ETD) for the analysis of posttranslational modifications. *Proteomics* **2008**, *8*, 4466-4483.

51. Nwosu, C. C.; Strum, J. S.; An, H. J.; Lebrilla, C. B. Enhanced detection and identification of glycopeptides in negative ion mode mass spectrometry. *Anal. Chem.* **2010**, *82*, 9654-9662.

52. Budnik, B. A.; Haselmann, K. F.; Zubarev, R. A. Electron detachment dissociation of peptide di-anions: an electron-hole recombination phenomenon. *Chem. Phys. Lett.* **2001**, *342*, 299-302.

53. Yang, J.; Mo, J. J.; Adamson, J. T.; Hakansson, K. Characterization of oligodeoxynucleotides by electron detachment dissociation Fourier transform ion cyclotron resonance mass spectrometry. *Anal. Chem.* **2005**, *77*, 1876-1882.

54. Yang, J.; Hakansson, K. Fragmentation of oligoribonucleotides from gas-phase ion-electron reactions. *J. Am. Soc. Mass. Spectrom.* **2006**, *17*, 1369-1375.

55. McFarland, M. A.; Marshall, A. G.; Hendrickson, C. L.; Nilsson, C. L.; Fredman, P.; Mansson, J. E. Structural characterization of the GM1 ganglioside by infrared multiphoton dissociation/electron capture dissociation, and electron detachment dissociation electrospray ionization FT-ICR MS/MS. *J. Am. Soc. Mass. Spectrom.* **2005**, *16*, 752-762.

56. Adamson, J. T.; Hakansson, K. Electron detachment dissociation of neutral and sialylated oligosaccharides. *J. Am. Soc. Mass. Spectrom.* **2007**, *18*, 2162-2172.

57. Wolff, J. J.; Amster, I. J.; Chi, L. L.; Linhardt, R. J. Electron detachment dissociation of glycosaminoglycan tetrasaccharides. *J. Am. Soc. Mass. Spectrom.* **2007**, *18*, 234-244.

58. Wolff, J. J.; Chi, L. L.; Linhardt, R. J.; Amster, I. J. Distinguishing glucuronic from iduronic acid in glycosaminoglycan tetrasaccharides by using electron detachment dissociation. *Anal. Chem.* **2007**, *79*, 2015-2022.

59. Wolff, J. J.; Laremore, T. N.; Busch, A. M.; Linhardt, R. J.; Amster, I. J. Electron detachment dissociation of dermatan sulfate oligosaccharides. *J. Am. Soc. Mass. Spectrom.* **2008**, *19*, 294-304.

60. Wolff, J. J.; Laremore, T. N.; Busch, A. M.; Linhardt, R. J.; Amster, I. J. Influence of charge state and sodium cationization on the electron detachment dissociation and infrared multiphoton dissociation of glycosaminoglycan oligosaccharides. *J. Am. Soc. Mass. Spectrom.* **2008**, *19*, 790-798.

61. Wolff, J. J.; Laremore, T. N.; Leach, F. E.; Linhardt, R. J.; Amster, I. J. Electron capture dissociation, electron detachment dissociation and infrared multiphoton dissociation of sucrose octasulfate. *Eur. J. Mass Spectrom.* **2009**, *15*, 275-281.

62. Chi, L. L.; Wolff, J. J.; Laremore, T. N.; Restaino, O. F.; Xie, J.; Schiraldi, C.; Toida, T.; Amster, I. J.; Linhardt, R. J. Structural analysis of bikunin glycosaminoglycan. *J. Am. Chem. Soc.* **2008**, *130*, 2617-2625.

63. Wolff, J. J.; Laremore, T. N.; Aslam, H.; Linhardt, R. J.; Amster, I. J. Electron-induced dissociation of glycosaminoglycan tetrasaccharides. *J. Am. Soc. Mass. Spectrom.* **2008**, *19*, 1449-1458.

64. Wuhrer, M.; Koeleman, C. A. M.; Hokke, C. H.; Deelder, A. M. Protein glycosylation analyzed by normal-phase nano-liquid chromatography-mass spectrometry of glycopeptides. *Anal. Chem.* **2005**, *77*, 886-894.

65. Temporini, C.; Perani, E.; Calleri, E.; Dolcini, L.; Lubda, D.; Caccialanza, G.; Massolini, G. Pronase-immobilized enzyme reactor: An approach for automation in glycoprotein analysis by LC/LC-ESI/MSn. *Anal. Chem.* **2007**, *79*, 355-363.

66. Zauner, G.; Koeleman, C. A. M.; Deelder, A. M.; Wuhrer, M. Protein glycosylation analysis by HILIC-LC-MS of Proteinase K-generated N- and O-glycopeptides. *J. Sep. Sci.* **2010**, *33*, 903-910.

67. Tsybin, Y. O.; Witt, M.; Baykut, G.; Kjeldsen, F.; Hakansson, P. Combined infrared multiphoton dissociation and electron capture dissociation with a hollow electron beam in Fourier transform ion cyclotron resonance mass spectrometry. *Rapid Commun. Mass Spectrom.* **2003**, *17*, 1759-1768.

68. Caravatti, P.; Allemann, M. The infinity cell - a new trapped-ion cell with radiofrequency covered trapping electrodes for Fourier-transform ion-cyclotron resonance mass-spectrometry. *Org. Mass Spectrom.* **1991**, *26*, 514-518.

69. Senko, M. W.; Canterbury, J. D.; Guan, S. H.; Marshall, A. G. A high-performance modular data system for Fourier transform ion cyclotron resonance mass spectrometry. *Rapid Commun. Mass Spectrom.* **1996**, *10*, 1839-1844.

70. Ledford, E. B.; Rempel, D. L.; Gross, M. L. Space-charge effects in Fourier-transform mass-spectrometry - mass calibration *Anal. Chem.* **1984**, *56*, 2744-2748.

71. Lohmann, K. K.; von der Lieth, C. W. GlycoFragment and GlycoSearchMS: web tools to support the interpretation of mass spectra of complex carbohydrates. *Nucleic Acids Res.* **2004**, *32*, W261-W266.

72. Spik, G.; Bayard, B.; Fournet, B.; Strecker, G.; Bouquelet, S.; Montreuil, J. Studies on glycoconjugates. 64. complete structure of 2 carbohydrate units of human serotransferrin *FEBS Lett.* **1975**, *50*, 296-299.

73. Green, E. D.; Adelt, G.; Baenziger, J. U.; Wilson, S.; Vanhalbeek, H. The asparagine-linked oligosaccharides on bovine fetuin - structural-analysis of N-glycanase-released oligosaccharides by 500-megahertz H-1-NMR spectroscopy *J. Biol. Chem.* **1988**, *263*, 18253-18268.

74. Coddeville, B.; Strecker, G.; Wieruszeski, J. M.; Vliegenthart, J. F. G.; Vanhalbeek, H.; Peterkatalinic, J.; Egge, H.; Spik, G. Heterogeneity of Bovine Lactotransferrin Glycans - Characterization of Alpha-D-GalP-(1-]3)-beta-D-Gal and Alpha-NeuAc-(2-]6)-beta-D-GalPNAc-(1-]4)-beta-D-GlcNAc-substituted N-linked Glycans. *Carbohydr. Res.* **1992**, *236*, 145-164.

75. Domon, B.; Costello, C. E. A systematic nomenclature for carbohydrate fragmentations in FAB-MS MS spectra of glycoconjugates *Glycoconj. J.* **1988**, *5*, 397-409.

76. Biemann, K. Nomenclature for Peptide Fragment Ion (Positive-ions). *Methods Enzymol.* **1990**, *193*, 886-887.

77. Zhang, J. H.; Schubothe, K.; Li, B. S.; Russell, S.; Lebrilla, C. B. Infrared multiphoton dissociation of O-linked mucin-type oligosaccharides. *Anal. Chem.* **2005**, *77*, 208-214.

78. Zhou, W.; Håkansson, K. In *Ion-electron reactions of sialylated N-linked glycans released from glycoproteins*, 57th ASMS Conference on Mass Spectrometry and Allied Topics, Philadelphia, PA, 2009.

79. Harvey, D. J. Fragmentation of negative ions from carbohydrates: Part 1. Use of nitrate and other anionic adducts for the production of negative ion electrospray spectra from N-linked carbohydrates. *J. Am. Soc. Mass. Spectrom.* **2005**, *16*, 622-630.

80. Harvey, D. J. Fragmentation of negative ions from carbohydrates: Part 2. Fragmentation of high-mannose N-linked glycans. *J. Am. Soc. Mass. Spectrom.* **2005**, *16*, 631-646.

81. Harvey, D. J. Fragmentation of negative ions from carbohydrates: Part 3. Fragmentation of hybrid and complex N-linked glycans. *J. Am. Soc. Mass. Spectrom.* **2005**, *16*, 647-659.

82. Harrison, A. G.; Young, A. B. Fragmentation reactions of deprotonated peptides containing proline. The proline effect. *J. Mass Spectrom.* **2005**, *40*, 1173-1186.

83. Edge, A. S. B.; Spiro, R. G. Presence of an O-glycosidically linked hexasaccharide in fetuin. *J. Biol. Chem.* **1987**, *262*, 16135-16141.

84. Haselmann, K. F.; Budnik, B. A.; Kjeldsen, F.; Nielsen, M. L.; Olsen, J. V.; Zubarev, R. A. Electronic excitation gives informative fragmentation of polypeptide cations and anions. *Eur. J. Mass Spectrom.* **2002**, *8*, 117-121.

Chapter 7

N-linked Glycan Profiling by Liquid Chromatography – Mass Spectrometry (LC-MS)

7.1 Introduction

Glycosylation is one of the most prevalent post-translational modifications (PTMs), playing key roles in biological activities, such as cell-cell interactions, molecular trafficking, immune response, and different disease states.[1-3] Aberrant glycosylation such as increased sialylation and increased branching of glycans have been linked to cancer metastasis and inflammation.[4-11] Even though the biological significance of glycosylation is well established, structural characterization of glycans and glycoconjugates is still far from routine and faces unique challenges. First, biosynthesis of glycans is non-template driven, which result in highly complex structures.[3] In order to fully characterize glycans, monosaccharide composition, sequence, branching, linkage, and anomeric configuration all need to be determined, which makes glycans highly challenging to characterize compared to other linear biomolecules such as proteins and nucleic acids.[12] Second, due to the hydrophilicity of glycans, they often suffer from ion suppression of hydrophobic molecules such as proteins and peptides and generate low abundance signals in mass spectrometry (MS). Therefore, sample purification steps or

separation by liquid chromatography (LC) prior to MS are often required, particularly for complex biological samples.[13,14]

N-linked glycans are branched oligosaccharides sharing a chitobiose core structure, often linked to the asparagine residue via an amide bond in an Asn-Xxx-Ser (or Thr) amino acid consensus sequence with Xxx ≠ proline.[12] N-linked glycans can be released from glycoproteins by peptide-*N*-glycosidase F (PNGase F), and are frequently identified either in native form, after permethylation, or after adding a fluorescent label at the reducing end.[13-19] Permethylated glycans and fluorescently labeled glycans are more hydrophobic than native glycans, and thus are more readily ionized by electrospray ionization (ESI).[20] However, such modifications often require extra clean-up steps, and may result in sample loss, particularly for low abundance species. Therefore, it is more desirable to analyze glycans in their native forms, particularly for complex biological samples such as human serum.[21,22] Reverse phase LC (RP-LC) is commonly used for separating hydrophobic biomolecules such as proteins and peptides. RP-LC has also been utilized to separate permethylated and fluorescently labeled glycans, but normally the resolution for native glycans is poor.[13,15,23-26] In contrast, hydrophilic interaction liquid chromatography (HILIC)[27] and graphitized carbon chromatography[14] of native glycans have just begun to emerge.

HILIC is a variant of normal-phase LC (NP-LC), but uses a highly hydrophilic stationary phase and a less hydrophilic mobile phase consisting of water and water-miscible organic solvents.[27] Retention of glycans is caused by partitioning (hydrogen bonding) between the water-rich layer that covers the stationary phase and the mobile phase.[28] NP-LC uses hydrophobic eluents (often hexane-based) in which glycans are

poorly soluble. Online HILIC-ESI-MS has been applied to native and fluorescently labeled N-linked and O-linked glycans at low femtomol sensitivity.[22,29-32] Because the retention is predominantly determined by multiple hydrogen bonding of glycans, modifications such as fluorescent labels and polar functional groups (e.g., sulfate) are compatible with HILIC of glycans.[28] Overall, HILIC LC-MS can be utilized for sensitive detection and identification of glycans with high resolution, both in their native and derivatized forms.

Graphitized carbon LC-MS of glycans has been developed since the early 1990s.[15,33-35] The graphitized carbon stationary phase participates in hydrophobic interactions, polar interactions, and also ionic interactions with glycans.[14,18,35] Both underivatized and derivatized glycans can be separated with good resolution using porous graphitized carbon (PGC) columns.[18,21,25,30,36-40] One advantage of such columns is their excellent physical and chemical stability.[13] A wide range of pH values is compatible with PGC columns, allowing MS detection both in positive- and negative-ion modes. Acidic glycans are often separated at basic pH and analyzed in negative-ion mode due to enhanced signal in MS, while neutral glycans are separated at acidic pH and analyzed in positive-ion mode.[14] Another feature of PGC LC-MS is its ability to separate glycan structural isomers, which significantly contributes to detailed structural analysis of glycans.[38-40] Overall, PGC LC-MS is a powerful tool for glycan analysis due to its high sensitivity, column stability, and ability to separate glycan structural isomers. Here, we investigate neutral and acidic N-linked glycan profiling by HILIC LC-MS and PGC LC-MS.

7.2 Experimental

7.2.1 Preparation and Purification of N-linked Glycans

α1-acid glycoprotein (AGP) from human plasma or ribonuclease B (Sigma, St. Louis, MO) was reduced in 5 mM DTT (Sigma) at 56 ^{o}C for 45 min, alkylated by 15 mM iodoacetamide (Sigma) in the dark at room temperature for 1 h, and digested with 2U PNGase F (EMD Chemicals, Gibbstown, NJ) in 50 mM NH_4HCO_3 (Fisher, Fair Lawn, NJ) overnight at 37 ^{o}C. Released glycans were purified by SPE graphitized carbon column (Sigma). For each sample, a carbon cartridge was washed with 0.1% (v/v) formic acid (Fisher) in 80% acetonitrile/H_2O (v/v, Fisher), followed by deionized water. The solution containing *N*-glycans was loaded and the cartridge was then washed with deionized water to remove salts and other contaminants. Glycans were eluted with 0.1% formic acid (v/v) in 20% or 40% acetonitrile/H_2O (v/v). The solution was then dried down in a vacuum concentrator (Eppendorf, Hamberg, Germany). For direct infusion mass spectrometry analysis, negative-ion mode solution was added (50% methanol, 0.1% NH_4OH) to reconstitute the glycans. For LC-MS analysis, 80% acetonitrile/H_2O (v/v) was added.

7.2.2 Liquid Chromatography – Mass Spectrometry

Glycans were separated on a Tosoh TSK-GEL amide-80 column (5 μm; 100 Å; 1 mm x 25 cm; Montgomeryville, PA) or a Thermo Hypercarb column (5 μm; 250 Å; 1 mm x 10 cm; West Palm Beach, FL) with an Agilent 1100 HPLC. For HILIC LC-MS, solvent A was acetonitrile with 2.5 mM ammonium acetate and solvent B was water with 2.5 mM ammonium acetate. For 1h separation of AGP *N*-glycans, the following gradient was used: t = 0 min, 0% solvent B; t = 10 min, 30% solvent B; t = 90 min, 35% solvent B,

t = 95 min, 95% solvent B; t = 115 min, 95% solvent B. For 2h separation of ovalbumin

N-glycans, the following gradient was used: t = 0 min, 0% solvent B; t = 10 min, 30%

solvent B; t = 90 min, 35% solvent B, t = 95 min, 95% solvent B; t = 115 min, 95%

solvent B.

For PGC LC-MS, solvent A was acetonitrile and solvent B was water with 10

mM ammonium bicarbonate. The flow rate was 50 μL/min. For 1h separation of AGP

N-glycans, the following gradient was used: t = 0 min, 0% solvent B; t = 10 min, 30%

solvent B; t = 90 min, 35% solvent B, t = 95 min, 95% solvent B; t = 115 min, 95%

solvent B. The HPLC was directly coupled to the mass spectrometer via an Apollo II ion

source.

7.2.3 Mass Spectrometry

All mass spectra were collected with an actively shielded 7 T FT-ICR mass

spectrometer with a quadrupole front-end (APEX-Q, Bruker Daltonics, Billerica, MA), as

previously described.[41] For direct infusion experiments, samples were infused via an

Apollo II electrospray ion source at a flow rate of 70 μL/h with the assistance of N_2

nebulizing gas. External CAD was performed in a hexapole following mass selective ion

accumulation.

For direct infusion experiments, mass spectra were acquired with ApexControl

software (Bruker Daltonics) with 256k data points and summed over 10 scans. LC-MS

data were acquired with Hystar software (Bruker Daltonics). LC-MS and MS data were

analyzed with Bruker Data Analysis software.

7.3 Results and Discussion

7.3.1 HILIC LC-FT-ICR MS of N-linked Glycans

AGP is a highly glycosylated glycoprotein, consisting of approximately 45% carbohydrate, including di-, tri-, and tetra-antennary complex type N-linked glycans.[42] Chicken ovalbumin is another well characterized glycoprotein which consists of a large number of neutral N-linked glycans.[43] We used AGP and ovalbumin as model systems to explore the utilization of HILIC LC-MS for sialylated and neutral *N*-glycans. Figure 7.1 compares the sialylated glycans detected in HILIC LC-MS and direct infusion experiments in negative-ion mode. The majority of *N*-glycans eluted between 60 and 70 minutes, as shown in the total ion chromatogram (TIC) (Figure 7.1a). The average mass spectrum between 60.0 and 66.4 min from the LC-MS run is shown in Figure 7.1b. Nine sialylated *N*-glycans were observed with different charge states, including di-, tri-, and tetra-antennary complex *N*-glycans. The most abundant peaks in the spectra were all assigned either as deprotonated *N*-glycans or their sodium adducts. In contrast, in direct infusion of the same sample, only five *N*-glycans were detected with relative abundances all lower than 8%. This result demonstrates high selectivity for sialylated *N*-glycans in HILIC LC-MS.

HILIC LC-FT-ICR MS of *N*-glycans released from chicken ovalbumin is demonstrated in Figure 7.2. The majority of *N*-glycans eluted between 45 and 65 minutes, and separated with high resolution. High-mannose, complex, and hybrid type[12] *N*-glycans were all observed and selected extracted ion chromatograms (EICs) are shown in Figure 7.2. Because retention on the HILIC column is primarily determined by multiple

hydrogen bonding of glycans, the retention of neutral *N*-glycans increased as the glycan length and size increased, which correlates well with previous reports.[31]

A. Total Ion Chromatogram (HILIC LC-MS)
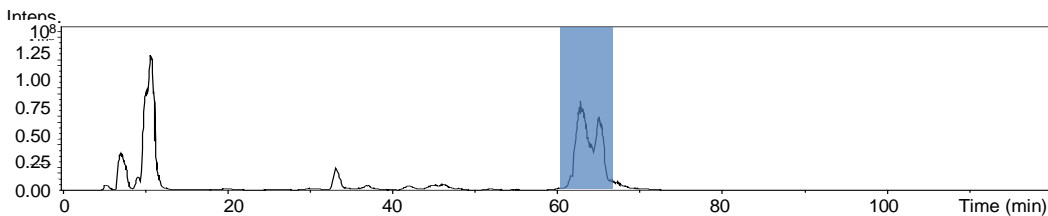
B. HILIC LC-MS (60.0 - 66.4 min)

C. ESI-FT-ICR MS
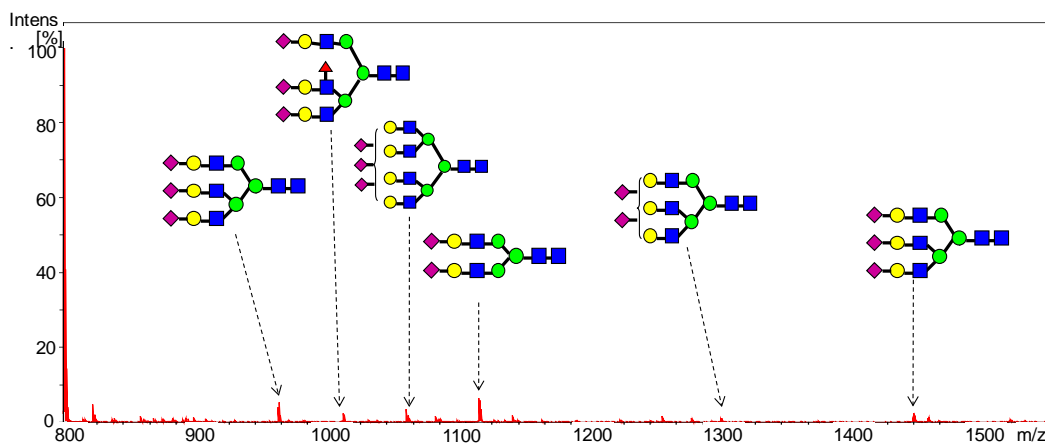
Figure 7.1. Analysis of *N*-glycans from AGP demonstrated by (A) TIC from HILIC LC-MS, (B) average mass spectrum summed from 60.0 to 66.4 min using HILIC LC-FT-ICR MS, and (C) direct infusion ESI-FT-ICR MS (10 scans). Highlighted range in (A) corresponds to 60.0–66.4 min.
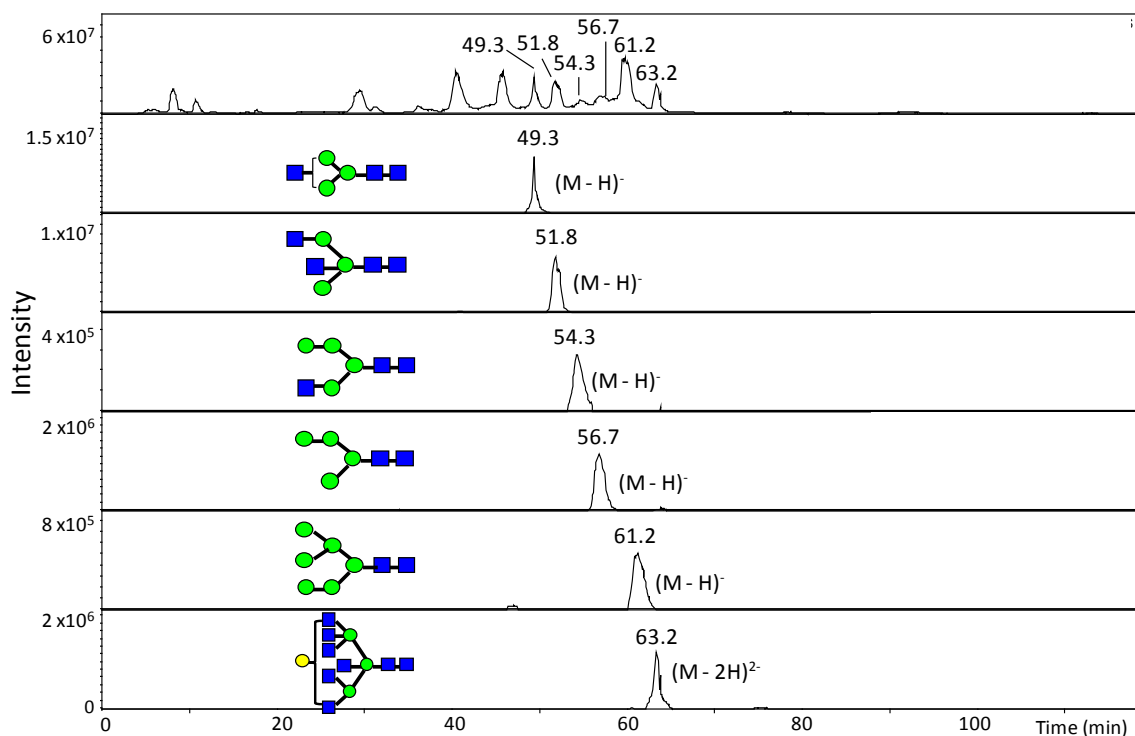
Figure 7.2. Total ion chromatogram and extracted ion chromatograms of *N*-glycans released from chicken ovalbumin using HILIC LC-FT-ICR MS.
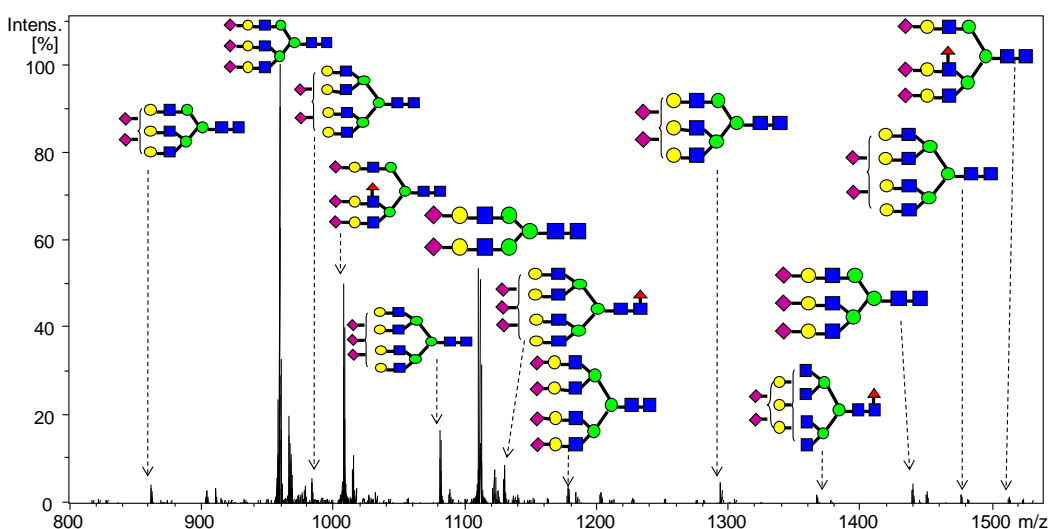
HILIC LC-FT-ICR MS of *N*-glycans released from chicken ovalbumin is demonstrated in Figure 7.2. The majority of *N*-glycans eluted between 45 and 65 minutes, and separated with high resolution. High-mannose, complex, and hybrid type[12] *N*-glycans were all observed and selected extracted ion chromatograms (EICs) are shown in Figure 7.2. Because retention on the HILIC column is primarily determined by multiple hydrogen bonding of glycans, the retention of neutral *N*-glycans increased as the glycan length and size increased, which correlates well with previous reports.[31]
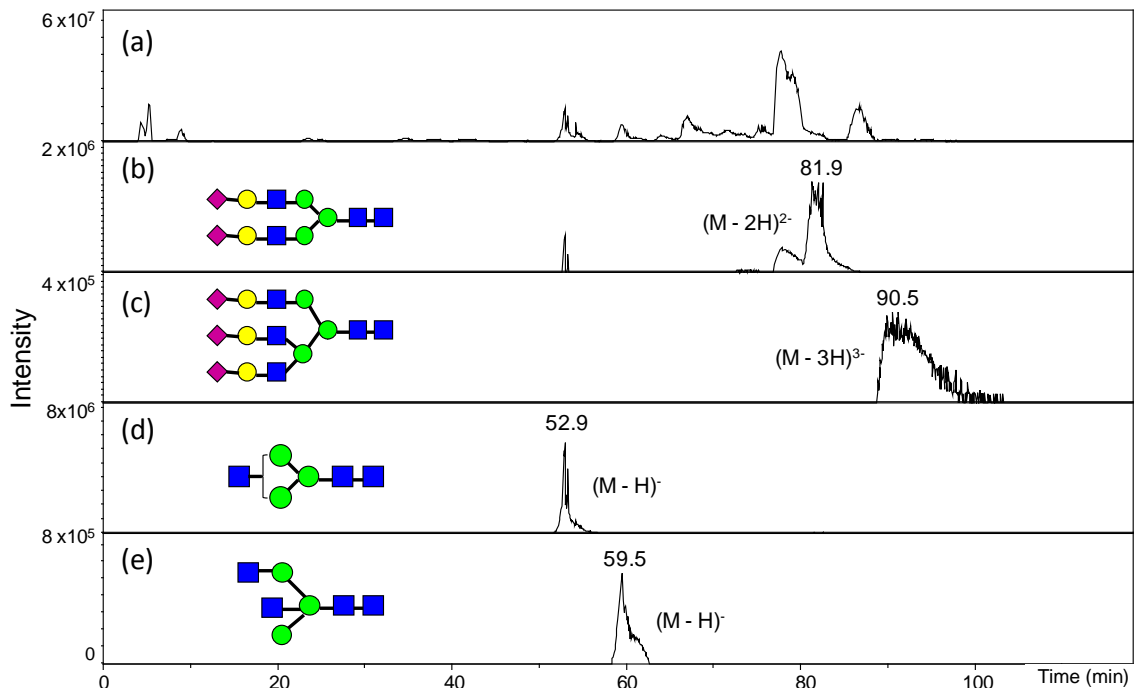
Figure 7.3. Total ion chromatogram (a) and selected extracted ion chromatograms of *N*-glycan mixtures from AGP ((b) and (c)) and ovalbumin ((d) and (e)) using HILIC LC-FT-ICR MS.

A 1:1 mixture of AGP *N*-glycans and ovalbumin *N*-glycans was also investigated by HILIC LC-FT-ICR MS. Figure 7.3 shows the TIC and selected EICs of sialylated and neutral *N*-glycans. Neutral and sialylated *N*-glycans were well separated, however, peaks with shoulders were observed in EICs (e.g., Figure 7.3e). Due to the electrostatic interaction between sialic acids and the positively charged amide stationary phase, sialylated *N*-glycans were better retained on the column and eluted later than the neutral *N*-glycans.[44] In sum, HILIC LC-FT-ICR MS can be utilized to separate and identify neutral and sialylated *N*-glycans, however, the column performance was not satisfactory and further optimization of conditions may still be needed.

7.3.2 PGC LC-FT-ICR MS of N-linked Glycans

N-linked glycans released from AGP were subjected to HILIC and PGC columns for online LC-FT-ICR MS and the TIC and EICs of sample glycans are displayed in Figure 7.4. In HILIC LC-FT-ICR MS, the di-antennary glycan (Figure 7.4b) and tri-antennary glycan (Figure 7.4c) were not fully separated, and co-eluted between 54 and 55 min. There was a shoulder peak at 55 min for the tri-antennary glycan $(HexNAc)_5(Hex)_6(NeuAc)_3$, indicating the presence of structural isomers which have been previously reported.[45] For PGC LC-FT-ICR MS, the two glycans mentioned above were fully separated, and potential separation of isomers was also observed for both glycans (Figure 7.4d and 7.4e). It has been reported that PGC columns provide excellent separation not only of structural isomers but also for anomeric isomers,[14] which contribute to detailed glycan structural characterization.
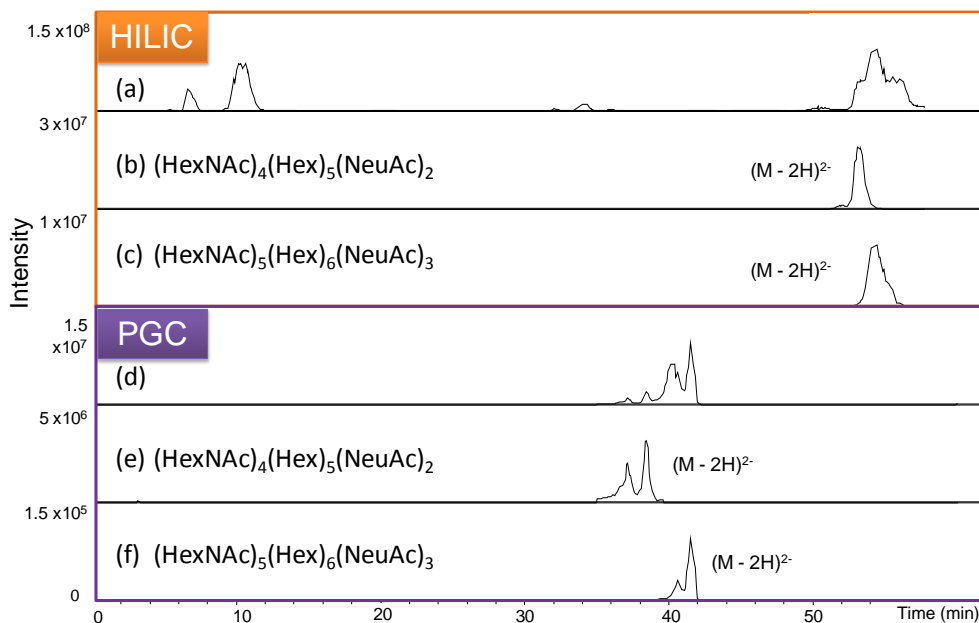

Figure 7.4. Total ion chromatogram and selected extracted ion chromatograms of *N*-glycan mixtures from AGP using HILIC LC-FT-ICR MS (a), (b), (c), and PGC LC-FT-ICR MS (d), (e), (f).
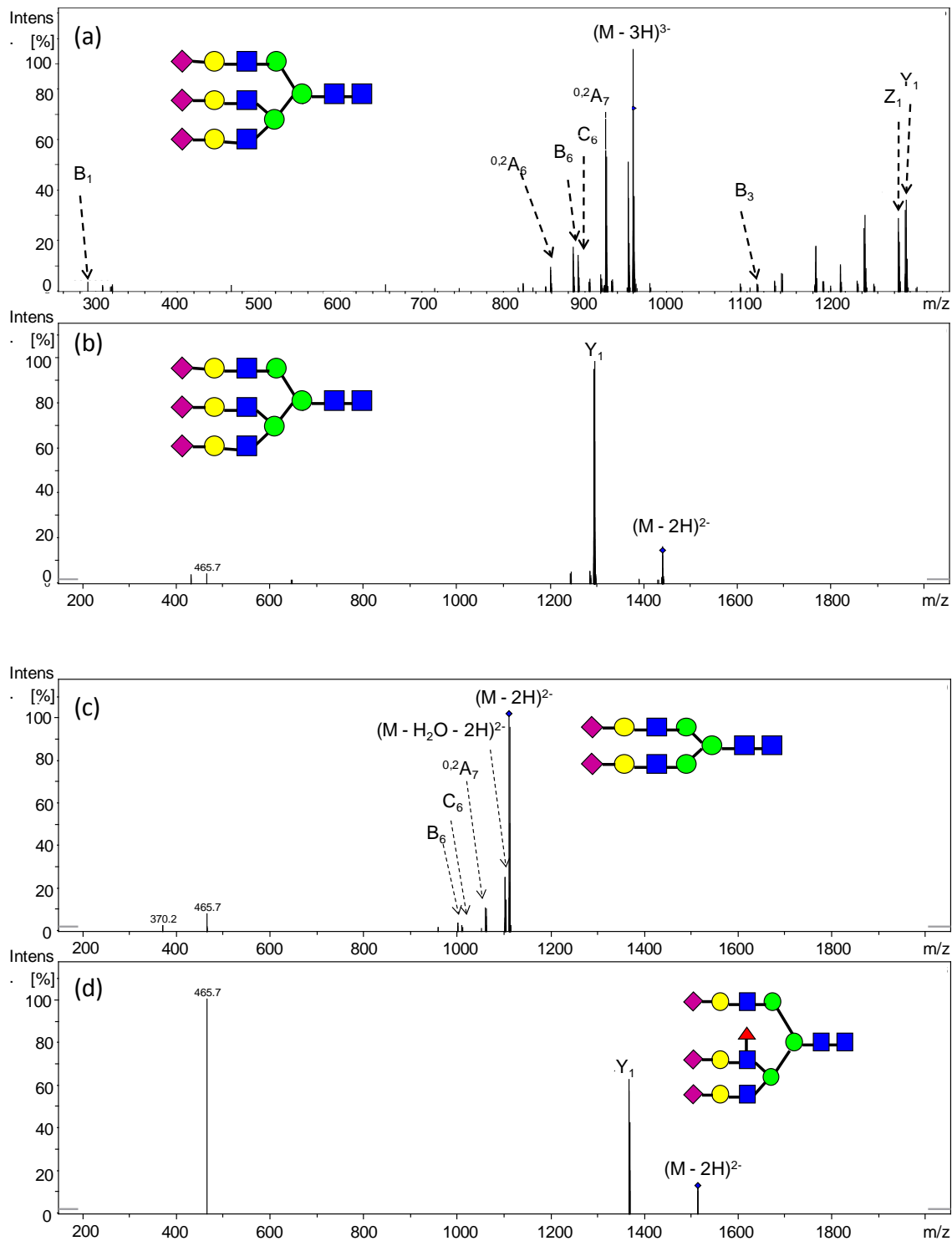
Figure 7.5. MS/MS of (a) *m/z* 959, (b) *m/z* 1438, (c) *m/z* 1110, and (d) *m/z* 1512 using PGC LC-FT-ICR MS.

Figure 7.5 displays online PGC LC-FT-ICR MS/MS spectra of sialylated glycans from AGP in negative-ion mode. We used a fixed voltage when fragmenting the precursor ions by collision activated dissociation (CAD), and found that the fragmentation efficiency for higher charge state precursor ions was significantly higher (see Figure 7.5a and 7.5b) than for lower charge states. For the tri-antennary glycan $(HexNAc)_5(Hex)_6(NeuAc)_3$, triply deprotonated species yielded several glycosidic and cross-ring cleavages, while doubly deprotonated species only generated one glycosidic fragment corresponding to loss of one sialic acid. The latter fragment helped determine that the glycan was sialylated, however, little structural information was obtained. In addition, tandem mass spectrometry (MS/MS) of glycans also depends on glycan size. Figures 7.5c and 7.5d show MS/MS spectra of a doubly charged di-antennary glycan $(HexNAc)_4(Hex)_5(NeuAc)_2$ and a doubly charged fucosylated tri-antennary glycan $(HexNAc)_5(Hex)_6(Fuc)(NeuAc)_3$. In Figure 7.5d, MS/MS of this tri-antennary glycan only produced one glycosidic cleavage, similar to Figure 7.5b. In contrast, MS/MS of the di-antennary glycan yielded both glycosidic and cross-ring cleavages. These results show that smaller glycans fragment more efficiently in on-line LC-MS/MS, but still not extensively enough to fully characterize the glycans. For further structural elucidation, offline LC-MS combined with alternative MS/MS techniques such as electron capture dissociation,[46] electron transfer dissociation,[47] and electron detachment dissociation[48] are powerful approaches for glycan analysis, as described in Chapter 2-5.

7.4 Conclusions

Strategies for N-linked glycan profiling using HILIC and PGC LC-FT-ICR MS/MS were developed. Acidic *N*-glycans from AGP and neutral *N*-glycans from ovalbumin were examined with an ESI FT-ICR mass spectrometer. HILIC LC-FT-ICR MS was able to separate neutral and acidic *N*-glycans, and demonstrated high resolution for neutral *N*-glycans. More glycans were identified based on high mass accuracy HILIC LC-FT-ICR MS than from direct infusion experiments. PGC LC-FT-ICR MS also achieved *N*-glycan profiling with good resolution, and potential separation of glycan isomers. Online PGC LC-FT-ICR MS/MS provided structural information both regarding monosaccharide composition and linkage type. In conclusion, HILIC and PGC LC-FT-ICR MS/MS are valuable tools for *N*-glycan profiling.

7.5 References

1.   Varki, A. Biological roles of oligosaccharides - All of the theories are correct. *Glycobiol.* **1993**, *3*, 97-130.
2.   Dwek, R. A. Glycobiology: Toward understanding the function of sugars. *Chem. Rev.* **1996**, *96*, 683-720.
3.   Bertozzi, C. R.; Kiessling, L. L. Chemical glycobiology. *Science* **2001**, *291*, 2357-2364.
4.   Kim, Y. J.; Varki, A. Perspectives on the significance of altered glycosylation of glycoproteins in cancer. *Glycoconj. J.* **1997**, *14*, 569-576.
5.   van den Steen, P.; Rudd, P. M.; Dwek, R. A.; Opdenakker, G. Concepts and principles of O-linked glycosylation. *Crit. Rev. Biochem. Mol. Biol.* **1998**, *33*, 151-208.
6.   Scanlin, T. F.; Glick, M. C. Terminal glycosylation and disease: Influence on cancer and cystic fibrosis. *Glycoconj. J.* **2000**, *17*, 617-626.
7.   Barchi, J. J. Emerging roles of carbohydrates and glycomimetics in anticancer drug design. *Curr. Pharm. Des.* **2000**, *6*, 485-501.
8.   Hakomori, S. Glycosylation defining cancer malignancy: New wine in an old bottle. *Proc. Natl. Acad. Sci. U. S. A.* **2002**, *99*, 10231-10233.
9.   Dube, D. H.; Bertozzi, C. R. Glycans in cancer and inflammation. Potential for therapeutics and diagnostics. *Nat. Rev. Drug Discov.* **2005**, *4*, 477-488.

10. Oppenheimer, S. B.; Alvarez, M.; Nnoli, J. Carbohydrate-based experimental therapeutics for cancer, HIV/AIDS and other diseases. *Acta Histochem.* **2008**, *110*, 6-13.

11. Krishnamoorthy, L.; Mahal, L. K. Glycomic analysis: an array of technologies. *ACS Chem. Biol.* **2009**, *4*, 715-732.

12. Mechref, Y.; Novotny, M. V. Structural investigations of glycoconjugates at high sensitivity. *Chem. Rev.* **2002**, *102*, 321-369.

13. Wuhrer, M.; Deelder, A. M.; Hokke, C. H. Protein glycosylation analysis by liquid chromatography-mass spectrometry. *Journal of Chromatography B-Analytical Technologies in the Biomedical and Life Sciences* **2005**, *825*, 124-133.

14. Ruhaak, L. R.; Deelder, A. M.; Wuhrer, M. Oligosaccharide analysis by graphitized carbon liquid chromatography-mass spectrometry. *Anal. Bioanal. Chem.* **2009**, *394*, 163-174.

15. ElRassi, Z. Recent progress in reversed-phase and hydrophobic interaction chromatography of carbohydrate species. *J. Chromatogr. A* **1996**, *720*, 93-118.

16. Novotny, M. V.; Mechref, Y. New hyphenated methodologies in high-sensitivity glycoprotein analysis. *J. Sep. Sci.* **2005**, *28*, 1956-1968.

17. Costello, C. E.; Contado-Miller, J. M.; Cipollo, J. F. A glycomics platform for the analysis of permethylated oligosaccharide alditols. *J. Am. Soc. Mass. Spectrom.* **2007**, *18*, 1799-1812.

18. Pabst, M.; Altmann, F. Influence of electrosorption, solvent, temperature, and ion polarity on the performance of LC-ESI-MS using graphitic carbon for acidic oligosaccharides. *Anal. Chem.* **2008**, *80*, 7534-7542.

19. Ruhaak, L. R.; Zauner, G.; Huhn, C.; Bruggink, C.; Deelder, A. M.; Wuhrer, M. Glycan labeling strategies and their use in identification and quantification. *Anal. Bioanal. Chem.* **2010**, *397*, 3457-3481.

20. Kebarle, P.; Verkerk, U. H. Electrospray: from ions in solution to ions in the gas phase, what we know now. *Mass Spectrom. Rev.* **2009**, *28*, 898-917.

21. Chu, C. S.; Ninonuevo, M. R.; Clowers, B. H.; Perkins, P. D.; An, H. J.; Yin, H. F.; Killeen, K.; Miyamoto, S.; Grimm, R.; Lebrilla, C. B. Profile of native N-linked glycan structures from human serum using high performance liquid chromatography on a microfluidic chip and time-of-flight mass spectrometry. *Proteomics* **2009**, *9*, 1939-1951.

22. Zhao, J.; Qiu, W. L.; Simeone, D. M.; Lubman, D. M. N-linked glycosylation profiling of pancreatic cancer serum using capillary liquid phase separation coupled with mass spectrometric analysis. *J. Proteome Res.* **2007**, *6*, 1126-1138.

23. Morelle, W.; Page, A.; Michalski, J. C. Electrospray ionization ion trap mass spectrometry for structural characterization of oligosaccharides derivatized with 2-aminobenzamide. *Rapid Commun. Mass Spectrom.* **2005**, *19*, 1145-1158.

24. Chen, X. Y.; Flynn, G. C. Gas-phase oligosaccharide nonreducing end (GONE) sequencing and structural analysis by reversed phase HPLC/mass spectrometry with polarity switching. *J. Am. Soc. Mass. Spectrom.* **2009**, *20*, 1821-1833.

25. Pabst, M.; Kolarich, D.; Poltl, G.; Dalik, T.; Lubec, G.; Hofinger, A.; Altmann, F. Comparison of fluorescent labels for oligosaccharides and introduction of a new postlabeling purification method. *Anal. Biochem.* **2009**, *384*, 263-273.

26. Chen, X. Y.; Flynn, G. C. Analysis of N-glycans from recombinant immunoglobulin G by on-line reversed-phase high-performance liquid chromatography/mass spectrometry. *Anal. Biochem.* **2007**, *370*, 147-161.

27. Hemstrom, P.; Irgum, K. Hydrophilic interaction chromatography. *J. Sep. Sci.* **2006**, *29*, 1784-1821.

28. Wuhrer, M.; de Boer, A. R.; Deelder, A. M. Structural glycomics using hydrophilic interaction chromatography (HILIC) with mass spectrometry. *Mass Spectrom. Rev.* **2009**, *28*, 192-206.

29. Zhao, J.; Simeone, D. M.; Heidt, D.; Anderson, M. A.; Lubman, D. M. Comparative serum glycoproteomics using lectin selected sialic acid glycoproteins with mass spectrometric analysis: Application to pancreatic cancer serum. *J. Proteome Res.* **2006**, *5*, 1792-1802.

30. Bereman, M. S.; Williams, T. I.; Muddiman, D. C. Development of a nanoLC LTQ orbitrap mass spectrometric method for profiling glycans derived from plasma from healthy, benign tumor control, and epithelial ovarian cancer patients. *Anal. Chem.* **2009**, *81*, 1130-1136.

31. Wuhrer, M.; Koeleman, C. A. M.; Deelder, A. M.; Hokke, C. N. Normal-phase nanoscale liquid chromatography - Mass spectrometry of underivatized oligosaccharides at low-femtomole sensitivity. *Anal. Chem.* **2004**, *76*, 833-838.

32. Wuhrer, M.; Koeleman, C. A. M.; Hokke, C. H.; Deelder, A. M. Nano-scale liquid chromatography-mass spectrometry of 2-aminobenzamide-labeled oligosaccharides at low femtomole sensitivity. *Int. J. Mass spectrom.* **2004**, *232*, 51-57.

33. Hounsell, E. F.; Davies, M. J.; Renouf, D. V. O-linked protein glycosylation structure and function. *Glycoconj. J.* **1996**, *13*, 19-26.

34. Davies, M. J.; Smith, K. D.; Carruthers, R. A.; Chai, W.; Lawson, A. M.; Hounsell, E. F. Use of a porous graphitized carbon column for the high-performance liquid-chromatography of oligosaccharides, alditols and glycopeptides with subsequent mass-spectrometry analysis. *J. Chromatogr.* **1993**, *646*, 317-326.

35. Fan, J. Q.; Kondo, A.; Kato, I.; Lee, Y. C. High-performance liquid-chromatography of glycopeptides and oligosaccharides on graphitized carbon columns *Anal. Biochem.* **1994**, *219*, 224-229.

36. Thomsson, K. A.; Backstrom, M.; Larsson, J. M. H.; Hansson, G. C.; Karlsson, H. Enhanced detection of sialylated and sulfated glycans with negative ion mode nanoliquid chromatography/mass spectrometry at high pH. *Anal. Chem.* **2010**, *82*, 1470-1477.

37. Kawasaki, N.; Ohta, M.; Hyuga, S.; Hyuga, M.; Hayakawa, T. Application of liquid chromatography/mass spectrometry and liquid chromatography with tandem mass spectrometry to the analysis of the site-specific carbohydrate heterogeneity in erythropoietin. *Anal. Biochem.* **2000**, *285*, 82-91.

38. Robinson, S.; Bergstrom, E.; Seymour, M.; Thomas-Oates, J. Screening of underivatized oligosaccharides extracted from the stems of Triticum aestivum using porous graphitized carbon liquid chromatography-mass spectrometry. *Anal. Chem.* **2007**, *79*, 2437-2445.

39.   Karlsson, H.; Halim, A.; Teneberg, S. Differentiation of glycosphingolipid-derived glycan structural isomers by liquid chromatography/mass spectrometry. *Glycobiol.* **2010**, *20*, 1103-1116.

40.   Wu, S. A.; Grimm, R.; German, J. B.; Lebrilla, C. B. Annotation and structural analysis of sialylated human milk oligosaccharides. *J. Proteome Res.* **2011**, *10*, 856-868.

41.   Yang, J.; Mo, J. J.; Adamson, J. T.; Hakansson, K. Characterization of oligodeoxynucleotides by electron detachment dissociation Fourier transform ion cyclotron resonance mass spectrometry. *Anal. Chem.* **2005**, *77*, 1876-1882.

42.   Fournier, T.; Medjoubi-N, N.; Porquet, D. Alpha-1-acid glycoprotein. *Biochimica Et Biophysica Acta-Protein Structure and Molecular Enzymology* **2000**, *1482*, 157-171.

43.   Harvey, D. J.; Wing, D. R.; Kuster, B.; Wilson, I. B. H. Composition of N-linked carbohydrates from ovalbumin and Co-purified glycoproteins. *J. Am. Soc. Mass. Spectrom.* **2000**, *11*, 564-571.

44.   Luo, Q. Z.; Rejtar, T.; Wu, S. L.; Karger, B. L. Hydrophilic interaction 10 mu m ID porous layer open tubular columns for ultratrace glycan analysis by liquid chromatography-mass spectrometry. *J. Chromatogr. A* **2009**, *1216*, 1223-1231.

45.   Shiyan, S. D.; Bovin, N. V. Carbohydrate composition and immunomodulatory activity of different glycoforms of alpha(1)-acid glycoprotein. *Glycoconj. J.* **1997**, *14*, 631-638.

46.   Zubarev, R. A.; Kelleher, N. L.; McLafferty, F. W. Electron capture dissociation of multiply charged protein cations. A nonergodic process. *J. Am. Chem. Soc.* **1998**, *120*, 3265-3266.

47.   Syka, J. E. P.; Coon, J. J.; Schroeder, M. J.; Shabanowitz, J.; Hunt, D. F. Peptide and protein sequence analysis by electron transfer dissociation mass spectrometry. *Proc. Natl. Acad. Sci. U. S. A.* **2004**, *101*, 9528-9533.

48.   Budnik, B. A.; Haselmann, K. F.; Zubarev, R. A. Electron detachment dissociation of peptide di-anions: an electron-hole recombination phenomenon. *Chem. Phys. Lett.* **2001**, *342*, 299-302.

Chapter 8

Conclusions and Prospects for Future Work

8.1 Purpose of Dissertation

Glycosylation characterization has been a challenging task due to the complexity of glycan structures and heterogeneity of glycoforms at a specific glycosylation site. Complete elucidation of glycosylation requires information of monosaccharide composition, sequence, linkage type, branching, anomeric configuration, and occupancy. It is essential to develop methods which can efficiently analyze glycosylation to facilitate better understanding of the functions it plays in various cellular processes. As mentioned in Chapter 1, exoglycosidase digestion, nuclear magnetic resonance (NMR) spectroscopy, X-ray crystallography, and gas chromatography/mass spectrometry (GC/MS) have all been used for structural characterization of glycans and glycoconjugates.[1] However, such methods do not provide the required sensitivity for current glycomics and glycoproteomics. Mass spectrometry (MS) is an indispensable tool for glycosylation analysis, due to its high sensitivity, high mass accuracy, and low sample consumption. In particular, Fourier transform ion cyclotron resonance mass spectrometry (FT-ICR MS) provides the highest resolution and resolving power of current mass spectrometers, and is

also capable to couple with various tandem mass spectrometric (MS/MS) techniques.[2,3]

In glycan and glycopeptide fragmentation studies, collision activated dissociation (CAD) preferentially generates glycosidic cleavages in both positive- and negative-ion modes.[4-10] Though glycosidic cleavages provide information regarding glycan composition and sequence, lack of cross-ring cleavages makes linkage determination difficult. Ion-electron and ion-ion based fragmentation techniques such as electron capture dissociation (ECD),[11] electron transfer dissociation (ETD),[12] and electron detachment dissociation (EDD)[13] have been utilized to characterize protein post-translational modifications (PTMs), and can generate complementary structural information compared to CAD and infrared multiphoton dissociation (IRMPD).[14-17] One major goal of this dissertation is to explore the utilization of ion-electron and ion-photon reactions to characterize neutral and acidic glycans in both native and derivatized forms, as well as acidic glycopeptides.

Another aim of this dissertation is to develop liquid chromatography (LC)-FT-ICR MS methods to separate and identify glycans. For complex biological samples such as blood and serum, sample purification prior to MS is essential for structural characterization, and LC-MS is the most commonly utilized strategy.[18-22] Here, we investigated online LC-FT-ICR MS of acidic and neutral N-linked glycans using columns with different stationary phases.

8.2 Summary of Results

Traditionally, most glycan structural analysis is conducted in positive-ion mode. Sulfated glycans have been associated with cancer metastasis processes,[23] but sulfated glycan analysis is challenging in MS due to the lability of sulfate groups. In Chapter 2,

we illustrated the application of metal-adduction with ECD for sulfated *N*-glycan analysis. ECD of metal-adducted sulfated *N*-glycans yielded complementary structural information compared to IRMPD, while preserving the labile sulfate groups in all the product ions. It was the first time ECD had been applied to N-linked glycans released from glycoproteins. The fragmentation behaviors of metal-adducted oligosaccharides in ECD, ETD, and CAD were also compared in Chapter 3. Fragmentation patterns in ECD and ETD of oligosaccharides are generally similar, but significantly different from those from CAD. For doubly charged oligosaccharide precursor ions, ECD typically generates more extensive fragmentation compared to ETD.

Some glycans are more suitable for analysis in negative-ion mode, such as sialylated glycans. Chapter 4 utilizes ion-electron reactions to characterize sialylated N-linked glycans both in positive- and negative-ion modes, and Chapter 5 examines fluorescently labeled sialylated oligosaccharides in negative-ion mode. For native sialylated glycans, negative-ion mode is more advantageous. IRMPD and EDD both produce extensive glycosidic and cross-ring cleavages, and the cross-ring fragments from the two approaches are completely complementary. For derivatized oligosaccharides, EDD also generates complementary structural information compared to IRMPD. We also found that fluorescent labels attached to oligosaccharides influence the fragmentation behavior.

In Chapter 6, we investigate structural characterization methods of N-linked and O-linked glycopeptides using negative ion mode IRMPD and EDD. Strategies involving use of the non-specific enzyme pronase combined with EDD are explored. For N-linked glycopeptides, EDD fragmentation efficiency decreased with increased peptide length.

For O-linked glycopeptides, EDD was able to yield peptide backbone, glycosidic, and cross-ring cleavages in the same spectrum, thus being a very promising tool for structural analysis of *O*-glycopeptides.

Finally, Chapter 7 focuses on LC-FT-ICR MS method development using hydrophilic interaction chromatography (HILIC) and porous graphitized carbon (PGC) columns to separate and identify *N*-glycans released from glycoproteins. Both HILIC and PGC LC-FT-ICR MS can separate *N*-glycans with good resolution, while PGC demonstrates better reproducibility and potential separation of isomers.

8.3 Prospects for Future Work

We have demonstrated the utilization of ECD, ETD, and EDD for structural characterization of N-linked glycans and glycopeptides, and complementary information was obtained compared to CAD and IRMPD. However, the ion-electron reactions all require precursor ions with at least two charges, which may be difficult to obtain for small glycans. Compared to N-linked glycans, O-linked glycans are in general smaller,[1] and are thus more difficult to multiply charge, particularly in positive-ion mode. Electron induced dissociation (EID) and negative-ion ECD (niECD) are promising tools for glycan structural analysis. EID has been applied to singly charged fatty acids, and allowed determination of double bond positions of several fatty acids.[24] EID can be performed both in positive- and negative-ion mode, which makes it potentially compatible with both neutral and acidic oligosaccharides. It has been proposed that EID involves both electronic excitation, similar to high energy CAD, as well as vibrational excitation, potentially generating additional information compared to CAD/IRMPD. niECD is a fragmentation technique recently developed in our lab. Negatively charged precursor

ions undergo electron capture and generate "charge-increased" radical species, to further yield c- and z-type ions for peptides. niECD could be a promising approach to study sialylated O-linked glycans in negative-ion mode.

Chapter 7 illustrates development of HILIC and PGC LC-FT-ICR MS methods for N-linked glycan profiling, and shows that acidic and neutral *N*-glycans can be separated. However, due to time limitations, factors that may influence the separation of glycans such as solvent, gradient, and temperature were not systematically studied and compared between the two stationary phases. In addition, the current study was conducted using *N*-glycans released from standard glycoproteins and capillary LC. The next logical step is to scale down to nano-scale LC (nanoLC) and implement that strategy to characterize more complex biological samples. NanoLC benefits from increased sensitivity and reduced sample consumption, and has been widely used to study glycans from complex mixtures such as human serum.[25-31] However, due to different instrumentation conditions, the method developed for capillary LC cannot be directly applied for nanoLC, and further optimization may still be required.

Aberrant glycosylation have been directly associated with different disease states. Therefore, complete characterization of glycosylation is crucial to understand the roles it plays in various biological activities. However, as described in Chapter 7, online LC-FT-ICR MS/MS does not provide extensive structural information of *N*-glycans, illustrating the limitation of CAD. ECD, ETD, and EDD are not easily combined with online LC separation due to the relatively long time for fragmentation. One possible solution to this issue is to obtain standard glycans of interest, and compare their CAD fragmentation to the online LC-MS/MS fragmentation profiles of unknown species. However, it may be

difficult to obtain such standard oligosaccharides, particularly if they are N- or O-linked glycans.

Another feasible approach is to combine ion-electron reactions with off-line LC, but further optimization is needed for future studies. The Advion Triversa Nanomate is the latest in chip-based electrospray ionization technology. The effluent is split with a portion directed to a LC/MS interface while the remainder of the split effluent is collected at time segments into a multi-well plate. Following LC/MS, we are able to select fractions of interest for further structural elucidation using alternative MS/MS strategies such as ion-electron and ion-ion reactions. The strategy of combining Nanomate robot and FT-ICR MS has been applied to characterize a glycoconjugate mixture from urine of a patient suffering from Schindler's disease, demonstrating the feasibility of the strategy to analyze complex biological samples.[32] Glycans and glycoconjugates are already used as targets in many therapeutic applications,[33-35] and detailed characterization of cancer associated glycans may permit the identification of cancer vaccine candidates.

8.4 References

1. Mechref, Y.; Novotny, M. V. Structural investigations of glycoconjugates at high sensitivity. *Chem. Rev.* **2002**, *102*, 321-369.
2. Marshall, A. G.; Hendrickson, C. L.; Jackson, G. S. Fourier transform ion cyclotron resonance mass spectrometry: A primer. *Mass Spectrom. Rev.* **1998**, *17*, 1-35.
3. Marshall, A. G.; Hendrickson, C. L. High-resolution mass spectrometers. *Annu. Rev. Anal. Chem.* **2008**, *1*, 579-599.
4. Harvey, D. J. Fragmentation of negative ions from carbohydrates: Part 2. Fragmentation of high-mannose N-linked glycans. *J. Am. Soc. Mass. Spectrom.* **2005**, *16*, 631-646.
5. Harvey, D. J. Fragmentation of negative ions from carbohydrates: Part 3. Fragmentation of hybrid and complex N-linked glycans. *J. Am. Soc. Mass. Spectrom.* **2005**, *16*, 647-659.
6. Harvey, D. J. Matrix-assisted laser desorption/ionization mass spectrometry of carbohydrates. *Mass Spectrom. Rev.* **1999**, *18*, 349-450.

7.   Zaia, J. Mass spectrometry of oligosaccharides. *Mass Spectrom. Rev.* **2004**, *23*, 161-227.

8.   Park, Y. M.; Lebrilla, C. B. Application of Fourier transform ion cyclotron resonance mass spectrometry to oligosaccharides. *Mass Spectrom. Rev.* **2005**, *24*, 232-264.

9.   Zaia, J. Mass spectrometry and glycomics. *Omics* **2010**, *14*, 401-418.

10. Sheeley, D. M.; Reinhold, V. N. Structural characterization of carbohydrate sequence, linkage, and branching in a quadrupole ion trap mass spectrometer: Neutral oligosaccharides and N-linked glycans. *Anal. Chem.* **1998**, *70*, 3053-3059.

11. Zubarev, R. A.; Kelleher, N. L.; McLafferty, F. W. Electron capture dissociation of multiply charged protein cations. A nonergodic process. *J. Am. Chem. Soc.* **1998**, *120*, 3265-3266.

12. Syka, J. E. P.; Coon, J. J.; Schroeder, M. J.; Shabanowitz, J.; Hunt, D. F. Peptide and protein sequence analysis by electron transfer dissociation mass spectrometry. *Proc. Natl. Acad. Sci. U. S. A.* **2004**, *101*, 9528-9533.

13. Budnik, B. A.; Haselmann, K. F.; Zubarev, R. A. Electron detachment dissociation of peptide di-anions: an electron-hole recombination phenomenon. *Chem. Phys. Lett.* **2001**, *342*, 299-302.

14. Zubarev, R. A. Reactions of polypeptide ions with electrons in the gas phase. *Mass Spectrom. Rev.* **2003**, *22*, 57-77.

15. Hakansson, K.; Cooper, H. J.; Hudgins, R. R.; Nilsson, C. L. High resolution tandem mass spectrometry for structural biochemistry. *Curr. Org. Chem.* **2003**, *7*, 1503-1525.

16. Mikesh, L. M.; Ueberheide, B.; Chi, A.; Coon, J. J.; Syka, J. E. P.; Shabanowitz, J.; Hunt, D. F. The utility of ETD mass spectrometry in proteomic analysis. *BBA-Proteins Proteomics* **2006**, *1764*, 1811-1822.

17. Wiesner, J.; Premsler, T.; Sickmann, A. Application of electron transfer dissociation (ETD) for the analysis of posttranslational modifications. *Proteomics* **2008**, *8*, 4466-4483.

18. Novotny, M. V.; Mechref, Y. New hyphenated methodologies in high-sensitivity glycoprotein analysis. *J. Sep. Sci.* **2005**, *28*, 1956-1968.

19. Chen, G. D.; Pramanik, B. N. LC-MS for protein characterization: current capabilities and future trends. *Expert Rev. Proteomics* **2008**, *5*, 435-444.

20. Ruhaak, L. R.; Deelder, A. M.; Wuhrer, M. Oligosaccharide analysis by graphitized carbon liquid chromatography-mass spectrometry. *Anal. Bioanal. Chem.* **2009**, *394*, 163-174.

21. Ruhaak, L. R.; Zauner, G.; Huhn, C.; Bruggink, C.; Deelder, A. M.; Wuhrer, M. Glycan labeling strategies and their use in identification and quantification. *Anal. Bioanal. Chem.* **2010**, *397*, 3457-3481.

22. Wuhrer, M.; de Boer, A. R.; Deelder, A. M. Structural glycomics using hydrophilic interaction chromatography (HILIC) with mass spectrometry. *Mass Spectrom. Rev.* **2009**, *28*, 192-206.

23. Kim, Y. J.; Varki, A. Perspectives on the significance of altered glycosylation of glycoproteins in cancer. *Glycoconj. J.* **1997**, *14*, 569-576.

24. Yoo, H. J.; Hakansson, K. Determination of double bond location in fatty acids by manganese adduction and electron induced dissociation. *Anal. Chem.* **2010**, *82*, 6940-6946.

25. Lochnit, G.; Geyer, R. An optimized protocol for nano-LC-MALDI-TOF-MS coupling for the analysis of proteolytic digests of glycoproteins. *Biomed. Chromatogr.* **2004**, *18*, 841-848.

26. Wuhrer, M.; Koeleman, C. A. M.; Hokke, C. H.; Deelder, A. M. Protein glycosylation analyzed by normal-phase nano-liquid chromatography-mass spectrometry of glycopeptides. *Anal. Chem.* **2005**, *77*, 886-894.

27. Bereman, M. S.; Williams, T. I.; Muddiman, D. C. Development of a nanoLC LTQ orbitrap mass spectrometric method for profiling glycans derived from plasma from healthy, benign tumor control, and epithelial ovarian cancer patients. *Anal. Chem.* **2009**, *81*, 1130-1136.

28. Karas, M.; Bahr, U.; Dulcks, T. Nano-electrospray ionization mass spectrometry: addressing analytical problems beyond routine. *Fresenius J. Anal. Chem.* **2000**, *366*, 669-676.

29. Karlsson, N. G.; Wilson, N. L.; Wirth, H. J.; Dawes, P.; Joshi, H.; Packer, N. H. Negative ion graphitised carbon nano-liquid chromatography/mass spectrometry increases sensitivity for glycoprotein oligosaccharide analysis. *Rapid Commun. Mass Spectrom.* **2004**, *18*, 2282-2292.

30. Wuhrer, M.; Koeleman, C. A. M.; Deelder, A. M.; Hokke, C. N. Normal-phase nanoscale liquid chromatography - Mass spectrometry of underivatized oligosaccharides at low-femtomole sensitivity. *Anal. Chem.* **2004**, *76*, 833-838.

31. Chu, C. S.; Ninonuevo, M. R.; Clowers, B. H.; Perkins, P. D.; An, H. J.; Yin, H. F.; Killeen, K.; Miyamoto, S.; Grimm, R.; Lebrilla, C. B. Profile of native N-linked glycan structures from human serum using high performance liquid chromatography on a microfluidic chip and time-of-flight mass spectrometry. *Proteomics* **2009**, *9*, 1939-1951.

32. Froesch, M.; Bindila, L. M.; Baykut, G.; Allen, M.; Peter-Katalinic, J.; Zamfir, A. D. Coupling of fully automated chip electrospray to Fourier transform ion cyclotron resonance mass spectrometry for high-performance glycoscreening and sequencing. *Rapid Commun. Mass Spectrom.* **2004**, *18*, 3084-3092.

33. Shriver, Z.; Raguram, S.; Sasisekharan, R. Glycomics: A pathway to a class of new and improved therapeutics. *Nat. Rev. Drug Discov.* **2004**, *3*, 863-873.

34. Dube, D. H.; Bertozzi, C. R. Glycans in cancer and inflammation. Potential for therapeutics and diagnostics. *Nat. Rev. Drug Discov.* **2005**, *4*, 477-488.

35. Krishnamoorthy, L.; Mahal, L. K. Glycomic analysis: an array of technologies. *ACS Chem. Biol.* **2009**, *4*, 715-732.

Appendix

Metal Oxide Enrichment of Acidic Oligosaccharides

A.1 Introduction

The analysis of protein glycosylation is crucial for understanding the important biological roles it plays in, e.g., cell-cell interactions and immune system response.[1-5] Aberrant glycosylation changes such as increased sialylation and sulfation have been directly associated with cancer metastasis.[6-9] Mass spectrometry (MS) has become an indispensable tool for structural analysis of glycans and glycoconjugates due to its high sensitivity, high mass accuracy, high mass resolution, and analytical versatility.[10-16] In addition, acidic glycans often suffer from ion suppression from neutral glycans in positive-ion mode analysis. Therefore, enrichment of glycans is essential prior to their characterization by mass spectrometry.

Lectin-based enrichment methods have been widely applied for glycoprotein and glycopeptide enrichment.[17,18] Lectins are a group of proteins which bind to glycans or glycan moieties of glycoproteins and glycolipids.[19] Concanavalin A (Con A) and wheat germ agglutinin (WGA) are among the most widely used lectins. Because lectins are highly specific to certain glycan structures, it is often necessary to use multi-dimensional

lectin-based approaches (e.g., lectin affinity chromatography) to fulfill the need of global-glycomics analysis.[19]   Metal oxide based enrichment methods have been extensively utilized to selectively enrich phosphopeptides[20-32] and sialylated glycopeptides.[33,34] TiO_2, ZrO_2, and HfO_2 demonstrated high selectivity for phosphorylated and sialylated peptides. Our lab demonstrated the application of metal oxide microtips for phosphopeptide enrichment with high specificity and high sensitivity.[21]   Here, we explore the application of TiO_2 and ZrO_2 microtips for the enrichment of sulfated and sialylated N-linked glycans prior to MS analysis.

A.2 Experimental

A.2.1 Reagents

Bovine thyroid stimulating hormone (bTSH), ribonuclease B (RNAse B), human transferrin, maltoheptaose, peptide-N-glycosidase F (PNGase F), 1,4-dithio-DL-threitol (DTT), and iodoacetamide were purchased from Sigma (St. Louis, MO).   Methanol, acetonitrile, NH_4HCO_3, NH_4OH, piperidine, and formic acid were obtained from Fisher (Fair Lawn, NJ).   Disialyl-lacto-N-tetraose (DSLNT) and lacto-N-fucopentaose (LNFP) were purchased from V-labs Inc (Covington, LA).   SPE graphitized carbon column was purchased from Alltech Associates Inc. (Deerfield, IL). ZrO_2 and TiO_2 microtips were obtained from Glygen Corp. (Columbia, MD).

A.2.2 Glycan Release and SPE Purification

Glycoproteins were reduced in 5 mM DTT at 56 °C for 45 min, alkylated by 15 mM iodoacetamide in the dark at room temperature for 1 h, and digested with PNGase F (2 U) in 50 mM NH_4HCO_3 (pH 8) overnight at 37 °C.   Released glycans were purified by SPE graphitized carbon column.   For each sample, a carbon cartridge was washed with

0.1% (v/v) formic acid in 80% acetonitrile/H_2O (v/v), followed by deionized water. The solution containing labeled oligosaccharides was loaded, and the cartridge was washed with deionized water to remove salts and other contaminants. Glycans were eluted with 0.1% formic acid (v/v) in 20% or 40% acetonitrile/H_2O (v/v). The solution was then dried down in a vacuum concentrator (Eppendorf, Hamberg, Germany) for further analysis.

A.2.3 Metal Oxide Microtip Enrichment

Oligosaccharides were reconstituted in binding solution, and loaded onto ZrO_2 microtips equilibrated with the same binding solution. Unbound glycans and other contaminants were removed with washing solution (H_2O), and bound sulfated glycans were eluted with eluting solution. Binding solution was either 3.3% formic acid (pH 2) or acetic acid (pH 4). Eluting solution was either deionized water (pH 7), 50 mM NH_4HCO_3 (pH 8), NH_4OH (pH 9), or 1% piperidine (pH 11). The eluted solution was dried down and reconstituted in 50% methanol, 0.1% NH_4OH (v/v) for negative-ion mode mass spectrometry analysis.

A.2.4 FT-ICR Mass Spectrometry

All mass spectra were collected with an actively shielded 7 T FT-ICR mass spectrometer with a quadrupole front-end (APEX-Q, Bruker Daltonics, Billerica, MA), as previously described.[35] Samples were infused via an Apollo II electrospray ion source at a flow rate of 70 μL/h with the assistance of N_2 nebulizing gas. Following ion accumulation in the first hexapole for 0.05 s, ions were mass selectively accumulated in the second hexapole for 1 s. Ions were then transferred through high voltage ion optics and captured with dynamic trapping in an Infinity ICR cell.[36] The accumulation

sequence up to the ICR cell fill was looped 3 times to optimize precursor ion signal to noise (S/N) ratio.

A.2.5 Data Analysis.

All mass spectra were acquired with XMASS software (Bruker Daltonics) with 256 data points from m/z 100 to 2000 and summed over 10-20 scans. Data processing was performed with MIDAS software.[37] Data were zero filled once, Hanning apodized, and exported to Microsoft Excel for internal frequency-to-mass calibration with a two-term calibration equation.[38] Product ions were not assigned unless the S/N ratio was at least 3.

A.3 Results and Discussion

A.3.1 Enrichment of Sulfated N-linked Glycans

Zirconium oxide and titanium oxide are known to have amphoteric properties. Depending on the pH of the solution, they can react either as a Lewis acid or a Lewis base, resulted from unsatisfied valencies of both oxygen and zirconium atoms in the surface layer.[39] Under acidic conditions, metal oxides act as a Lewis acid, and demonstrates high binding affinity with polyoxy anions, including phosphate, carboxylate, and sulfate.[21] In basic solutions, metal oxides act as a Lewis base and show low binding affinity. Therefore, biomolecules containing such functional groups can be released from metal oxides by increasing pH.

Figure A.1 shows sulfated N-linked glycans released from bTSH before and after TiO_2 enrichment in negative-ion mode MS. Among all the solutions examined 3.3% formic acid as binding solution, H_2O as eluting solution, and no washing step yielded the best enrichment results (data not shown). Before enrichment, many contamination peaks

from *m/z* 800–1200 were detected. Several sulfated *N*-glycans were observed with low abundance, both as singly and doubly charged species. After enrichment, the abundance of contamination peaks significantly decreased, leaving sulfated glycans as the most abundant peaks in the spectrum. Structures of the four glycans compared and the abundance change (normalized to charge state) after enrichment are shown in Table A.1. After TiO_2 enrichment, the increase in abundance of sulfated *N*-glycans was between 50 and 222%, indicating effective enrichment in this approach. Similar experiments were conducted using ZrO_2 microtips, and there was no significant difference in the results compared to TiO_2 microtips.
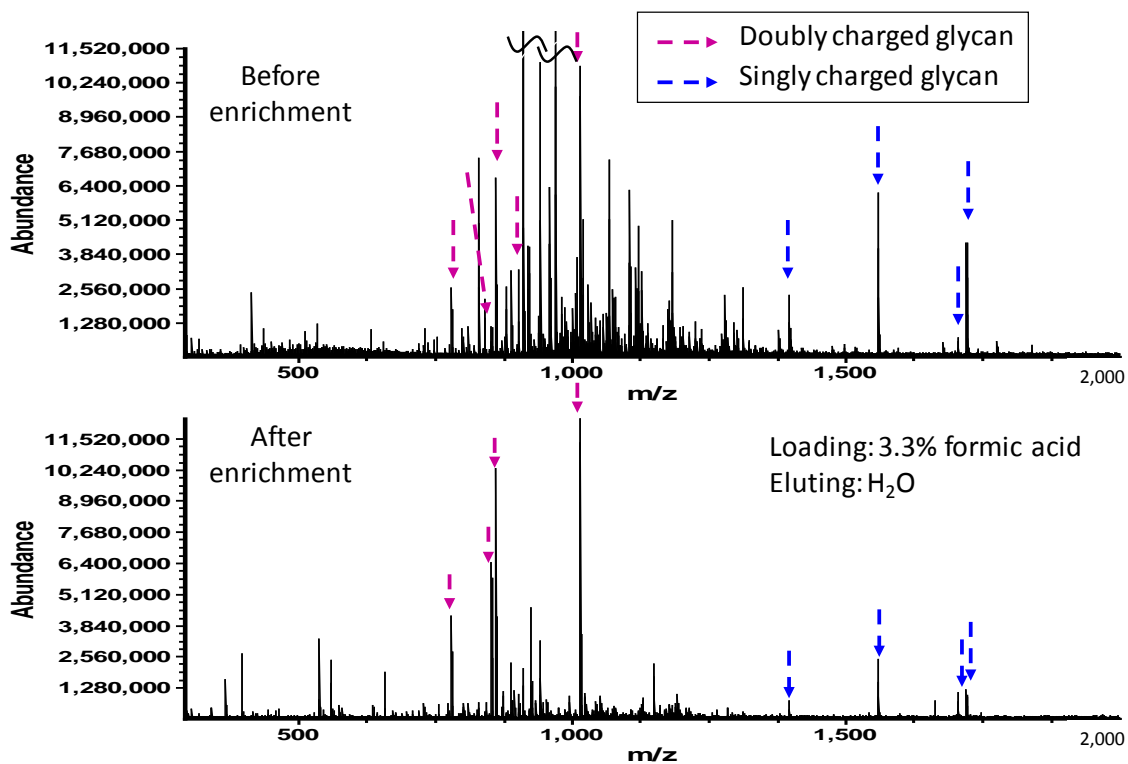

Figure A.1. Negative-ion mode MS of sulfated N-linked glycans released from bTSH before (top) and after (bottom) TiO_2 enrichment. Doubly charged glycan peaks are indicated by purple arrows, and singly charged glycan peaks are indicated by blue arrows.

No.	Glycan	Abundance increase after enrichment (%)
1	$(GlcNAc)_3(GalNAc)(Man)_4(SO3)$	59.5
2	$(GlcNAc)_3(GalNAc)(Man)_4(Fuc)(SO3)$	222.2
3	$(GlcNAc)_3(GalNAc)(Man)_5(Fuc)(SO3)$	175.3
4	$(GlcNAc)_4(GalNAc)_2(Man)_3(Fuc)(SO3)_2$	108.3

Table A.1. List of sulfated *N*-glycans and abundance changes before and after TiO_2 enrichment.

Figure A.2 illustrates the MS spectra of sulfated *N*-glycans from bTSH and maltoheptaose prior to and following TiO_2 enrichment. Similar to the previous results, the abundance of all four sulfated glycans increased. However, the abundance of maltoheptaose, which is not sulfated, also increased, demonstrating low selectivity of this approach. It is possible that not only sulfate groups bind to TiO_2 (ZrO_2) the large number of hydroxyl groups in the glycan may also bind to TiO_2 (ZrO_2). Because the surface properties of TiO_2 and ZrO_2 are not fully uncovered,[40,41] the binding properties of different functional groups are not well understood yet, and still requires further investigation.
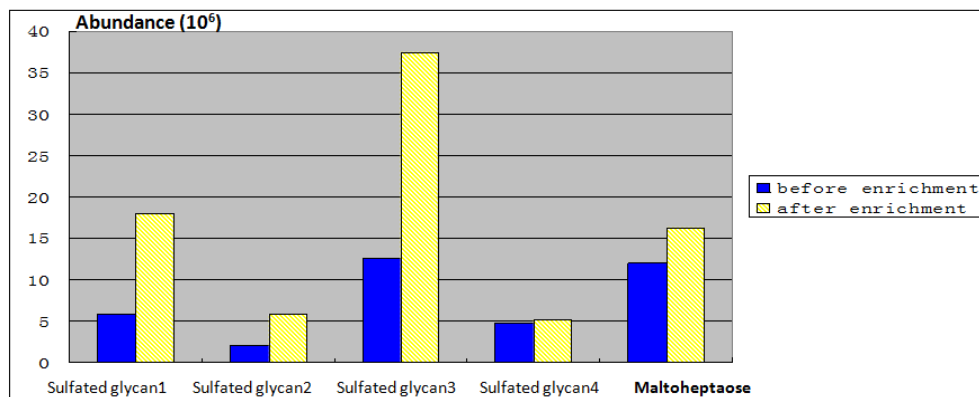

Figure A.2. The abundances of sulfated *N*-glycans from bTSH and maltoheptaose before (blue bars) and after (yellow bars) enrichment.

A.3.2 Enrichment of Sialylated Oligosaccharides

DSLNT (a doubly sialylated oligosaccharide) and LNFP (a neutral oligosaccharide) were mixed 1:100, and subjected to metal oxide enrichment before negative-ion mode MS analysis. The optimum binding solution was acetic acid (pH 4) and the optimum eluting solution was NH_4HCO_3 (pH 8). In Figure A.3, the MS spectra prior to and following zirconium oxide enrichment are compared. Prior to enrichment, LNFP was the dominant species in the spectrum, while only singly charged DSLNT was observed with very low abundance. After enrichment, both singly and doubly deprotonated DSLNT were observed and the abundance of these peaks were comparable with that of LNFP, demonstrating high selectivity of sialylated oligosaccharides over neutral ones.
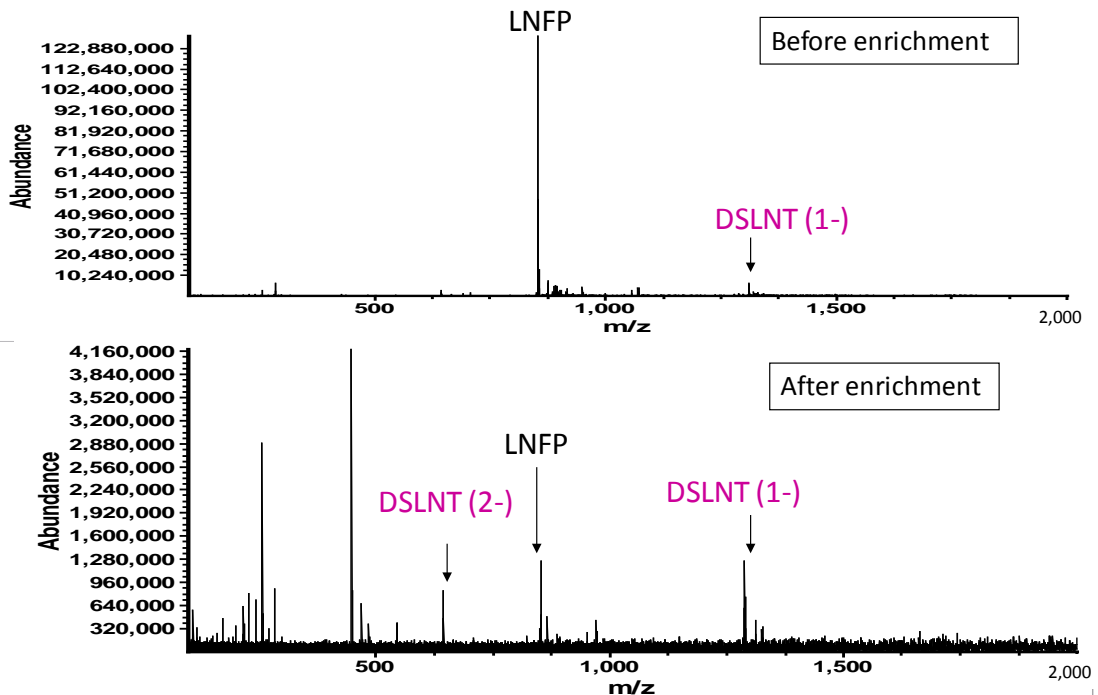

Figure A.3. Negative-ion mode MS of a 1:100 mixture of DSLNT (sialylated) and LNFP (neutral) before and after ZrO_2 enrichment.

In Figure A.4, MS before and after ZrO_2 enrichment were compared for a mixture of N-linked glycans released from human transferrin and RNAse B. The same number of moles of each glycoprotein was incubated with PNGase F separately, and 1/20 of *N*-glycans from transferrin (all sialylated) and all the *N*-glycans from RNAse B were mixed and subjected to ZrO_2 enrichment. The glycans present in the spectra are listed in Table A.2. Because acidic sialylated glycans readily generate abundant signal in negative-ion mode, the absolute abundance of a sialylated glycan (mass 2222) was higher than a neutral glycan (mass 1234) prior to enrichment. After enrichment, two additional sialylated glycans from transferrin were observed, and the peak corresponding to the neutral glycan was negligible. Again, these results demonstrated that ZrO_2 microtips are effective for enriching sialylated oligosaccharides over neutral oligosaccharides.
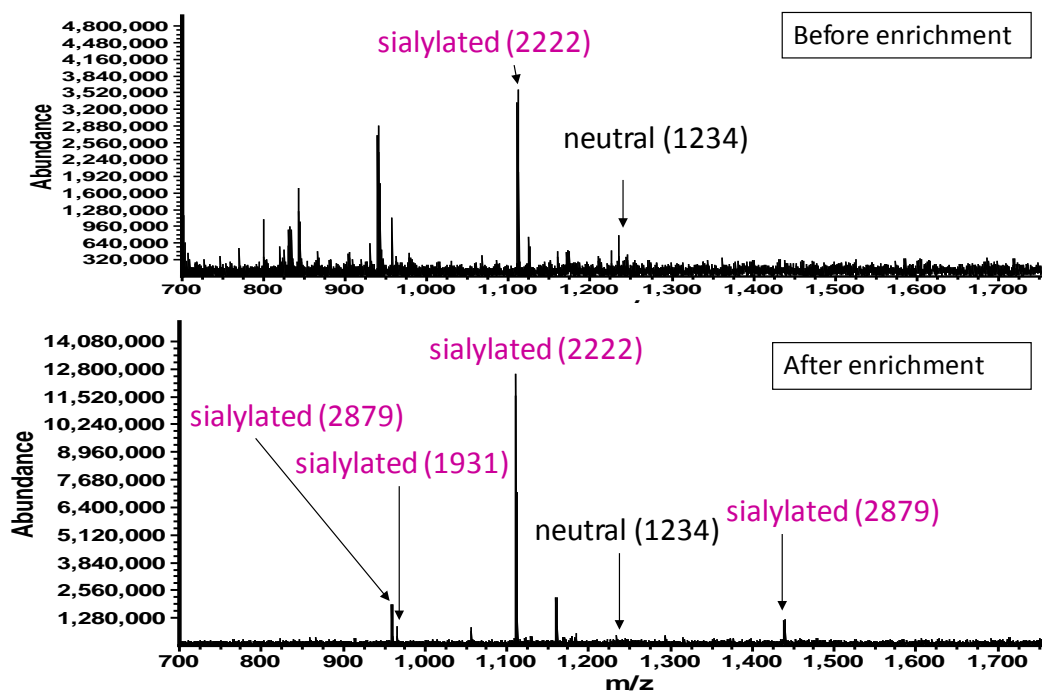

Figure A.4. Negative-ion mode MS of a 1:20 mixture of N-linked glycans from human transferrin and RNAse B before and after ZrO_2 enrichment. Masses of the glycans are indicated in brackets.

No.	Glycan	Mass	pH	Glycoprotein
1	$(GlcNAc)_4(Gal)_2(Man)_3(NeuAc)_2$	2222.7830	Acidic	transferrin
2	$(GlcNAc)_4(Gal)_2(Man)_3(NeuAc)$	1931.6876	Acidic	transferrin
3	$(GlcNAc)_5(Gal)_3(Man)_3(NeuAc)_3$	2879.0106	Acidic	transferrin
4	$(GlcNAc)_2(Man)_5$	1234.4334	Neutral	RNAse B

Table A.2. List of sialylated and neutral *N*-glycans in Figure A.4.

A.4 Conclusions

Here, we explore sulfated and sialylated glycan enrichment using ZrO_2 and TiO_2 microtips. For sulfated N-linked glycans, the optimum binding solution was formic acid (pH 2), and the optimum eluting solution was H_2O (pH 7). After enrichment, the abundance of sulfated glycans increased, and they became the dominant species in the spectrum. However, the neutral oligosaccharide maltoheptaose in the mixture was also enriched, demonstrating low selectivity of this approach. For sialylated oligosaccharides, the optimum binding solution was acetic acid (pH 4), the optimum washing solution was H_2O, and the optimum eluting solution was NH_4HCO_3 (pH 8). Mixtures of standard sialylated and neutral oligosaccharides, and acidic and neutral N-linked glycans released from glycoproteins were examined. In both cases, the sialylated species were enriched over the neutral species, showing high selectivity for sialylated oligosaccharides.

A.5 References

1. Varki, A. Biological roles of oligosaccharides - All of the theories are correct. *Glycobiol.* **1993**, *3*, 97-130.
2. Dwek, R. A. Glycobiology: Toward understanding the function of sugars. *Chem. Rev.* **1996**, *96*, 683-720.
3. Bertozzi, C. R.; Kiessling, L. L. Chemical glycobiology. *Science* **2001**, *291*, 2357-2364.
4. Rudd, P. M.; Elliott, T.; Cresswell, P.; Wilson, I. A.; Dwek, R. A. Glycosylation and the immune system. *Science* **2001**, *291*, 2370-2376.
5. Hakomori, S. Glycosylation defining cancer malignancy: New wine in an old bottle. *Proc. Natl. Acad. Sci. U. S. A.* **2002**, *99*, 10231-10233.
6. Barchi, J. J. Emerging roles of carbohydrates and glycomimetics in anticancer drug design. *Curr. Pharm. Des.* **2000**, *6*, 485-501.
7. Dube, D. H.; Bertozzi, C. R. Glycans in cancer and inflammation. Potential for therapeutics and diagnostics. *Nat. Rev. Drug Discov.* **2005**, *4*, 477-488.
8. Brown, J. R.; Crawford, B. E.; Esko, J. D. Glycan antagonists and inhibitors: A fount for drug discovery. *Crit. Rev. Biochem. Mol. Biol.* **2007**, *42*, 481-515.
9. Krishnamoorthy, L.; Mahal, L. K. Glycomic analysis: an array of technologies. *ACS Chem. Biol.* **2009**, *4*, 715-732.
10. Harvey, D. J. Matrix-assisted laser desorption/ionization mass spectrometry of carbohydrates. *Mass Spectrom. Rev.* **1999**, *18*, 349-450.
11. Mechref, Y.; Novotny, M. V. Structural investigations of glycoconjugates at high sensitivity. *Chem. Rev.* **2002**, *102*, 321-369.
12. Zaia, J. Mass spectrometry of oligosaccharides. *Mass Spectrom. Rev.* **2004**, *23*, 161-227.
13. Park, Y. M.; Lebrilla, C. B. Application of Fourier transform ion cyclotron resonance mass spectrometry to oligosaccharides. *Mass Spectrom. Rev.* **2005**, *24*, 232-264.
14. Morelle, W.; Michalski, J. C. Glycomics and mass spectrometry. *Curr. Pharm. Des.* **2005**, *11*, 2615-2645.
15. Zaia, J. Mass spectrometry and the emerging field of glycomics. *Chem. Biol.* **2008**, *15*, 881-892.
16. Zaia, J. Mass spectrometry and glycomics. *Omics* **2010**, *14*, 401-418.
17. Dai, Z.; Zhou, J.; Qiu, S. J.; Liu, Y. K.; Fan, J. Lectin-based glycoproteomics to explore and analyze hepatocellular carcinoma-related glycoprotein markers. *Electrophoresis* **2009**, *30*, 2957-2966.
18. Wu, A. M.; Lisowska, E.; Duk, M.; Yang, Z. G. Lectins as tools in glycoconjugate research. *Glycoconj. J.* **2009**, *26*, 899-913.
19. Zhang, L. J.; Lu, H. J.; Yang, P. Y. Specific enrichment methods for glycoproteome research. *Anal. Bioanal. Chem.* **2010**, *396*, 199-203.
20. Larsen, M. R.; Thingholm, T. E.; Jensen, O. N.; Roepstorff, P.; Jorgensen, T. J. D. Highly selective enrichment of phosphorylated peptides from peptide mixtures using titanium dioxide microcolumns. *Mol. Cell. Proteomics* **2005**, *4*, 873-886.

21.	Kweon, H. K.; Hakansson, K. Selective zirconium dioxide-based enrichment of phosphorylated peptides for mass spectrometric analysis. *Anal. Chem.* **2006**, *78*, 1743-1749.

22.	Carrascal, M.; Ovefletro, D.; Casas, V.; Gay, M.; Ablan, J. Phosphorylation analysis of primary human T lymphocytes using sequential IMAC and titanium oxide enrichment. *J. Proteome Res.* **2008**, *7*, 5167-5176.

23.	Han, G. H.; Ye, M. L.; Zou, H. F. Development of phosphopeptide enrichment techniques for phosphoproteome analysis. *Analyst* **2008**, *133*, 1128-1138.

24.	Yu, Y. Q.; Fournier, J.; Gilar, M.; Gebler, J. C. Phosphopeptide enrichment using microscale titanium dioxide solid phase extraction. *J. Sep. Sci.* **2009**, *32*, 1189-1199.

25.	Leitner, A.; Sturm, M.; Smatt, J. H.; Jarn, M.; Linden, M.; Mechtler, K.; Lindner, W. Optimizing the performance of tin dioxide microspheres for phosphopeptide enrichment. *Anal. Chim. Acta* **2009**, *638*, 51-57.

26.	Gates, M. B.; Tomer, K. B.; Deterding, L. J. Comparison of metal and metal oxide media for phosphopeptide enrichment prior to mass spectrometric analyses. *J. Am. Soc. Mass. Spectrom.* **2010**, *21*, 1649-1659.

27.	Nelson, C. A.; Szczech, J. R.; Dooley, C. J.; Xu, Q. G.; Lawrence, M. J.; Zhu, H. Y.; Jin, S.; Ge, Y. Effective enrichment and mass spectrometry analysis of phosphopeptides using mesoporous metal oxide nanomaterials. *Anal. Chem.* **2010**, *82*, 7193-7201.

28.	Nie, S.; Dai, J.; Ning, Z. B.; Cao, X. J.; Sheng, Q. H.; Zeng, R. Comprehensive profiling of phosphopeptides based on anion exchange followed by flow-through enrichment with titanium dioxide (AFET). *J. Proteome Res.* **2010**, *9*, 4585-4594.

29.	Leitner, A.; Sturm, M.; Hudecz, O.; Mazanek, M.; Smatt, J. H.; Linden, M.; Lindner, W.; Mechtler, K. Probing the phosphoproteome of HeLa cells using nanocast metal oxide microspheres for phosphopeptide enrichment. *Anal. Chem.* **2010**, *82*, 2726-2733.

30.	Mazanek, M.; Roitinger, E.; Hudecz, O.; Hutchins, J. R. A.; Hegemann, B.; Mitulovic, G.; Taus, T.; Stingl, C.; Peters, J. M.; Mechtler, K. A new acid mix enhances phosphopeptide enrichment on titanium- and zirconium dioxide for mapping of phosphorylation sites on protein complexes. *Journal of Chromatography B-Analytical Technologies in the Biomedical and Life Sciences* **2010**, *878*, 515-524.

31.	Aryal, U. K.; Ross, A. R. S. Enrichment and analysis of phosphopeptides under different experimental conditions using titanium dioxide affinity chromatography and mass spectrometry. *Rapid Commun. Mass Spectrom.* **2010**, *24*, 219-231.

32.	Dunn, J. D.; Reid, G. E.; Bruening, M. L. Techniques for phosphopeptide enrichment prior to analysis by mass spectrometry *Mass Spectrom. Rev.* **2010**, *29*, 29-54.

33.	Larsen, M. R.; Jensen, S. S.; Jakobsen, L. A.; Heegaard, N. H. H. Exploring the sialiome using titanium dioxide chromatography and mass spectrometry. *Mol. Cell. Proteomics* **2007**, *6*, 1778-1787.

34.	Palmisano, G.; Lendal, S. E.; Engholm-Keller, K.; Leth-Larsen, R.; Parker, B. L.; Larsen, M. R. Selective enrichment of sialic acid-containing glycopeptides using

titanium dioxide chromatography with analysis by HILIC and mass spectrometry. *Nat. Protoc.* **2010**, *5*, 1974-1982.

35. Yang, J.; Mo, J. J.; Adamson, J. T.; Hakansson, K. Characterization of oligodeoxynucleotides by electron detachment dissociation Fourier transform ion cyclotron resonance mass spectrometry. *Anal. Chem.* **2005**, *77*, 1876-1882.

36. Caravatti, P.; Allemann, M. The infinity cell - a new trapped-ion cell with radiofrequency covered trapping electrodes for Fourier-transform ion-cyclotron resonance mass-spectrometry. *Org. Mass Spectrom.* **1991**, *26*, 514-518.

37. Senko, M. W.; Canterbury, J. D.; Guan, S. H.; Marshall, A. G. A high-performance modular data system for Fourier transform ion cyclotron resonance mass spectrometry. *Rapid Commun. Mass Spectrom.* **1996**, *10*, 1839-1844.

38. Ledford, E. B.; Rempel, D. L.; Gross, M. L. Space-charge effects in Fourier-transform mass-spectrometry - mass calibration *Anal. Chem.* **1984**, *56*, 2744-2748.

39. Dobson, K. D.; McQuillan, A. J. In situ infrared spectroscopic analysis of the adsorption of aromatic carboxylic acids to TiO2, ZrO2, Al2O3, and Ta2O5 from aqueous solutions. *Spectrochimica Acta Part a-Molecular and Biomolecular Spectroscopy* **2000**, *56*, 557-565.

40. Nawrocki, J.; Dunlap, C.; McCormick, A.; Carr, P. W. Part I. Chromatography using ultra-stable metal oxide-based stationary phases for HPLC. *J. Chromatogr. A* **2004**, *1028*, 1-30.

41. Nawrocki, J.; Dunlap, C.; Li, J.; Zhao, J.; McNeff, C. V.; McCormick, A.; Carr, P. W. Part II. Chromatography using ultra-stable metal oxide-based stationary phases for HPLC. *J. Chromatogr. A* **2004**, *1028*, 31-62.